ADDENDUM

p 2 line 3: Citation added "…less than 3% w/w **(Stadler *et al*., 2004)**."

p 4 line 5: "...pharmaceutical grade..." is changed to "... clinical grade ..."

p 195 para 4 line 2: Additional comment " Species A is tetraanionic LPS existing in solution at lower pH. As pH is increased, another LPS species B (pentaanion) is generated as a result of dissociation of a single proton. Both species A and B contribute to the total LPS solubility and exist in equilibrium. The two carboxylate groups in the tetraanionic species are completely dissociated and each of the two phosphate groups is monoanionic. There is also an increase in the pentaanionic LPS fraction with increasing pH (Din *et al*., 1993)"

p 199 line 4: Additional comment "In this work, homogeneous LPS solution was prepared at 1 mg/mL"

Section 5.3 Figure 1 to 7: Comment: At least three replicates were examined for each sample.

p 202 Figure 6: Additional comment "Results shown in Figure 6 (also in Table 1) indicate that LPS cannot be completely removed with $ZnSO_4$. However, the percentage of LPS removal reported herein was quite impressive, suggesting that the method can be applied as an initial step towards pDNA purification, hence less problematic"

p 1993 Figure 2: Additional comment "The immediate increase of LPS size upon $ZnSO_4$ addition is still not fully understood but is believed to be the results of shift in the polydispersity index value. The subsequent decrease of LPS size is due to LPS entanglement as a result of reduced repulsive force between the negatively charged groups of LPS as observed from the reduced magnitude of Zeta potential. The samples for time-course experiment were prepared as described in section 2.4"

p 217 line 5 to 10: The following statement replaces line 5 – 10 "An intuitive method was used to calculate the number of pDNA molecules in an average pDNA aggregate. The average volume (nm^3) was divided by 27500 nm^3/molecule and calculations were based on the following known parameters. The base pairs size of the pDNA molecule was 25 kbp. A single base pair is approximately equivalent to 660 daltons [9]. One dalton is equivalent to 1 g/mole, thus the molecular weight was approximated to be 1.65×10^7 g/mole. Dividing by 6×10^{23} molecules/mole gave 2.75×10^{-17} g/molecule. The density was assumed to be 1 g/cm^3"

Section 5.3 Table 1: Caption is changed to "Analysis of Zeta potential of pDNA in different cation-containing solutions"

Section 5.3 Table 2: Caption is changed to “Analysis of Zeta potential of LPS in different cation-containing solutions”

p 219 line 6: “This suggests.....untreated” is changed to “This suggests that LPS aggregates were more cationic in the presence of Zn^{2+}, Ca^{2+} and Mg^{2+} compared to untreated LPS”

p 219 last line: Citation added “...the value is still lower than ±30 mV **(DTS Nano Series Manual)**”

p 222 line 2: “...were consisted of partially aggregated...” is changed to “...consisted of ~ 99% aggregated...”

p 222 Table 3: Table 3 is moved to the next page after the text

p 222 Table 3: The following table replaces Table 3

	Plasmid DNA particles		
Cation	Average diameter (nm)	Volume (nm^3)	No. of molecules/particle
No cation	501	6.6E+07	2.4E+03
Zn^{2+}	507	6.8E+07	2.5E+03
Mg^{2+}	166	2.4E+06	8.7E+01
Ca^{2+}	542	8.3E+07	3.0E+03

p 222 Table 3: Additional comment to Table 3 “The relative number of molecules neither represents the actual number of molecules per particle nor its actual volume. It is an estimated value to indicate how many more molecules per particle there are in cation-containing solutions compared to that in the control experiment”

p 226 line 6: “From the literature .... plasmid in this case” is changed to ”Literature findings demonstrate that the value of nK is dependent on biomolecular concentration [16].’

p 228 para 2 line 7: “the curve for” is added and read “At higher concentrations of LPS, the curve for Mg^{2+} indicated…”

p 228 Figure 4: Additional comment “Similar to Fig. 4, the positive gradient of $ZnSO_4$-LPS curve hints that there is a minimum concentration of LPS that is required before a significant aggregation occur, and that LPS-cation binding is not significant at low cation concentrations”

p 236 basis and assumptions: Additional comment: Due to the absence of actual literature data, many assumptions were made for the purpose of calculation and these assumptions were subject to discrepancy. Many aspects of the process design and calculations are likely to have significant

errors as the plasmid DNA production facility was assumed to be similar to that of production of recombinant protein using a bacterial host. However, assumptions were clearly spelt out where actual data were absence and all calculations were performed correctly based on available data. This article concludes that pDNA vaccine production facility could be more economical in the long run compared to that of inactivated virus vaccine. As suggested in the future work, the economics of the production process can be enhanced by using pilot-scale experimental data generated for DNA production and integrated with advanced process engineering economics for biological process upstream and downstream systems.

List of references

Stadler, J., Lemmens, R., and Nyhammar, T. 2004. Plasmid DNA purification. *J. Gene. Med.* 6: 54-66.

Din ZZ, Mukerjee P, Kastowsky M, Takayama K. Effect of pH on Solubility and Ionic State of Lipopolysaccharide Obtained from the Deep Rough Mutant of *Escherichia- Coli. Biochem* 1993;32:4579-4586.

DTS Nano Series and HPPS Customer Training Manual Chapter 5: Zeta Potential Theory

ERRATA

p 236 para 3 line 6: “1 batch per year” for “1 batch I year”

MONASH University

Bioprocess development for plasmid-based vaccine production

A thesis submitted for the degree of Doctor of Philosophy

by

Clarence M. Ongkudon

Department of Chemical Engineering
Monash University, Clayton
Australia

July, 2011

General Declaration

Monash University

Monash Research Graduate School

Declaration for thesis based or partially based on conjointly published or unpublished work

In accordance with Monash University Doctorate Regulation 17/Doctor of Philosophy and Master of Philosophy (MPhil) regulations, the following declarations are made:

I hereby declare that this thesis contains no material which has been accepted for the award of any other degree or diploma at any university or equivalent institution and that, to the best of my knowledge and belief, this thesis contains no material previously published or written by another person, except where due reference is made in the text of the thesis.

This thesis includes 10 original papers published in and submitted to international peer-reviewed journals and 3 peer-reviewed conference abstracts. There is also 1 Australian provisional patent application which is based predominantly on the body of work represented by this thesis. The core theme of the thesis is "bioprocess development for plasmid-based vaccine production". The ideas, development and writing up of all the papers in the thesis were the principal responsibility of myself, the candidate, working within the Department of Chemical Engineering under the supervision of Dr. Michael K. Danquah. The inclusion of co-authors reflects the fact that the work came from active collaboration between researchers and acknowledges input into team-based research.

The following international peer-reviewed academic journal articles are presented in this thesis:

Item no.	Thesis chapter	Publication title	Publication status	Nature and extent of candidate's contribution
1	**2**	Mitigating the looming vaccine crisis: production and delivery of plasmid-based vaccines	Critical Reviews in Biotechnology. 31: 32 – 52 (2011)	Initiation, Key ideas, Writing up [90 %]
2	**2**	Versatility of polymethacrylate monoliths for chromatographic purification of biomolecules	Journal of Separation Science. 32: 2485 – 2494 (2009)	Initiation, Key ideas, Writing up [40 %]
3	**3**	Cultivation of *E. coli* carrying a plasmid-based Measles vaccine construct (4.2 kbp pcDNA3F) employing medium optimisation and pH-temperature induction techniques	Microbial Cell Factories. 10: 16 (2011)	Initiation, Key ideas, Experimental, Development, Results interpretations, Writing up [85 %]
4	**4**	Process optimisation for anion exchange monolithic chromatography of 4.2 kbp plasmid vaccine (pcDNA3F)	Journal of Chromatography B. 878: 2719 – 2725 (2010)	Initiation, Key ideas, Experimental, Development, Results interpretations, Writing up [90 %]
5	**4**	Anion exchange chromatography of 4.2 kbp plasmid based vaccine (pcDNA3F) from alkaline lysed *E. coli* lysate using amino functionalised polymethacrylate conical monolith	Separation and Purification Technology. 78: 303 – 310 (2011)	Initiation, Key ideas, Experimental, Development, Results interpretations, Writing up [90 %]
6	**5**	Endotoxin removal and plasmid DNA recovery in various metal ion solutions	Separation Science and Technology. 46: 1280 – 1282 (2011)	Initiation, Key ideas, Experimental, Development, Results interpretations, Writing up [90 %]
7	**5**	Analysis of selective metal-salt-induced endotoxin precipitation in plasmid DNA purification using improved LAL assay and central composite design	Analytical Chemistry. 83: 391 – 397 (2011)	Initiation, Key ideas, Experimental, Development, Results interpretations, Writing up [90 %]
8	**5**	Analysis of $ZnSO_4$-induced lipopolysaccharides precipitation by measurement of hydrodynamic sizes and Zeta potentials	Process Biochemistry (Under review 2011)	Initiation, Key ideas, Experimental, Development, Results interpretations, Writing up [90 %]
9	**5**	The study of aggregative interaction of cations with endotoxins and plasmid DNA	Chemical Engineering Journal (Under review 2011)	Initiation, Key ideas, Experimental, Development, Results interpretations, Writing up [85 %]

10	**6**	Inactivated influenza virus vaccine versus plasmid DNA influenza vaccine: Cost per dose estimation and economic comparison	BMC Health Service Research (Under review 2011)	Initiation, Key ideas, Experimental, Development, Results interpretations, Writing up [35 %]

The following provisional patent application has emerged from this thesis:

Item no.	Thesis chapter	Publication title	Publication status	Nature and extent of candidate's contribution
11	**Appendix A1**	Elimination of wall channel in monolithic column preparation through the use of a conical column design and method of making a conical monolith design	Provisional patent no. 2011900918 filed by Watermark Intellectual Asset Management	Initiation, Key ideas, Experimental, Development, Results interpretations, Writing up [90 %]

The following peer-reviewed conference publications have emerged from this thesis:

Item no.	Thesis chapter	Publication title	Publication status	Nature and extent of candidate's contribution
12	**Appendix B1**	The performance of a triethylamine activated polymethacrylate conical monolith for plasmid vaccine purification	Victorian Infection and Immunity Network Symposium proceedings (2010)	Initiation, Key ideas, Experimental, Development, Results interpretations, Writing up [90 %]
13	**Appendix B2**	A novel technology for continuous enzyme free isolation of plasmid DNA	Bioprocessing Network Conference proceedings (2010)	Initiation, Key ideas, Experimental, Development, Results interpretations, Writing up [90 %]
14	**Appendix B3**	A novel technology for continuous isolation of large biomolecules: A study on plasmid DNA production	UMS Biotechnology Symposium IV proceedings (2010)	Initiation, Key ideas, Experimental, Development, Results interpretations, Writing up [90 %]

Signed by: …… **Date: …….……..**

(Clarence M. Ongkudon)

TABLE OF CONTENTS

ACKNOWLEDGEMENTS

First and foremost, praise to the Almighty God whose blessings and will have enabled me to develop this valuable PhD thesis. Next, I wish to express my heartfelt appreciation to my supervisor, Dr. Michael K. Danquah for his dedication and intellectual advice in conducting systematic and professional research. Special thanks also go to Prof. Datin Ann Anton, Director of Biotechnology Research Institute, University Malaysia of Sabah, Malaysia for giving me the opportunity to pursue my PhD. I also want to acknowledge several people especially Dr. Gareth Forde, Prof. Nick Birrell, Prof. Pauline Doran, and my fellow postgraduate researchers for their ideas and assistance at various occasions in my research. I also thank my family members and friends for their supports, words of encouragement and prayers. They have indeed helped me to face the difficulties I encountered along the journey. I wish and pray for good health and fortunes for them in the days to come. Last but not least, I want to thank all the staff in the Chemical Engineering Department of Monash University, Australia for their direct and indirect supports which have been very pleasant and worthwhile. The invaluable experiences gained during my candidature have nurtured me to take up bigger challenges in my on-going career.

ABSTRACT

Plasmid DNA (pDNA) vaccine is a promising vaccine technology, with better safety profile, more economical production and transport logistics, than conventional viral vaccines. Most importantly, pDNA vaccines elicit different immune responses including antibody-mediated, CD4 T-cell-mediated and CD8 T-cell-mediated immune responses, for defending against viral infections and cancer. The increasing number of preclinical and clinical trials on plasmid vaccines has triggered the need to make more in less time. Recent developments in the production of plasmid therapeutics involve the establishment of innovative and cost effective methods as well as simplified operations. This dissertation reports fundamental studies essential to the development of a rapid economically-viable plasmid production system which is cGMP-compatible. Optimisation of upstream bacterial fermentation and continuous downstream purification of the plasmid vaccine fraction are the main aspects considered in the project of this dissertation. Process variables required to improve the volumetric and specific yields of a model plasmid-based measles vaccine (pcDNA3F) harboured in *E. coli* DH5α were investigated. A cGMP-compatible method offering the capacity to continuously produce homogeneous supercoiled pDNA from clarified bacterial lysate using a monolithic adsorbent was developed. The method involved optimisation of the adsorbent characteristics, ligand functionalisation and chromatographic process conditions. The feasibility of using free metal ions to preferentially precipitate endotoxins (LPS) from a clarified plasmid DNA-containing bacterial lysate was investigated. Screening of various free metal ions for effective endotoxin removal and optimisation of process conditions, such as pH, ion concentration, temperature and incubation time, using central composite design experiments were performed. The potential and advantages of using Zn^{2+}-induced LPS aggregation as a secondary pDNA purification method was validated by studying the interaction of Zn^{2+} with LPS and pDNA. A comparative economic analysis on the basis of vaccine cost per dose for influenza vaccine produced via pDNA vaccine technology and fertilised egg-based technology was also studied. Experimental results from growth medium optimisation in 500 mL culture showed a maximum volumetric yield of 13.65 mg/L, twice the amount generated using a standard medium (PDM). Fed-batch fermentation in combination with exponential

glycerol feeding strategy resulted in a significant increase of 110 mg/L pcDNA3F volumetric yield and a specific yield of 14 mg/g. In addition, growth pH variation (6 to 8.5) and temperature fluctuation (35 ^{o}C to 45 ^{o}C) also resulted in improved plasmid yield. Chromatographic purification of pDNA using a triethylamine-activated conical monolithic adsorbent resulted in preferential pcDNA3F adsorption with optimum resolution achieved under the conditions of 400 nm pore size of monolith, 0.7 M NaCl (pH 6) of binding buffer and 3 % B/min of gradient elution up to 1 M NaCl. Plasmid volumetric yield and recovery of ~3g/L and ~90% were obtained. Contaminant levels recorded were protein (0.01 mg/L), LPS (0.12 EU/mg) with no detectable gDNA and RNA. Results from endotoxin removal and analysis showed that $ZnSO_4$ displayed the highest endotoxin removal efficiency (~91%) and plasmid recovery (~100%). It was found that selective endotoxin precipitation (< 0.05 EU/μg) could effectively be carried out during neutralisation in alkaline cell lysis at a pH condition similar to that of clarified cell lysate, a low $ZnSO_4$ concentration (0.5 M), a minimum incubation time (30 min) and a temperature of 15 ^{o}C. Apparently, the lipopolysaccharide (LPS) showed a decreased aggregate size at the start of the $ZnSO_4$ addition before increasing gradually. Results from the LPS aggregation analysis drew a hypothesis that cationic close range encounter and interaction with LPS monomers may contribute to LPS self-aggregation whilst bridging of LPS monomers may increase the LPS aggregate size to a greater extent compared to that of self-aggregation. Specifically, addition of Zn^{2+} resulted in the largest number of LPS particles per aggregate and the value of aggregation constant (K_m) for LPS-Zn^{2+} was substantially low (0.28 M) and considerably large (>2 M) for pDNA-Zn^{2+}, indicating its preferential ability to remove LPS from pDNA-containing solutions. The economic studies suggested that pDNA-based influenza vaccine production was highly dependent on the selling price and production volume. A similar cost per dose of about $2 was calculated although most of the manufacturing costs for plasmid DNA vaccine were lower than inactivated virus vaccine. This dissertation has developed a simple bioprocess framework to successfully improve production specification of plasmid vaccines using pcDNA3F as a model. The method offers ease of plasmid DNA purification due to reduced bulk impurities, cost-efficiency and most importantly high endotoxin removal (> 80%) and plasmid recovery (> 90%). The technology will have a great impact on overall plasmid production and in particular on the development of axial flow monolithic purification in combination with selective endotoxin precipitation.

DETAILS OF PUBLICATIONS

Details of the findings in this dissertation are described in 10 published/submitted peer-reviewed international journal papers, 1 provisional patent application and 3 peer-reviewed conference proceedings. This constitutes the requirements based on Monash University guidelines for PhD thesis by publications. The following articles are organised in the order of appearance in the thesis.

Peer-Reviewed Journal Papers

1. **Clarence M. Ongkudon**, Jenny Ho, Michael K. Danquah (2011). Mitigating the looming vaccine crisis: production and delivery of plasmid-based vaccines. Critical Reviews in Biotechnology. 31: 32 – 52.
2. Michael W. H. Roberts, **Clarence M. Ongkudon**, Gareth M. Forde, Michael K. Danquah (2009). Versatility of polymethacrylate monoliths for chromatographic purification of biomolecules. Journal of Separation Science. 32: 2485 – 2494.
3. **Clarence M. Ongkudon**, Raelene Pickering, Diane Webster, Michael K. Danquah (2011). Cultivation of *E. coli* carrying a plasmid-based Measles vaccine construct (4.2 kbp pcDNA3F) employing medium optimisation and pH-temperature induction techniques. Microbial Cell Factories. 10: 16.
4. **Clarence M. Ongkudon,** Michael K. Danquah (2010). Process optimisation for anion exchange monolithic chromatography of 4.2 kbp plasmid vaccine (pcDNA3F). Journal of Chromatography B. 878: 2719 – 2725.
5. **Clarence M. Ongkudon,** Michael K. Danquah (2011). Anion exchange chromatography of 4.2 kbp plasmid based vaccine (pcDNA3F) from alkaline lysed *E. coli* lysate using amino functionalised polymethacrylate conical monolith. Separation and Purification Technology. 78: 303 – 310.
6. **Clarence M. Ongkudon,** Michael K. Danquah (2011). Endotoxin removal and plasmid DNA recovery in various metal ion solutions**.** Separation Science and Technology. 46: 1280 –1282.

7. **Clarence M. Ongkudon,** Michael K. Danquah (2011). Analysis of selective metal-salt-induced endotoxin precipitation in plasmid DNA purification using improved LAL assay and central composite design. Analytical Chemistry. 83: 391 – 397.
8. **Clarence M. Ongkudon,** Michael K. Danquah (2011). Analysis of $ZnSO_4$-induced lipopolysaccharides precipitation by measurement of hydrodynamic sizes and Zeta potentials. Process Biochemistry (Under Review).
9. **Clarence M. Ongkudon,** Emma Hodges, Kathleen Murphy, Michael K. Danquah (2011). The study of aggregative interaction of cations with endotoxins and plasmid DNA. Chemical Engineering Journal (Under Review).
10. **Clarence M. Ongkudon**, Lorraine Angstetra, Michael K. Danquah, Gareth M. Forde (2011). Inactivated influenza virus vaccine versus plasmid DNA influenza vaccine: Cost per dose estimation and economic comparison. BMC Health Service Research (Under Review).

Patent

1. **Clarence M. Ongkudon** and Michael K. Danquah. Elimination of wall channel in monolithic column preparation through the use of a conical column design and method of making a conical monolith design. Australian provisional patent no. 2011900918.

Peer-Reviewed Conference Proceedings

1. **Clarence M. Ongkudon** and Michael K. Danquah. The performance of a triethylamine activated polymethacrylate conical monolith for plasmid vaccine purification. Victorian Infection and Immunity Network symposium, Melbourne, Australia, 3rd June 2010.
2. **Clarence M. Ongkudon** and Michael K. Danquah. A novel technology for continuous enzyme free isolation of plasmid DNA. Bioprocessing Network conference, Melbourne, Australia, 12th – 14th October 2010.
3. **Clarence M. Ongkudon** and Michael K. Danquah. A novel technology for continuous isolation of large biomolecules: A study on plasmid DNA production. UMS Biotechnology Symposium IV, Kota Kinabalu, Malaysia, 1st – 3rd December 2010.

Specially dedicated to…

♥Mom and Dad;

Jessica, Edven, Fayleanne and Kayla♥

… whom I owe all that I am

CHAPTER ONE

INTRODUCTION

1.1 Introduction

DNA vaccines have significantly made its way into providing relatively high levels of protection against many diseases. However, plasmid DNA (pDNA) existing in *E. coli* cells accounts for only less than 3 % w/w. This yield also varies slightly from one recombinant construct to the other. Therefore, it is very desirable to maintain a high specific yield in each construct since it leads to high product purities and ease of downstream processing (Carnes *et al.*, 2006). Improved plasmid yield results from high plasmid stability and preferential plasmid synthesis over other contaminating biomolecules syntheses (Prather *et al.*, 2003). Plasmid DNA is highly viscous in solution, non globular, highly electronegative and have high molecular weight (MW). In designing a purification scheme for pDNA molecules, it is important to retain its intact structure (Prazeres *et al.*, 1999). The need for DNA supercoilty in plasmid vaccine formulation is not fully understood but it is generally known that supercoiled plasmid DNA (scpDNA) is more efficient in transfecting eukaryotic cells and stimulating cell-mediated responses (Prazeres *et al.*, 1999; Sousa *et al.*, 2008).

Numerous methods have been widely suggested as ways to control the biomass growth rate in order to achieve high plasmid specific yields. In batch cultivations, cell growth can be controlled by altering growth temperature, pH, dissolved oxygen (DO) concentration and nutrient composition (Filomena *et al*., 2009). However, optimum plasmid replication is limited by nutrient availability during batch fermentation (Nan *et al*., 2005). Cell growth regulation by the provision of a medium limiting substrate to make intracellular activities viable is the method of choice currently used in pilot-scale pDNA vaccine production (Carnes, 2007; Danquah and Forde, 2008; Prazeres, *et al*. 1999). Recent advancements in pDNA purification involve the development of monolithic chromatographic supports which provide higher capacity and flow rates at lower pressure drops compared to particulate supports. Current studies aim at developing a technology to efficiently manufacture a clinical grade, endotoxin free plasmid DNA vaccine via monolithic chromatography. Consequently, this technology would have a great impact on the overall vaccine production and its economic viability. In *in vivo* administration of pDNA vaccines, the presence of endotoxin can cause severe health effects such as fever and even death. Therefore, it is vital to effectively reduce the level of endotoxin in pDNA vaccines preparations both in laboratory and production scales. Endotoxins are often co-purified with pDNA when using conventional purification

technique such as anion exchange chromatography due to their highly negatively charged groups.

Currently, pDNA vaccine purification for *in vivo* administration is performed through a series of chromatographic steps. In recent years, the concept of single-stage chromatographic purification of pDNA molecules via anion exchange or affinity chromatography has been found to effectively separate supercoiled pDNA from its impurities (Han and Forde, 2008). However, its commercial viability is mired due to problems such as low plasmid recovery, high salt concentration for elution, dialysis requirements and instability of biological based ligands used in high affinity chromatography (Diogo *et al*., 2005). This has called for the development of novel technologies for single-stage chromatographic purification of pDNA molecules. An alternative method would be to design a selective purification scheme for pDNA vaccine by integrating anion exchange chromatography (AEC) and selective metal ion-induced precipitation to improve endotoxin removal, and maximise pDNA purity and recovery. AEC could be used to remove lower charged impurities from the bulk scpDNA, RNA, and endotoxins through electrostatic interactions between less positively charged ligands, such as diethylamine and triethylamine, and more negatively charged biomolecules (Diogo *et al*., 2005). The metal ion-induced precipitation is targeted to selectively bind RNA and endotoxins while keeping pDNA in the flowthrough.

An economic analysis of vaccine production process can also be carried out using an in-depth cost budgeting and profitability analysis to examine the commercial viability of pDNA vaccine production technology in comparison to current vaccine technologies. The different costs, including cost of fermentation, cell concentration and lysis including utilities as well as the cost of polymer preparation, functionalisation and purification requirements can be evaluated for an estimated plant life, and key economic indicators such as payback period, rate of return and net present value can then be estimated.

1.2 Scope of Work

This project utilised a plasmid vector harbouring a measles vaccine candidate as the model plasmid vaccine (pcDNA3F). Similar to other plasmid vaccines, the overall production of plasmid DNA measles vaccine involves the design of the vaccine construct, cell transformation, fermentation, cell lysis, vaccine purification, vaccine formulation and filling.

This research focuses mainly on the fermentation and purification parts of the pDNA vaccine production scheme as these two unit operations are very critical to plasmid productivity and process economics. Many of the production schemes employed by cGMP and GCP (Good Clinical Practice) facilities combine at least three purification steps to achieve a pharmaceutical grade pDNA vaccine. Increasing the number of unit operations results in product loss and cost ineffectiveness. Although the concept of single-stage pDNA vaccine purification has been found to effectively separate supercoiled pDNA, there exist many technological problems as mentioned earlier, thus making this process not commercially viable. This research focuses on the development of a novel process for pDNA vaccine production via fed-batch bacterial fermentation and a single-stage chromatographic purification combined with an innovative endotoxin removal technique.

1.3 Research Objectives

Based on an in-depth review of the production of plasmid DNA vaccines, three main objectives were set apart for this research. Eight specific objectives were also designed to assist in the realisation of the main objectives.

1.3.1 Main Objectives

1. To develop a fully scalable bacterial fermentation scheme for the production of high-yield clinical grade plasmid DNA vaccine.
2. To develop a commercially viable single-stage monolithic purification system for plasmid DNA measles vaccine via liquid chromatography.
3. To develop a selective endotoxin removal method to improve plasmid DNA purification.

1.3.2 Specific Objectives

1. To improve lab-scale volumetric titres of plasmid vaccine production.
2. To develop a pilot-scale production system via fed-batch fermentation optimisation for the production plasmid vaccines.
3. To optimise chromatographic process conditions in anion-exchange purification of plasmid vaccines from bacterial lysate.

4. To study the performance of amino functionalised anion exchange system for chromatographic purification of plasmid DNA using a proprietary conical monolithic support.
5. To develop an analytical method for endotoxin quantification in different metal-ion-containing solutions.
6. To develop a selective endotoxin precipitation method to enhance plasmid DNA purification using metal salts.
7. To characterise selective endotoxin-plasmid DNA precipitation by measurement of hydrodynamic parameters, binding kinetics and aggregation constants.
8. To economically evaluate plasmid-based vaccine production technology.

1.4 Chapter Layout

The specific objectives of the project as outlined above are expressed and tackled in the body of work contained in the publications which form the main chapters of the thesis. A chronological presentation of the thesis structure in the context of these publications is included below.

Chapter 1: This chapter forms the thesis background and clearly describes the scope and objectives of the research.

Chapter 2: This chapter reviews earlier research works in the field of DNA therapeutics and production methodologies. An in-depth review is presented on the potential use of plasmid DNA molecules as vaccine vectors including the design of DNA vaccine constructs as well as methods currently employed in plasmid DNA production. Some major challenges in plasmid DNA vaccine production were identified to include low plasmid yield, low plasmid purity, low plasmid selectivity, and the routine use of high volumes of disposable materials. A specific review on a novel chromatographic adsorbent selected for this research was also performed to substantiate and adapt its application to work.

Chapter 3: This chapter describes methods to improve plasmid DNA measles vaccine (pcDNA3F) lab/pilot-scale production yields by optimising growth conditions such as pH, temperature, medium and feeding strategy. The attainment of high plasmid specific yields during fermentation is vital to the success of further downstream processing.

Chapter 4: This chapter describes the purification of pcDNA3F using a novel polymethacrylate monolithic adsorbent. A major bottleneck commonly experienced with the preparation and application of organic-based monoliths is the tendency of the monolith to shrink, resulting in the formation of flow gaps between the monolith surface and the column wall (called as 'wall channel'). This chapter describes the development of a conical monolith-based chromatographic column, its application to the elimination of wall channel and its utilisation for enhanced plasmid DNA purification. The body of work in this chapter is the focus of a provisional patent application.

Chapter 5: This chapter describes a novel endotoxin removal technique based on selective free metal ion-induced precipitation as a pre-chromatographic step. Under certain chromatographic conditions, plasmid yield could be substantially lower than could be predicted from binding capacity analysis. This could be due to co-binding of impurities such as RNA, protein and endotoxin electrostatically to the anion exchange ligand. Although the amount of bound impurities could be reduced by increasing the ionic strength of the binding buffer, this results in apparent decrease in plasmid DNA yield. Removal of impurities prior to column purification would better exploit the monolith for maximum plasmid binding. Endotoxin removal was considered in this case. The structural dynamics of endotoxin lipopolysaccharides make their removal from vaccine titers problematic, thus making vaccine endotoxin removal very challenging.

Chapter 6: This chapter describes the comparison of the economic analysis between plasmid DNA vaccine production via recombinant DNA technology and fertilised egg-based technology using influenza vaccine as the model vaccine. It presents a detailed economic understanding of the different vaccine production techniques and provides a framework for assessing cost efficiency. This study will be useful to pharmaceutical or biotechnology companies when considering their production and investment strategies for vaccines.

Chapter 7: This chapter concludes the research work by reiterating the core findings and relevant applications to improve plasmid DNA production. The chapter also proposes some future works that can be performed to further improve plasmid DNA production.

CHAPTER TWO

LITERATURE REVIEW

Section 2.1

Mitigating the looming vaccine crisis: Production and delivery of plasmid-based vaccines

Critical Reviews in Biotechnology. 31: 32 – 52 (2011)

Monash University

Declaration for Thesis Section 2.1

Declaration by candidate

In the case of Section 2.1, the nature and extent of my contribution to the work was the following:

Nature of contribution	Extent of contribution (%)
Initiation, Key ideas, Writing up	90

The following co-authors contributed to the work. Co-authors who are students at Monash University must also indicate the extent of their contribution in percentage terms:

Name	Nature of contribution
Dr. Jenny Ho	Initiation, Key ideas, Writing up
Dr. Michael K. Danquah	Initiation, Key ideas, Writing up

Candidate's signature		**Date**

Declaration by co-authors

The undersigned hereby certify that:

1. the above declaration correctly reflects the nature and extent of the candidate's contribution to this work, and the nature of the contribution of each of the co-authors;
2. they meet the criteria for authorship in that they have participated in the conception, execution, or interpretation, of at least that part of the publication in their field of expertise;
3. they take public responsibility for their part of the publication, except for the responsible author who accepts overall responsibility for the publication;
4. there are no other authors of the publication according to these criteria;
5. potential conflicts of interest have been disclosed to (a)granting bodies, (b) the editor or publisher of journals or other publications, and (c) the head of the responsible academic unit; and
6. the original data are stored at the following location (s) and will be held for at least five years from the date indicated below:

Location	Chemical Engineering Department, Monash University, Clayton, Australia

Signature		**Date**

Mitigating the Looming Vaccine Crisis: Production and Delivery of Plasmid-Based Vaccines

Clarence M. Ongkudon, Jenny Ho, Michael K. Danquah

ABSTRACT

The exponentially growing human population and the emergence of new diseases are clear indications that the world can no longer depend solely on conventional vaccine technologies and production schemes. The race to find a new vaccine technology is crucial to help speed up and complement the WHO disease elimination program. The ultimate goal is to uncover fast and efficient production schemes in the event of a pandemic, and also to effectively fight deadly diseases such as malaria, bird flu, hepatitis and HIV. Plasmid DNA vaccines, if properly formulated, offer specific priming of the immune system and similar or even better prophylactic effects than conventional vaccines. This article discusses many of the critical issues that need to be considered when developing fast, effective and reliable plasmid DNA vaccine manufacturing processes. Different modes of plasmid production via bacterial fermentation are compared. Plasmid purification by chromatography is specifically discussed as it is the most commercially-viable bioprocess engineering technique for continuous purification of supercoiled plasmid DNA. Current techniques and progress covering the area of plasmid DNA vaccine design, formulation and delivery are also put forward.

Keywords: Plasmid DNA; DNA vaccine; Vaccine production; Vaccine delivery, Bioprocess

INTRODUCTION

Vaccine Evolution

The so called first generation or conventional vaccines involve the introduction of whole organism vaccines into the immune system to induce immunological responses. These vaccines could be in the form of live, attenuated, or killed pathogens such as smallpox and polio vaccines (WHO, 2007). The efficiency of these vaccines lies in their ability to trigger both B- and T- cell responses. T cell mediated response is the generation of cytolytic T lymphocytes (CTL) against viral infection and tumour while B cell response is the antibody production against antigens (Shroff *et al.*, 1999). A list of some current vaccines in the market

and under evaluation is given in Table 1. Measles vaccine (MV) was first formulated in the 1960s using formalin or Tween inactivated virus adjuvanted with alum. This formulation however, is incapable of inducing relatively sufficient amounts of CTL and was discontinued in 1967. Live attenuated vaccine (LAV) was introduced later and resulted in a major decline of measles casualties even though it led to rash and fever in almost 50% of the children immunized.

The presence of maternally derived MV specific antibodies and immunological maturity of the recipient has the most profound effect on the success of measles vaccination (Vries *et al.*, 2008). In 2005, after nearly a decade of intensive research, the Food and Drug Administration (FDA) issued a license to a new vaccine combining measles, mumps, rubella, and varicella (MMRV) vaccines. The MMRV which is commercially known as ProQuad® contains LAV and albumin. The level of antibody response reflects in a similar way in patients who are given separate vaccines but contraindicated in patients with known hypersensitivity to any component of the vaccine including neomycin and gelatine (Buck, 2005). The second generation vaccines consist of subcomponent vaccines such as defined protein antigens and recombinant viral proteins. Examples of these vaccines are tetanus, diphtheria toxoid and hepatitis B surface antigen. Merozoite surface proteins such as MSP1, MSP2, and MSP3 or the apical membrane antigen (AMA)-1, are among the target subunit vaccines for malaria disease. Long synthetic peptides such as CSP, GLURP and Exp-1 have also been tried in an attempt to fight against this deadly disease (Genton, 2008).

Plasmid DNA Vaccine

Plasmid DNA (pDNA) based vaccine, as the third generation vaccine technology, has been escalating since early 1990s. Generally, it involves the introduction of one or more functional genes to a human recipient to prevent or treat infectious diseases (Prazeres *et al.*, 1999). Plasmid is an extra chromosomal DNA, it replicates autonomously and is mostly found in bacteria. It carries only accessory genes rather than indispensable genes (Shroff *et al.*, 1999). DNA vaccine development uses not only plasmid but also adjuncts to help deliver and direct the immune system. Although it is not well established in humans, protection against diseases in animals has been achieved (WHO, 2007). Studies in mice have characterized both B- and T- cell mediated responses where T is more profound. B response is non-neutralizing and therefore is not relevant for protection. In human studies, pDNA vaccination also leads to a prominent T type of response. These studies also suggest that pDNA immunization mimics

the native intracellular antigen expression. The most commonly reported side effects following pDNA vaccination are mild tenderness and erythema (Shroff *et al.*, 1999).

Table 1: Vaccines candidates for measles, malaria, hepatitis C and HIV-1 virus

	Measles	Malaria	Hepatitis C	HIV
Viral and protein based vaccines	a) Formalin- and Tween inactivated MV and Live attenuated MV (Vries *et al*., 2008) b) MMR and MMRV (Buck, 2005)	a) MSP1, MSP2, MSP3 and (AMA)-1 subunit proteins b) Long synthetic peptides C SP, GLURP and Exp-1 (Genton, 2008)	a) HCV core proteins (Lechmann and Liang, 2000)	a) HIV subunit proteins (ORFs) (Sahloff, 2005; Huang *et al*., 2008)
DNA vaccines	a) Plasmid encoding hemaglutinin protein (H), fusion protein (F) and nucleoprotein (N) (Vries *et al*., 2008)	a) Plasmid encoding AMA-1 (Ser-22 to Gln-479) and MSP4/5 (Met-1 to Ser-190) (Rainczuk *et al*., 2008)	a) Plasmid encoding HCV conserved proteins (Lechmann and Liang, 2000)	a) Plasmid encoding ORFs b) ADVAX (Vical, Inc., San Diego, CA) and VRC-HIVDNA009-00-VP (Vical, Inc.) (Sahloff, 2005; Huang *et al*., 2008)

Table 2: Pros and cons of plasmid-based vaccine technology

PROS	CONS
• Ability to trigger both humoral and cell mediated responses	• Poor immune response or zero seroconversion
• Poses no risk of developing the disease	• Insufficient level of antigen expression
• Flexibility to prime different arms of the immune system like CTL, helper T cell and B	• Limited to protein antigen and not useful for non protein antigens like bacterial polysaccharides
• Easy to construct due to its small size	• Unforeseen risk of genomic DNA (gDNA) integration,
• Obviates the need for high cost peptide synthesis, expression and purification of complex proteins	• Possibility of antibody response against pDNA and possible tolerance to the antigen
• pDNA is stable under variable temperature	
• Easily stored and transported since a cold chain may not have to be maintained	

The development of pDNA vaccines against diseases such as Hepatitis C still poses a major problem. Hepatitis C virus (HCV) represents high sequence variations of multiple isolates in the world and being an RNA virus, it can mutate rapidly. On top of that, the complete identification of epitopes in at least 6 HCV genotypes and more than 50 subtypes has not been achieved (Lechmann *et al.*, 2000). However, HCV core protein is highly conserved among various genotypes and therefore an excellent target for the design of pDNA HCV vaccines. AIDS is another lethal disease and with the complexity of the viral invasion into the human immune system, its absolute cure may never be found at least for the next five to ten years period. The history of human immunodeficiency virus (HIV) infection has recently entered its third decade. There are many vital questions that need to be addressed regarding the immune response to HIV as well as some sensitive ethical issues. These include the understanding and identification of specific immune responses that are actually protective against HIV infection,

addressing the ability of HIV to invade the system, where to conduct the study and how HIV volunteers will be treated (Corey, 1999; Sahloff, 2005). Like Hepatitis C virus, HIV also possesses high genetic variability and rate of mutation, which are the major barriers to the successful development of an HIV pDNA vaccine.

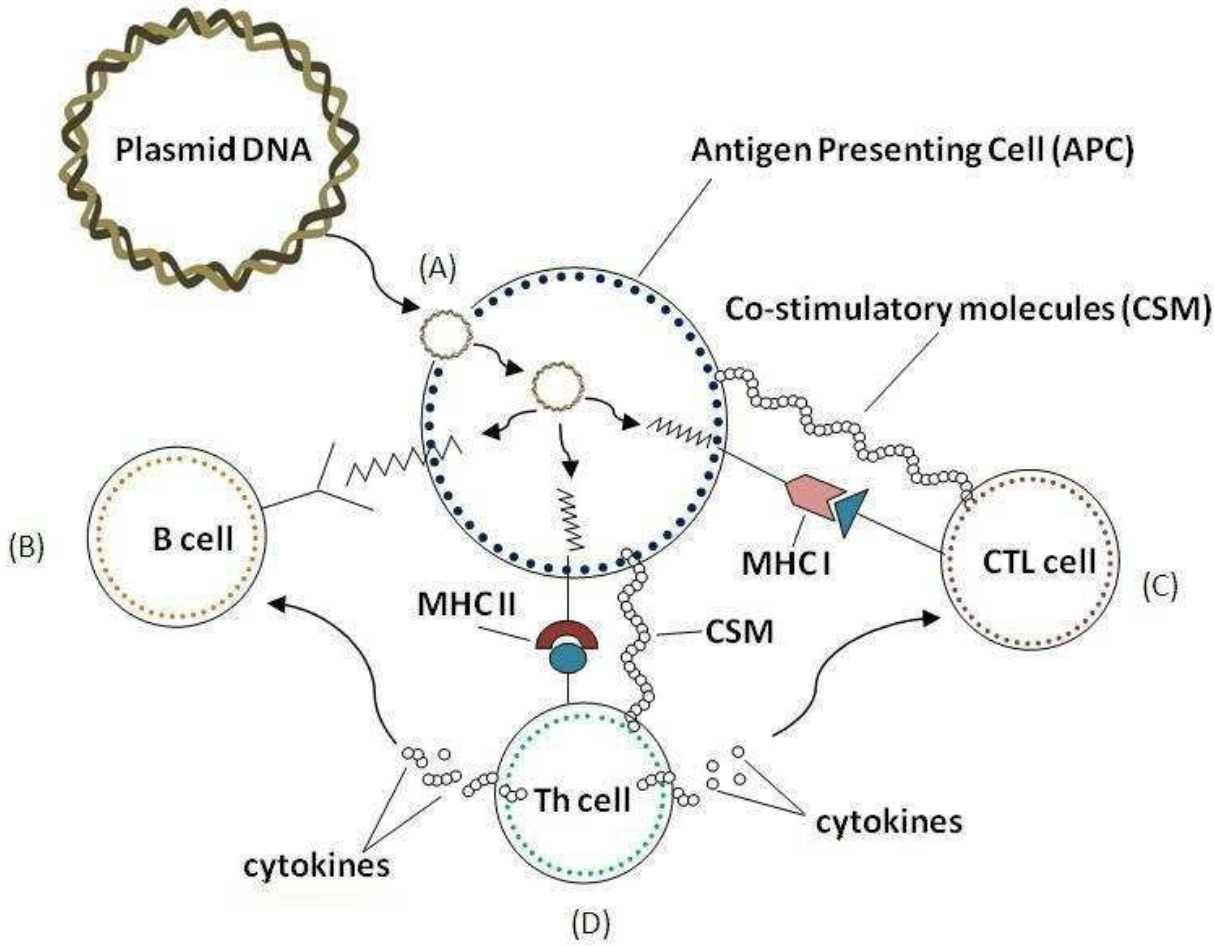

Figure 1: Immunological pathways of plasmid DNA vaccines. (A)In order to be expressed in target cells, exogenous plasmid DNA vaccine has to overcome the endosomal degradatory pathways. (B) Humoral B cell recognizes antigenic proteins that are expressed extracellularly and produces antibodies. (C) Antigenic protein undergoes further process intracellularly and produces MHC Class I peptide which is recognized by CTL cell. (D) MHC Class II peptide is recognized by Th cell which is then activated to produce cytokines. Cytokines are used in activating B cell to produce antibody and stimulating CTL cell to produce CTLs and kill infected APC. The interaction between Th cell, CTL cell and APC is enhanced by the co-stimulatory molecules (CSM).

Mechanism of Defense of pDNA Vaccines

The immunological pathway of pDNA vaccination is assumed to inhibit the natural antigen expression and system. Plasmid DNA vaccine can be delivered via intravenous, intratracheal, intraorbital and intradermal means. In order to be expressed, pDNA has to reach the appropriate antigen presenting cells (APC), cross over the cell membrane, escape the endosomal degradatory pathways and enter the cytoplasm. Plasmid DNA is normally coated with adjuvants such as gold beads to improve the delivery and expression level of antigens (Shroff *et al.*, 1999). Generally, there are three components in the immune system that help to terminate an invading pathogen. These are the killer T cells, helper T cells and B antibody producing cells (refer to Figure 1). In order to activate the killer T cells, an antigen from the cytoplasm will enter a cellular processing pathway and results in peptides known as MHC Class I molecules which are recognized by the appropriate T cells. The T cells are then activated to kill the infected cell. In the same way, helper T cells can recognize antigen peptides or MHC Class II molecules produced in the infected cells and then are activated to produce cytokines. These cytokines help in stimulating B cells to produce antibodies and also activating the killer T cell to produce CTLs. Successful activation of both T cells depends heavily on the interaction of other molecules between the APC and naïve T cells known collectively as co-stimulatory molecules. B cells can recognize and respond to antigens that are present or exposed extracellularly from inside the infected cells (Liu, 2003). Although it has been shown that a muscle cell can take up a recombinant pDNA and synthesize the encoded antigen, it is not exactly known whether the use of pDNA vaccine could generate the desired quality of cell mediated response especially in highly diverged viral strains. However, this technique can be used to develop a vaccine that encodes the conserved viral core proteins thus producing CTLs against various strains of a virus.

Pros and Cons

Scientifically sound fundamentals of DNA vaccine production are mandatory for application in humans. Safety issues like human DNA integration, antibodies against pDNA vaccine, long term expression of pDNA and other biological activities need to be fully characterized (WHO, 2007). Table 2 shows a list of the advantages and disadvantages of pDNA vaccines. The undoubted potential of pDNA vaccines lies in their versatility, stability, ease of manufacture, safety and most importantly their ability to trigger both humoral and cell mediated responses (Shroff *et al.*, 1999; WHO, 2007). Plasmid DNA vaccines can be presented by both MHC class I and class II molecules and are able to polarize T cells towards type 1 and 2 (Robinson

and Pertmer, 2000). Studies have shown that pDNA vaccines based on viral core proteins were able to induce both humoral antibody and cytolytic responses against various Hepatitis C viral proteins (Meacle *et al.*, 2007). Clinical studies of pDNA vaccination against HIV in chimpanzees indicated promising B- and T- cell responses (Shroff *et al.*, 1999). In another review, scientists have also made significant discoveries in HIV DNA vaccine research including the recent DNA vaccines (ADVAX and VRC-HIVDNA009-00-VP) which have gone into Clinical Trial Phase III. DNA vaccines encoding for HIV subunit proteins from different HIV subtypes are also being studied (Sahloff, 2005).

Plasmid DNA vaccines consist of only selected subcomponents of a virus and therefore pose no risk of developing the disease. The flexibility to manipulate DNA and prime different arms of the immune system such as CTL, helper T cells and B cells is one of the major advantages of this technology as it mimics the native viral infection (Lechmann *et al.*, 2000). This includes reducing full-length genes to minigenes to help focus on the target immune response; recruiting help from helper T cells to treat cancer in genetic immunization; linking multiple epitopes to create polytope vaccines; and incorporating different enhancers such as Kozak consensus sequence and CpG motifs to boost the immune response (Lechmann and Liang, 2000; Garmory *et al*., 2003, Genton, 2008; Corey, 1999) In animal studies however, injection with pDNA may sometimes lead to poor immune response and zero seroconversion. This is often due to an insufficient level of antigen expression to elicit strong immune response. Therefore, the amount of pDNA vaccine administered has to be increased (Luckay *et al.*, 2007; Prather *et al.*, 2003; Vries *et al.*, 2008). Plasmid DNA application is somehow limited to protein antigens and not useful for non protein antigens like bacterial polysaccharides. Further details on the delivery of DNA vaccines are given in the Formulation and Delivery section.

Other issues regarding the use of pDNA vaccines are unforeseen risk of genomic DNA (gDNA) integration, possibility of antibody response against pDNA and possible tolerance to the antigen. Theoretically, the injection of exogenous DNA into cells could lead into gene transformations (e.g. gene controlling cell growth) that quite often result in the occurrence of cancer cells. These transformations can be caused by random integration and homologous recombination where the former is much likely to occur (WHO, 2007). Many studies have shown that pDNA vaccines are safe because of the lack of genetic integration. Basically, pDNA will remain episomally in infected cells before being eliminated by cytotoxic T killer

cells. These studies used an assay that can identify and quantify one integration event in 1×10^{-6} cells (Prather *et al.*, 2003; Shroff *et al.*, 1999). A high sensitivity gel purification assay revealed that essentially all detectable pDNA in vaccinated cells was extra-chromosomal and the integration frequency (1 in 150000 diploid cells) was far below the spontaneous mutation rate (Henke, 2000). Plasmid DNA vaccine can be amplified in the well studied gram negative *Escherichia coli* bacteria and is also easy to construct due to its small size (1-100kbp) (Corey, 1999; Genton, 2008). It also obviates the need for high cost peptide synthesis, expression and purification of complex proteins and use of toxic adjuncts. Generally, it only takes about one week from bacterial transformation to plasmid purification as compared to nine weeks using the conventional fertilized eggs and it eliminates the costs related to longer processing times. Plasmid DNA vaccine purification has been widely studied and many techniques are available to prepare a high grade endotoxin free pDNA vaccine (Zhang *et al.*, 2005; Magalhães *et al*., 2007). Plasmid DNA is stable under variable temperatures therefore; it is easily stored and transported since a cold chain may not have to be maintained. All of these factors contribute to the cost effectiveness of pDNA vaccines.

PLASMID DESIGN

Effect of Replicon, Promoter and Marker

The first step in ensuring the success of DNA vaccines is to maximize the potential components in pDNA (Figure 2). All elements in pDNA serve as a cloning vehicle for a gene of interest (Shroff *et al.*, 1999). Plasmid DNA vaccines should contain necessary elements for maintenance and propagation in the bacterial hosts (selectable marker, origin of replication ORI) and for expression of antigen genes in human recipients (promoter, gene of interest, polyadenylation/terminator) (Garmory *et al.*, 2003; Prather *et al.*, 2003). Other genes that engage the immature immune system in infants may also be included. However, it is strictly necessary to avoid sequence homology to human genome or any biological significance (WHO, 2007). Plasmid DNA should also be designed to be as small as possible (1-100kbp) in order to avoid extra metabolic burdens on *E. coli* host which may reduce the resources for plasmid replication and cell growth (Huber *et al.*, 2008).

Most scientists from the academic/research institutions and manufacturing companies have settled on the Co1E1-type of plasmid as the base replicon/vector for their DNA vaccine and gene therapeutic drug production (Prather *et al.*, 2003). This naturally occurring plasmid (Co1E1) was found to localize as a cluster on one or both of the *E. coli* cell poles. Other

plasmids which were also found such as F, P1, R1 and R27 were located at quarter- or mid-cell positions near the cell pole (Yao *et al.*, 2007). They have been modified and derived into many successful plasmids that have better copy numbers and overall plasmid yields.

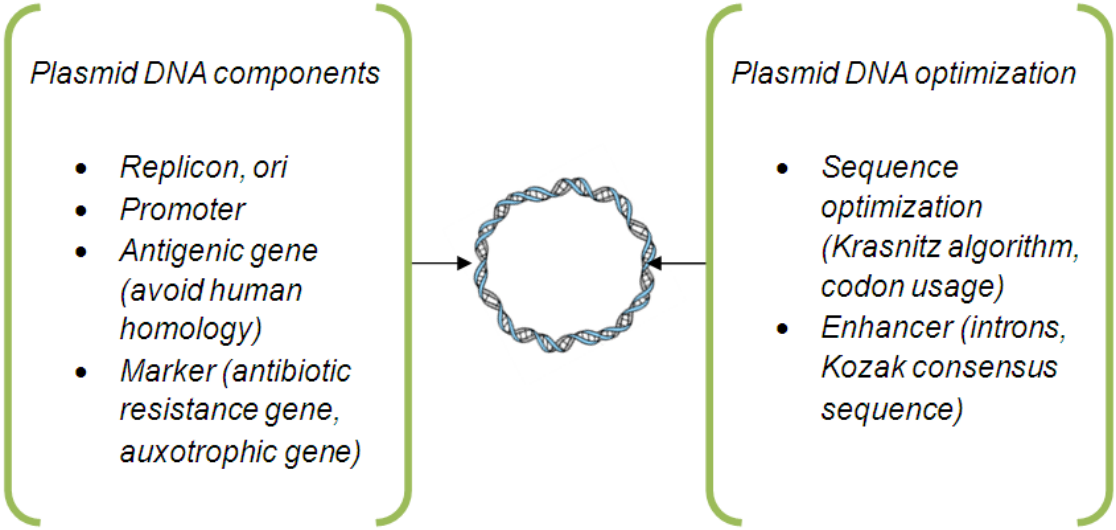

Figure 2: Fundamental plasmid DNA vaccine construction and optimization.

One of the first successful plasmids, pAT153 was found to exclude Rop/Rom gene from pBR322 and exhibited 1-150 copy numbers per cell. pUC18 and pUC19 were also constructed without Rop/Rom protein but with much better copy numbers (Prather *et al.*, 2003).

The negative control of plasmid replication is actually mediated by the stabilizing interaction between two RNA molecules (RNAI and RNAII). The activity of these RNAs is aided and enhanced by Rop/Rom protein by increasing the affinity between the two complementary RNAs (Castagnoli *et al.*, 1989). The removal of Rop/Rom gene has become an attractive choice to increase plasmid yield since the use of chemical enhancers such as chloramphenicol and rifampicin has been banned from pharmaceutical products (Prather *et al.*, 2003). Although high copy number plasmids are widely used as DNA vaccines, some low copy number plasmids can still have high plasmid yields when induced by a temperature shift ($32^{o}C - 42^{o}C$). This results in the loss of replication control and accumulation of up to 1000 plasmids per cell (Remaut *et al*., 1983).

The rate of transcriptional initiation is increased by the use of strong promoters such as virally derived promoters or eukaryotic promoters. SV40 promoter which is derived from the Simian

virus was conventionally used until it was found that Rous Sarcoma virus promoter (RSV) gave a much higher plasmid yield than SV40. The most currently used promoters are derived from Cytomegalovirus (CMV) and are able to direct the highest level of recombinant gene expression in eukaryotic systems. The choice of promoters may also depend on the target antigens. In the case of a Hepatitis B vaccine, the desmin promoter which controls the expression of protein desmin, has successfully been used to drive the expression of Hepatitis B surface antigens (Garmory *et al.*, 2003).

A specific marker is needed to provide means of identification of plasmid DNA carrying the gene of interest. One method is by incorporating an antibiotic resistance gene into the plasmid. Since the use of beta-lactams (e.g. ampicillin) resistance gene is precluded for human use, one should rather select aminoglycosides (e.g. neomycin, kanamycin) resistance gene (Garmory *et al.*, 2003; Prather *et al.*, 2003; Shroff *et al.*, 1999). The use of antibiotic resistance genes as selection markers may impact on the process economics considering the cost of antibiotics for a large-scale plasmid manufacturing facility. Therefore, a concept for antibiotic free plasmid selection has been developed. This method is based on the host encoded growth inhibitor (gene murA). If plasmid DNA is present in the host system, the copy number controlling RNAI will inhibit the expression of murA and ensure a positive cell growth (Huber *et al.*, 2008). The polyA gene such as the bovine growth hormone (BGH) and SV40 provide stabilization of mRNA transcripts. It is also possible to insert a second SV40 promoter downstream of the SV40 polyA sequence to construct more efficient vectors.

Effects of Codon Usage and Kozak Sequence

Another approach to improve DNA vaccine expression is by optimizing the codon usage of antigenic mRNAs for eukaryotic cells. There are 4 types of nucleotides in DNA and 64 possible triplets encoding 20 amino acids. Due to this variance, 18 amino acids are often encoded by more than one triplet. Eucaryotic organisms often show a particular preference for one codon for an amino acid. Substituting these wild type codons with codons mostly expressed in human genes will improve the expression of DNA vaccines in antigen presenting cells (Garmory *et al.*, 2003; Ko *et al.*, 2005). How these enhancing effects prevail is still a much debated topic in molecular biology. A much better codon optimization scheme can be achieved using the Robins-Krasnitz algorithm method. Instead of replacing wild type amino acid codons with codons from human genes, the Robins-Krasnitz algorithm finds short codons in human genome that are independent of amino acids and codon usage. For example,

the triplet AGG is more frequently found in HIV than in human genome. Recoding the HIV ORFs gene by reducing the occurrences of single triplets, AGG, improves the immune response to an HIV DNA vaccine in a mouse model (Huang *et al.*, 2008). The inclusion of a Kozak consensus sequence has been found by many researchers to improve the expression initiation of DNA vaccines. In a study on HIV DNA vaccine, a Kozak sequence was located immediately upstream of the initial ATG and was cloned into NotI and XbaI of the pVAX1 (Invitrogen) vector. This resulted in an improved expression compared to a wild type initiator sequence (Huang *et al.*, 2008). In another study on animal DNA vaccines, a Kozak sequence which was inserted into two types of pUC vectors significantly increased the *in vitro* expression of HAS gene in primary horse cells derived from skin, lung, duodenum and kidney (Ólafsdóttir *et al.*, 2008). Other enhancers such as CMV intron A may also improve the level of transgene expression by the CMV promoter. This is attributed to the enhanced rate of polyadenylation and mRNA stability (Garmory *et al.*, 2003).

Antigenic Gene Selection and CpG motif

The ultimate goal of DNA vaccines is to elicit immune responses specifically against the antigenic transgene. Two of the greatest hurdles in developing vaccines are the high mutation rate and existence of diverse virus strain isolates. Therefore, careful selection of DNA vaccine targets is very crucial. In developing candidate vaccines against HIV-1, the relative immunogenicities of individual HIV-1-derived vaccine antigens (Env, Gag, Pol, Nef, Tat and Vif) were studied followed by two, three and four combined vaccine antigens. The CTL responses were widely varied whether the antigen was expressed individually or as part of a fusion protein (Luckay *et al.*, 2007). To develop a safe and effective DNA vaccine against Measles challenge, it is necessary to determine the specific immune response elicited by hemagglutinin (MV-H) and fusion (MV-F) antigens individually and when combined (Song *et al.*, 2005). The most reasonable malaria vaccine will require the expression of multiple proteins from different phases of the life cycle of the malaria parasite. One way of doing this is by constructing a bicistronic pIRES (Clontech) plasmid vector encoding the AMA-1 (Ser 22-to-Gln 479) ectodomain of *Plasmodium chabaudi adami* DS fused into a tissue plasminogen activator (TPA) secretion signal in the first position of the vector. The gene encoding MSP4/5 (Met 1 to Ser 190) of *Plasmodium chabaudi adami* DS is then fused into the monocyte chemotactic protein 3 (MCP-3) DNA coding site in the second position of the vector (Rainczuk *et al.*, 2004). By doing systematic screenings, scientists will be able to

understand and direct specific immune responses for better protection against hard-to-fight diseases.

The recognition of unmethylated CpG dinucleotides of bacterial DNA in particular base contexts (CpG motif) is known to be the first line of mechanism used by human immune systems to detect the presence of microbes or viruses and has been included in DNA vaccines for more than a decade (Hartmann and Krieg, 2000). The addition of CpG motifs in DNA vaccines has been shown to increase IL-12 mRNA expression in draining lymph nodes and enhance Th-1 based microenvironment (Liu *et al*., 2005). A newly found CpG motif has strongly stimulated primary human B cells to express high levels of CD86, CD40, CD54 and MHC-II and was associated with the sustained induction of NF-kBp50/p65 heterodimer and transcription factor complex AP-1 (Hartmann and Krieg, 2000). A number of factors can influence the success of CpG DNA vaccines including number of CpG motifs inserted, site of insertion of CpG motifs, up-take rate and adjuvanticity of unmethylated CpG motifs (Coban *et al*., 2005). Naked plasmid DNA, even if it contains CpG motifs, is still susceptible to degradation via the endososomal degradatory pathway leading to a poor level of gene expression. To overcome this problem, CpG-modified plasmids can be packaged into fusogenic liposomes (FL) derived from conventional liposomes and Sendai virus-derived accessory proteins. It was found that CpG DNA vaccine fused into FL enhanced ovalbumin (OVA)-specific T cell propagation and CTL induction post vaccination (Yoshikawa *et al*., 2006).

FERMENTATION

Process development of large scale pDNA production and purification to meet product specifications and regulatory standards is a challenge. Factors such as purity, potency, identity, efficacy and safety related to the intended therapeutic use have to be taken into consideration when designing each unit operation as these will directly influence the immunogenicities of the DNA vaccines produced. General steps involved in pDNA production are fermentation, primary isolation and purification (Prazeres *et al.*, 1999). Figure 3 shows the basic unit operations involved in a typical pDNA vaccine manufacturing plant. Fermentation strategies and medium designs are known to have profound effects on pDNA yields (Carnes, 2008; Wang *et al.*, 2001). The required principles for high quality and high yield plasmid production are the use of a defined growth medium, employing a fed batch feeding strategy and allowing the cells to grow at a reduced growth rate that promotes

plasmid replication (Listner *et al.*, 2006). The use of a semi defined medium can also provide a relatively high plasmid yield especially in fed-batch fermentations (Carnes, 2008; Danquah *et al.,* 2007a). It is speculated that the mechanisms that contribute to an increase in plasmid yield are reduced metabolic burden during plasmid synthesis; reduced plasmid mediated protein production and altered DNA compaction during plasmid induction. Current top plasmid DNA productions are shown in Table 3.

Growth Media Formulation

Cultivation medium for *E. coli* growth and protein production is well established and widely available. It is important to note that like chromosomal DNA, plasmid DNA is made up of sugar-phosphate backbone and nitrogen based nucleotides (ATGC). Sugar, phosphorus and nitrogen are the main ingredients in pDNA biopolymers. Thus, the cultivation medium for pDNA production in *E. coli* is substantially different from those used for the production of other biomolecules such as antibodies, hormones and glycoproteins (Danquah *et al.*, 2008c). Medium design also has a higher impact on pDNA yield compared to using different plasmid strains. To compliment with metabolic engineering study or quality control, it is preferable to consider a chemically defined medium. A defined medium that promotes plasmid DNA synthesis should also support higher plasmid stability up to 63% as compared to complex media (Prather *et al.*, 2003). A growth medium for pDNA vaccine production should not cause major problems during downstream processing and it should meet regulatory requirements (WHO, 2007). The use of animal-derived products for plasmid production should be avoided to eliminate the risk of adventitious agent contamination (Carnes, 2007).

The presence of antibiotics in the medium does not complicate the process since it is easily removed during the cell concentration process. However, the use of antibiotics may pose an economic challenge during large-scale production (Prather *et al.*, 2003). The first step in achieving an effective medium formulation is to identify the desired nutrient that is limiting. The culture media should be designed to support high pDNA quality, high specific pDNA yield, high biomass yield, and reduced cell growth rate (Carnes, 2007). Inorganic nitrogen sources such as ammonia and ammonium salts are important to support high plasmid yields and are included in a defined media. More complex components such as yeast extract, peptone and casamino acids are usually included in semi defined and complex media (Carnes, 2008; Nan *et al.*, 2005). Unlike yeast extract, tryptone is carbohydrate-deficient and is very useful when establishing the consumption rate of an already established carbon source

(Filomena *et al.*, 2009). According to Saldanha *et al.*, (2004), when a medium lacking in tryptophan is prepared and different known concentrations of the nutrient are added each time, the final *E. coli* density is proportional to the amount of added tryptophan at low concentrations but is not significantly affected at high concentrations. It has also been reported that a high pDNA specific yield of ~ 20.43 mg/g DCW can be achieved using a low tryptone concentration of ~0.5 g/L at 37^{o}C (Filomena *et al.*, 2009).

Another approach to nutrient evaluation is by using statistical methods particularly the experimental design and response surface methodology to systematically formulate and optimize a defined medium (Ongkudon *et al.*, 2006). In this method, a series of potential nutrients is varied in concentrations and tested in different combinations. After analysis, a few nutrients are identified and further studied by using central composite experiments to gain a better understanding of the effects of nutrient on product yield (Ongkudon *et al.*, 2005). Glycerol can be employed as a carbon source to replace glucose in fed-batch cultivation and to adjust the *E. coli* growth rate conducive for plasmid DNA replication. It has also been suggested that C:N ratio might affect the pDNA yield (Córdoba *et al.*, 2008). O'Kennedy *et al.,* (2000) found that an optimum C:N ratio of 2.78:1 affected the physiology of the microbes and promotes plasmid DNA synthesis. Our research group (BEL, Monash University, Australia) has designed a cost effective semi defined medium PDMR for industrial scale pUC-based plasmid DNA production.

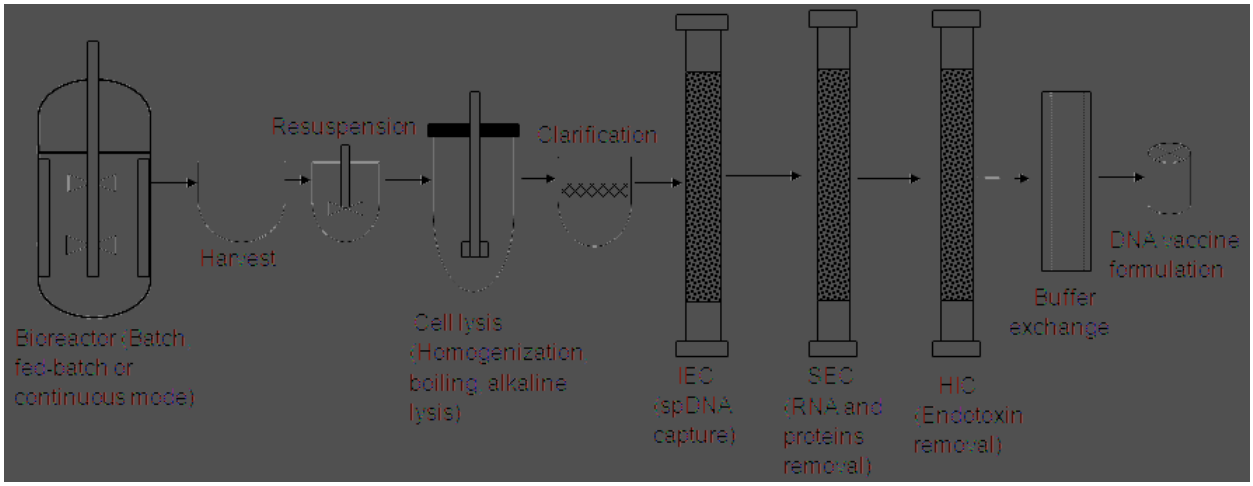

Figure 3: Typical unit operations involved in plasmid DNA production. IEC–Ion exchange chromatography column. SEC–Size exclusion chromatography column. HIC–Hydrophobic interaction chromatography column.

Table 3: Current top plasmid DNA production

Reference	Process type	Plasmid	Cell conc (gDCW/L)*	pDNA vol. yield (mg/L)	pDNA specific yield (mg/gDCW)
Danquah *et al*., 2008a-c	Batch Fed-batch	pUC19	4 11	63 530	17 49
Listner *et al.*, 2008	Fed-batch 1st generation 2nd generation	pV1Jns	 21-23 38-41	 500-750 1000-1600	 24-33 26-39
Carnes *et al.*, 2006	Batch Fed-batch	pW2.0 pBR322 gWiz GFP pNTC7264-hmPA-EGFP	29 61 49 43	230 438 1070 1497	8 7 22 35
Filomena *et al*., 2008	Shake flask	pVAX1-LacZ	5	100	20
Carnes *et al*., 2008	Fed-batch	gWiz-GFP	22	1100	50
Phue *et al*., 2008	Fed-batch	pVRC5737Ap	94	1923	21
Williams *et al*., 2009	Fed-batch	pNTCUltra1	44	2220	51

*DCW estimation (OD600nm = 100 correspond to 50 g DCW).

This medium was developed based on elemental balances and stoichiometric analysis of the major nutrients in yeast extract, tryptone, glucose, $Na_2HPO_4.7H_2O$, KH_2PO_4, NH_4Cl and $MgSO_4$ (Danquah *et al.*, 2007a, Wang *et al.*, 2001). Nan *et al.* (2005) designed a medium MMBL (for *E. coli* BL21) that supports high plasmid volumetric yield and specific yield of 58.3 mg/L and 37.9 mg/g respectively. This medium was composed of 5.0 g/L glucose, 15.0 g/L yeast extract, 2.0 g/L phosphate salts and less than 3.0 g/L acetate.

Cultivation Method

Controlled Parameters

High growth rates have always been correlated with acetate production, plasmid instability, and low yield of supercoiled pDNA (Carnes, 2007).The strong correlation that exists between pDNA yields and cell growth rates has become a key principle in maximizing pDNA production. Co1E1 type plasmid copy number varies inversely with *E. coli* growth rates which signifies that the pDNA yield is increased when the cell is grown at reduced rates and *vice versa* (Filomena *et al.*, 2009; Prather *et al.*, 2003). Schmidt *et al.*, (2003) obtained a supercoiled pDNA yield of 225 mg/L when employing a growth rate of 0.15/hr in a fed batch culture. It is presumed that a reduced growth rate supports growth-dependent plasmid production by synchronizing the time for plasmid replication and cell division (Carnes, 2007). There are different methods that can be employed to achieve reduced growth rates and maximize pDNA yields. One of these methods is the novel temperature shift technique. It has been found that pUC ori sites have high copy numbers and are temperature sensitive (Danquah *et al.*, 2008c). Temperature shift induces plasmid replication and reduces contaminating RNAs and gDNAs synthesis rates by down regulating the growth rate of the cells (Prather *et al.*, 2003; Prazeres *et al.*, 1999). In a study by Filomena *et al*. (2009), *E. coli* DH5α cells bearing the pVAX1-LacZ plasmid were grown at 30, 32, 37, and 40^{o}C. Higher pDNA specific yields (4.60 and 5.56 mg/g) and purity degrees (35.68% and 45.72%) were obtained at 37 and 40^{o}C respectively. Cells grown at 37 and 40^{o}C were found to exhibit a filamentous morphology in which cells elongated and replicated their DNA without being separated. Therefore, the enhanced plasmid amplification induced by the temperature-growth shift may be explained by the inhibition of cell wall synthesis leading to filamentation and reduced cell growth. Carnes *et al*., (2006) suggested that temperature shifts should be performed from 30 ^{o}C to 37 ^{o}C or 42 ^{o}C at OD_{600} = 60 to increase the plasmid copy number prior to harvesting the culture.

Another approach has been introduced by Carnes, (2008) using the temperature induced fed-batch fermentation method. After the cells reached OD_{600} = 75, the culture was cooled down to a temperature between 15 and 25°C for 30 minutes in order to stop the accumulation of biomass. The cooling period enabled the pDNA yield to increase by 29% (814 mg/L) compared to 663 mg/L when the cooling step was excluded. Based on these findings, it can be hypothesized that by incorporating a cooling step at the end of a fed-batch phase, the cells are driven to its maximum potential plasmid copy number which may not be possible at higher temperatures. Other factors that can regulate cell growth such as dissolved oxygen (DO) concentration and antibiotics also need to be investigated when designing an optimum process for pDNA production. Dissolved oxygen concentration (DOC) also can act as a probe to detect nutrient deficiency especially in fed-batch fermentations (Prather *et al.*, 2003). It has been shown that under a sufficient oxygen supply, cells are able to achieve higher densities. Additionally, the amount of DO in the culture can be altered to support both high cell densities and pDNA yields (Chen, 1999)**.** Passarinha *et al*., (2006) obtained higher specific plasmid concentrations under low DOC compared to those obtained at higher DOC as a result of decreased growth rate. Higher specific yield also means higher pDNA purity due to reduced amount of materials to be processed. In a study by Passarinha *et al*., (2006) using ColE1-type plasmid (pVAX1-LacZ) and DH5α host strain as a model, it was found that under an oxygen limitation (5% DOC), the specific growth rate was half the value obtained when an antibiotic was present in the medium. At 60% DOC, the specific growth rate of 0.7/h was independent of the use of antibiotic. Generally, the control of a dissolved oxygen level in a standard bioreactor can be achieved by the cascade control of the agitation speed and oxygen enrichment in air supply whereas the airflow rate is maintained the same.

Batch Mode

The most commonly used bacterial fermentation method for pDNA production is the batch method owing to its flexibility in controlling the production of pDNA. Recently, continuous cultures have successfully been employed for bench top and pilot scale pDNA production. Batch cultures have predominantly been used to initiate the preliminary phase of fed-batch and continuous cultures (Carnes, 2008; Carnes *et al.*, 2006; Listner *et al.*, 2006). Simplicity is the key to batch fermentation because all of the nutrients required for growth are present at the time of inoculation and modeling issues related to batch cultures are rather straight forward compared to fed-batch and continuous cultures. The growth profile for a batch culture which consists of a lag phase, an exponential growth phase and a stationary phase can be adequately represented by the Monod equation and the logistic equation (Shuler *et al.*, 2002)**.**

As discussed earlier, a reduced growth rate is strongly correlated to an increased plasmid specific yield (Filomena *et al.*, 2009; Prather *et al.*, 2003) and this can be achieved in a batch fermentation by using a lower growth temperature (e.g. 30^{o}C) (Carnes, 2008). A medium design that supports high plasmid specific yields can also be incorporated into batch fermentation although this may result in reduced total cell density or poor plasmid volumetric yield. To maintain high cell density and pDNA volumetric yield at reduced growth rates, glycerol can be used as a carbon source at higher concentrations than glucose without causing any inhibition (Carnes, 2007). Depending on the type of plasmid host and vector used, cell densities of 4 to 29 gDCW/L can be obtained in batch fermentation with plasmid specific yield of 8-17 mg/g (Table 3).

Fed-Batch Mode

Production of extended cell density and growth-related pDNA yield can be achieved in a fed-batch culture by expanding the cultivating time. Cell density of 10 gDCW/L and pDNA volumetric yield of 500 mg/L were obtained in a fed-batch fermentation of *E. coli* DH5α-pUC19 during 10-30 hr of cultivation (Danquah *et al.*, 2008c). Listner *et al.,* (2006) obtained a cell density and pDNA yield of 50 gDCW/L and 1200 mg/L respectively using different *E. coli*-bearing HIV DNA vaccine constructs in 20-48 hr of extended cultivating time. In another article, it was reported that an outstanding pDNA yield of up to 1500 mg/L (cell density = 43 gDCW/L) was obtained using *E. coli*-pUC host cells and employing an inducible fed-batch (15-45 hr) method (Carnes *et al.*, 2006). The multi-fold high pDNA yields in high cell density cultures poses major concerns such as accumulation of byproducts (e.g. toxins and proteins) as well as possible loss of supercoiled pDNA integrity (Carnes *et al.*, 2006; Prather *et al.*, 2003). To address this problem, the first stage of a cultivation may be initiated at 30 ^{o}C to reduce the accumulation of unstable plasmids and followed by a temperature shift (37 or 42^{o}C) after a suitable biomass concentration is achieved. This will help with the amplification of healthy cell lines and in the reduction of metabolic burdens imposed by plasmid mediated transcriptions during fermentation. The amplification of plasmid copy number during the temperature shift and shortly before the harvest should also help maintain high plasmid integrity and stability (Carnes *et al.*, 2006). Fed-batch production of pDNA can be categorized under fixed-volume and variable-volume. The former means that a limiting substrate is fed as a very concentrated liquid (100-200 g/L) and the latter indicates volumetric changes over time due to addition of diluted substrates. Fed-batch mode has been an important technique in *E. coli* fermentation and has many advantages over batch mode (Shuler *et al.*, 2002)**.**

The main advantage of using fed-batch mode for pDNA production is that the accumulation of by-products or metabolic repressors is limited due to the controlled provision of substrates (e.g. glucose, phosphate and oxygen) conducive to pDNA formation and cell growth (Prather *et al.*, 2003). Apart from the extension of working time and controlled provision of substrates, fed-batch automation mode requires no additional special piece of equipment as compared to the batch mode of operation. It allows the provision of a correspondent antibiotic to increase the antibiotic-marked plasmid stability during fermentation. A good fed-batch fermentation practice is based on the supplementation of a substrate at a rate such that it is completely consumed. The fermentation begins with a batch mode under non-limiting conditions and an optimum growth rate. When one or more substrates are exhausted which normally occurs at the late exponential phase, the batch mode is then switched to fed-batch mode (Carnes, 2008; Park *et al.*, 2004).

There are two reliable approaches that can be incorporated to synchronize between the substrate feed and demand if real time measurement of the medium substrate is not possible. The first strategy is an open-loop control scheme where the feeding rate is controlled based on previously established data or fixed model (Furuichi *et al.*, 2007). The feeding strategy for an open loop control scheme may consist of constant, linear and exponential feeding rates (Carnes *et al.*, 2006). In the cultivation of *E. coli*-bearing HIV DNA vaccine constructs, a 75% (w/v) glycerol feed solution was initiated at a rate of 42.9 g min^{-1} during the batch-fed-batch transition. The feeding rate was linearly amplified to 171.5 g min^{-1} during the first 5 hr of the fed-batch phase. The feeding rate was then maintained at 171.5 g min^{-1} until the end of the fed-batch phase where cell growth began to decline. A maximum cell concentration of 41.0 gDCW/L was achieved when a glycerol feeding rate of 7.2$gL^{-1}h^{-1}$ was employed (Listner *et al.*, 2006). Meacle *et al.,* (2007) has designed a combination of exponential glucose feeding (40%) and linear amino acids feeding to attain a cell-carrying plasmid growth rate of 0.1h^{-1}. The exponential feeding was introduced during 15.5-19.5hr and amino acids were fed at 20.5-35hr of the fermentation process. The second fed-batch feeding scheme is known as the indirect control of substrate feed based on on-line physiological parameters such as pH, dissolved O_2 and cell concentration. As a rule of thumb, a nutrient solution is fed when the DO rises to 50% which indicates a decrease in the cellular activity or when the pH rises to 7.2 which indicates a glucose constraint (Park *et al.*, 2004; Prather *et al.*, 2003). Schmidt *et al.,* (2003) describe the DO feedback-control (DO-stat) by using glycerol and yeast-extract as the feed medium to produce up to 230mg/L of plasmid. A rational equation based on the biomass yield coefficient $Y_{X/S}$ (g DCW/g substrate) may be employed for a better control of the

substrate feeding. The initial feed rate (F_o) is given as $F_o = \mu.V_{b.}\ X_b\ /S_{fo}.Y_{S/X}$ where μ is the specific growth rate, V_b is the volume of the culture, X_b is the amount of biomass produced, S_{fo} is the amount of substrate consumed, and $Y_{S/X}$ is the yield coefficient. $Y_{S/X}$ (g/g/h) = r_X/r_S where r_X is the volumetric rate of biomass production and r_S is the volumetric rate of substrate consumption (Thatcher *et al*., 1999). After every two hours, the feed rate needs to be adjusted based on the total biomass produced and total substrate consumed to compensate for the exponentially increasing demand for substrate.

Continuous Mode

Continuous culture or often referred to as chemostat (i.e. perfusion in animal cell culture) is of particular interest in the highest throughput process (Mutschlechner *et al.*, 2000). It enables the cells to grow at a constant density and growth rate exclusive to pDNA production at a much longer working time than in batch and fed-batch cultures. Continuous steady state cultures at a constant cell density of 30 g/L DCW and a dilution rate of $0.2h^{-1}$ can produce four times the amount of cell mass in 20 hours at a reduced growth rate as compared to the same duration in batch culture (Carnes, 2008). In pDNA production, continuous cultures may often fail to prevail due to a drop in copy number and plasmid integrity over a long run which signifies that the cells are not starving but have become unstable (Saldanha *et al.*, 2004). Problems such as mechanical failures and contaminations also need to be given a greater emphasis when running a continuous culture.

POST FERMENTATION

In a large scale production, cell harvest and concentration can affect the intact structure of supercoiled pDNA. A study shows that cells harvested and concentrated using a disc stack centrifuge suffer from membrane disruption and subsequent degradation of released materials. Cells harvested using solid bowl centrifuge and processed within 2 hours at below 13^oC retain the highest supercoiled pDNA. The extra holding time required in achieving a large homogenous cell suspension may lead to extended enzymatic reaction and reduced intact supercoiled pDNA yield (Kong *et al.*, 2008). Thus, the isolation of supercoiled pDNA from other impurities needs to be carefully designed to attain a maximum amount of supercoiled pDNA in the final bulk.

There are several methods for cell disruption and each contributes significantly to the final supercoiled pDNA yield. Thermal based cell disintegration uses lysozymes to break down cell membranes upon boiling thus releasing plasmid DNA. Undesired DNAs and proteins are

precipitated during the heat step. This method requires a very fine tuning of the heating step and uses large heat exchangers in a large scale production. The use of lysozymes does not lead to product degradation but poses safety issues regarding the use of animal-derived components (Prather *et al.*, 2003). Mechanical cell lysis is usually applied in a continuous process of protein production. A homogenizer can be run at set temperature and pressure, and repeated passes can also be conducted in order to obtain a complete cell rupture under minimal product degradation. The use of a homogenizer however, does not seem to be feasible since plasmid DNAs are highly sensitive to shear forces greater than $10^4 s^{-1}$. An HPLC analysis shows that the shear forces during homogenization result in smaller fragments of gDNA and damaged pDNA which may complicate the downstream column elution (Urthaler *et al.*, 2007). Chemical (or Alkaline) cell lysis seems to be the most reliable technique for shear sensitive supercoiled pDNA production even in a large continuous process. Alkaline lysis results in the release of intracellular materials and upon neutralization leads to the precipitation of proteins and gDNAs (Prather *et al.*, 2003). The use of NaOH in a large continuous cell lysis process will require optimizations of the mixing procedure, contact time and holding time in order to achieve the desired release of intact supercoiled pDNA (Urthaler *et al.*, 2007; Urthaler *et al.*, 2005b).

PLASMID DNA PURIFICATION

The clarified lysate from cell lysis typically contains fragmented gDNA, endotoxins, proteins, RNA and nicked pDNA along with the supercoiled pDNA (Danquah *et al.*, 2007b). The major bottleneck in pDNA purification is poor selectivity because most of the impurities share common features with the supercoiled pDNA such as electronegativity (Sousa *et al.*, 2008). Conventional plasmid purification using chloride/ethidium bromide ultracentrifugation is not scalable because of hazardous materials although it is still used as a purity benchmark for plasmid DNA. Other methods such as selective precipitation, aqueous two-phase separation and tangential flow filtration have some drawbacks such as low purification effect, need for dedicated equipments, time consuming and not scalable (Levy *et al.*, 2000; Stadler *et al.*, 2004; Urthaler *et al.*, 2005a). However these methods are commonly used in the intermediate purification of plasmid DNA. Commercial benchtop purification kits such as Promega miniprep and Qiagen miniprep use alkaline lysis and disposable chromatographic columns which are not scalable and large amounts of resins and enzymes are employed (Prather *et al.*, 2003). Chromatographic technique however, is the most reliable and widely applied method due to its ability to exploit the size, charge, hydrophobicity, nucleotide accessibility and affinity of pDNA (Sousa *et al.*, 2008). When developing a large scale pDNA

chromatographic process, the design aims at volume reduction, achieving a high flow rate, attaining a better resolution and higher capacity. These will have significant impacts on the equipment design, amount of liquid used, man hours and overall economics (Stadler *et al.*, 2004).

Currently there are many companies that produce high grade plasmid DNA utilized in phase I, II, and III clinical trials. Proprietary purification procedures were specifically designed for scale up and regulatory conformance. Boehringer Ingelheim (Austria) and BIA Separations (Slovenia) have developed a novel process involving three chromatographic steps (HIC, AIEX and SEC) and using this combination they produced more than 98% of supercoiled pDNA (Huber *et al*., 2008). VGTC (China) also uses several chromatographic separation steps to achieve ultrapure supercoiled pDNA. Recent advancement in plasmid purification also involves the development of a chromatography support which provides higher capacity and flowrates at lower pressure drops compared to the particle-based systems. Prometic Biosciences Inc. (USA) and Boehringer Ingelheim (Austria) have designed their own proprietary columns (Perfluorosorb® and convective interactive media CIM® respectively) that are chemically stable and have high functionalized-resin retention. This would ensure that the final bulk of DNA vaccines are not contaminated by resin wash-outs which would otherwise become unsafe for *in vivo* application in human. Pall (USA) and Sartorius Stedim (Germany) designed membrane based techniques for plasmid purification and endotoxin removal. These technologies including Mustang Q (Pall) and Sartobind Q (Sartorius Stedim) are anion-exchange membrane supports that provide ease of handling and high dynamic binding capacities at exceptional high flow rates.

Chromatographic Adsorbents

An effective chromatographic medium for the purification of pDNA must allow variable flow rates under reasonable pressure drops. Conventional chromatographic medium is prepared by packing a column with microbeads/microparticles. Smaller proteins are normally adsorbed on the inner surface of the particle micropores (2-50nm) as well as the outer surface of each particle. Large pDNA molecules (>100nm) which are unable to pass through these micropores are only adsorbed on the outer surface. Consequently, column capacities are significantly reduced for pDNA compared to proteins. Increase in flowrate for particulate columns results in higher pressure drop as well as low plasmid purity (Danquah *et al.*, 2007a, 2008b; Sousa *et al.*, 2008; Urthaler *et al.*, 2005a). Single macroporous monolithic support and adsorptive membranes are regarded as high performance materials and an advanced

technology that can be used in dealing with problems of low capacity (Sousa *et al.*, 2008). In monolithic supports, band resolution is broadened by multiple flow paths, slow equilibration of solutes between the mobile and stationary phase as well as solute diffusion in the mobile phase. Larger pore-skeleton size ratio can support high permeability, high column efficiency and high performance close to ultra high performance liquid chromatography UHPLC (Tanaka *et al.*, 2003). Monolithic supports also provide high convective flow rates under low pressure drops through its large pores thus boosting the high throughput pDNA purification process (Danquah *et al.*, 2007b). Problems that are often related to the formation of a monolith are polymerization temperature, pores homogeneity, monolith stability and durability (Danquah *et al.*, 2008b). The search for advanced and super durable materials in monolith synthesis is still ongoing. Materials that have high chemical resistance, solvent resistance and high tensile strength may eventually become the materials of choice in a large commercial scale plasmid DNA production.

The 8000 ml CIM DEAE (diethyl amino ethyl) monolithic column by Boehringer Ingelheim (Austria) is currently the largest commercially available chromatographic medium that can produce up to 15g of purified pDNA. The advantage of using this monolith is that only a small elution volume (5 column volumes) is required and the resulting pool contains highly concentrated pDNA (Urthaler *et al.*, 2005a). Polymethacrylate polymer has been shown as an attractive monolith material due to its flexibility and ease of pore formation. Macroporous polymethacrylate possesses persistent porous structures even in the dry state (Danquah *et al.*, 2007c). They contain epoxy groups which can be functionalized with ionic, hydrophobic and affinity ligands. A method for producing large volumes of methacrylate monolith with homogenous pore sizes has been introduced using the thermal expulsion technique (Danquah *et al.*, 2008a). A customarily-made DEAE-functionalised polymethacrylate monolith proved to be very stable with persistent binding capacity after several uses for plasmid purification (Danquah *et al.*, 2007c).

Chromatographic Techniques

Four main types of liquid chromatographic techniques that have been widely used in pDNA purification either as a single-step or multiple-steps process are size exclusion, anion exchange, affinity interaction and hydrophobic interaction. Size exclusion chromatography (SEC) is mainly used to separate pDNAs from the bulk RNAs and other smaller molecules present in the clarified lysate (Sousa *et al.*, 2008). Plasmid DNA isolation using SEC is rather limited due to the common characteristics it exhibits amongst its impurities. Due to this, SEC

is usually employed as the last purification step to achieve both buffer exchange and further removal of impurities (Urthaler *et al.*, 2005a). When SEC is to be employed prior to ion-exchange chromatography, a concentration of 0.5M NaCl or 2M ammonium sulphate is required in order to obtain the desired separation of pDNA from other impurities (Stadler *et al.*, 2004).

Supercoiled pDNA has a high negative charge density compared to its counter-isoforms and other impurities (Smith *et al*., 2007). Anion-exchange chromatographic (AEC) purification is based on the interaction between the negatively charged phosphate groups of the plasmid and the positively charged stationary matrix (Danquah *et al.*, 2007c; Sousa *et al.*, 2008). Elution of supercoiled pDNA can be done by size compaction and ionic shield using the right combination of NaCl concentration and flow rate (Danquah *et al.*, 2007b). By gradually increasing the ionic strength of the washing/binding buffer, lower charged impurities will form part of the flow through thus leaving only highly charged supercoiled pDNA on the matrix. However, endotoxins and large RNAs may co-elute with supercoiled pDNA during elution due to their high negative charge thus resulting in low pDNA purity and recovery (Diogo *et al*., 2005, Anspach, 2001). Another limitation of AEC is related to the high salt load during elution which calls for additional steps prior to in vivo administration of pDNA vaccine (Diogo *et al*., 2005). Nonetheless, this technique is considered highly advantageous because of lack of organic solvents, possible in-place sanitation using NaOH and most of all efficient separation of supercoiled pDNA from its lower charged isoforms (Sousa *et al.*, 2008). The leaching of AEC ligands from the polymer matrix is minimal since an ionic ligand density loss of less than 10% after 7 weeks of repeated runs has been achieved (Danquah *et al.*, 2007c). Under optimal conditions, AEC can be used as both single-stage purification and to concentrate supercoiled pDNA solution (Urthaler *et al.*, 2005a). Anion-exchange ligands that are commonly used as functional groups on the epoxy matrix include urea, DEAE and ammonia (Danquah *et al.*, 2007c).

A highly specific chromatographic technique uses specific ligands such as 16-mer or 24-mer proteins and amino acids (e.g. arginine or histidine) to selectively bind supercoiled pDNA (Sousa *et al.*, 2008; Sousa *et al.*, 2009b). This type of chromatographic technique which is known as affinity chromatography (AC) can be run as either a single-stage purification or a polishing step due to its high specificity to supercoiled pDNA (Sousa *et al.*, 2008; Sousa *et al.*, 2009b). Histidine and arginine have shown specific binding to supercoiled pDNA probably because the degree of base exposure in supercoiled pDNA is higher than that in

open circular (OC) and linear pDNA (Sousa *et al.*, 2009a). Major problems associated with AC are high salt (NaCl) gradient required to elute supercoiled pDNA from the high affinity interaction and low recovery (Arakawa *et al.*, 2007). A strategy based on a competitive ligand can be used to tackle this problem. In this method arginine is supplemented to the NaCl elution buffer at an optimized composition in order to achieve 80% supercoiled pDNA recovery as compared to 60% when using NaCl alone (Arakawa *et al.*, 2007; Sousa *et al.*, 2009b). Another drawback of this method is the limitation in regards to the use of animal derived ligands. This problem can be addressed by using synthetic ligands such as synthetic peptides although this process is complex and time consuming. A synthetic 16-mer peptide has shown a high preference for supercoiled pDNA over other plasmid isoforms and requires a low concentration of elution buffer (Han *et al.*, 2008).

Hydrophobic interaction chromatography (HIC) is particularly important when the removal of endotoxins is concerned. This method is based on the differences in surface hidrophobicity of pDNA and endotoxins. Amphiphilic endotoxins typically present a high hidrophobicity due the exposure of their hydrophobic bases whereas pDNA molecules present a low hydrophobicity since the majority of the bases are shielded inside the double helix (Freitas *et al.*, 2009). In pDNA purification, pDNA retention occurs at a high salt concentration due to the displacement of water molecules (Sousa *et al.*, 2008). Thiophilic aromatic ligand in combination with hydrophobic matrix is the method of choice when it comes to selective separation of supercoiled pDNA and endotoxins. In this method, supercoiled pDNAs and endotoxins are bound to a thioether ligand under a high salt concentration. Selective supercoiled pDNA elution can be done by a combination of 2M AS and 1.4M NaCl. Endotoxins typically remain in the matrix and can be washed out during the sanitation using NaOH (Stadler *et al.*, 2004). Under optimised conditions, this method is also capable of separating pDNA isoforms thus producing pure supercoiled plasmid DNA for use in gene therapy and DNA vaccine applications (Lemmens *et al*., 2003). GE Healthcare (USA) has designed PlasmidSelect to selectively purify supercoiled pDNA in a three-process step (removal of RNA, plasmid capture and endotoxin removal). PlasmidSelect is based on a thiophilic aromatic adsorption chromatography support with 2-mercaptopyridine as the functionalised group.

Immobilised Metal Ion Affinity Chromatography (IMAC) can be used to simultaneously remove RNA and endotoxins from the alkaline cell lysate. It was found that RNA and endotoxins bound to IDA-Cu^{2+}, -Zn^{2+}, -Fe^{3+} and –Ni^{2+} whereas pDNA did not interact to any

of the IMAC chemistries (Tan *et al*., 2007). The presence of salt in IMAC enhanced the binding of RNA and endotoxins due to reduced repulsive interaction with IDA-metal ion ligands and improved access to adsorption sites due to salt-promoted molecules compaction (Tan *et al*., 2007b). One precaution that needs to be considered in IMAC is the possibility of ligand leaching although metal chelated IDA was found to be stable up to 5 IMAC recycles (Ma *et al*., 2005).

FORMULATION AND DELIVERY

Challenges in Plasmid DNA Vaccine Delivery

In the early of 1990s, Johnston and co-workers reported that introducing a protein-coding gene into the skin of living mice using a gene-gun could elicit antibody responses against the delivered antigen (Tang *et al.*, 1992). At the same time, several groups of researchers also described the ability of DNA plasmids to drive both humoral and cellular immune responses for protection against influenza virus (Fynan *et al.*, 1993; Ulmer *et al.*, 1993) and human immunodeficiency virus (HIV-1) (Wang *et al.*, 1993) antigens in mice using different formulations and delivery methods. Plasmid based vaccine is a promising new technology for the prevention of cancer, intracellular bacterial and viral infections due to its ability to generate both B-cell and T-cell responses. The first clinical trial of naked plasmid DNA was started in 1993 through intramuscular injection of pDNA encoded with specific anti-Idiotype genes (http://www.wiley.co.uk/genmed/clinical/). Naked pDNA is susceptible to degradation by serum enzymes such as endonucleases, thereby reducing the amount of pDNA that is available in hosts to express the antigen gene. Upon entry into a host cell, the transport of pDNA across cell membranes is limited by its net negative surface charge and large hydrodynamic diameter. In addition to that, one possible mechanism of pDNA uptake is endocytosis, after which the pDNA travels through the endosome-lysosome compartment, where it may be degraded. The acidic condition in endosome promotes acidic hydrolysis and activates the lysosomal enzymes that can rapidly degrade plasmids (Patil *et al.*, 2005; Thierry *et al.*, 2003). Thus, improved pDNA delivery strategies are needed. At present, pDNA-based vaccine deliveries in preclinical and clinical animal studies are achieved by using mechanical (e.g. injection, particle bombardment), electrical (e.g. electroporation), and chemical (e.g. liposomal or polymeric complexes) approaches (Patil *et al.*, 2005). However, despite these efforts, the failure rates of DNA vaccine clinical trials remain high. The recent licensing of several veterinary DNA vaccine products has re-inspirited the DNA vaccine research in humans despite its poor performance in larger animals especially non-human primates and human clinical trials (Kutzler *et al.*, 2008).

Table 4: Methods for plasmid DNA vaccine delivery

Methods of delivery	Features
naked pDNA injection [intramuscular (IM), intradermal (ID) and intraperitoneal (IP)]	▪ Simple and inexpensive ▪ Large amounts of DNA required ▪ Inefficient uptake by cells and limited distribution within tissue ▪ Low transfection efficiency
Particle bombardment (Gene Gun)	▪ DNA-coated beads bombarded to cell membranes ▪ Less amount of DNA required ▪ High transfection efficiency ▪ Limited to local expression ▪ Special device and formulation (gold or tungsten beads) required
Electroporation (EP)	▪ Greatly increases the uptake of plasmid DNA into cells ▪ High transfection efficiency ▪ Special device required ▪ Causes severe tissue damage and high mortality of cells ▪ Limited clinical experience
Microneedle patches	▪ Controlled depth below skin surface for stronger gene expression ▪ Invasive and localized immunization

A primary focus of the delivery systems has been to increase the level of DNA expression and to target its delivery to the appropriate cell type. A summary of the currently used methods for pDNA vaccine delivery is given in Table 4.

Direct injection of naked pDNA is simple and inexpensive, but the amount of uptake and expression is dwarfed by the total amount of plasmid administered (< 0.01% of total) (Manthorpe *et al.*, 1993), and this is due to the high molecular weight and the polyanionic nature of the nucleic acids. Intramuscular injection of naked pDNA resulted in low *in situ* transfection of cells, and several limitations such as distribution of the vaccine solution within the injected tissue, cellular uptake, and intracellular delivery to the nucleus need to be improved (Dupuis *et al.*, 2000). Also on a global scale, unsafe injection practice is a serious issue which has contributed to substantial morbidity and mortality rates. Particle bombardment, which introduce DNA-coated beads (composed of gold or tungsten) at high velocity to penetrate cell membranes or cell walls is widely employed to increase the potency and this method requires 2 – 3 orders of magnitude less DNA compared to direct intramuscular injection (Fynan *et al.*, 1993; Pertmer *et al.*, 1995) . This delivery method has gained popularity in DNA vaccination because limited local expression of delivered DNA (in cells of the epidermis or muscle) is adequate to achieve immune responses. However, since direct exposure of target tissue is required, particle bombardment is limited to local expression and has yet to be widely used systemically (Luo *et al.*, 2000). Electroporation uses electric pulses temporarily disrupt the cellular membrane and physically translocates pDNA into the cell. It was first shown able to increase the *in vivo* gene transfer into the muscle of mice using plasmid DNA as the vector (Aihara *et al.*, 1998). Several studies have shown that intradermal or intramuscular injections, followed by electroporation of the injection sites, resulted in higher transfection efficiency and immune responses in mice and pigs (Bodles-Brakhop *et al.*, 2009; Manoj *et al.*, 2004). However, severe tissue damage and high mortality of cells could accompany electroporation, and this is due to the release of heat during the transfer of electric pulses of high strength into the tissues (Manoj *et al.*, 2004). Although these mechanical and electrical approaches have achieved significant transfection efficiencies, they are considered laborious and invasive for clinical setting.

Plasmid DNA Vaccine Adjuvants

The immune response associated with pDNA vaccination is influenced by the site and mode of immunisation. Various types of carriers such as liposomes, biodegradable polymeric particles, hydrogel, inorganic nanoparticles (Table 5) have been evaluated based on their

ability to improve the efficiency of pDNA vaccines. Liposomes are spherical vesicles composed of natural or synthetic amphiphilic phospholipids, which self-associate into bilayers (Bhattacharya *et al.*, 2009; Felgner *et al.*, 1994; Patil *et al.*, 2005). The potency of liposomes depends on their composition, charge and method of formulation, and can be categorised as conventional liposomes, pH-sensitive liposomes, cationic liposomes, immunoliposomes, and long-circulating liposomes (Bawarski *et al.*, 2008; Smith *et al.*, 1997). However, conventional liposomes prepared with a neutral zwitterionic lipid or an anionic lipid showed low entrapment efficiency for plasmid DNA with a high molecular weight (Lindner *et al.*, 2006). This property was improved by the inclusion of cationic lipids to promote the plasmid DNA condensation by forming lipoplexes and to encourage cellular uptake (de Lima *et al.*, 2001; Felgner *et al.*, 1994; Felgner, 1996; May *et al.*, 2000; Stephan *et al.*, 1996). There are *in vitro* and *in vivo* evidence that cationic liposomes can enhance both humoral and cell-mediated immune responses induced in mice by plasmid DNA immunogens (Canonico *et al.*, 1994; Hofland *et al.*, 1997; Hofland *et al.*, 1996; Perrie Y, 2001). Unfortunately, lipolexes progress slowly in clinical trials because its polycationic nature pronounces the tendency to bind to proteins in serum, thus resulting in the release of the associated plasmid DNA after loss of cationic surface charge (McNeil *et al.*, 2006; Patil *et al.*, 2005). The transfection efficiencies of liposomal systems are significantly lower than those viral vectors. Some *in vivo* studies have revealed that the gene transduction responses obtained by liposomal were transient and short-lived (Liu *et al.*, 1997; Wheeler *et al.*, 1996). The number of gene therapy clinical trials using liposomes as the vector has dropped drastically since 2001 (http://www.wiley.co.uk/genmed/clinical/). Continuing efforts such as incorporating agents to enhance plasmid endosomal escape, peptides to promote nuclear localisation, steric coating to stabilise the vectors in sera and targeting moieties to improve cellular specificity for liposome systems have been summarised elsewhere (McNeil *et al.*, 2006).

In recent years, polymeric particles including natural and synthetic ones are gaining interest as promising controlled delivery systems for introducing pDNA into cells for several reasons including: 1) The ability to protect plasmid payload from extracellular degradation; 2) The ability to accommodate large size plasmids and other immunostimulatory agents; 3) The ability to offer a phagocytosis-based passive targeting to APCs; and 4) The ability to be conjugated with appropriate functionalities to enhance target and uptake (Kang *et al.*, 2005; Nguyen *et al.*, 2009; O'Hagan *et al.*, 2006). The polymer most often utilized in antigen and plasmid encapsulation is polylactide-co-glycolide (PLGA).

Table 5: Plasmid DNA vaccine adjuvants

Vaccine adjuvants	Features
Liposomal systems	▪ High transfection efficiency and immunogenicity ▪ Enhance both humoral and cell-mediated immune responses ▪ Incorporation of cationic lipids can promote condensation and cellular uptake of pDNA ▪ Ineffectiveness in serum ▪ Transient gene expression
Polymeric particles	▪ Protect pDNA from extracellular degradation ▪ Can accommodate larger size plasmids and other immunostimulatory agents ▪ Controlled delivery ▪ Surface can be modified to enhance target and uptake ▪ Cationic polymers can condense pDNA into virus-like sizes to enhance transfection efficiency ▪ Cellular toxicity for certain polymeric materials
Hydrogels	▪ High biocompatibility ▪ Sustained release ▪ Localized gene expression
Inorganic nanoparticles	▪ Increase DNA transfection efficiency up to several fold ▪ Less DNA required ▪ Directed delivery (magnetic iron oxide) ▪ Need biomaterial coating to prevent aggregation and to suppress toxicity

This biodegradable and biocompatible polymer is approved by the US FDA, making it more easily advanced to clinical trials; and its chemical composition, total molecular weight and block length ratios can easily be changed to allow control of the size and morphology of the polymeric carriers. Hedley and co-workers first reported that the plasmid encapsulated in PLGA microspheres can elicit stronger CTL responses after intraperitoneal injection and subcutaneous administration as compared to naked pDNA injection (Hedley *et al.*, 1998). Studies have demonstrated the ability of PLGA to function as an attractive genetic vaccine delivery system (Ando *et al.*, 1999; Jones *et al.*, 1996; Sheets *et al.*, 2003; Stern *et al.*, 2003). However, issues such as an acidic microclimate pH deactivation of supercoiled plasmid and the denature of pDNA due to high shear stresses encountered during the double emulsion fabrication procedure need to be addressed. In response to that, polyethylenimines (PEI)/pDNA complexes were encapsulated in monodisperse PLGA microspheres using ultrasonic atomization to shield pDNA from shear stress and to eliminate organic/aqueous interfaces which is deleterious to biomolecules (Ho *et al.*, 2008). Alternatively, cationic polymers such as poly-L-lysine (PLL) (Zauner *et al.*, 1998), polyethylenimines (PEI) (Goula *et al.*, 1998; Lungwitz *et al.*, 2005), polyamidoamine (PAMAM) dendrimers (Dufes *et al.*, 2005; KukowskaLatallo *et al.*, 1996) and chitosan (Borchard, 2001; MacLaughlin *et al.*, 1998) can be applied as carriers for complexing gene vectors into polyplexes to form defined virus-like sizes. When applied to cells, the positively charged polyplexes will mediate transfection via a multistage process including cationic binding to the negatively charged cell membrane to facilitate entrance into the cytoplasm (Lungwitz *et al.*, 2005; Petersen *et al.*, 2002). As a result, formulated or encapsulated therapeutics have shown to exhibit greater therapeutic efficacy compared to unformulated biomolecules (Pouton *et al.*, 2001). With the assistance of cationic polymers, it is noticeable that transfection activity parallels the membrane toxicity. The general association between cytotoxicity and transfection suggests that a degree of membrane damage must be caused for the cells to gain access to the cytoplasm (Godbey *et al.*, 2001; Panyam *et al.*, 2003; Wagner *et al.*, 1991). Successful transfection relies on achieving the correct balance between gaining adequate accesses by the DNA molecules into the cytoplasm and causing excessive and lethal damage to the cells. Additionally, poly(β-amino-ester)s have been developed by incorporating hydrolyzable moieties that allow this cationic polymers readily degrade into nontoxic metabolites for long term and repeated application in *in vivo* use (Lynn *et al.*, 2000).

Recently, block copolymers including diblock or multiblock copolymers have attracted attentions as promising gene carriers (Choi *et al.*, 2000; Nishiyama *et al.*, 2006). The block

copolymer is a linear copolymer with one segment covalently joined to the head of another segment (Kakizawa *et al.*, 2002), and provides a core-shell structure where pharmaceutical complexes surrounded by a protective and stabilising hydrophilic corona. To date, several micelles gene carriers have been intensively studied in preclinical and clinical trials. A series of block copolymers containing a poly-(ethylene glycol) block were synthesised using a combination of click chemistry and ring-opening metathesis polymerization (Wigglesworth *et al.*, 2008). A triblock copolymer consisting of a lactosylated poly(ethylene glycol), a pH-responsive polyamine segment and a DNA-condensing polyamine segment was associated with plasmid DNA to form three-layered polyplex micelles as a targetable and endosome disruptive non-viral gene vector (Oishi *et al.*, 2006). In addition, a polycation-based micelles gene delivery system which introduces a lysine (Lys) unit in poly(ethylene glycol)-*b*-cationic poly(*N*-substituted asparagine) with a flanking *N*-(2-aminoethyl)-2-aminoethyl group (PEG-*b*-Asp(DET)) resulting in PEG-*b*-P[Lys/Asp(DET)] has displayed improved stability and transfection efficacy (Miyata *et al.*, 2007).

Hydrogels are water-saturated turgid networks which mimic the three-dimensional environments of various cells in native cartilaginous tissues (Kushibiki *et al.*, 2006; Wieland *et al.*, 2007). They represent an improvement as a class of biodegradable polymeric materials with excellent biocompatibility and allow protracted localized gene expression. New biodegradable pluronic hydrogels with different cross-linking densities and mechanical strengths that are capable of releasing pDNA in a sustained manner were prepared by UV-induced photo-polymerization (Chun *et al.*, 2005). Recently, incorporation of pDNA in hyaluronan (Kim *et al.*, 2003; Segura *et al.*, 2005), gelatin (Fukunaka *et al.*, 2002; Kushibiki *et al.*, 2003) and thermosensitive (Li *et al.*, 2003) hydrogels has been demonstrated. Other delivery mode like magnetofection has been described (Plank *et al.*, 2003; Xiang *et al.*, 2003). In this method, DNA-loaded superparamagnetic iron oxide nanoparticles are guided along a magnetic gradient field to the cells during the transfection procedure (Huth *et al.*, 2004; Scherer *et al.*, 2002). Several recent studies also demonstrated that modifying the surfaces of superparamagnetic iron oxide nanoparticles with pullulan (Gupta *et al.*, 2005) or PEI-PEG-chitosan copolymer (Kievit *et al.*, 2009) can suppress the toxic effect and enhanced cellular uptake. Gold nanoparticles provide attractive candidate for pDNA delivery through the functional diversity of monolayer protected clusters systems on the surfaces that allow tuning of the charge and hydrophobicity to maximize transfection efficiency while minimizing toxicity (Ghosh *et al.*, 2008). At the optimized branched polyethylenimine (PEI, 2 kDa) to gold nanoparticles ratio, this transfection vector is more potent than the unmodified

polycation itself and its 25-kDa counterpart at the same concentration (Thomas *et al.*, 2003). Other recent studies demonstrated the ability of gold nanoparticles to deliver plasmid DNA into breast cancer cells (MCF-7) (Wang *et al.*, 2007) and human embryonic kidney cells (HEK 293) (Li *et al.*, 2008) with modified coating biomaterials. Recent advances also include the use of microneedle arrays/patches to breach the skin barrier which enables topical immunization with naked pDNA and induce stronger and less variable immune responses than needle-based injections (Kendall, 2006; Mikszta *et al.*, 2002).

Routes of Administration of pDNA Vaccines

New methods such as subcutaneous, intraperitoneal, intravenous and mucosal (oral, vaginal, intranasal, intratracheal or pulmonary) deliveries of pDNA carry a number of potential advantages over conventional methods (Goya *et al.*, 2008). Such advantages include increased safety, acceptability and treatment compliance; increased efficacy linked to a broader tissue distribution of the antigen; ease of use leading to self-administration; and administration of smaller doses of the antigen. The mucous membranes covering all body passages such as the respiratory and alimentary tracts are endowed with powerful protection network against foreign matters through the immunocytes that form mucosa-associated lymphoid tissues (MALT) (Holmgren *et al.*, 2005). Most infectious pathogens such as HIV and influenza virus enter the body through mucosal tissues; therefore, the induction of humoral, mucosal and cellular immune response via non-invasive DNA therapeutic conduit is gaining attention. Mucosal immunisation was reported to induce stronger antigen-specific responses in comparison to parenteral immunisation (Goya *et al.*, 2008). Mucoadhesive properties of colloidal delivery systems have been reported for their ability to prolong retention time at the mucosal surfaces for enhanced gene expression (Alpar *et al.*, 2005; Goya *et al.*, 2008). Oral gene therapy is an attractive mode for its significant potentials to treat local and systemic diseases (Romano *et al.*, 2000), and to provide both mucosal and systemic immunity (Jones *et al.*, 1996; Li *et al.*, 2009). Nevertheless, oral delivery of nonviral gene medicine has proven to be extremely challenging, owing to the poor stability of the biomolecules in the acidic and enzyme-rich environment of the gastrointestinal tract. Several strategies including liposome and polymeric nanoparticle delivery systems have been adapted to efficiently bypass the barriers in the gastrointestinal tract, and to protect the delicate gene vector; so that it can selectively target a specific cell type and express the therapeutic genes in a regulated fashion. The efficiency of oral formulations has been established in animal studies. However, attempts to scale up the results to humans are generally problematic as substantially high doses are required and the clinical experience has been mixed. The future success of oral formulations

for DNA gene therapy will depend on their ability to bypass the barriers in the gastrointestinal tract, to enhance payload uptake and absorption by gut-associated lymphoid tissues (GALT) and to reduce the doses needed in inducing significant therapeutic effects.

In the last decade, intranasal delivery has been recognised as a very promising route for vaccine administration as it offers a faster and more effective therapeutic effect. The loss of drug by first-pass metabolism in the liver can be avoided because the venous blood from the nose passes directly into the systemic circulation. The mucosal surface in the nasal cavity is highly vascularised and interspersed with immunologically active tissues identified as nasopharyngeal lymphoid tissues (NALT), which are responsible for the induction and mediation of immune responses against the potential pathogenic organisms (Boyaka *et al.*, 2003). The nasal mucosa is also lined with extensive pseudostratified columnar epithelium that enhances the uptake and absorption of carrier systems. Induction of antigen-specific immunoglobulin G (IgG) antibodies in serum, saliva and respiratory tract secretions has also been reported in human trials (Kozlowski *et al.*, 2002). The major limitation of nasal delivery is inadequate absorption of carriers. Factors such as physiochemical properties of gene medicine, nasal mucociliary clearance and nasal absorption enhancers greatly affect absorption in the nasal mucosa. Several enhancers such as mucoadhesive polymers (Alpar *et al.*, 2005) and gels (Turker *et al.*, 2004) have been utilised to improve the nasal absorption.

The immediate pharmacological effect after the translocation of antigens from the lung to the lymph node, and the clearance of carriers from the lung by alveolar phagocytosing cells proved to be prominent in generating immune responses (Helson *et al.*, 2008; Lu *et al.*, 2007). Several preliminary clinical gene therapies using a variety of formulations including lipoplexes and polyplexes to treat a variety of diseases have been completed and more studies are in progress (Bivas-Benita *et al.*, 2004; Gorman *et al.*, 1997; Hyde *et al.*, 2008; Li *et al.*, 2000; Stern *et al.*, 2003). Regardless of its eminent advantages for gene therapy, the lung epithelium has a number of features that discourage the uptake of formulations. These features include the tight junctions between cells, mucus secreted by goblet cells and apical surface coated with cilia. Most recently, the incorporation of positively charged moieties such as PEI to increase the loading of plasmid DNA as well as to formulate highly porous PLGA microspheres may offer interesting strategy for the pulmonary delivery of DNA (Alpar *et al.*, 2005; Ho *et al.*, 2008). The porous structure confers the porogenous formulation with less density and aerodynamic diameter, but increases its propensity for deep lung deposition (Edwards *et al.*, 1997).

REGULATORY STANDARDS

As to date, there is no ultimate standards for ensuring the quality of DNA vaccines used in humans. It is still open to public debate and further improvements. All of the prerequisites discussed below are some of the Food and Drug Administration's (FDA), World Health Organization's (WHO) and Office of Vaccine Research and Review's (OVRR) current opinion on this issue. They are only guidelines instead of standard regulations because more work is needed to ensure the stability, efficacy and safety of DNA vaccines (USFDA, 2007). Generally, thorough characterizations covering all manufacturing aspects as well as product testing need to be conducted before a DNA vaccine can go into a Clinical Trial Phase I. Sources, genotypes and phenotypes of the plasmid strain and bacterial host need to be fully characterized as well as their means of isolations. The construction and complete sequence of plasmid DNA vaccines need to be well presented. These should include their origins of replication, promoters, markers, eukaryotic codons, enzyme restriction map and other enhancing genes such as Kozak consensus sequence or secondary promoters (WHO, 2007). The protocols explaining preparation and maintenance of master cell banks (MCB) and working cell banks (WCB) are required in order to track down any possibility of genetic instability after multiple cell/plasmid passages (USFDA, 2007).

The properties of bulk plasmid DNA obtained after purification should be qualified and quantified. High specificity and high sensitivity assays should be used in all analyses. Standardized procedures should be maintained throughout all analyses and have references such as ASTM, ISO, FDA and any other certified standards. Samples can be sent to these organizations for further verification of the product quality. Generally, the pDNA isoforms content varies from lot to lot but FDA recommends more than 80% of supercoiled pDNA (USFDA, 2007). Various methods can be used for identity testing including restriction enzyme mapping and polymerase chain reaction (PCR). In vitro or in vivo expression followed by confirmation of the identity of the antigen must also be considered (WHO, 2007). Sterility test must rule out presence of any bacteria or fungi using ISO 11737:1 method (Prazeres *et al.*, 1999). Polyacrylamide gel electrophoresis, HPLC and capillary electrophoresis can be used to evaluate the presence of impurities such as RNAs, gDNAs, nicked pDNAs and medium residuals which should represent less than 1% by mass volume of the total vaccine. Endotoxins which generally refer to lipopolysaccharides (LPS) are major contaminants in biological products especially when produced via gram-negative bacteria (Glenting and Wessels, 2005). When the body is exposed to LPS even in small amounts, a range of pro-inflammatory mediators such as TNF, IL-6 and IL-1 are released and lead to

multiple side effects such as endotoxin shock, tissue injury or even death (Magalhães *et al*., 2007). Therefore, in order to ensure the safety of DNA vaccine, the endotoxin level should be kept below 40 EU/mg plasmid when tested using the Limulus Amebocyte Lysate (LAL) test (USFDA, 2007). Anion exchange, affinity, hydrophobic interaction chromatography, synthetic adsorbent of crystalline calcium silicate hydrate (Zhang *et al.*, 2005), and two-phase micellar system using surfactant Triton (Magalhães *et al*., 2007) are currently being used in endotoxin removal procedures. Alternatively, gram-positive hosts such as L. *lactis* (none of which produces endotoxins and biogenic amines) can be employed to eliminate the absolute dependency on LPS removal strategies although they may not produce as high plasmid yields as gram-negative bacteria (Glenting and Wessels, 2005).

Before a DNA vaccine can be brought into human trial, preclinical immunogenicity and safety studies need to be conducted in an animal model. This study may include the evaluation of seroconversion rates, humoral and cell mediated immune response, autoimmunity, genome integration, immunosupression and other biological responses in relation to vaccine administration (WHO, 2007). Clinical vaccination aspects such as number of doses, prime-boost vaccination, methods of delivery and histological effects in animal models will have a significant impact on the design of an immunization program for human recipients (USFDA, 2007).

CONCLUSION

Plasmid based vaccine is a promising new alternative to viral and protein based vaccines as it has shown the ability to stimulate both B- and T- cell mediated responses. As of February 2006, WHO has reported several pDNA vaccines on trial including 1 cholera, 1 influenza, 5 AIDS, 1 dengue, 1 West Nile, 4 hepatitis and 2 papilomavirus DNA vaccines. The major drawback is low levels of immune responses against diseases. Since the magic formulation of pDNA vaccine has not been discovered yet, the provision of naked pDNA vaccine is normally boosted by prime boost vaccination using live attenuated vaccines. Plasmid design, fermentation control and novel purification techniques significantly contribute to the efficacy, reproducibility and most importantly cost-effectiveness of the plasmid based vaccine manufacture.

The choice of replicons, promoters, markers, antigenic genes, codons and CpG motifs is very crucial and has a significant impact on the effectiveness of pDNA vaccines. Genes that engage the immature immune system in infants should be taken into consideration whilst

genes that portray sequence homology to human genome must be avoided. For plasmid cultivation, the obtention of high quality and high yield pDNA vaccines are greatly dependent on the use of defined growth medium, fed batch cultivation strategy and reduced growth rate that promotes high plasmid replication rather than high cell biomass. In a large scale production, cell harvest and concentration methods can adversely affect the intact structure of supercoiled pDNA. The extended mixing time required in achieving a large homogenous cell suspension may lead to reduced intact supercoiled pDNA yield. Alkaline cell lysis seems to be more favorable than mechanical or thermal based cell lysis for shear sensitive supercoiled pDNA production. However, the use of NaOH in a large continuous cell lysis process will require optimizations of the mixing procedure, contact time and holding time in order to retain the intact nature of supercoiled pDNA. The major challenges in pDNA purification are poor selectivity and recovery due to the common features (e.g. electronegativity and size) shared by supercoiled pDNA and other impurities such as endotoxins and plasmid isoforms. When developing a large scale pDNA purification process, the design aims at volume reduction, attaining a better resolution and higher capacity at reasonable flow rates and pressure drops. Single macroporous monolithic support and adsorptive membranes are promising new and advanced materials that can deal with problems of low capacity. In the vaccine delivery section, it has been shown that the injection of naked pDNA did not result in a sufficient level of protection against the disease due to degradation by serum enzymes such as endonucleases. Recent progresses have shown that intradermal or intramuscular injections, followed by electroporation of the injection sites, resulted in improved immune responses in mice and pigs although the heat released during the transfer of electric pulses could adversely affect the sites of injection. This has called for a concerted research to ensure the effectiveness and safety of this technique. Oral and intranasal deliveries of nonviral gene medicine are promising new methods for pDNA vaccine administration although more studies are needed to overcome the problems such as plasmid instability and vaccine loss during administration and tranfection. To ensure process viability, thorough economic analysis of the entire production scheme needs to be evaluated. Further information on bioprocess economics can be found in Bailey *et al.* (1986), Bungay (1963), and Harrison *et al.* (2002).

REFERENCES

Aihara, H., and Miyazaki, J. 1998. Gene transfer into muscle by electroporation in vivo. *Nat. Biotechnol.* 16: 867-870.

Alpar, H. O., Somavarapu, S., Atuah, K. N., and Bramwell, V. 2005. Biodegradable mucoadhesive particulates for nasal and pulmonary antigen and DNA delivery. *Adv. Drug Delivery Rev.* 57: 411-430.

Ando, S., Putnam, D., Pack, D. W., and Langer, R. 1999. PLGA microspheres containing plasmid DNA: Preservation of supercoiled DNA via cryopreparation and carbohydrate stabilization. *J. Pharm. Sci.* 88: 126-130.

Anspach, F. B. 2001. Endotoxin removal by affinity sorbents. *J. Biochem. Biophys. Methods*. 49: 665-681.

Arakawa, T., Ejima, D., Tsumoto, K., Ishibashi, M., and Tokunaga, M. 2007. Improved performance of column chromatography by arginine: Dye-affinity chromatography. *Protein Expression Purif.* 52: 410-414.

Bailey, J. E., and Ollis, D. F. 1986. *Biochemical Engineering Fundamentals*. McGraw Hill, Singapore.

Bawarski, W. E., Chidlowsky, E., Bharali, D. J., and Mousa, S. A. 2008. Emerging nanopharmaceuticals. *Nanomed. Nanotechnol. Bio. Med.* 4: 273-282.

Bhattacharya, S., and Bajaj, A. 2009. Advances in gene delivery through molecular design of cationic lipids. *Chem. Commun.* 4632-4656.

Bivas-Benita, M., van Meijgaarden, K. E., Franken, K., Junginger, H. E., Borchard, G., Ottenhoff, T. H. M., and Geluk, A. 2004. Pulmonary delivery of chitosan-DNA nanoparticles enhances the immunogenicity of a DNA vaccine encoding hla-a*0201-restricted t-cell epitopes of mycobacterium tuberculosis. *Vaccine.* 22: 1609-1615.

Bodles-Brakhop, A. M., Heller, R., and Draghia-Akli, R. 2009. Electroporation for the delivery of DNA-based vaccines and immunotherapeutics: Current clinical developments. *Mol. Ther.* 17: 585-592.

Borchard, G. 2001. Chitosans for gene delivery. *Adv. Drug Delivery Rev.* 52: 145-150.

Boyaka, P. N., Tafaro, A., Fischer, R., Fujihashi, K., Jirillo, E., and McGhee, J. R. 2003. Therapeutic manipulation of the immune system: Enhancement of innate and adaptive mucosal immunity. *Curr. Pharm. Des.* 9: 1965-1972.

Buck, M. L. 2005. Combination measles, mumps, rubella, and varicella vaccine. *Pediatr. Pharm.* 11: 1-5.

Bungay, H. R. 1963. Economic definition of continuous fermentation goals. *Biotechnol. Bioeng.* 5: 1-7.

Canonico, A. E., Conary, J. T., Meyrick, B. O., and Brigham, K. L. 1994. Aerosol and intravenous transfection of human alpha-1-antitrypsin gene to lungs of rabbits. *Am. J. Respir. Cell Mol. Biol.* 10: 24-29.

Carnes, A. E. 2007. *Process for Plasmid DNA Fermentation*. U.S. patent 20070254342.

Carnes, A. E. 2008. *Fermentation Process for Continuous Plasmid DNA Production*. U.S. patent 20080318283.

Carnes, A. E., Hodgson, C. P., and Williams, J. A. 2006. Inducible *Escherichia coli* fermentation for increased plasmid DNA production. *Biotechnol. Appl. Biochem.* 45: 155-166.

Castagnoli, L., Scarpa, M., Kokkinidis, M., Banner, D. W., Tsernoglou, D., and Cesareni, G. 1989. Genetic and structural analysis of the ColE 1 Rop (Rom) protein. *EMBO.* 8: 621 -629.

Chen, W. 1999. *Automated high-yield fermentation of plasmid DNA in Escherichia coli*. U.S. patent 5955323.

Choi, J. S., Joo, D. K., Kim, C. H., Kim, K., and Park, J. S. 2000. Synthesis of a barbell-like triblock copolymer, poly(L-lysine) dendrimer-block-poly(ethylene glycol)-block-poly(L-lysine) dendrimer, and its self-assembly with plasmid DNA. *J. Am. Chem. Soc.* 122: 474-480.

Chun, K. W., Lee, J. B., Kim, S. H., and Park, T. G. 2005. Controlled release of plasmid DNA from photo-cross-linked pluronic hydrogels. *Biomaterials.* 26: 3319-3326.

Coban, C., Ishii, K. J., Gursel, M., Klinman, D. M., and Kumar, N. 2005. Effect of plasmid backbone modification by different human CpG motifs on the immunogenicity of DNA vaccine vectors. *J. Leukocyte Biol.* 778: 1-9.

Córdoba, L. T., Bocanegra, A. R. D., Llorente, B. R., Hernández, E. S., Echegoyen, F. B., Borja, R., Bejines, F. R., and Morcillo, M. F. C. 2008. Batch culture growth of *Chlorella zofingiensis* on effluent derived from two-stage anaerobic digestion of two-phase olive mill solid waste. *Electr. J. Biotech.* 11: 1-8.

Corey, L. 1999. HIV vaccines. *Medscape HIV/AIDS.* 5: 1-3.

Danquah, M. K., and Forde, G. M. 2007a. Growth medium selection and its economic impact on plasmid DNA production. *J. Biosci. Bioeng.* 104: 490-497.

Danquah, M. K., and Forde, G. M. 2007b. The suitability of DEAE-Cl active groups on customized poly(GMA-*co*-EDMA) continuous stationary phase for fast enzyme-free isolation of plasmid DNA. *J. Chromatogr. B.* 853: 38-46.

Danquah, M. K., and Forde, G. M. 2008a. Large-volume methacrylate monolith for plasmid purification: Process engineering approach to synthesis and application. *J. Chromatogr. A.* 1188: 227-233.

Danquah, M. K., and Forde, G. M. 2008b. Preparation of macroporous methacrylate monolithic material with convective flow properties for bioseparation: Investigating

the kinetics of pore formation and hydrodynamic performance. *Chem. Eng. J.* 140: 593-599.

Danquah, M. K., and Forde, G. M. 2008c. Development of a pilot-scale bacterial fermentation for plasmid-based biopharmaceutical production using a stoichiometric medium. *Biotechnol. Bioprocess Eng.* 13: 1-10.

Danquah, M. K., Ho, J., and Forde, G. M. 2007c. Performance of R-N(R9)-R99 functionalised poly(glycidyl methacrylate-co-ethylene glycol dimethacrylate) monolithic sorbent for plasmid DNA adsorption. *J. Sep. Sci.* 30: 2843 - 2850.

de Lima, M. C. P., Simoes, S., Pires, P., Faneca, H., and Duzgunes, N. 2001. Cationic lipid-DNA complexes in gene delivery: From biophysics to biological applications. *Adv. Drug Delivery Rev.* 47: 277-294.

Diogo, M. M., Queiroz, J. A., and Prazeres, D. M. F. 2005. Chromatography of plasmid DNA. *J. Chromatogr. A*. 1069: 3-22.

Dufes, C., Uchegbu, I. F., and Schatzlein, A. G. 2005. Dendrimers in gene delivery. *Adv. Drug Delivery Rev.* 57: 2177-2202.

Dupuis, M., Denis-Mize, K., Woo, C., Goldbeck, C., Selby, M. J., Chen, M. C., Otten, G. R., Ulmer, J. B., Donnelly, J. J., Ott, G., and McDonald, D. M. 2000. Distribution of DNA vaccines determines their immunogenicity after intramuscular injection in mice. *J. Immunol.* 165: 2850-2858.

Edwards, D. A., Hanes, J., Caponetti, G., Hrkach, J., BenJebria, A., Eskew, M. L., Mintzes, J., Deaver, D., Lotan, N., and Langer, R. 1997. Large porous particles for pulmonary drug delivery. *Science.* 276: 1868-1871.

Felgner, J. H., Kumar, R., Sridhar, C. N., Wheeler, C. J., Tsai, Y. J., Border, R., Ramsey, P., Martin, M., and Felgner, P. L. 1994. Enhanced gene delivery and mechanism studies with a novel series of cationic lipid formulations. *J. Biol. Chem.* 269: 2550-2561.

Felgner, P. L. 1996. Improvements in cationic liposomes for in vivo gene transfer. *Hum. Gene Ther.* 7: 1791-1793.

Filomena, S., Passarinha, L., Sousa, F., Queiroz, J. A., and Domingues, F. C. 2009. Influence of growth conditions on plasmid DNA production. *J. Microbiol. Biotechnol.* 19: 1408-1414.

Freitas, S. S., Santos, A. L., and Prazeres D. M. F. 2009. Plasmid purification by hydrophobic interaction chromatography using sodium citrate in the mobile phase. *Sep. Purif. Tech*. 65: 95-104

Fukunaka, Y., Iwanaga, K., Morimoto, K., Kakemi, M., and Tabata, Y. 2002. Controlled release of plasmid DNA from cationized gelatin hydrogels based on hydrogel degradation. *J. Controlled Release.* 80: 333-343.

Furuichi, K., Katakura, Y., Ninomiya, K., and Shioya, S. 2007. Enhancement of 1,4-dihydroxy-2-naphthoic acid production by *Propionibacterium freudenreichii* ET-3 fed-batch culture. *Appl. Environ. Microbiol.* 73: 3137-3143.

Fynan, E. F., Webster, R. G., Fuller, D. H., Haynes, J. R., Santoro, J. C., and Robinson, H. L. 1993. DNA vaccines - protective immunizations by parenteral, mucosal, and gene-gun inoculations. *Proceedings of the National Academy of Sciences of the United States of America.* 90: 11478-11482.

Garmory, H. S., Brown, K. A., and Titball, R. W. 2003. DNA vaccines: improving expression of antigens. *Genet. Vaccines Ther.* 1: 1-5.

Genton, B. 2008. Malaria vaccines: A toy for travelers or a tool for eradication? *Expert Rev. Vaccines.* 7: 597-611.

Ghosh, P., Han, G., De, M., Kim, C. K., and Rotello, V. M. 2008. Gold nanoparticles in delivery applications. *Adv. Drug Delivery Rev.* 60: 1307-1315.

Glenting, J., and Wessels, S. 2005. Ensuring safety of DNA vaccines. *Microb. Cell Factories.* 4: 26-30.

Godbey, W. T., Wu, K. K., and Mikos, A. G. 2001. Poly(ethylenimine)-mediated gene delivery affects endothelial cell function and viability. *Biomaterials.* 22: 471-480.

Gorman, C. M., Aikawa, M., Fox, B., Fox, E., Lapuz, C., Michaud, B., Nguyen, H., Roche, E., Sawa, T., and WienerKronish, J. P. 1997. Efficient in vivo delivery of DNA to pulmonary cells using the novel lipid edmpc. *Gene Ther.* 4: 983-992.

Goula, D., Benoist, C., Mantero, S., Merlo, G., Levi, G., and Demeneix, B. A. 1998. Polyethylenimine-based intravenous delivery of transgenes to mouse lung. *Gene Ther.* 5: 1291-1295.

Goya, A. K., Khatri, K., Mishra, N., and Vyas, S. P. 2008. New patents on mucosal delivery of vaccines. *Expert Opin. Ther. Pat.* 18: 1271-1288.

Gupta, A. K., and Gupta, M. 2005. Cytotoxicity suppression and cellular uptake enhancement of surface modified magnetic nanoparticles. *Biomaterials.* 26: 1565-1573.

Han, Y., and Forde, G. M. 2008. Single step purification of plasmid DNA using peptide ligand affinity chromatography. *J. Chromatogr. B.* 874: 21-26.

Harrison, R. G., Todd, P. W., Rudge, S. R., and Petrides, D. 2002. *Biosep. Sci. Eng.* Oxford University Press, UK.

Hartmann, G., and Krieg, A. M. 2000. Mechanism and Function of a Newly Identified CpG DNA Motif in Human Primary B Cells1. *J. Immunol.* 164: 944-953.

Hedley, M. L., Curley, J., and Urban, R. 1998. Microspheres containing plasmid-encoded antigens elicit cytotoxic t-cell responses. *Nat. Med.* 4: 365-368.

Helson, R., Olszewska, W., Singh, M., Megede, J. Z., Melero, J. A., Hagan, D. O., and Openshaw, P. J. M. 2008. Polylactide-co-glycolide (plg) microparticles modify the immune response to DNA vaccination. *Vaccine.* 26: 753-761.

Henke, A. 2000. DNA immunization– a new chance in vaccine research? *Med. Microbiol. Immunol.* 191: 187–190

Ho, J., Wang, H. T., and Forde, G. M. 2008. Process considerations related to the microencapsulation of plasmid DNA via ultrasonic atomization. *Biotechnol. Bioeng.* 101: 172-181.

Hofland, H. E. J., Nagy, D., Liu, J. J., Spratt, K., Lee, Y. L., Danos, O., and Sullivan, S. M. 1997. In vivo gene transfer by intravenous administration of stable cationic lipid DNA complex. *Pharm. Res.* 14: 742-749.

Hofland, H. E. J., Shephard, L., and Sullivan, S. M. 1996. Formation of stable cationic lipid/DNA complexes for gene transfer. *Proceedings of the National Academy of Sciences of the United States of America.* 93: 7305-7309.

Holmgren, J., and Czerkinsky, C. 2005. Mucosal immunity and vaccines. *Nat. Med.* 11: S45-S53.

http://www.wiley.co.uk/genmed/clinical/. Gene therapy clinical trials worldwide: Wiley.

Huang, Y., Krasnitz, M., Rabadan, R., Witten, D. M., Song, Y., Levine, A. J., Ho, D. D., and Robins, H. 2008. A recoding method to improve the humoral immune response to an HIV DNA vaccine. *PLoS ONE.* 3: 3214-3218.

Huber, H., Buchinger, W., Diewok, J., Ganja, R., Keller, D., Urthaler, J., and Necina, R. 2008. *Industrial Manufacturing of Plasmid DNA:Boehringer's New cGMP Production System Employs Prudent Vector Design as a Backbone*. Genetic Engineering & Biotechnology News, Vol. 28: 4-6. USA.

Huth, S., Lausier, J., Gersting, S. W., Rudolph, C., Plank, C., Welsch, U., and Rosenecker, J. 2004. Insights into the mechanism of magnetofection using PEI-based magnetofectins for gene transfer. *J. Gene Med.* 6: 923-936.

Hyde, S. C., Pringle, I. A., Abdullah, S., Lawton, A. E., Davies, L. A., Varathalingam, A., Nunez-Alonso, G., Green, A. M., Bazzani, R. P., Sumner-Jones, S. G., Chan, M., Li, H., Yew, N. S., Cheng, S. H., Boyd, A. C., Davies, J. C., Griesenbach, U., Porteous, D. J., Sheppard, D. N., Munkonge, F. M., Alton, E., and Gill, D. R. 2008. Cpg-free

plasmids confer reduced inflammation and sustained pulmonary gene expression. *Nat. Biotechnol.* 26: 549-551.

Jones, D. H., Corris, S., McDonald, S., Clegg, J. C. S., and Farrar, G. H. 1996. Poly(DL-lactide-co-glycolide)-encapsulated plasmid DNA elicits systemic and mucosal antibody responses to encoded protein after oral administration. *Proceedings of the International Meeting on Nucleic Acid Vaccines for the Prevention of Infectious Diseases*. Bethesda, Md.

Kakizawa, Y., and Kataoka, K. 2002. Block copolymer micelles for delivery of gene and related compounds. *Adv Drug Delivery Rev.* 54: 203-222.

Kang, H. C., Lee, M., and Bae, Y. H. 2005. Polymeric gene carriers. *Crit. Rev. Eukaryotic Gene Expression.* 15: 317-342.

Kendall, M. 2006. Engineering of needle-free physical methods to target epidermal cells for DNA vaccination. *Vaccine.* 24: 4651-4656.

Kievit, F. M., Veiseh, O., Bhattarai, N., Fang, C., Gunn, J. W., Lee, D., Ellenbogen, R. G., Olson, J. M., and Zhang, M. Q. 2009. PEI-PEG-Chitosan-Copolymer-Coated Iron Oxide Nanoparticles for Safe Gene Delivery: Synthesis, Complexation, and Transfection. *Adv. Func. Mater.* 19: 2244-2251.

Kim, A., Checkla, D. M., Dehazya, P., and Chen, W. L. 2003. Characterization of DNA-hyaluronan matrix for sustained gene transfer. *J. Controlled Release.* 90: 81-95.

Ko, H. J., Ko, S. Y., Kim, Y. J., Lee, E. G., Cho, S. N., and Kang, C. Y. 2005. Optimization of codon usage enhances the immunogenicity of a DNA vaccine encoding mycobacterial antigen Ag85B. *Infect. Immun.* 73: 5666-5674.

Kong, S., Rock, C. F., Booth, A., Willoughby, N., O'Kennedy, R. D., Relton, J., Ward, J. M., Hoare, M., and Levy, M. S. 2008. Large-scale plasmid DNA processing: Evidence that cell harvesting and storage methods affect yield of supercoiled plasmid DNA. *Biotechnol. Appl. Biochem.* 51: 43-51.

Kozlowski, P. A., Williams, S. B., Lynch, R. M., Flanigan, T. P., Patterson, R. R., Cu-Uvin, S., and Neutra, M. R. 2002. Differential induction of mucosal and systemic antibody responses in women after nasal, rectal, or vaginal immunization: Influence of the menstrual cycle. *J. Immunol.* 169: 566-574.

KukowskaLatallo, J. F., Bielinska, A. U., Johnson, J., Spindler, R., Tomalia, D. A., and Baker, J. R. 1996. Efficient transfer of genetic material into mammalian cells using Starburst polyamidoamine dendrimers. *Proceedings of the National Academy of Sciences of the United States of America.* 93: 4897-4902.

Kushibiki, T., Tomoshige, R., Fukunaka, Y., Kakemi, M., and Tabata, Y. 2003. In vivo release and gene expression of plasmid DNA by hydrogels of gelatin with different cationization extents. *J. Controlled Release.* 90: 207-216.

Kushibiki, T., Tomoshige, R., Iwanaga, K., Kakemi, M., and Tabata, Y. 2006. Controlled release of plasmid DNA from hydrogels prepared from gelatin cationized by different amine compounds. *J. Controlled Release.* 112: 249-256.

Kutzler, M. A., and Weiner, D. B. 2008. DNA vaccines: Ready for prime time? *Nat. Rev. Genetics.* 9: 776-788.

Lemmens, R., Olsson, U., Nyhammar, T., and Stadler, J. 2003. Supercoiled plasmid DNA: selective purification by thiophilic/aromatic adsorption. *J. Chromatogr. B*. 784: 291-300.

Lechmann, M., and Liang, T. J. 2000. Vaccine development for Hepatitis C. *Semin. Liver Dis.* 20: 211-226.

Levy, M. S., O'Kennedy, R. D., Shamlou, P. A., and Dunnill, P. 2000. Biochemical engineering approaches to the challenges of producing pure plasmid DNA. *TIBTECH*. 18: 296-304.

Li, G. P., Liu, Z. G., Liao, B., and Zhong, N. S. 2009. Induction of Th1-type immune response by chitosan nanoparticles containing plasmid DNA encoding house dust mite allergen Der p 2 for oral vaccination in mice. *Cell. Mol. Immunol.* 6: 45-50.

Li, P. C., Li, D., Zhang, L. X., Li, G. P., and Wang, E. K. 2008. Cationic lipid bilayer coated gold nanoparticles-mediated transfection of mammalian cells. *Biomaterials.* 29: 3617-3624.

Li, S., Tan, Y. D., Viroonchatapan, E., Pitt, B. R., and Huang, L. 2000. Targeted gene delivery to pulmonary endothelium by anti-pecam antibody. *Am. J. Physiology-Lung Cell. Mol. Physiol.* 278: L504-L511.

Li, Z. H., Ning, W., Wang, J. M., Choi, A., Lee, P. Y., Tyagi, P., and Huang, L. 2003. Controlled gene delivery system based on thermosensitive biodegradable hydrogel. *Pharm. Res.* 20: 884-888.

Lindner, L. H., Brock, R., Arndt-Jovin, D., and Eibl, H. 2006. Structural variation of cationic lipids: Minimum requirement for improved oligonucleotide delivery into cells. *J. Controlled Release.* 110: 444-456.

Listner, K., Bentley, L., Okonkowski, J., Kistler, C., Wnek, R., Caparoni, A., Junker, B., Robinson, D., Salmon, P., and Chartrain, M. 2006. Development of a highly productive and scalable plasmid DNA production platform. *Biotechnol. Prog.* 22: 1335-1345.

Liu, F., Qi, H., Huang, L., and Liu, D. 1997. Factors controlling the efficiency of cationic lipid-mediated transfection in vivo via intravenous administration. *Gene Ther.* 4: 517-523.

Liu, L., Zhou, X., Liu, H., Xiang, L., and Yuan, Z. 2005. CpG motif acts as a 'danger signal' and provides a T helper type *1*-biased microenvironment for DNA vaccination. *Immunology.* 115: 223-230.

Liu, M. A. 2003. DNA vaccines: a review. *J. Intern. Med.* 253: 402-410.

Lu, D. M., and Hickey, A. J. 2007. Pulmonary vaccine delivery. *Exp. Rev. Vaccines.* 6: 213-226.

Luckay, A., Sidhu, M. K., Kjeken, R., Megati, S., Siew-Yen Chong, Roopchand, V., Garcia-Hand, D., Abdullah, R., Braun, R., Montefiori, D. C., Rosati, M., Felber, B. K., Pavlakis, G. N., Mathiesen, I., Israe, Z. R., Eldridge, J. H., and Egan, M. A. 2007. Effect of plasmid DNA vaccine design and in vivo electroporation on the resulting vaccine-specific immune responses in *Rhesus Macaques*. *J. Virol.* 81: 5257-5269.

Lungwitz, U., Breunig, M., Blunk, T., and Gopferich, A. 2005. Polyethylenimine-based non-viral gene delivery systems. *Eur. J. Pharm. Biopharm.* 60: 247-266.

Luo, D., and Saltzman, W. M. 2000. Synthetic DNA delivery systems. *Nature Biotechnology.* 18: 33-37.

Lynn, D. M., and Langer, R. 2000. Degradable poly(beta-amino esters): Synthesis, characterization, and self-assembly with plasmid DNA. *J. Am. Chem. Soc.* 122: 10761-10768.

Ma, Z. Y., Guan, Y. P., and Liu, H. Z. 2005. Synthesis of monodisperse nonporous crosslinked poly(glycidyl methacrylate) particles with metal affinity ligands for protein adsorption. *Polym. Int.* 54: 1502-1507.

MacLaughlin, F. C., Mumper, R. J., Wang, J. J., Tagliaferri, J. M., Gill, I., Hinchcliffe, M., and Rolland, A. P. 1998. Chitosan and depolymerized chitosan oligomers as condensing carriers for in vivo plasmid delivery. *J. Controlled Release.* 56: 259-272.

Magalhães, P. O., Lopes, A. M., Mazzola, P. G., Rangel-Yagui, C., Penna, T. C. V., and Jr., A. P. 2007. Methods of Endotoxin Removal from Biological Preparations: a Review. *J. Pharm. Pharmaceut. Sci.* 10: 388-404.

Manoj, S., Babiuk, L. A., and Hurk, S. v. D. L.-v. d. 2004. Approaches to enhance the efficacy of DNA vaccines. *Crit. Rev. Clin. Lab. Sci.* 41: 1-39.

Manthorpe, M., Cornefertjensen, F., Hartikka, J., Felgner, J., Rundell, A., Margalith, M., and Dwarki, V. 1993. Gene-therapy by intramuscular injection of plasmid DNA - studies on firefly luciferease gene-expression in mice *Hum. Gene Ther.* 4: 419-431.

May, S., Harries, D., and Ben-Shaul, A. 2000. The phase behavior of cationic lipid-DNA complexes. *Biophys. J.* 78: 1681-1697.

McNeil, S. E., and Perrie, Y. 2006. Gene delivery using cationic liposomes. *Exp. Opin. Ther. Pat.* 16: 1371-1382.

Meacle, F. J., Zhang, H., Papantoniou, I., Ward, J. M., Titchener-Hooker, N. J., and Hoare, M. 2007. Degradation of supercoiled plasmid DNA within a capillary device. *Biotechnol. Bioeng.* 97: 1148-1157.

Mikszta, J. A., Alarcon, J. B., Brittingham, J. M., Sutter, D. E., Pettis, R. J., and Harvey, N. G. 2002. Improved genetic immunization via micromechanical disruption of skin-barrier function and targeted epidermal delivery. *Nat. Med.* 8: 415-419.

Miyata, K., Fukushima, S., Nishiyama, N., Yamasaki, Y., and Kataoka, K. 2007. Peg-based block catiomers possessing DNA anchoring and endosomal escaping functions to form polyplex micelles with improved stability and high transfection efficacy. *J. Controlled Release.* 122: 252-260.

Montgomery, D. L., Ulmer, J. B., Donnelly, J. J., and Liu, M. A. 1997. DNA vaccines. *Pharmacol. Ther.* 74: 195-205.

Mutschlechner, O., Swoboda, H., and Gapes, J. R. 2000. Continuous two-stage ABE-fermentation using *Clostridium beijerinckii* NRRL B592 operating with a growth rate in the first stage vessel close to its maximal value. *J. Mol. Microbiol. Biotechnol.* 2: 101-105.

Nan, X. Z., He, S. W., Hao, C., and Lin, C. P. 2005. Effects of medium composition on the production of plasmid DNA vector potentially for human gene therapy. *J. Zhejiang Univ. SCI.* 6B: 396-400.

Nguyen, D. N., Green, J. J., Chan, J. M., Longer, R., and Anderson, D. G. 2009. Polymeric materials for gene delivery and DNA vaccination. *Adv. Mater.* 21: 847-867.

Nishiyama, N., and Kataoka, K. 2006. Current state, achievements, and future prospects of polymeric micelles as nanocarriers for drug and gene delivery. *Pharmacol. Ther.* 112: 630-648.

O'Hagan, D. T., Singh, M., and Ulmer, J. B. 2006. Microparticle-based technologies for vaccines. *Methods.* 40: 10-19.

Oishi, M., Kataoka, K., and Nagasaki, Y. 2006. Ph-responsive three-layered pegylated polyplex micelle based on a lactosylated abc triblock copolymer as a targetable and endosome-disruptive nonviral gene vector. *Bioconjugate Chem.* 17: 677-688.

O'Kennedy, R., Baldwin, C., and Moore, E. K. 2000. Effects of growth medium selection on plasmid DNA production and initial processing steps. *J. Biotechnol.* . 76: 175-183.

Ólafsdóttir, G., Svansson, V., Ingvarsson, S., Marti, E., and Torsteinsdóttir, S. 2008. In vitro analysis of expression vectors for DNA vaccination of horses: the effect of a Kozak sequence. *Acta. Vet. Scand.* 50: 1-7.

Ongkudon, C. M., Rahman, B. A., and Aziz, A. A. 2005. Screening of the Sf900-II SFM insect cell culture medium and recombinant baculovirus for the expression of recombinant human transferrin. *Proceedings of the 15th MSMBB Scientific Meeting*. Kuala Lumpur, Malaysia.

Ongkudon, C. M., Rahman, B. A., and Aziz, A. A. 2006. Optimization of critical medium components for the expression of recombinant human transferrin in insect cells baculovirus system. *J. Teknologi F.* 45: 19-30.

Pan, C. H., Jimenez, G. S., Nair, N., Wei, Q., Adams, R. J., Polack, F. P., Rolland, A., Vilalta, A., Griffin, D. E. 2008. Use of Vaxfectin adjuvant with DNA vaccine encoding the measles virus hemagglutinin and fusion proteins protects juvenile and infant rhesus macaques against measles virus. *Clin. Vaccine Immunol*. 15:1214-1221.

Panyam, J., and Labhasetwar, V. 2003. Biodegradable nanoparticles for drug and gene delivery to cells and tissue. *Adv. Drug Delivery Rev.* 55: 329-347.

Park, Y.-C., Kim, S.-G., Park., K., Lee, K. H., and Seo, J.-H. 2004. Fed-batch production of D-ribose from sugar mixtures by transketolase-deficient *Bacillus subtilis* SPK1. *Appl. Microbiol. Biotechnol.* 66: 297-302.

Passarinha, L. A., Diogo, M. M., Queiroz, J. A., Monteiro, G. A., Fonseca, L. P., and Prazeres, D. M. F. 2006. Production of ColE1 type plasmid by *Escherichia coli* DH5α cultured under nonselective conditions. *J. Microbiol. Biotechnol.* 16: 20-24.

Patil, S. D., Rhodes, D. G., and Burgessp, D. J. 2005. DNA-based therapeutics and DNA delivery systems: A comprehensive review. *AAPS.* 7: 61-77.

Perrie Y, F. P., Gregoriadis G. 2001. Liposome-mediated DNA vaccination: The effect of vesicle composition. *Vaccine.* 19: 3301-3310.

Pertmer, T. M., Eisenbraun, M. D., McCabe, D., Prayaga, S. K., Fuller, D. F., and Haynes, J. R. 1995. Gene-gun based nucleic-acid immunization - elicitation of humoral and cytotoxic t-lymphocyte responses following epidermal delivery of nanogram quantities of DNA. *Vaccine.* 13: 1427-1430.

Petersen, H., Kunath, K., Martin, A. L., Stolnik, S., Roberts, C. J., Davies, M. C., and Kissel, T. 2002. Star-shaped poly(ethylene glycol)-block-polyethylenimine copolymers enhance DNA condensation of low molecular weight polyethylenimines. *Biomacromolecules.* 3: 926-936.

Phue, J.-N., Lee, S. J., Trinh, L., and Shiloach1, J. 2008. Modified *Escherichia Coli* B (BL21), a superior producer of plasmid DNA compared with *Escherichia coli* K (DH5a). *Biotechnol Bioeng.* 101: 831-836.

Plank, C., Schillinger, U., Scherer, F., Bergemann, C., Remy, J. S., Krotz, F., Anton, M., Lausier, J., and Rosenecker, J. 2003. The magnetofection method: Using magnetic force to enhance gene delivery. *Bio. Chem.* 384: 737-747.

Pouton, C. W., and Seymour, L. W. 2001. Key issues in non-viral gene delivery. *Adv. Drug Delivery Rev.* 46: 187-203.

Prather, K. J., Sagar, S., Murphy, J., and Chartrain, M. 2003. Industrial scale production of plasmid DNA for vaccine and gene therapy: plasmid design, production, and purification. *Enzyme Microb. Technol.* 33: 865-883.

Prazeres, D. M. F., Ferreira, G. N. M., Monteiro, G. A., Cooney, C. L., and Cabral, J. M. S. 1999. Large-scale production of pharmaceutical-grade plasmid DNA for gene therapy: problems and bottlenecks. *TIBTECH.* 17: 168-174.

Rainczuk, A., Scorza, T., Spithill, T. W., and Smooker, P. M. 2004. A bicistronic DNA vaccine containing apical membrane antigen 1 and merozoite surface protein 4/5 can prime humoral and cellular immune responses and partially protect mice against virulent *Plasmodium chabaudi adami* DS malaria. *Infect. Immun.* 72: 5565-5573.

Remaut, E., Tsao, H., and Fiers, W. 1983. Improved plasmid vectors with a thermoinducible expression and temperature-regulated runaway replication. *Gene* 22: 103–113.

Robinson, H. L., and Pertmer, T. M. 2000. DNA vaccines for viral infections: basic studies and applications. *Adv. Virus Res*. 55:1-74.

Romano, G., Mitcheli, P., Pacilio, C., and Giordano, A. 2000. Latest developments in gene transfer technology: Achievements, perspectives, and controversies over therapeutic applications. *Stem Cells.* 18: 19-39.

Sahloff, E. G. 2005. Current issues in the development of a vaccine to prevent human immunodeficiency virus: Insights from the society of infectious diseases pharmacists. *Pharmacother.* 25: 741-747.

Saldanha, A. J., Brauer, M. J., and Botstein, D. 2004. Nutritional homeostasis in batch and steady-state culture of yeast. *Mol. Biol. Cell.* 15: 4089-4104.

Scherer, F., Anton, M., Schillinger, U., Henkel, J., Bergemann, C., Kruger, A., Gansbacher, B., and Plank, C. 2002. Magnetofection: enhancing and targeting gene delivery by magnetic force in vitro and in vivo. *Gene Ther.* 9: 102-109.

Segura, T., Chung, P. H., and Shea, L. D. 2005. DNA delivery from hyaluronic acid-collagen hydrogels via a substrate-mediated approach. *Biomaterials.* 26: 1575-1584.

Sheets, E. E., Urban, R. G., Crum, C. P., Hedley, M. L., Politch, J. A., Gold, M. A., Muderspach, L. I., Cole, G. A., and Crowley-Nowick, P. A. 2003. Immunotherapy of human cervical high-grade cervical intraepithelial neoplasia with microparticle-delivered human papillomavirus 16 e7 plasmid DNA. *Am. J. Obstet. Gynecol.* 188: 916-926.

Shroff, K. E., Smith, L. R., Baine, Y., and Higgins, T. J. 1999. Potential for plasmid DNAs as vaccines for the new millennium. *Pharm. Sci. Technol. Today.* 2: 205-212.

Shuler, M. L., and Kargi, F. 2002. *Bioprocess Engineering Basic Concepts*. Prentice Hall, USA.

Schmidt, T., Friehs, K., Flaschel, E., and Schleef, M. 2003. *Method for the Isolation of CCC plasmid DNA*. U.S. patent 6664078.

Smith, C. R., DePrince, R. B., Dackor, J., Weigl, D., Griffith, J., and Persmark, M. 2007. Separation of topological forms of plasmid DNA by anion-exchange HPLC: Shifts in elution order of linear DNA. *J. Chromatogr. B*. 854: 121–127

Smith, J., Zhang, Y. L., and Niven, R. 1997. Toward development of a non-viral gene therapeutic. *Adv. Drug Delivery Rev.* 26: 135-150.

Smith, J. M., Amara, R. R., McClure, H. M., Patel, M., Sharma, S., Yi, H., Chennareddi, L., Herndon, J. G., Butera, S. T., Heneine, W., Ellenberger, D. L., Parekh, B., Earl, P. L., Wyatt, L. S., Moss, B., and Robinson, H. L. 2004. Multiprotein HIV type 1 clade B DNA/MVA vaccine: construction, safety, and immunogenicity in macaques. *AIDS Res. Hum. Retroviruses.* 20: 654 - 665.

Song, M. K., Vindurampulle, C. J., Capozzo, A. V. E., Ulmer, J., Polo, J. M., Pasetti, M. F., Barry, E. M., and Levine, M. M. 2005. Characterization of immune responses induced by intramuscular vaccination with DNA vaccines encoding measles virus hemagglutinin and/or fusion proteins. *J. Virol.* 79: 9854-9861.

Sousa, F., Duarte, M. F., Prazeres, and Queiroz, J. A. 2008. Affinity chromatography approaches to overcome the challenges of purifying plasmid DNA. *Trends Biotechnol.* 26: 518-525.

Sousa, F., Prazeres, D. M. F., and Queiroz, J. A. 2009a. Binding and elution strategy for improved performance of arginine affinity chromatography in supercoiled plasmid DNA purification. *Biomed. Chromatogr.* 23: 160-165.

Sousa, F., Prazeres, D. M. F., and Queiroz, J. a. A. 2009b. Improvement of transfection efficiency by using supercoiled plasmid DNA purified with arginine affinity chromatography. *J. Gene. Med.* 11: 79-88.

Stadler, J., Lemmens, R., and Nyhammar, T. 2004. Plasmid DNA purification. *J. Gene. Med.* 6: 54-66.

Stephan, D. J., Yang, Z. Y., San, H., Simari, R. D., Wheeler, C. J., Felgner, P. L., Gordon, D., Nabel, G. J., and Nabel, E. G. 1996. A new cationic liposome DNA complex enhances the efficiency of arterial gene transfer in vivo. *Hum. Gene Ther.* 7: 1803-1812.

Stern, M., Ulrich, K., Geddes, D. M., and Alton, E. 2003. Poly (d, l-lactide-co-glycolide)/DNA microspheres to facilitate prolonged transgene expression in airway epithelium in vitro, ex vivo and in vivo. *Gene Ther.* 10: 1282-1288.

Tan, L., Lai, W. B., Lee, C. T., Kim, D. S., and Choe, W-S. 2007a. Differential interactions of plasmid DNA, RNA and endotoxin with immobilised and free metal ions. *J. Chromatogr. A*. 1141: 226-234.

Tan, L., Kim, D-S., Yoo, I-K, and Choe, W-S. 2007b. Harnessing metal ion affinity for the purification of plasmidDNA. *Chem. Eng. Sci*. 62: 5809-5820.

Tanaka, N., and Kobayashi, H. 2003. Monolithic columns for liquid chromatography. *Anal. Bioanal. Chem.* 376: 298-301.

Tang, D. C., Devit, M., and Johnston, S. A. 1992. Genetic immunization is a simple method for eliciting an immune-response. *Nature.* 356: 152-154.

Thatcher, D. R., Hitchcock, A., Hanak, J. A. J., and Varley, D. L. 1999. *Method of plasmid DNA production and purification*. U. S. patent 5981735.

Thierry, A. R., Vives, E., Richard, J. P., Prevot, P., Martinand-Mari, C., Robbins, I., and Lebleu, B. 2003. Cellular uptake and intracellular fate of antisense oligonucleotides. *Curr. Opin. Mol. Ther.* 5: 133-138.

Thomas, M., and Klibanov, A. M. 2003. Conjugation to gold nanoparticles enhances polyethylenimine's transfer of plasmid DNA into mammalian cells. *Proceedings of the National Academy of Sciences of the United States of America.* 100: 9138-9143.

Turker, S., Onur, E., and Ozer, Y. 2004. Nasal route and drug delivery systems. *Pharm. World Sci.* 26: 137-142.

Ulmer, J. B., Donnelly, J. J., Parker, S. E., Rhodes, G. H., Felgner, P. L., Dwarki, V. J., Gromkowski, S. H., Deck, R. R., Dewitt, C. M., Friedman, A., Hawe, L. A., Leander, K. R., Martinez, D., Perry, H. C., Shiver, J. W., Montgomery, D. L., and Liu, M. A. 1993. Heterologous protection against influenza by injection of DNA encoding a viral protein. *Science.* 259: 1745-1749.

United States Food and Drug Administration US FDA. 2007. *Considerations for plasmid DNA vaccines for infectious disease indications*. Office of Vaccines Research and Review. Rockville, USA

Urthaler, J., Ascher, C., W¨ohrer, H., and Necina, R. 2007. Automated alkaline lysis for industrial scale cGMP production of pharmaceutical grade plasmid-DNA. *J. Biotech.* 128: 132-149.

Urthaler, J., Buchinger, W., and Necina, R. 2005a. Improved downstream process for the production of plasmid DNA for gene therapy. *Acta Biochim. Pol.* 52: 703-711.

Urthaler, J., Buchinger, W., and Necina, R. 2005b. Industrial Scale cGMP Purification of Pharmaceutical Grade Plasmid DNA. *Chem. Eng. Technol.* 28: 1408-1420.

Vries, R. D. d., Stittelaar, K. J., Osterhaus, A. D., and Swart, R. L. d. 2008. Measles vaccination: new strategies and formulations. *Expert Rev. Vaccines.* 7: 1215-1223.

Wagner, E., Cotten, M., Foisner, R., and Birnstiel, M. L. 1991. Transferrin polycation DNA complexes - the effect of polycations on the structure of the complex and DNA delivery to cells *Proceedings of the National Academy of Sciences of the United States of America.* 88: 4255-4259.

Wang, B., Ugen, K. E., Srikantan, V., Agadjanyan, M. G., Dang, K., Refaeli, Y., Sato, A. I., Boyer, J., Williams, W. V., and Weiner, D. B. 1993. Gene inoculation generates immune-responses against human immunodeficiency virus type 1 *Proceedings of the National Academy of Sciences of the United States of America.* 90: 4156-4160.

Wang, H., Chen, Y., Li, X. Y., and Liu, Y. 2007. Synthesis of oligo(ethylenediamino)-beta-cyclodextrin modified gold nanoparticle as a DNA concentrator. *Mol. Pharm.* 4: 189-198.

Wang, Z., Le, G., Shi, Y., and Wegrzyn, G. 2001. Medium design for plasmid DNA production based on stoichiometric model. *Process Biochem.* 36: 1085-1093.

Wheeler, C. J., Felgner, P. L., Tsai, Y. J., Marshall, J., Sukhu, L., Doh, S. G., Hartikka, J., Nietupski, J., Manthorpe, M., Nichols, M., Plewe, M., Liang, X. W., Norman, J., Smith, A., and Cheng, S. H. 1996. A novel cationic lipid greatly enhances plasmid DNA delivery and expression in mouse lung. *Proceedings of the National Academy of Sciences of the United States of America.* 93: 11454-11459.

Wieland, J. A., Houchin-Ray, T. L., and Shea, L. D. 2007. Non-viral vector delivery from PEG-hyaluronic acid hydrogels. *J. Controlled Release.* 120: 233-241.

Wigglesworth, T. J., Teixeira, F., Axthelm, F., Eisler, S., Csaba, N. S., Merkle, H. P., Meier, W., and Diederich, F. 2008. Dendronised block copolymers as potential vectors for gene transfection. *Org. Biomol. Chem.* 6: 1905-1911.

Williams, J. A., Luke, J., Langtry, S., Anderson, S., Hodgson, C. P., and Carnes, A. E. 2009. Generic plasmid DNA production platform incorporating low metabolic burden seed-stock and fed-batch fermentation processes. *Biotechnol. Bioeng.* 103: 1129-1143.

World Health Organization WHO. 2007. *Guidelines for assuring the quality and nonclinical safety evaluation of DNA vaccines*. World Health Organization. Geneva, Switzerland.

Xiang, J. J., Tang, J. Q., Zhu, S. G., Nie, X. M., Lu, H. B., Shen, S. R., Li, X. L., Tang, K., Zhou, M., and Li, G. Y. 2003. Ionp-pll: A novel non-viral vector for efficient gene delivery. *J. Gene Med.* 5: 803-817.

Yao, S., Helinsk, D. R., and Toukdarian, A. 2007. Localization of the naturally occurring plasmid ColE1 at the cell pole. *J. Bacteriol.* 189: 1946-1953

Yoshikawa, T., Imazu, S., Gao, J.-Q., Hayashi, K., Tsuda, Y., Okada, N., Tsutsumi, Y., Akashit, M., Mayumi, T., and Nakagawa, S. 2006. Non-Methylated CpG Motif Packaged into Fusogenic Liposomes Enhance Antigen-Specific Immunity in Mice. *Biol. Pharm. Bull.* 29: 105-109.

Zauner, W., Ogris, M., and Wagner, E. 1998. Polylysine-based transfection systems utilizing receptor-mediated delivery. *Adv. Drug Delivery Rev.* 30: 97-113.

Zhang, J. P., Wang, Q., Smith, T. R., Hurst, W. E., and Sulpizio, T. 2005. Endotoxin Removal Using a Synthetic Adsorbent of Crystalline Calcium Silicate Hydrate. *Biotechnol. Prog.* 21: 1220-1225.

Section 2.2

.

Versatility of polymethacrylate monoliths for chromatographic purification of biomolecules

Journal of Separation Science. 32: 2485 – 2494 (2009)

Monash University

Declaration for Thesis Section 2.2

Declaration by candidate

In the case of Section 2.2, the nature and extent of my contribution to the work was the following:

Nature of contribution	Extent of contribution (%)
Initiation, Key ideas, Writing up	40

The following co-authors contributed to the work. Co-authors who are students at Monash University must also indicate the extent of their contribution in percentage terms:

Name	Nature of contribution
Michael W. H. Roberts	Initiation, Key ideas, Writing up
Dr. Gareth M. Forde	Initiation, Key ideas, Writing up
Dr. Michael K. Danquah	Initiation, Key ideas, Writing up

Candidate's signature		**Date**

Declaration by co-authors

The undersigned hereby certify that:

1. the above declaration correctly reflects the nature and extent of the candidate's contribution to this work, and the nature of the contribution of each of the co-authors;
2. they meet the criteria for authorship in that they have participated in the conception, execution, or interpretation, of at least that part of the publication in their field of expertise;
3. they take public responsibility for their part of the publication, except for the responsible author who accepts overall responsibility for the publication;
4. there are no other authors of the publication according to these criteria;
5. potential conflicts of interest have been disclosed to (a)granting bodies, (b) the editor or publisher of journals or other publications, and (c) the head of the responsible academic unit; and
6. the original data are stored at the following location (s) and will be held for at least five years from the date indicated below:

Location	Chemical Engineering Department, Monash University, Clayton, Australia

Signature		**Date**

Versatility of poly(GMA-*co*-EDMA) monoliths for chromatographic purification of biomolecules

Michael W. H. Roberts, Clarence M. Ongkudon, Gareth M. Forde, Michael K. Danquah

ABSTRACT

Polymethacrylate monoliths, poly(GMA-*co*-EDMA), are a new generation of chromatographic supports and are significantly different to conventional particle-based adsorbents, membranes and other monolithic supports for biomolecule purification. Similar to other monoliths, polymethacrylate monoliths possess large pores which allow convective flow of mobile phase and results in high flow rates at reduced pressure drop, unlike particulate supports. The simplicity of adsorbent synthesis, pH resistance and the ease and flexibility of tailoring its pore size to that of the target biomolecule are the key properties which differentiate polymethacrylate monoliths from other monoliths. Polymethacrylate monoliths are endowed with reactive epoxy groups for easy functionalisation (with anion-exchange, hydrophobic and affinity ligands), and high ligand retention and this is very essential especially when the ligand is expensive and efficiency of immobilization and retention are highly desired in chromatography. In this review, the structure and performance of polymethacrylate monoliths for chromatographic purification of biomolecules are evaluated and compared to that of other supports. The development and use of polymethacrylate monoliths for research applications has grown rapidly in recent times and has enabled the achievement of high through-put biomolecule purification on semi-preparative and preparative scales.

Keywords: Polymethacrylate monolith; Biomolecules; Purification; Chromatography

INTRODUCTION

There are many different ways that biomolecule separation and purification is performed. Of all the techniques available, liquid chromatography is the most versatile technique for the purification different biomolecules. Stationary phases for chromatographic purification of

biomolecules have conventionally been particulate based supports consisting of many beads with small internal pores. These supports are designed for efficient separation of smaller biomolecules. Issues arise when larger biomolecules are to be separated. These large biomolecules are too large to enter the pores of the bead so interactions occur only on the outer surface, thus leading to poor binding. Poor binding results in under-exploitation of the available capacity of the resin and may also result in high levels of non-specific binding in the intra-particle volume [1].

Monolithic supports are new developing technology and have many benefits over particulate supports. In the past decade there has been increasing research and development in the area of monolithic supports for use as the stationary phase in chromatographic separation. Monolithic supports comprise a single structure with a highly interconnected or honey-combic network of channels, a significant variation from conventional particulate supports. Monolithic supports have many inherent advantages when compared to conventional particulate based supports due to their physical and chemical structure. A major reason for many of the advantages of monolithic supports is the large pores (> 200 nm) in diameter found in the matrix [2, 3]. These pores are much larger than those found in particulate supports and allow convective mass transport, far superior to mass transfer by diffusion found in particulate supports. In chromatographic separations, with the exception of affinity purification, mass transfer has been considered the rate limiting factor [4]. With the convective transport mechanism of monolithic structures, this bottleneck has largely been relieved especially for larger molecules which are too large to penetrate the internal structure of particulate supports. A lower pressure drop is observed when passing a fluid though a monolithic support and different pressure drops can be observed in monoliths with different pore structure orientations. Lower pressure drops allow higher flow rates of the mobile phase to be applied. This has the benefit of increasing the capacity of separation. When separating smaller biomolecules, this can be used to offset the capacity losses by the monoliths lower specific surface area. Generally for larger biomolecules this increase in flow rate more than makes up for the lost capacity due to lower specific surface area [5]. The physical attributes extend much further than pore size when comparing monolithic supports to particulate supports.

Due to the distinct solid structure of monoliths a single crack could cause column failure and loss of valuable product [6]. Monolithic structures have generally been shown to exhibit good mechanical stability [5, 7], though the level of stability depends on the material of construction. This mechanical stability allows larger monolithic supports to be cast, currently

up 8 L in volume [2]. The increased volume allows a greater capacity for separation which is a limiting factor for particulate supports.

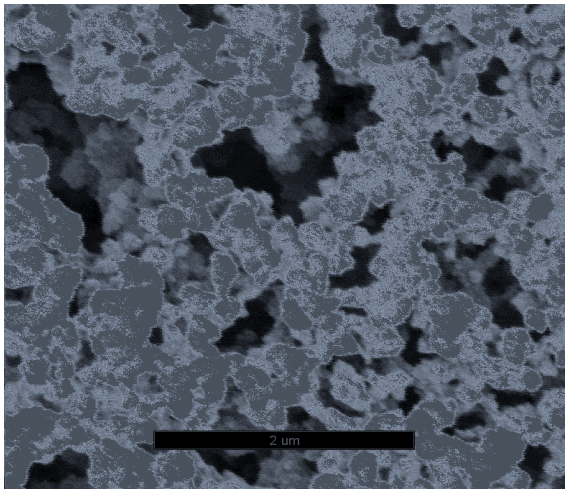

Figure 1: Scanning electron microscopy image of a porous polymethacrylate monolith showing heterogeneous pore structure and channel interconnectivities.

A typical monolithic polymer make-up commonly employed for biomolecule purification is the polymethacrylate resin which is an organic polymer with flexible surface and pore characteristics modification through precise alteration in synthesis conditions. Polymethacrylate monolithic polymer is synthesized via a free radical polymerization process in an unstirred mould, thus resulting in a shape that conforms to that of the mould as well as a porous structure which allows direct flow of a liquid through it. The unimpeded flow fashion of the monolithic medium, as oppose to the flow around a classical bead has offered new opportunities in bioseparation targeting different biomolecules with distinct hydrodynamic sizes and nature. The size distribution of pores existing within polymethacrylate monolithic matrix may cover a wide range up to the second order of magnitude. The morphology of polymethacrylate monoliths is made of interconnected globules that are partly aggregated. The pores in the polymer actually consist of irregular voids existing between clusters of globules or between globules of a given cluster or even within globules (Figure 1). The pore size distribution reflects the internal organization of both globules and clusters within the polymer matrix and this mainly depends on the composition of the polymerization mixture and reaction conditions. This makes it flexible for the pore size to be fine-tuned. The chemical stability of polymethacrylate monoliths is an additional important property that is vital during

repeated process of elution and regeneration and this differentiates it from other types of monoliths. During elution, retained biomolecules are easily separated from polymethacrylate monoliths without any damage to the support or ligand. This feature is more important when the ligand is expensive, as is often the case with affinity chromatography [2, 8]. Degradation of ligands could result in leaching of ligand moieties into purified products and this could be unpleasant in the case of therapeutic or food products. Regeneration is frequently completed with the use of strong basic solutions. Similar to elution, the ligands remain bonded to the polymethacrylate support during regeneration and not significantly degraded over time [2, 5, 7]. The chemical composition of polymethacrylate monoliths dictates the pore structure of the monolith. For example, altering the composition of the porogen and/or the ratio of monomers to porogen in the initial polymerization mixture can change the pore characteristics of the monolith dramatically [4]. In addition to the physical and chemical characteristics of the polymethacrylate monolithic structure, there are also significant advantages associated with the preparation of the support. The synthesis technique of polymethacrylate monoliths allows the supports to be produced in various shapes including disks, rods and tubes, to satisfy a variety of different chromatographic purifications [5]. Some of these geometries are shown in Figure 2.

Pressure drop dependence on pore structure of monoliths

The pressure drop across a monolithic bed is dependent on the type of porous media, channel size and network structure. Two types of monolithic structures were investigated; (1) a honey-combic structure with straight channels of equal diameters which are not interconnected, and (2) a non-uniform structure with interconnected channels (Figure 3). Polymethacrylate monolithic supports show pore structures similar to the latter. They have identical and non-identical structure between nodes with pore interconnectivities. Let's assume that the same flow rate is applied to both structures, both structures have similar voidage with equal pore volume and that the pore volume existing in a nodal plane N_i is negligible. D_s is the pore diameter of the first porous media, D_j is the pore diameter of the second porous media and ΔP_i^k (k = 1, 2) is the pressure drop across N_{i-1} and N_i nodal planes for porous media 1 and 2. Considering the first structure, pores of the same length have the same pore volume and since the nodal planes are considered at the same intervals the pressure drop between successive nodal planes is the same. For m number of nodal planes;

$$\Delta P_1^1 = \Delta P_2^1 = \ldots\ldots = \Delta P_i^1 = \Delta P_{i+1}^1 = \ldots\ldots = \Delta P_m^1 = \Delta P_{m+1}^1 \ldots\ldots\ldots\ldots \quad [1]$$

Consequently, the total pressure drop ΔP_1 over the bed is given by;

$$\Delta P^1 = \Delta P_1{}^1 + \Delta P_2{}^1 + \ldots\ldots + \Delta P_i{}^1 + \Delta P_{i+1}{}^1 + \ldots\ldots + \Delta P_m{}^1 + \Delta P_{m+1}{}^1 = \sum_{i=1}^{i=m+1} \Delta P_i^1 = (m+1)$$

$$\Delta P_i{}^1 \ldots\ldots\ldots \text{[2]}$$

Total pore volume for a unit distance between successive nodal planes, V_{p1} existing in pore media 1 is given by;

$$V_{p1} = n(m+1)\frac{\pi D_s^2}{4} \quad \ldots\ldots\ldots\ldots\ldots \text{[3]}$$

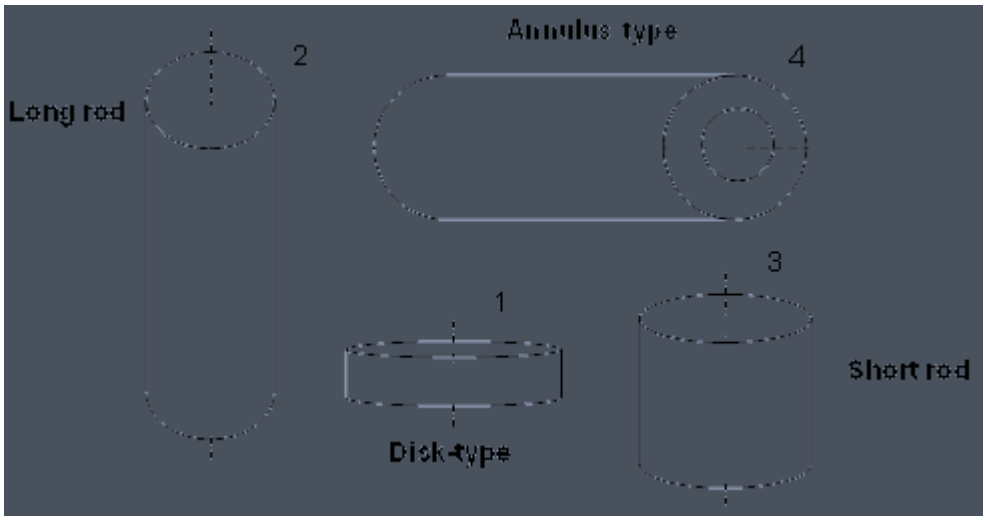

Figure 2: Examples of different polymethacrylate monoliths geometries including membrane or disk type, a long rod, a short rod and annulus type columns.

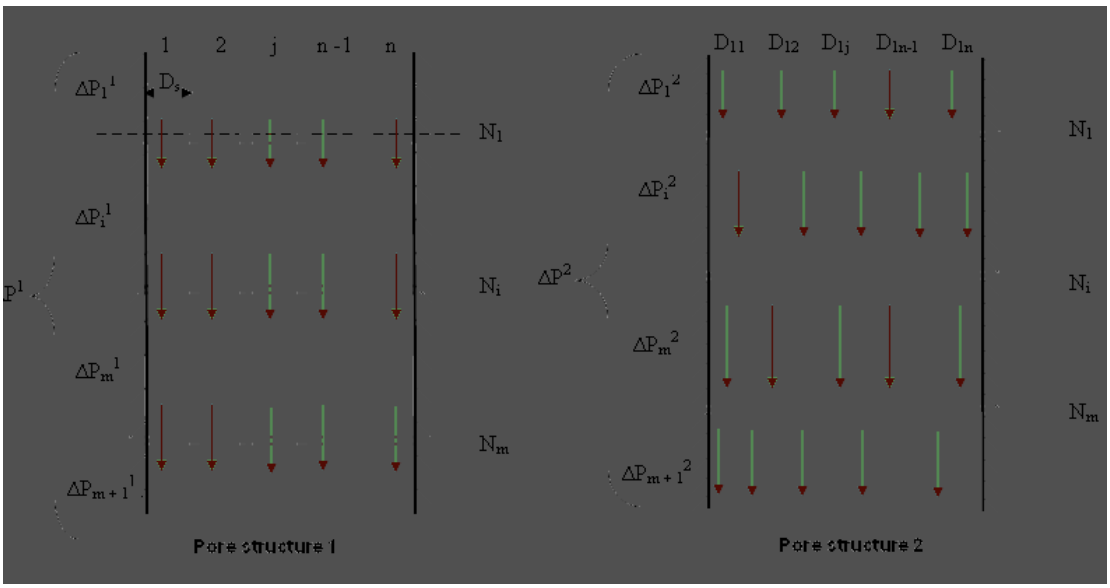

Figure 3: A representation of monolithic structures made of a structure with homogeneous pores and equal diameters with no interconnected channels (Pores structure 1) and a structure made of non-uniform pores with interconnected channels (Pore structure 2).

For the second structure, pore diameters between nodes are different so the pressure drops are different for any two consecutive nodal planes. Liquid flowing through this structure can randomly switch through the nodal planes from one pore to the other due to the pore structure interconnectivities.

$$\Delta P_1^2 \neq \Delta P_2^2 \neq \ldots\ldots \neq \Delta P_i^2 \neq \Delta P_{i+1}^2 \neq \ldots\ldots \neq \Delta P_m^2 \neq \Delta P_{m+1}^2 \ldots\ldots\ldots\ldots [4]$$

Consequently, the total pressure drop ΔP_2 over the bed is given by;

$$\Delta P^2 = \Delta P_1^2 + \Delta P_2^2 + \ldots\ldots + \Delta P_i^2 + \Delta P_{i+1}^2 + \ldots\ldots + \Delta P_m^2 + \Delta P_{m+1}^2 = \sum_{i=1}^{i=m+1} \Delta P_i^2 \ldots\ldots\ldots\ldots [5]$$

Total flow through in media 2 is equal to the sum of the individual flows in all the pores. D_{ij} represents the diameter of the jth pore entering the ith nodal plane. Total pore volume for a unit distance between successive nodal planes, V_{p2} existing in pore media 2;

$$V_{p2} = \frac{\pi}{4}\left(\sum_{j=1}^{j=n} D_{1j}^2 + D_{2j}^2 + ... + D_{ij}^2 + ... + D_{mj}^2 + D_{(m+1)j}^2\right) = \frac{\pi}{4}\sum_{j=1}^{j=n}\sum_{i=1}^{i=m+1} D_{ij}^2 \quad .....[6]$$

Since the total pore volume for structures 1 and 2 are the same, $V_{p1} = V_{p2}$

$$n(m+1)D_s^2 = \sum_{j=1}^{j=n}\sum_{i=1}^{i=m+1} D_{ij}^2 \quad \ldots\ldots\ldots\ldots\ldots [7]$$

Pressure drop of a laminar flow through a cylindrical pore can be computed using Hagen-Poiseuille equation. Application of Hagen-Poiseuille equation on structure 1 gives;

$$\varphi_v^1 = n(m+1)\pi\frac{\Delta P^1 D_s^4}{128\,\eta\, L} \quad \ldots\ldots\ldots\ldots\ldots\ldots [8]$$

Application of Hagen-Poiseuille equation on structure 2 gives;

$$\varphi_v^2 = \frac{\pi}{128\,\eta\, L}\sum_{j=1}^{j=n}\sum_{i=1}^{i=m+1}\Delta P_{ij} D_{ij}^4 \quad \ldots\ldots\ldots\ldots\ldots [9]$$

Since the total pore volume existing in structures 1 and 2 are considered the same, $\varphi_v^1 = \varphi_v^2$

$$n(m+1)D_s^4\Delta P^1 = \sum_{j=1}^{j=n}\sum_{i=1}^{i=m+1}\Delta P_{ij} D_{ij}^4 \quad \ldots\ldots\ldots\ldots\ldots\ldots [10]$$

Combining equations [7] and [10] gives;

$$\frac{\sum_{j=1}^{j=n}\sum_{i=1}^{i=m+1}\frac{\Delta P_{ij}}{\Delta P^1} D_{ij}^4}{D_s^2\sum_{j=1}^{j=n}\sum_{i=1}^{i=m+1} D_{ij}^2} = 1 \quad \ldots\ldots\ldots\ldots\ldots\ldots [11]$$

Scenario 1:

Consider a single nodal plane (i = 1) of a non-uniform methacrylate monolithic structure which is bimodal (j = 2) with modal pore diameters D_1 and D_2 in the ratio $D_1/D_2 = \xi$. Assume the monolith has a structure of parallel type non-uniformity. The pressure drop analysis for this system is carried out in comparison with a monolith of uniform structure having the same pore volume, single node (i = 1) and unimodal pore diameter D_o.

Pore volume equality for the two systems can be written as;

$$D_0^2 = \frac{D_1^2}{2} + \frac{D_2^2}{2} = \frac{D_1^2}{2}\left(1 + \frac{D_2^2}{D_1^2}\right) = \frac{D_1^2}{2}\left(1 + \frac{1}{\xi^2}\right) \quad \text{..... [12]}$$

Applying Hagen-Poiseuille equation to evaluate pressure drop and equalizing results gives;

$$2\Delta P_0\, D_0^4 = \Delta P_1\, D_1^4 + \Delta P_2\, D_2^4 \quad \text{..... [13]}$$

For parallel type non-uniform structure, the total pressure drop above (ΔP_1) and below (ΔP_2) the nodal plane are the same; hence $\Delta P_1 = \Delta P_2 = \Delta P$

$$2\Delta P_0\, D_0^4 = \Delta P\left(D_1^4 + D_2^4\right) = \Delta P\, D_1^4\left(1 + \frac{D_2^4}{D_1^4}\right) = \Delta P\, D_1^4\left(1 + \frac{1}{\xi^4}\right) \quad \text{..... [14]}$$

Combining equations [12] and [14] gives;

$$\frac{\Delta P_0}{\Delta P} = 2\left(1 + \frac{1}{\xi^4}\right)\left(1 + \frac{1}{\xi^2}\right)^{-2} \quad \text{..... [15]}$$

Differentiating equation [15] gives;

$$\frac{d\left(\Delta P_0/\Delta P\right)}{d\xi} = \frac{8\xi}{\left(\xi^2+1\right)^2}\left(\xi^2 - \frac{\xi^4+1}{\xi^2+1}\right) \quad \text{..... [16]}$$

The minimum value of $\left(\Delta P_0 / \Delta P\right)$ occurs at $\xi = 1$

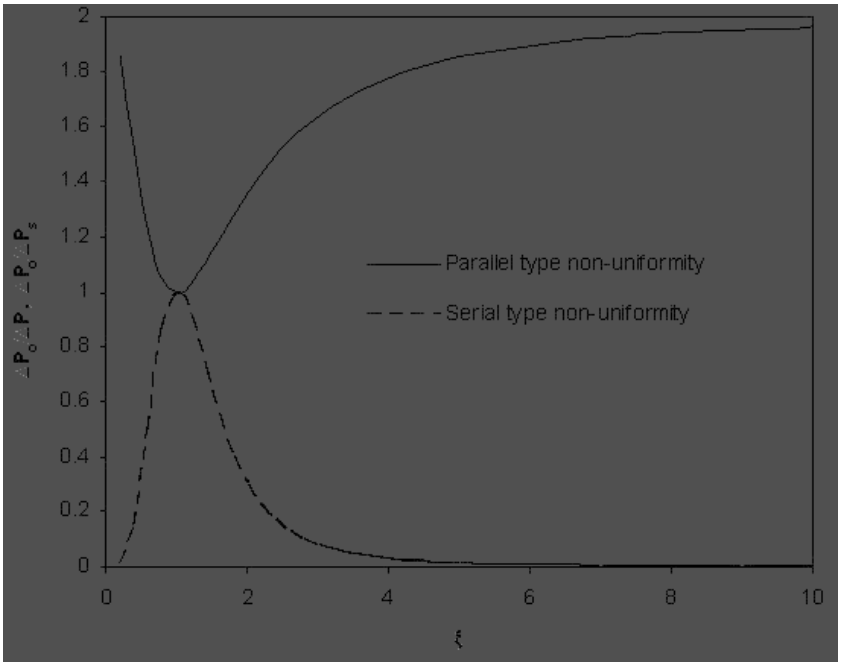

Figure 4: The dependencies of pressure drop on heterogeneous pore structure types: parallel type non-uniformity and serial type non-uniformity.

Scenario 2:

Considering a single nodal plane (i = 1) of a non-uniform methacrylate monolithic structure which is bimodal (j = 2) with modal pore diameters D_{1s} and D_{2s} in the ratio $D_{1s} / D_{2s} = \xi$.

Assume the monolith has a structure of serial type non-uniformity. Pore geometry existing in this structure changes periodically between nodes. The pressure drop analysis for this system is also carried out in comparison with a monolith of uniform structure having the same pore volume, single node (i = 1) and unimodal pore diameter D_o.

Pore volume equality for the 2 systems can be written as;

$$D_0^2 = \frac{D_{1s}^2}{2} + \frac{D_{2s}^2}{2} = \frac{D_{1s}^2}{2}\left(1 + \frac{D_{2s}^2}{D_{1s}^2}\right) = \frac{D_{1s}^2}{2}\left(1 + \frac{1}{\xi^2}\right) \text{..... [17]}$$

Applying Hagen-Poiseuille equation to evaluate pressure drop and equalizing results gives;

$$2\Delta P_0 D_0^4 = \Delta P_{1s} D_{1s}^4 + \Delta P_{2s} D_{2s}^4 \ldots\ldots\ldots\ldots\ldots [18]$$

Where ΔP_{1s} and ΔP_{2s} are the pressure drops before and after the nodal plane. With a monolith having a serial type non-uniformity structure, where diameter changes periodical between nodes to a constant specific diameter, it can be assumed that the flow rate before and after the nodal plane are the same. Therefore from Hagen-Poiseuille equation;

$$\Delta P_{1s} D_{1s}^4 = \Delta P_{2s} D_{2s}^4 \ldots\ldots\ldots\ldots [19]$$

The total pressure drop, ΔP_s across the monolithic bed is given by;

$$\Delta P_s = \Delta P_{1s} + \Delta P_{2s} \ldots\ldots\ldots\ldots\ldots [20]$$

Combining equations [17], [18], [19] and [20] gives;

$$\frac{\Delta P_o}{\Delta P_s} = \frac{8}{\left(1+\xi^4\right)\left(1+ 1/\xi^2\right)^2} \ldots\ldots\ldots\ldots [21]$$

Differentiating equation [21] gives;

$$\frac{d\left(\Delta P_o/\Delta P_s\right)}{d\xi} = \frac{32\left(1-\xi^6\right)}{\xi^3\left(1+\xi^4\right)^2\left(1+ 1/\xi^2\right)^3} \ldots\ldots\ldots\ldots [22]$$

The maximum value of $\left(\Delta P_0/\Delta P_s\right)$ occurs at $\xi = 1$

The dependency of pressure drop on the media types is shown in Figure 4 for single node structures with parallel type non-uniformity and serial type non-uniformity. It is quite obvious that for $0 < \xi < 1$, the parallel type non-uniform structure gives a higher pressure drop in comparison to the structure with a uniform pore size distribution whilst the serial type non-

uniform structure gives a lower pressure drop in comparison to the structure with a uniform pore size distribution. For $\xi \geq 1$, the parallel type non-uniform structure gives a lower pressure drop in comparison to the structure with a uniform pore size distribution whilst the serial type non-uniform structure gives a higher pressure drop in comparison to the structure with a uniform pore size distribution. The profiles obtained shows that low pressure drop can be obtained simply by modifying the extent of pore size distribution. For polymethacrylate monoliths, this can be achieved by altering synthesis conditions such as polymerisation temperature, reactant mixture composition and heat transfer mechanisms.

Hydrodynamics of polymethacrylate monoliths and particulate supports

Polymethacrylate monolith, as a continuous highly porous interconnected material, exhibits flow hydrodynamics such that there is a linear relationship between flow rate of mobile phase and the back pressure as shown in Figure 5. Polymethacrylate monoliths generally display high performance efficiency in chromatography and in some cases the efficiency is enhanced as the flow rate increases. This is because when the flow rate increases some pores that were stagnant at lower flow rates open up and are included in convective mass transport as the mobile phase flows through [9]. This is a significant advantage over particulate supports, where an increased flow rate causes an exponential increase in back pressure due to the particulate bed compressing and reducing void volumes. Though are there obvious differences between monolithic and particulate supports, it is possible to compare the hydrodynamics of the mobile phase as it flow through either support. The macroscopy of monolithic and particulate media are usually coherent, however, all porous media are characterized by diameter, characteristic lengths and shape of their respective interparticle or interskeleton macropore system [10]. Darcy's law governs the flow of Newtonian fluids through a fixed bed which can be either a monolithic or particulate bed.

$$u_{sf} = -\frac{K}{\eta}\nabla P \quad \ldots\ldots\ldots\ldots\ldots\ldots \quad [23]$$

Where u_{sf} is the superficial velocity, K is the specific permeability, η is the dynamic viscosity and ∇P is the pressure gradient. This equation is valid for laminar flows when the porous media and the mobile phase are incompressible. Figure 6 shows results from tests performed by Leinweber and Tallarek, 2003 [10] which confirms the equation when applied

to both non-porous particulate and silica monolithic supports. The linear relationship demonstrates that the equation is valid for laminar flow rates.

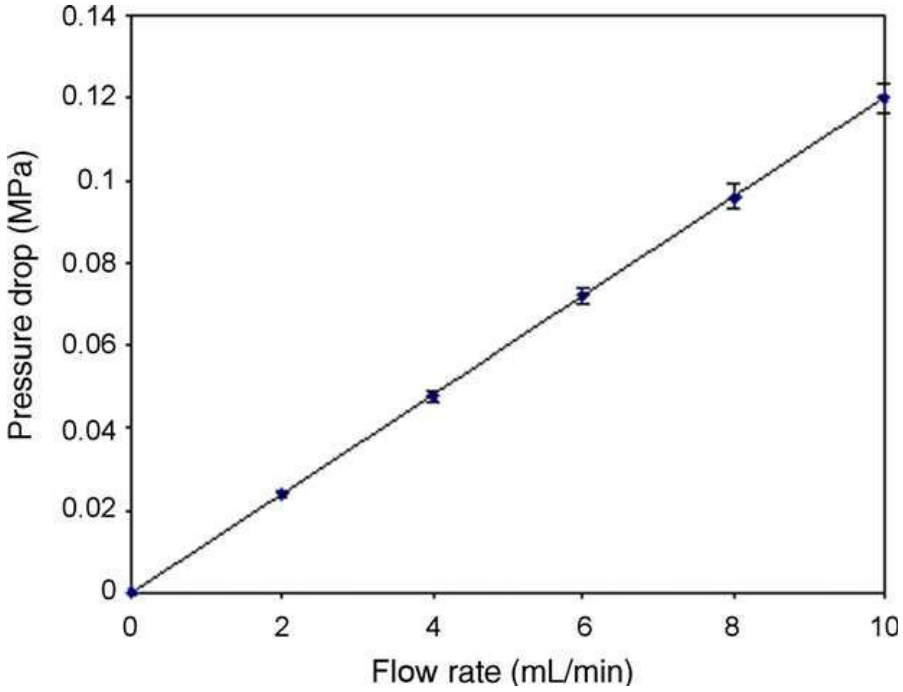

Figure 5: The dependence of pressure drop on flow rate of mobile phase through a polymethacrylate monolithic column [11].

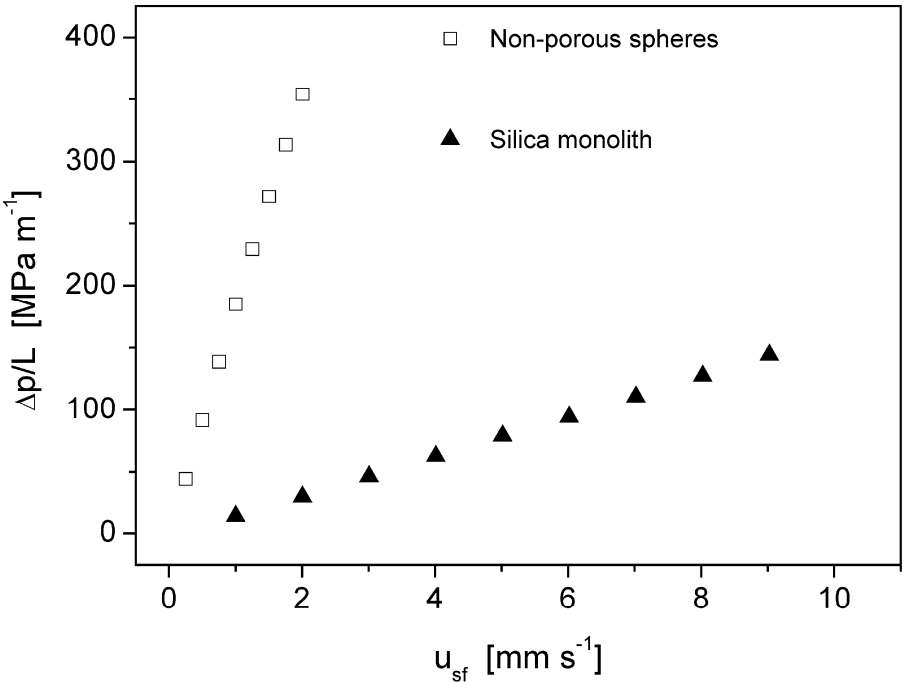

Figure 6: Hydraulic permeability (using water as the liquid) of non-porous particulates and monolithic supports showing flow resistance against superficial velocity [10].

However, it should be noted that significantly higher pressure drop were developed in the particulate support. It is also expected that at higher flow rates the linear relationship of the particulate support would become non-linear due to bed compression and subsequent increase in pressure. The monolithic support would continue in a linear fashion at much higher flow rates. This data shows the general trends and a rough comparison that can be made between the supports; however, it is not enough to allow a direct comparison to be made.

The data for the monolithic support must be transformed into a dimensionless form to allow direct application to equivalent particulate spheres. This enables quantitative treatment of hydraulic permeability accounting for different interstitial porosities and particle diameters and gives a direct comparison between monolithic and particulate supports. A general approach of dimensional analysis for hydraulic permeability can be represented as follows:

$$\frac{\Delta p}{\rho u_{sf}^2} = f\left(\mathrm{Re} = \frac{u_{sf}\bar{x}}{v}, \frac{L}{\bar{x}}, \varepsilon_{inter}, q_i, \psi_i, \mathrm{packing-structure} \right) \ldots\ldots\ldots\ldots\ldots [24]$$

Where ρ is the volumetric density of the liquid, $\bar{x}$ is the mean characteristic length of the porous medium, L is the bed length, ε_{inter} is the interstitial porosity, q_i is the particle size distribution factor and ψ_i is the particle shape distribution factor. Leinweber and Tallarek, 2003 [10] showed that there was seemingly no clear relationship between bed structure properties such as porosity or macropore structure and permeability according to Darcy's law. An approach using the Darcy-Weißbach friction factor-Reynolds number relationship was used for scaling permeability data for porous media.

$$F = \frac{\Delta p}{\rho u_{sf}^2}\frac{L_{flow}}{L_{bed}} = f\left[\mathrm{Re} = \frac{u_{sf}L_{flow}}{v}, \varepsilon_{inter}, q_i, \psi_i \right] \ldots\ldots\ldots\ldots\ldots [25]$$

Where F is the Darcy-Weißbach friction factor, L_{flow} is the ratio of bed length divided by the mean characteristic length of the porous media and L_{bed} is the bed length. Using this equation allows monolithic materials to be given a value which describes the macroscopic permeability in terms of average particle size diameter spheres for a particulate medium. This allows a straightforward comparison between monolithic and particulate media and has been used by Leinweber and Tallarek, 2003 [10] for silica based monoliths.

BIOPRODUCT PURIFICATION

Polymethacrylate monolith for anion-exchange purification

Ion-exchange chromatography (IEC) is the most widely used chromatographic method for separation and purification of biomolecules [3, 5, 12]. This process involves the separation of biomolecules based on their ionic charge and molecular size. The mixture of biomolecules to be separated is contained in the mobile phase which is passed over a solid stationary phase. The stationary phase is functionalized with an ion-exchange ligand attached to the surface to allow the ionic interactions to occur. Since most intercellular biomolecules are negatively charged in nature, the type of ion-exchange chromatography used for most biomolecule separation is anion-exchange chromatography. In anion-exchange chromatography, the anions in the mobile phase are retained by the stationary phase and the remaining mixture flows through. After the desired anions are retained on the support, they are eluted out of the stationary phase by passing an ion-exchange with a stronger anionic strength, commonly NaCl or NaOH [12, 13]. The rate of migration along the stationary phase is dependent on the charge density of the biomolecules, thus, enabling the separation of different biomolecules attached to the stationary phase. A high salt concentration solution containing the desired product is produced and is purified using membrane filtration with water to remove the salt. An important factor in IEC is the binding capacity of the support [5]. The binding capacity depends on many factors including the availability of ion-exchange ligands for interaction with the biomolecules in the mobile phase. Polymethacrylate monoliths are suitable for activation with different functional groups due to the presence of reactive epoxy group found on the monomers. This epoxy group can be functionalized with an ion-exchange ligand and by changing the monomer ratio the density of available ion-exchange ligands which allows tailoring for a specific application can be dictated [4]. This flexibility in ligand density has been extended to look at specific supports for the separation of large biomolecules using weakly activated supports. Controlling the density of ligands to a minimum for the retention of the desired biomolecule allows a much milder elution and avoids high ionic strength and pH solutions passing through the support. This concept is well presented in Figure 7. The chemical stability of polymethacrylate monoliths allows significant ligand retention and becomes very important when ligand cost is high. During the elution and regeneration phases of the chromatographic process, strong basic solutions are passed through the column severally so if the column is not resistant to such reagents the support will degrade and the ion-exchange ligand would be lost.

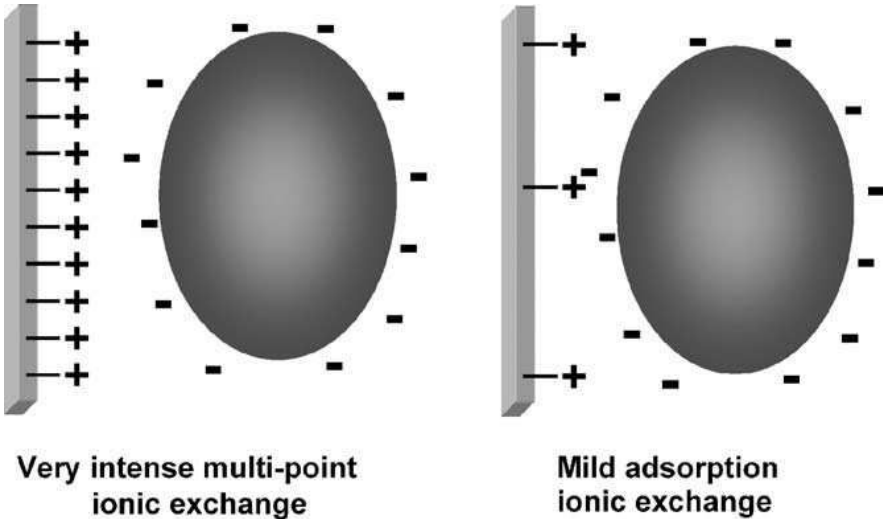

Figure 7: Adsorption mechanism of proteins on differently activated anion-exchange supports [14].

Polymethacrylate monolith for hydrophobic interaction purification

Hydrophobic interaction chromatography (HIC) is a less widely used method of purification of biomolecules compared to ion-exchange chromatography [5]. The technique involves passing a mobile phase across a stationary phase immobilized with hydrophobic interaction ligands [15]. The biomolecules that are to be purified possess hydrophobic characteristics which enable them to interact with the immobilized ligands on the support when in a solution. This process is usually used for the purification of proteins, however, it can be used for the separation of nucleic acids, viruses, cells and carbohydrates [4]. The process is much milder than other chromatographic separation methods because the retained molecules are eluted in increasing order of hydrophobicity [16]. The separation of biomolecules through HIC depends on the hydrophobicity of the biomolecule surface and density as well as the type of hydrophobic ligands attached to the surface of the support. The hydrophobicity of a biomolecule is an intrinsic property and often cannot be changed absolutely; however, the total hydrophobicity of the separation medium can be adjusted during preparation. The adjustments can be made through alterations in ligand density and/or the number of C-atoms on the ligand chains [5]. Polymethacrylate monoliths possess epoxy groups that can easily be

activated with hydrophobic ligands and also exhibits the flexibility of altering the degree of hydrophobicity. The total ligand density can be altered on polymethacrylate monoliths by changing the monomer ratio prior to polymerization.

Polymethacrylate monolith for affinity purification

Affinity chromatography (AC) is one of the most selective methods of purification. However issues around stability and cost of affinity ligands gives this method limited industrial applications despite widespread use in the laboratory [17, 18]. This method relies on the attractive force between different molecules or functional groups; for example an antibody and an antigen, enzymes and substrates, and receptors and ligands. As with other chromatographic methods, there is a mobile phase that passes through a stationary phase. The mobile phase contains the molecule to be purified and the stationary support contains a surface with preference to retain only the desired molecule. Slow adsorption kinetics are considered to be the rate limiting step in AC rather than mass transfer which limits other chromatographic methods [4]. As a result, the major advantage of convective transport in monolithic stationary phases generally plays a little role in AC. However, there are other conditions of affinity chromatography process where monolithic supports are vital. Due to the variety of AC, there are no set rules for an ideal separation but there are some important factors the support should have. With AC, the cost of ligand can often be very high and therefore ligand selectivity of the support is important to ensure the most efficient functionalisation of the support. Polymethacrylate monolithic supports may contain relatively reactive functional groups that can either be used directly for purification or can be functionalized to give a variety of affinity orientations. Polymethacrylate monoliths also tend to have a low non-specific binding for many biological agents which is a benefit when trying to maximize ligand immobilization efficiency [19]. If desired, the monolith can be functionalized during preparation by attaching the affinity ligand to a co-monomer prior to polymerization [4]. A method has been developed by Jungbauer and Hahn, 2008 [2] for functionalisation of monolithic supports where ligands are only attached to sites which are able to be reached by the target molecule. This increases the efficiency of affinity chromatography when using monolithic supports. Table 1 summarizes the conditions and performances of different biomolecule purification technologies reported in literature.

BIOMOLECULAR PRODUCTS

Peptides and oligonucleotides

Peptides and oligonucleotides are less predictable than other biomolecules during separation due to their irregular charge distribution and subsequent irregular adsorption sites. A short monolithic column has been used to separate three linear lysine homologues and the support showed similar performance to conventional packed columns. This shows that the thin monolithic columns have enough theoretical plates to fulfill the requirements of isocratic separation. Yamamoto et al, 2007 [20] have also reported retention of oligonucleotides of various sizes at linear gradient conditions using anion exchange chromatography on thin monolithic columns. Podgornik et al, 1999 [21] separated four oligodeoxynucleotides using commercially available Convective Interaction Media (CIM) disks which are methacrylate-based. The separation was reported to improve by increasing column length. A similar result was obtained by Podgornik et al, 2002 [22] when separating organic acids.

Proteins

There are a very wide variety of proteins and many research papers have reported on protein separation using monolithic supports. Podgornik et al, 1999 [23] and Podgornik et al, 2001 [24] have looked at the use of disks to separate manganese peroxidase and lignin peroxidase.

The result was a faster separation than was possible with a packed column. Also, the lower bed volume of the monolithic disk compared to the packed column gave a higher peak height of the same sample. The sensitivity of analysis is higher and therefore monolithic supports are recommended for purification of proteins in dilute solutions. Branovich et al, 2003 [25] demonstrated using 8, 80 and 500 mL DEAE functionalised poly(GMA-co-EDMA) and DEAE-Sephadex tubes to isolate factor IX from human plasma. The result was a reduced separation time and increased specific activity of the product when using DEAE functionalised poly(GMA-*co*-EDMA).

Nucleic Acids

The separation of nucleic acids is generally governed by the overall negative charge carried by the molecule in the case anion-exchange chromatography as well as the sequences available in the case of affinity chromatography. The number of theoretical binding sites for a pDNA molecule is much higher than that for proteins as an average protein binds with 3–10 sites the pDNA binds with 50 sites on the same support [2]. Short monolithic columns have been used by Benčina et al, 2004 [26] for the separation of DNA molecules and the dynamic

binding capacity was unaffected by flow rate. Double stranded RNA has also been separated by Jerman et al, 2005 [27] using monoliths. They revealed the presence of pathogens in total nucleic acid extracts originating from an infected plant tissue in only 15 minutes, thus, avoiding nucleic acid precipitation and electrophoretic analysis. Monolithic columns were applied in high performance liquid chromatography (HPLC) by Brgles et al, 2007 [28] to separate DNA molecules and the results were positive. The separation was fast and effective in contrast to other methods, avoiding DNA labeling. Danquah and Forde, 2007 [29] reported a detailed study on the properties of the mobile and stationary phases and their influence on separation efficiency using poly(GMA-*co*-EDMA) monoliths. The stationary phase pore size and ligand density were studied and it was observed that the pDNA binding capacity increased as the pore size decreased due to increase in the specific surface area of the stationary phase.

Viral particles

Viral particles are basically nucleic acids inside a protein capsid which is surrounded by a lipid bilayer and glycoproteins. This structure gives the particle a charge and can be separated by IEC. Monolithic disks have been widely used to concentrate viral particles [30-32]. All the different applications were successful with high levels of product recovery and purification.

CONCLUSION

The objective of this review is to highlight the versatility of polymethacrylate monolithic supports for chromatographic purification of biomolecules. Polymethacrylate monolithic supports are a relatively new technology when compared to the particulate supports and even other monolithic supports which have been extensively used in process chromatography. The benefits associated with polymethacrylate monolithic support are significant, in particular for retention and purification of large biomolecules. The large pore diameter of polymethacrylate monolith allows a greater variety of biomolecules to be retained by the immobilized ligands and also provides convective mass transfer which is superior to diffusion based transport found in particulate supports. The large pores also allow higher flow rates through the support at low pressure drops. This leads to high capacity of separation and product recovery. The advantages and rapid developments in polymethacrylate monolith applications point towards a more extensive use in the future.

Table 1: Performance of different chromatographic purification technologies

Technology	Adsorbent	Chromatography	Feedstock	Performance
Polymerization of a High Internal Phase Emulsion (HIPE) [7]	PolyHIPE Methacrylate Monolith (90% pore volume)	HPLC	Protein solution (Myoglibin, conalbumin and soybean trypsin inhibitor)	Breakthrough is much lower than commercially available supports however an optimized process with smaller pore volume (greater surface area) could provide higher capacities.
Weak ion-exchange grafted methacrylate monolith [33]	Grafted weak anion-exchange methacrylate monolith	Anion-exchange	Protein solution (BSA, Thyroglobulin and β-lactoglobulin)	Capacity and separation are flow unaffected up to higher linear velocities than commercially available monoliths. Higher capacity (80mg/ml) compared to CIM disks (25mg/ml).
Weakly activated anion-exchange supports [14]	Particulate and monolithic	Anion-exchange	B-galactosidase and Catalase	Purity was much higher after elution compared to highly activated supports. However does show lower activation degree (less of the protein was retained).
Magnetic particulates [34]	Particulate	Anion-exchange	pDNA from an untreated bacterial lysate	Recovery yield was 91.7% and nearly 100% protein and 62.5% RNA removal. Work shows strategy can be used with high recovery and yield.
Customized biporous hydrophobic adsorbent [35]	Particulate	Hydrophobic	pDNA (0.32mg/ml), RNA (0.42mg/ml) and protein (50μg/ml)	pDNA recovered was ~100 %. Mobile phase flow rate is 5–10 times higher than normal preparative chromatography.
Intein-mediated protein litigation (IPL) in conjunction with chitin affinity chromatography [36]	N/A	Affinity	Animal sera	The column specifically retained the antibodies raised against the antigen present on the resin.

REFERENCES

[1] Lyddiatt, A., *Current Opinion in Biotechnology* 2002, *13*, 95-103.

[2] Jungbauer, A., Hahn, R., *Journal of Chromatography A* 2008, *1184*, 62-79.

[3] Zou, H., Huang, X., Ye, M., Luo, Q., *Journal of Chromatography A* 2002, *954*, 5-32.

[4] Urban, J., Jandera, P., *Journal of Separation Science* 2008, *31*, 2521-2540.

[5] Vlakh, E. G., Tennikova, T. B., *Journal of Chromatography A* 2009, *1216*, 2637-2650.

[6] Podgornik, A., Jancar, J., Merhar, M., Kozamernik, S.*, et al.*, *Journal of Biochemical and Biophysical Methods* 2004, *60*, 179-189.

[7] Krajnc, P., Leber, N., Stefanec, D., Kontrec, S., Podgornik, A., *Journal of Chromatography A* 2005, *1065*, 69-73.

[8] Mondal, K., Gupta, M. N., Roy, I., *Analytical Chemistry* 2006, *78*, 3499-3504.

[9] Du, K.-F., Yang, D., Sun, Y., *Journal of Chromatography A* 2007, *1163*, 212-218.

[10] Leinweber, F. C., Tallarek, U., *Journal of Chromatography A* 2003, *1006*, 207-228.

[11] Danquah, M. K., Forde, G. M., *Journal of Chromatography A* 2008, *1188*, 227-233.

[12] Vidic, J., Podgornik, A., Jancar, J., Frankovic, V.*, et al.*, *Journal of Chromatography A* 2007, *1144*, 63-71.

[13] Guiochon, G., *Journal of Chromatography A* 2007, *1168*, 101-168.

[14] Pessela, B. C. C., Munilla, R., Betancor, L., Fuentes, M.*, et al.*, *Journal of Chromatography A* 2004, *1034*, 155-159.

[15] Ikegami, T., Tomomatsu, K., Takubo, H., Horie, K., Tanaka, N., *Journal of Chromatography A* 2008, *1184*, 474-503.

[16] Diogo, M. M., Queiroz, J. A., Prazeres, D. M. F., *Journal of Chromatography A* 2005, *1069*, 3-22.

[17] Labrou, N. E., *Journal of Chromatography B* 2003, *790*, 67-78.

[18] Frey, D. D., Kang, X., *Current Opinion in Biotechnology* 2005, *16*, 552-560.

[19] Rangan Mallik, D. S. H., *Journal of Separation Science* 2006, *29*, 1686-1704.

[20] Yamamoto, S., Nakamura, M., Tarmann, C., Jungbauer, A., *Journal of Chromatography A* 2007, *1144*, 155-160.

[21] Podgornik, A., Barut, M., Jancar, J., Strancar, A., *Journal of Chromatography A* 1999, *848*, 51-60.

[22] Podgornik, A., Barut, M., Jaksa, S., Jancar, J., Strancar, A., *Journal of Liquid Chromatography & Related Technologies* 2002, *25*, 3099 - 3116.

[23] Podgornik, H., Podgornik, A., Perdih, A., *Analytical Biochemistry* 1999, *272*, 43-47.

[24] Podgornik, H., Podgornik, A., Milavec, P., Perdih, A., *Journal of Biotechnology* 2001, *88*, 173-176.
[25] Branovic, K., Buchacher, A., Barut, M., Strancar, A., Josic, D., *Journal of Chromatography B* 2003, *790*, 175-182.
[26] Bencina, M., Podgornik, A., Strancar, A., *Journal of Separation Science* 2004, *27*, 801-810.
[27] Jerman, S., Podgornik, A., Cankar, K., Cadez, N*., et al.*, *Journal of Chromatography A* 2005, *1065*, 107-113.
[28] Brgles, M., Halassy, B., Tomasic, J., Santak, M*., et al.*, *Journal of Chromatography A* 2007, *1144*, 150-154.
[29] Danquah, M. K., Forde, G. M., *Biotechnology and Applied Biochemistry* 2007, *48*, 85-91.
[30] Branovic, K., Forcic, D., Ivancic, J., Strancar, A*., et al.*, *Journal of Virological Methods* 2003, *110*, 163-171.
[31] Kramberger, P., Peterka, M., Boben, J., Ravnikar, M., Strancar, A., *Journal of Chromatography A* 2007, *1144*, 143-149.
[32] Kramberger, P., Petrovic, N., Strancar, A., Ravnikar, M., *Journal of Virological Methods* 2004, *120*, 51-57.
[33] Frankovic, V., Podgornik, A., Lendero Krajnc, N., Smrekar, F*., et al.*, *Journal of Chromatography A* 2008, *1207*, 84-93.
[34] Zhang, H.-P., Bai, S., Xu, L., Sun, Y., *Journal of Chromatography B* 2009, *877*, 127-133.
[35] Li, Y., Dong, X.-Y., Sun, Y., *Biochemical Engineering Journal* 2005, *27*, 33-39.
[36] Sun, L., Ghosh, I., Xu, M.-Q., *Journal of Immunological Methods* 2003, *282*, 45-52.

CHAPTER 3

LAB-SCALE BACTERIAL FERMENTATION FOR PLASMID PRODUCTION

Section 3.1

Cultivation of *E. coli* carrying a plasmid-based Measles vaccine construct (4.2 kbp pcDNA3F) employing medium optimisation and pH-temperature induction techniques

Microbial Cell Factories. 10: 16 (2011)

Monash University

Declaration for Thesis Section 3.1

Declaration by candidate

In the case of Section 3.1, the nature and extent of my contribution to the work was the following:

Nature of contribution	Extent of contribution (%)
Initiation, Key ideas, Experimental, Development, Results interpretations, Writing up	85

The following co-authors contributed to the work. Co-authors who are students at Monash University must also indicate the extent of their contribution in percentage terms:

Name	Nature of contribution
Raelene Pickering	Experimental
Dr. Diane Webster	Experimental
Dr. Michael K. Danquah	Initiation, Key ideas, Experimental, Development, Results interpretations, Writing up

Candidate's signature		**Date**

Declaration by co-authors

The undersigned hereby certify that:

1. the above declaration correctly reflects the nature and extent of the candidate's contribution to this work, and the nature of the contribution of each of the co-authors;
2. they meet the criteria for authorship in that they have participated in the conception, execution, or interpretation, of at least that part of the publication in their field of expertise;
3. they take public responsibility for their part of the publication, except for the responsible author who accepts overall responsibility for the publication;
4. there are no other authors of the publication according to these criteria;
5. potential conflicts of interest have been disclosed to (a)granting bodies, (b) the editor or publisher of journals or other publications, and (c) the head of the responsible academic unit; and
6. the original data are stored at the following location (s) and will be held for at least five years from the date indicated below:

Location	Chemical Engineering Department, Monash University, Clayton, Australia

Signature		**Date**

Cultivation of *E. coli* carrying a plasmid-based Measles vaccine construct (4.2 kbp pcDNA3F) employing medium optimisation and pH-temperature induction techniques

Clarence M. Ongkudon, Raelene Pickering, Diane Webster, Michael K. Danquah

ABSTRACT

Background: Plasmid-based measles vaccines offer great promises over the conventional fertilised egg method such as ease of manufacture and mimic wild-type intracellular antigen expression. The increasing number of clinical trials on plasmid-based measles vaccines has triggered the need to make more in less time. **Results:** In this work, we investigated the process variables necessary to improve the volumetric and specific yields of a model plasmid-based measles vaccine (pcDNA3F) harboured in *E. coli* DH5*α*. Results from growth medium optimisation in 500 mL shake flasks by response surface methodology (RSM) generated a maximum volumetric yield of 13.65 mg/L which was 1.75 folds higher than that of the base medium. A controlled fed-batch fermentation employing strategic glycerol feeding and optimised growth conditions resulted in a remarkable pcDNA3F volumetric yield of 110 mg/L and a specific yield of 14 mg/g. In addition, growth pH modification and temperature fluctuation between 35 and 45 ^{o}C were successfully employed to improve plasmid production. **Conclusion:** Production of a high copy number plasmid DNA containing a foreign gene of interest is often hampered by the low plasmid volumetric yield which results from the over expression of foreign proteins and metabolic repressors. In this work, a simple bioprocess framework was employed and successfully improved the production of pcDNA3F.

Background

Plasmid DNA (pDNA) vaccine is a third generation of vaccine technology which offers an attractive new alternative to conventional immunisation techniques. In human trials, pDNA has been shown to induce protective immunity similar to that of natural infection for not only measles, but across a broad range of virus families [1]. From a production stand point, the lyophilised form of the current vaccine lacks thermal stability, requiring an uninterrupted cold

chain for maximum efficacy [2]. The enhanced thermal stability of plasmid DNA at room temperature and above offers a great promise for the treatment of measles and other diseases in tropical and economically disadvantaged areas [3]. General steps involve in the production of plasmid vaccines are similar to that of protein production that include fermentation, primary isolation and purification [4]. It is presumed that the mechanisms that contribute to yield improvement are reduced metabolic burden during plasmid synthesis; reduced plasmid mediated protein production and altered DNA compaction during plasmid induction [5]. Various bioprocess engineering approaches that can be employed to alter the growth of *E. coli* hence gene expression have extensively been discussed by Razali *et al*. [6] that include temperature shift techniques, feeding strategies, timing of induction and plasmid stabilisation.

It is important to note that like chromosomal DNA, plasmid DNA is made up of sugar-phosphate backbone and nitrogen base nucleotides (ATGC). Carbon, phosphorus and nitrogen are the main ingredients in DNA biopolymers unlike proteins. Also, in the central dogma of molecular biology, only replication is required for DNA synthesis whilst transcription and translation are added mechanisms for protein synthesis. Thus, cultivation medium for DNA production in *E. coli* is substantially different from protein production [7]. In our previous work [8], we have developed an economically viable semi-complex stoichiometric medium for pUC based plasmid production. In this work, we used the same media and optimised it specifically for plasmid-based Measles vaccine (pcDNA3F) production. Growth temperature up-shifts may be employed to induce plasmid replication and reduce contaminating RNAs and gDNAs by down regulating the growth rate of the cells [3-4]. Several researchers have attempted multiple temperature induction schemes that included constant, gradual and fluctuating temperature shifts specific to a product expression [9-11]. The duration at which the cells are exposed to a certain temperature shift is known to affect the maximum recombinant protein production [12-13]. The use of fluctuating temperatures to achieve selective gene expression has also been reported in other biological systems [14-15]. It is further suggested that a cooling step may be required to drive cells to maximum potential plasmid copy number which may not be possible at higher temperatures [16].

Production of extended cell density and growth-related pDNA yield can be achieved in a fed-batch culture by expanding the cultivation time under the controlled provision of substrates (e.g. glucose, phosphate and oxygen) conducive to pDNA formation and cell growth [3]. A good fed-batch fermentation practice is based on the supplementation of a substrate at a rate such that it is completely consumed. The fermentation commences with a batch mode under

non-limiting conditions and an optimum cell growth rate. When one or more substrates are exhausted, the batch mode is then switched to fed-batch mode [17]. Several methods have been suggested to synchronize substrate feed and demand including an open-loop control scheme where the feeding rate is controlled based on previously established data or fixed model [5, 18-20] and an indirect control of substrate feed based on on-line physiological parameters such as pH, dissolved O_2 and cell concentration [3, 17]. A rational equation based on the biomass yield coefficient $Y_{X/S}$ (g DCW/g substrate) may be employed for a better control of the substrate feeding. In this article, we present bioprocess methods for the improvement of volumetric and specific yields of a model plasmid-based measles vaccine production. It involves medium optimisation, growth pH alteration, varied temperature shifting, fed-batch cultivation and glycerol exponential feeding strategy specific to pcDNA3F-harbouring *E. coli* DH5α cells. pcDNA3F was derived from plasmid pcDNA3 (Invitrogen) and fusion protein gene (F) of measles virus. This work was motivated by the fact that under a pre-defined culture condition, pcDNA3F yields were lower than that of pcDNA3. Consequently, methodologies and results from this study may be used to favour the subsequent development of commercial scale production of pcDNA3F.

Table 1. Composition of basic (PDM) and optimised (PDM-pcDNA3F) medium for DH5α-pcDNA3F cultivation.

Nutrient	PDM (g/L)	PDM-pcDNA3F (g/L)
yeast extract	4.41	4.41
tryptone	7.93	10.60
glucose	10.00	6.50
Na_2HPO_4	12.80	15.70
K_2HPO_4	3.00	3.00
NH_4Cl	0.50	0.50
$MgSO_4$	0.24	0.24

Results and discussions

Medium optimisation

The basic composition of pUC-based plasmid DNA semi-defined medium (PDM) as depicted in Table 1 was reported by [7] which was developed from a stoichiometric analysis. Prior to the medium optimisation, a preliminary medium screening based on Plackett Burman design [21-22] was carried out to select three most significant medium components in PDM and the results showed that tryptone, glucose and disodium hydrogen orthophosphate (Na_2HPO_4) significantly affected pcDNA3F volumetric yield (data not shown).

Following the medium screening, a series of 16 central composite design (CCD) [23] experiments as shown in Table 2 were conducted to optimise tryptone, glucose and disodium hydrogen orthophosphate (Na_2HPO_4) contents in PDM. The concentrations of tryptone, glucose, and Na_2HPO_4 in each experiment were varied from 0.5 g/L (coded value = -2) to 18.5 g/L (coded value = +2). The central value of 10 g/L (coded value = 0) was chosen as the average concentration of tryptone, glucose, and Na_2HPO_4 in PDM. The parameters' coefficients obtained from the ANOVA (Table 3) were used to construct the second-order polynomial model which explained the correlation of each nutrient and their second-order interactions with the plasmid volumetric yield. Thus, pcDNA3F volumetric yields were predicted by the following equation.

$$y = a_o + a_1 x_1 - a_2 x_1^2 - a_3 x_2 - a_4 x_2^2 + a_5 x_3 - a_6 x_3^2 + a_7 x_1 x_2 - a_8 x_1 x_3 - a_9 x_2 x_3 \qquad (1)$$

where $a_0, a_1, a_2, a_3, a_4, a_5, a_6, a_7, a_8, a_9$ are parameters' coefficients as shown in Table 3, x_1 is the coded value of tryptone concentration, x_2 is the coded value of glucose concentration, x_3 is the coded value of Na_2HPO_4 concentration and y is the pcDNA3F volumetric yield (mg/L). The quadratic model in equation (1) involves nine terms consisting of three linear terms, three quadratic terms, and three two-factor interactions. All terms were included in the model to give the best fit of the experimental data. Generally, the equation shows a good agreement between predicted and observed experimental data (Table 2). The lack of fit of the model was checked by the determination coefficient (R^2) which is the ratio of *SS* (regression) to *SS* (total). R^2 is a measure of the amount of reduction in the variability of y obtained by using the parameters' coefficients in the model. The value of the determination coefficient ($R^2 = 0.95$) indicates that 95% of the data are well matched by equation (1). The significance of each coefficient was determined by student's *t*-test, *F* and *P* values, which are listed in Table 3.

Table 2. Central composite design for the optimization of tryptone, glucose and disodium hydrogen orthophosphate concentrations.

	Coded Values*			Real Values*			*y*= pDNA (mg/L)	
				g/L	g/L	g/L		
Run no.	x_1	x_2	x_3	X_1	X_2	X_3	**Actual**	**Predicted**
1	-1	-1	-1	5	5	5	6.99	6.75
2	-1	-1	1	5	5	15	11.7	10.98
3	-1	1	-1	5	15	5	6.03	6.06
4	-1	1	1	5	15	15	7.95	7.74
5	1	-1	-1	15	5	5	7.65	7.2
6	1	-1	1	15	5	15	12.03	11.31
7	1	1	-1	15	15	5	8.43	8.46
8	1	1	1	15	15	15	10.44	10.02
9	-1.7	0	0	1.5	10	10	6.27	6.6
10	1.7	0	0	18.5	10	10	8.34	8.94
11	0	-1.7	0	10	1.5	10	9.06	9.96
12	0	1.7	0	10	18.5	10	8.25	8.28
13	0	0	-1.7	10	10	1.5	6.66	6.69
14	0	0	1.7	10	10	18.5	10.71	11.61
15	0	0	0	10	10	10	11.79	11.55
16	0	0	0	10	10	10	11.43	11.55

* x_1, x_2 and x_3 are coded values of tryptone, glucose and disodium hydrogen orthophosphate concentrations respectively whilst X_1, X_2 and X_3 correspond to real values of tryptone, glucose and disodium hydrogen orthophosphate concentrations respectively.

Table 3. ANOVA.

Parameter*	**Coefficients,** a_n		***SS***	***t*-Stat**	***MS***	***F***	***P***
Intercept	$a_0 =$	11.55		20.99			0.00
x_1	$a_1 =$	0.69	6.41	3.25	6.41	10.54	0.02
$x_1 . x_1$	$a_2 =$	-1.32	16.35	-5.19	16.35	26.88	0.00
x_2	$a_3 =$	-0.51	3.48	-2.38	3.48	5.68	0.05
$x_2 . x_2$	$a_4 =$	-0.84	6.78	-3.34	6.78	11.15	0.02
x_3	$a_5 =$	1.44	28.75	6.88	28.75	47.28	0.00
$x_3 . x_3$	$a_6 =$	-0.84	6.61	-3.30	6.61	10.87	0.02
$x_1 . x_2$	$a_7 =$	0.48	1.90	1.77	1.90	3.13	0.13
$x_1 . x_3$	$a_8 =$	-0.03	0.01	-0.11	0.01	0.01	0.92
$x_2 . x_3$	$a_9 =$	-0.66	3.33	-2.34	3.33	5.47	0.06
	residual		6.08		6.08		
	R^2		94.60				
	Adjusted R		86.78				

*x_1 is the coded value of tryptone concentration, x_2 is the coded value of glucose concentration and x_3 is the coded value of Na_2HPO_4 concentration.

The *F* values show how larger the mean square of the coefficients compared to mean square of the residuals (errors). The significance of *F* value or sometimes referred to as *P* value is the probability to get larger *F* value by chance alone. The larger the magnitude of the *t* and *F* values and the smaller the *P* value, the more significant the corresponding coefficient is. As a rule of thumb, coefficients with $P < 0.05$ are considered significant. In general, the linear (x_1, x_2, x_3) and quadratic (x_1^2, x_2^2, x_3^2) interactions between the coefficients and plasmid yield are significant thus contribute to the adequacy of the regressed model. The magnitudes of the linear and quadratic terms are evenly large which show that they all contributed significantly to the plasmid volumetric yield.

Table 4. Analysis of plasmid production and cell growth in different commercially available media and PDM-pcDNA3F.

Medium	pcDNA3F volumetric yield* (mg/L)	pcDNA3F specific yield* (mg/g)	pcDNA3F production rate* (mg/L/h)	Final cell density* (g/L)	Cell growth rate* (h^{-1})
Terrific Broth	8.40	4.31	0.56	1.95	0.85
Luria Broth	5.80	7.94	0.39	0.73	0.31
2xYT	6.42	3.82	0.43	1.68	0.77
PDM	7.80	3.57	0.52	2.18	0.89
PDM-pcDNA3F	13.65	9.10	0.91	1.50	0.75

*Cells were cultured in 250 ml of medium containing 100 μg/mL ampicillin using 500 mL shake flasks at 200 rpm, 37 ^{o}C and halted after 15 h. Each value represents an average of triplicates. Standard deviations for all data are 1 – 5% of the values shown.

The negative values of the quadratic terms also indicate that there are maximum values for each nutrient's concentration. Based on the corresponding *t*, *F* and *P* values, Na_2HPO_4 seems to have the most profound impact on pcDNA3F volumetric yield. This is true since phosphate forms a major component in the plasmid structure. Meanwhile, the two-way interaction between tryptone (x_1) and Na_2HPO_4 (x_3) yields the lowest *F* value. This indicates that both nutrients have a distinct role in plasmid synthesis possibly due to lack of phosphate in tryptone. Glucose (x_2) and tryptone (x_1) also have insignificant interaction possibly due to lack of carbon source in tryptone while glucose (x_2) and Na_2HPO_4 (x_3) generally have a high

degree interaction possibly because glucose and Na_2HPO_4 are the main components in plasmid backbone.

RSM was carried out to predict the highest point of plasmid yield as well as optimum values of tryptone, glucose and Na_2HPO_4 concentration using equation (1). The optimum values of the parameters in coded values are $x_1 = 0.12$, $x_2 = –0.69$, and $x_3 = 1.13$ with the corresponding response y = 12.59 mg/L. This translates to real values of the test variables which are given in Table 1. Actual experiments using the optimised medium were carried out and the results showed that the optimised medium for pcDNA3F cultivation resulted in an improved volumetric yield of 13.65 $\pm$ 0.10 mg/L which is 1.75 folds higher than the non-optimised medium (7.80 $\pm$ 0.2 mg/L). In summary, the utilisation of experimental design and RSM on three important factors of the plasmid DNA medium resulted in a markedly improved plasmid pcDNA3F yield.

To evaluate the performance of the optimised medium against commercial medium, *E. coli* carrying pcDNA3F was cultured in different commercially available growth media. Parameters such as plasmid volumetric and specific yields as well as production rates were compared and the results are shown in Table 4. Although the results are mixed, but it can immediately be seen that the optimised medium (PDM-pcDNA3F) has significant advantages over other medium in terms of highest plasmid production rate and specific yield.

Effect of growth conditions on cell growth and pcDNA3F production

E. coli has traditionally been grown at pH~7. In plasmid DNA production, it is conjectured that a moderate pH deviation might have a positive effect on plasmid yield. Thus, pcDNA3F volumetric and specific yields were assessed at different initial pH ranging from 6 to 8.5. The result as shown in Fig. 1 demonstrates that reduced cell growth rate does not necessarily followed by an increase in pcDNA3F yield.

Generally at lower pH, cell growth and pcDNA3F production were suppressed whilst at higher pH; pcDNA3F yield was improved with decreased cell growth. At pH 6 – 7, pcDNA3F yield was dependent on biomass yield; thus plasmid yield increased as maximum cell growth rate increased. At pH 7 – 7.5, a non-growth dependent or inverse correlation profile was displayed. A maximum cell growth rate of ~ 0.9 h^{-1} was obtained at pH 7 where pcDNA3F volumetric and specific yields were ~ 5 mg/L and ~ 3 mg/g respectively. Optimum pcDNA3F yield of ~ 7 mg/L (4 – 5 mg/g) was achieved at pH 7.5 when the cell growth rate was only 0.8

h^{-1}. From a molecular perspective, pH gradient across a cell membrane is theoretically related to the generation of proton motive force (PMF). Subsequently, PMF is likened to the production of ATP for use in different cellular metabolic pathways including DNA replication. It is presumed that when the extracellular pH condition deviates from neutral to acidic condition, PMF hence ATP drastically drop and suppress both cell growth and plasmid DNA synthesis. This profile is indicated in the pH range of 6 to 7 of Fig. 1. This can be explained by the impairment of ATP production at acidic condition as a result of fuelling pathways and enzyme inhibition as described by [24-25]. Under a low pH stress, ATPases are activated to compensate for pH variations in the cytoplasmic region by proton intrusion into the periplasm with the concomitant consumption of ATPs [25-26].

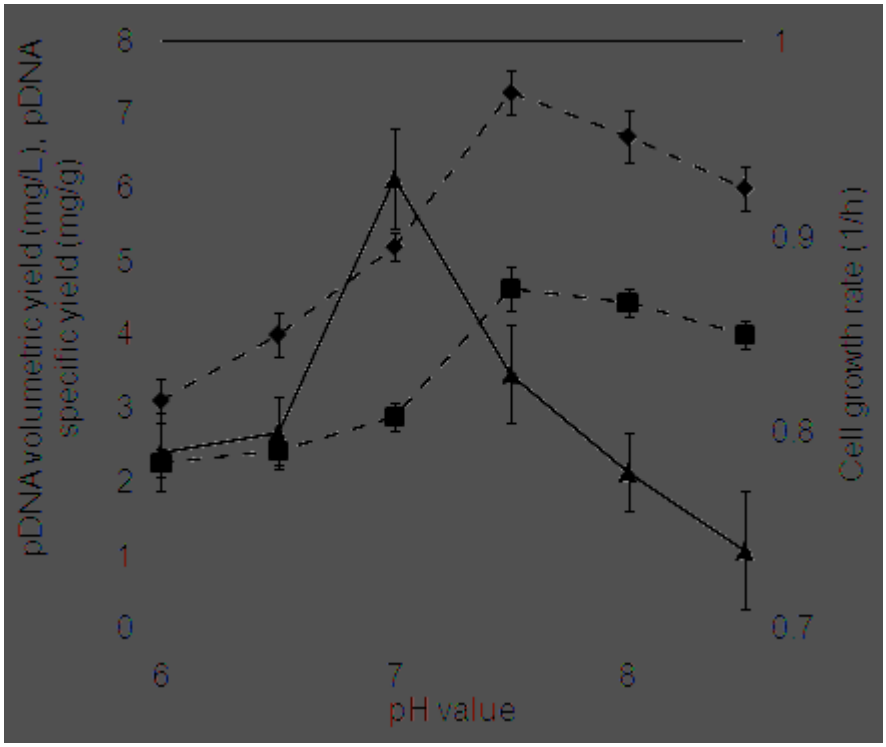

Fig. 1. Effect of pH on cell growth rate and plasmid yield. Cells were cultured in 250 ml of PDM medium using 500 mL shake flasks at 200 rpm, 37 ^{o}C and halted after 15 h. Each data point represents an average of triplicates. Rhombus: pcDNA3F volumetric yield; square: pcDNA3F specific yield; triangle: cell growth rate.

However, it is speculated that a small pH deviation to the alkaline region is needed to generate PMF which preferentially improves plasmid yield over cell growth. In other words, optimum synchronization of cell growth, plasmid synthesis and PMF is achievable in a slightly alkaline condition. These results of effect of pH on plasmid production however, are rather contradictory to studies reported by [27]. In their studies, plasmid pEGFP-N1 was cultivated at initial pH values ranging from 6.5 to 8.5 and the highest plasmid specific yield was obtained at a slightly acidic condition at pH 6.5.

A unique temperature fluctuation (Fig. 2A) was conducted to increase plasmid productivity theoretically by inactivating the synthesis of repressor at higher temperatures and periodically maintaining plasmid stability at lower temperatures. The solid line in Fig. 2A represents equation (2) where $T(t)$ is temperature at time t, $T(0)$ is based temperature, ΔT is temperature deviation, f is frequency of temperature fluctuation, and ϕ is phase at the start of the temperature shift.

$$T(t) = T(0) + \Delta T \sin(2\pi f t + \phi) \quad (2)$$

The duration of temperature shift exposure as indicated by the reciprocal of frequency f in equation (2) shows an optimum value of $1/f$ = 5 h corresponding to an optimum plasmid specific yield of ~ 15 mg/g DCW (Fig. 2B). In addition to that, the use of controlled temperature fluctuation shows great advantages over single step temperature shifts in terms of maximum plasmid volumetric and specific yields (Fig. 2C). Cells exposed to a high temperature regime exhibit diminished growth which can be explained by the over expression of foreign proteins and metabolic repressors [28-29]. An increase in growth temperature results in cloned gene expression as a result of promoter activation which in turn triggers expression of growth inhibitors and metabolic repressors [29]. Plasmid DNA being a temperature stable molecule continues to replicate under this condition. However, prolonged exposure of conditions that derepress the promoter can lead to a decreased ratio of plasmid-harbouring cells[9]. High temperature is also associated with low oxygen solubility and decreased TCA activity hence higher acetate production[10] as well as inhibition of cell wall synthesis leading to filamentation and reduced cell growth [30]. It is thought that returning the culture to a lower temperature regime just before the accumulation of plasmid segregants favours high level of plasmid-harbouring cells for an extended period of time hence higher plasmid volumetric and specific yields are achieved.

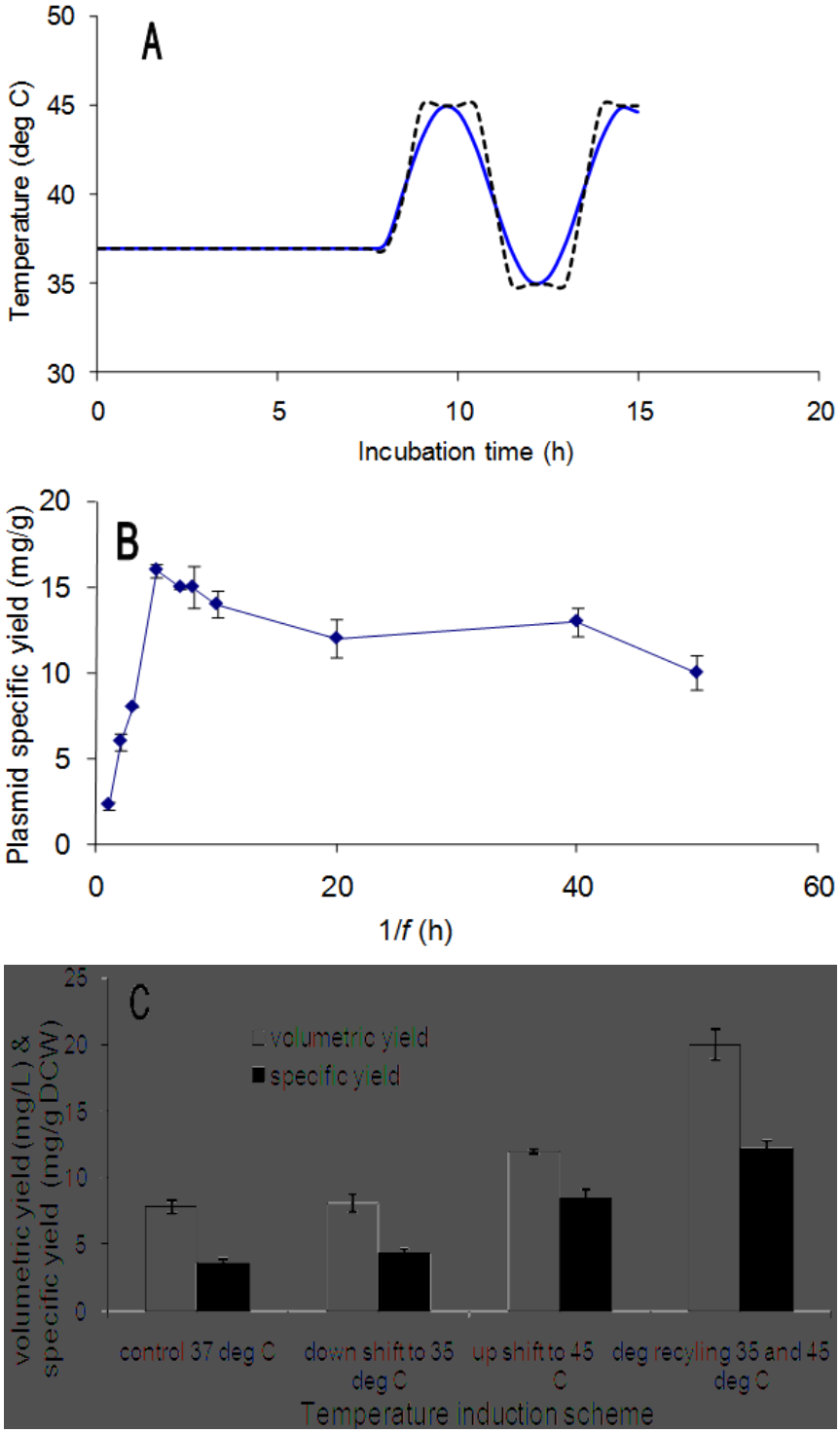

Fig. 2. Effect of different growth temperature induction schemes on plasmid production. Temperature inductions were performed at 8 h post inoculation. Cells were cultured in 250 ml PDM medium using 500 mL shake flasks at 200 rpm, initial temperature of 37 ^{o}C and halted after 15 h. Each data point represents an average of five replicates (n=5). (A) Profiles of an actual (dashed line) and a model (solid line) growth temperature fluctuations. (B) Effect of frequency of temperature fluctuation (1/*f*) on plasmid specific yield. (C) Analysis of plasmid volumetric and specific yields from different temperature induction schemes.

Fed-batch fermentation

Prior to performing the fed-batch fermentation, the effect of *E. coli* cell growth rate on pcDNA3F specific yield (Fig. 3) was studied by growing the culture in batch mode in PDM medium containing different initial concentrations of glucose. Samples were collected every 30 min during the batch fermentations and analysed for cell concentration and pcDNA3F volumetric yield. Glucose was found to affect the cell growth rate (μ) and the final biomass concentration which in turn resulted in different levels of pcDNA3F specific yield as depicted in Fig. 3. A maximum pcDNA3F specific yield of 11 mg/g was achieved at a considerably low cell growth rate of 0.1 h^{-1}. The strong dependency of plasmid specific yield on cell growth rate was evident since a drastic drop in specific yield was observed even at a slight deviation of the cell growth rate. We speculate that the molecular mechanism contributing to this phenomenon is associated with the synchronization of cell growth and plasmid replication. pcDNA3F plasmid is constructed based on pUC plasmid which has high copy number due to the removal of protein repressor (Rop/Rom) gene from its genetic sequence. To reach at the maximum plasmid copy number, it has to undergo multiple cycles of RNA transcription, DNA pairing and ligation in a single *E. coli* cell.

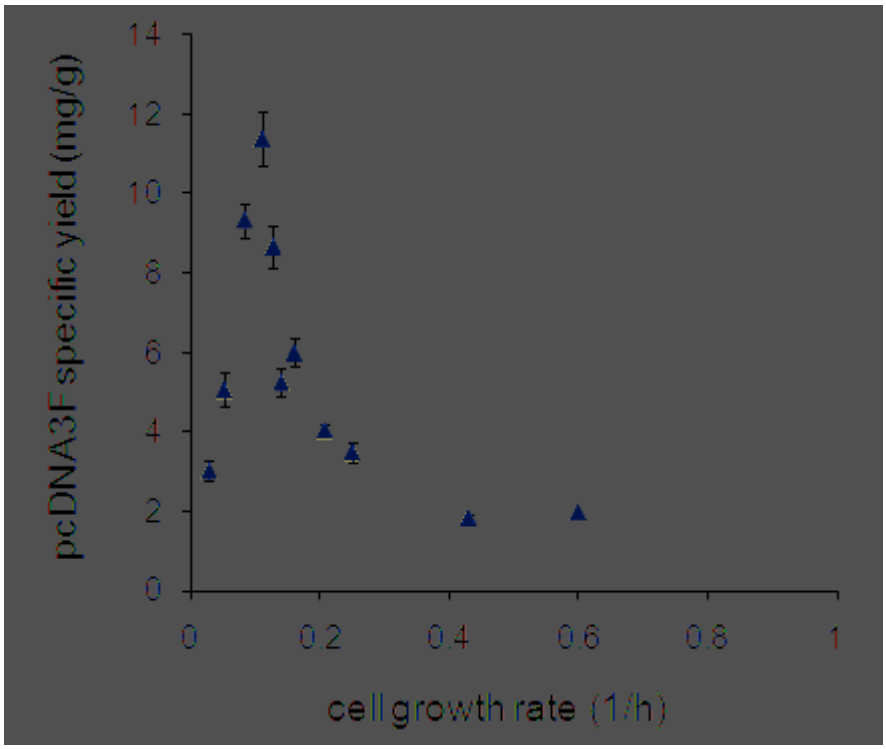

Fig. 3. Effect of cell growth rate of *E. coli* DH5α on pcDNA3F specific yield. Data were obtained from batch fermentations at different initial glucose concentrations. Each data point represents an average of triplicates.

Therefore, cell replication has to be slowed down to give time for the plasmid to complete its continuous extra chromosomal replication.

Batch fermentation was used to initiate a culture under a non limiting environment. This was to accumulate the biomass density within a short period of time thus reducing the initial fermentation cost. In batch fermentation, the cells were cultivated in PDM-pcDNA3F medium at a cell growth rate of 0.6 h^{-1} which was equivalent to a biomass doubling time, t_d of 1.1 h (Fig. 4). As the fermentation progressed, there was a downward trend of cell growth rate which was mainly due to a nutrient depletion. The decreased cell growth rate and increased biomass density both contributed to increase in plasmid volumetric and specific yields. When the carbon source was fully consumed, no significant increase in biomass density was observed. Fed batch process was then initiated under the controlled provision of glycerol into the fermentor.

During the fed-batch phase, the amount of substrate (glycerol) fed into the bioreactor was controlled via an automated peristaltic pump according to equation (3) where F_t is the substrate feeding rate at t h after the fed-batch mode is initiated, F_i is the initial substrate feeding rate, α is the specific exponential feeding rate, and t is the cultivation time during the fed-batch phase. According to equation (3), F_t can be optimised by fine-tuning the values of F_i and α. The value of F_i can be approximated by integration of equation (4) where $\int S_t$ is the cumulative amount of substrate consumed in the batch phase and S_i is the initial substrate consumption rate in the batch phase.

$$F_t = F_i.e^{\alpha t} \quad (3)$$

$$S_t = S_i.e^{\alpha t} \quad (4)$$

$$\int S_t = \int S_i.e^{\alpha t}\,(dt) \quad (5)$$

Therefore,

$$F_i = -S_t \quad \text{(at the start of the fed-batch phase)} \quad (6)$$

A series of experiments was conducted at different α values until the highest point of plasmid specific yield was obtained. Samples were collected every 30 min during the fed-batch phases at different α values and analysed for cell growth rate and the results are shown in Fig 5.

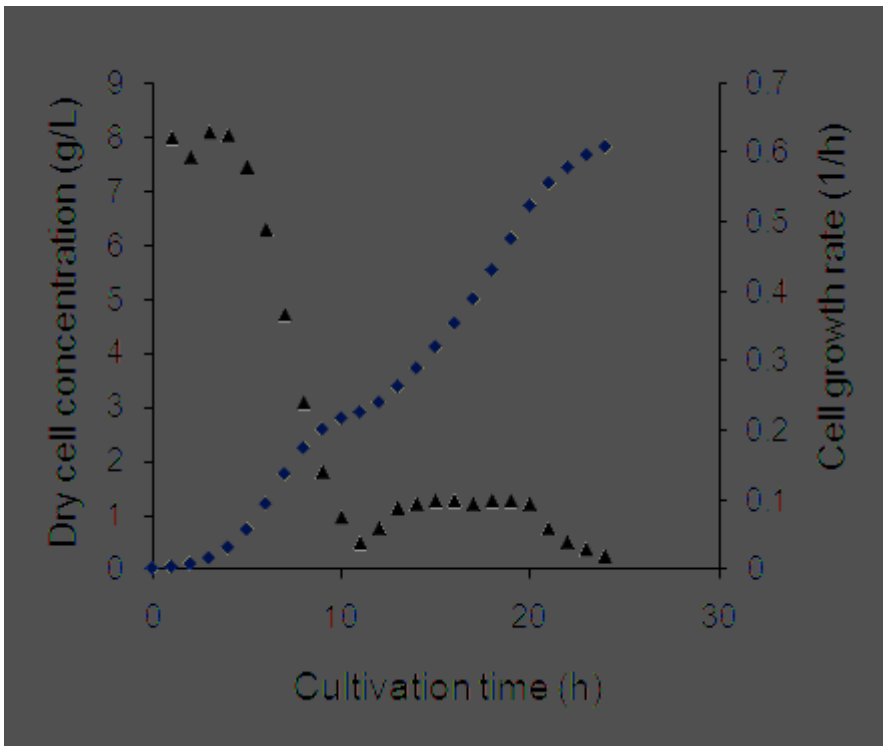

Fig. 4. Dry cell concentration and cell growth rate profiles during fed-batch fermentation of *E. coli* DH5α-pcDNA3F. Glycerol feeding was initiated at 10 h post culture and temperature upshift (37 ^{o}C to 45 ^{o}C) was performed at 20 h post inoculation. Rhombus: dry cell concentration; triangle: cell growth rate.

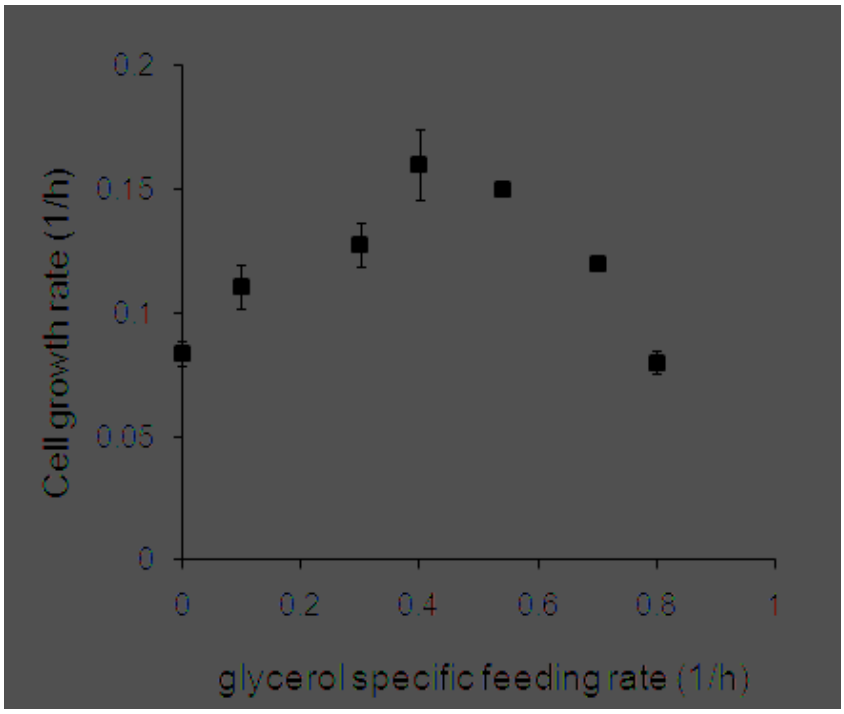

Fig. 5. Cell growth rates of *E. coli* DH5α carrying pcDNA3F at different glycerol exponential feeding rates, α. Data were obtained from fed-batch fermentations at different glycerol feeding rates. Each data point represents an average of triplicates.

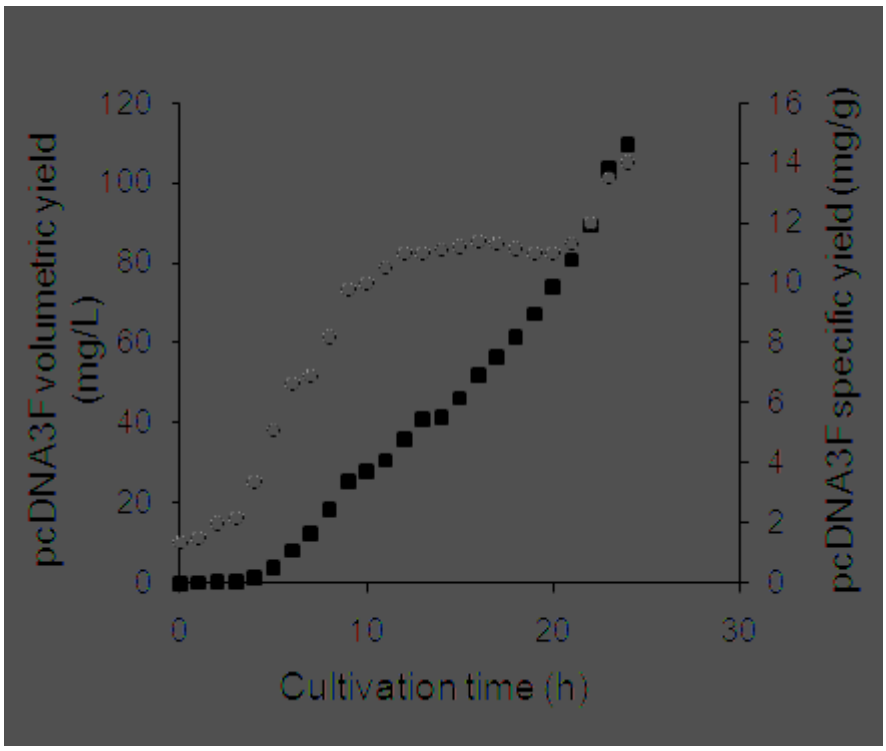

Fig. 6. pcDNA3F volumetric yield and specific yield profiles during fed-batch fermentation of *E. coli* DH5α-pcDNA3F. Glycerol feeding was initiated at 10 h post culture and temperature upshift (37 ^{o}C to 45 ^{o}C) was performed at 20 h post inoculation. Square: volumetric yield; rhombus: specific yield.

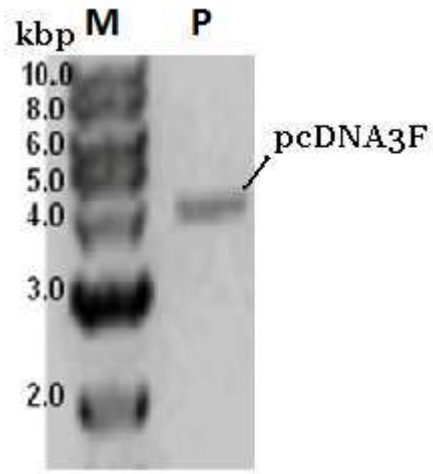

Fig. 7. Ethidium bromide agarose gel electrophoresis of pDNA samples from fed batch fermentation of DH5α-pcDNA3F. Loading volume = 1µL. Analysis was performed using 1% agarose in TAE x 1 buffer, 3 µg/mL ethidium bromide at 65 V for 90 min. Lane M is 1 kb DNA ladder and lane P represents 55.0 mg/L of purified pcDNA3F.

Glycerol exponential feeding strategy greatly affects the cells growth by maintaining the cell growth rate below 0.2 h^{-1} with improved plasmid specific yields. Although a low cell growth rate is beneficial for plasmid replication, this may not hold true at $\alpha > 0.4$. This is due to the significantly large amount of glycerol that needs to be pumped into the bioreactor every hour at $\alpha > 0.4$. As the cultivation time *(t)* and exponential feeding rate (α) increase, the dilution rate (D) becomes extremely large and impractical. In this case, the optimum α value is ~0.1 h^{-1} which is equivalent to a pcDNA3F specific yield of ~12 mg/g.

In this work, the initial glycerol feeding rate was successfully estimated by using an exponential feeding rate equation and assuming that the carbon consumption rate equalled the cell growth rate (μ) in the batch phase. Therefore, the final carbon consumption rate in the batch phase was used as the initial glycerol feeding rate in the fed-batch phase. Using the calculated initial glycerol feeding rate and increasing it exponentially, the biomass proliferated at a reduced cell growth rate of 0.1 h^{-1} (t_d = 6.9 h) (Fig. 4) conducive to pcDNA3F propagation. By maintaining this low cell growth rate throughout the fed-batch phase, a considerably high plasmid specific yield of about 12 mg/g was obtained (Fig. 6). At 20 h post culture, the growth temperature was shifted from 37^{o}C to 45^{o}C. The final plasmid pcDNA3F yields showed a profound improvement compared to that was normally achieved in batch fermentations.

It has been reported elsewhere that the plasmid DNA medium can provide as high as 12 g/L dry cell concentration in a fed-batch system using pUC based plasmid system [7]. We speculated that the fairly low dry cell density obtained in this work using the same base plasmid was due to over expression of foreign gene (MV-F). At the start of the fed-batch mode, cells density was around 3 g/L. Further increase in cell density was observed at 12 h onwards before reaching 6 g/L at 19 h which correlated to a cell growth rate of 0.1 h^{-1} and a biomass doubling time of 7 h. The fermentation was halted at 24 h (early stationary phase) which was equivalent to a final cell density of ~ 8 g/L. Again the harvest time was chosen as the optimum combination between cell growth and plasmid yield. At this point, one or more nutrients became limiting since only carbon substrate was provided in the fed-batch mode. DNA gel electrophoresis of purified pcDNA3F (Fig. 7) showed pure supercoiled plasmid DNA with no nicked plasmid DNA isoforms.

Fed-batch cultivation with glycerol feeding commenced after an initial glucose carbon source in the initial batch fermentation phase has starved. Hence, the fed-batch mode occurred at a

fairly high cell concentration in the late exponential phase. The inconsistency in the source of carbon for the cells during the batch and fed-batch contexts could result in the mismatched pattern in the somewhat initial low growth phase. However, glucose was not used in the fed-batch case as the interest here was to boost plasmid replication and not cell growth. Glycerol was used to tweak cell metabolism to support plasmid replication as the kinetics of glycerol transportation and uptake is slower than glycolysis.

Conclusions

It has been observed that the inclusion of fusion protein gene (F) of measles virus into base plasmid pcDNA3 resulted in reduced plasmid volumetric yields during fermentation compared to naked pcDNA3. This was possibly due to extra factors introduced by the F gene into the culture which interfered with normal plasmid production and *E. coli* cell growth. Higher plasmid yields are often the results of higher plasmid stability and preferential plasmid synthesis over other biomolecules syntheses. Bioreactor and medium designs are known to have significant effects on plasmid yields. One of the unifying criteria for high purity and high yield plasmid cultivation is the use of defined or semi-defined medium that allows the cells to grow at a reduced cell growth rate whilst preferentially boosting plasmid replication rate. At a molecular level, the mechanisms that contribute to plasmid yield improvement are reduced metabolic burden during plasmid synthesis; reduced plasmid mediated protein production and altered DNA compaction during plasmid induction. In this article, concise presentations on the optimisation of medium specifically for pcDNA3F cultivation and the development of fed-batch fermentation by strategic glycerol feeding to improve pcDNA3F volumetric and specific yields were presented. In addition, two simple methods to boost plasmid yield based on the alteration of growth pH and temperature fluctuation were also included. A method for pilot-scale fermentation of *E. coli* carrying plasmid DNA measles vaccine construct was successfully developed based on controlled fed-batch fermentation and optimised growth conditions. This method resulted in an improved plasmid based (pcDNA3) measles (F) vaccine volumetric yield of 110 mg/L and specific yield of 14 mg/g. *In vitro* study also showed that the MV-F protein was successfully expressed (data not shown) from pcDNA3F produced using the optimised fed-batch cultivation method.

Materials and methods

Materials

Maximum efficiency *E. coli* DH5*α* and pcDNA3 vector were purchased from Invitrogen, VIC, Australia. Tryptone, yeast extract, KH_2PO_4 (99.5%) and glucose (99%) were purchased

from Merck, NJ, USA. NH_4Cl (99.5%), ethidium bromide (1%), NaOH (99%), HCl (36.5%), and $MgSO_4$ (99.5%) were purchased from Sigma-Aldrich, NSW, Australia. Glycerol (99.5%) and NaCl (99.5%) were purchased from Amresco, OH, USA and disodium hydrogen orthophosphate, Na_2HPO_4 (99%) was purchased from Univar, WA, USA.

Plasmid design

To construct pcDNA3F vaccine, 1.65 kb open reading frame of the measles virus fusion (MV-F) gene from plasmid pTM1-F was amplified by PCR using the oligonucleotides: 5'ACGTAAGC TTACCATGGGTCTCAAGGTGAACGTC 3' and 5' ATGCTCTAGAGCTCAGAGCGACCT TACATAGG 3' containing *Hind*III and *Xba*I restriction enzyme sites respectively. This was followed by ligation into the pcDNA3 vector, and transformation into competent *E. coli* DH5*α* cells.

Cell propagation and monitoring

10 µL of transformed cells (*E. coli* DH5*α*-pcDNA3F) was cultured in LB-agar-ampicillin plate at 37°C overnight. A single *E. coli* DH5*α*-pcDNA3F colony was picked from the LB-agar-ampicillin plate and subcultured with 250 mL of LB media containing 100 µg/mL ampicillin at 37°C overnight under 200 rpm shaking. Subsequently, 2 mL of the culture was inoculated into 250 mL medium containing 100 µg/mL ampicillin. The batch fermentation was run at 37°C under 200 rpm shaking and was halted at late exponential phase at 15 h. 15 h was selected as the harvest time for batch fermentation as it provided a good combination between optimum cell growth and plasmid production. 1 mL of culture was sampled after every hour for cell growth and plasmid yield analysis.

Growth media optimisation

2 mL of fresh innoculums were cultured in 500 mL shake flasks containing 250 mL of each of the designated medium (Table 2) at pH 7.0. The culture was incubated at 37°C under 200 rpm shaking, harvested after 15 h and was analysed for plasmid content. The modified PDM medium was known as PDM-pcDNA3F medium. The pcDNA3F volumetric yields were incorporated to multiple non-linear regression analysis to determine the model coefficients. The significance of the models was determined to check their efficiency. All statistical analyses were done using the software Statistica (Statsoft, v. 5.0). The optimum values for tryptone, glucose and Na_2HPO_4 were predicted using the steepest ascent method of RSM.

Effect of pH and temperature on plasmid production and cell growth

All experiments were carried out using the same master cell bank to minimize errors due to cell age. 2 mL fresh inoculums were dispensed into each 500 mL conical flask containing 100 µg/ml ampicillin and 250 mL PDM. The cultures were incubated at 37 °C and 200 rpm for 15 h. Effect of pH on plasmid production and cell growth was investigated by varying the initial cultivation pH values between 6 and 8.5. To explore the effect of temperature shift on plasmid production, one step and periodic temperature inductions at 35 and 45 ^{o}C were performed at 8 h post innoculation at 37 ^{o}C. For periodic temperature induction, a simple sinusoidal wave model (equation (2)) was used to represent the temperature fluctuation. More specifically, the objective of the temperature fluctuation was to find the frequency f at which the plasmid production was optimum. All samples were analysed for plasmid yield and biomass growth periodically.

Fed-batch fermentation

A single bacterial colony carrying the plasmid pcDNA3F (*E. coli* DH5*α*-pcDNA3F) was picked from an LB-agar-ampicillin plate and subcultured overnight in 500 mL shake flask containing 250 mL PDM-pcDNA3F medium, 1% ampicillin and 0.25% v/v glycerol at 37°C and 200 rpm shaking. Subsequently, the culture was inoculated into a 20 L fermentor (New Brunswick Scientific, BioFlo 410, USA) containing 15 L of PDM-pcDNA3F medium and 0.25% v/v glycerol. The initial temperature was set at 37°C and the DO value which was subjected to a previous optimisation was maintained at 10% by the PID controller. The pH was maintained at 7.5 using 4.0 M NaOH and 1.0 M HCl. The inflowing air was set at 20 psi and foaming was controlled by using polypropylene glycol as antifoam. In the fed-batch phase, a carbon substrate feed containing 50% glycerol was added into the fermentor according to equation (3). Temperature shift from 37 to 45°C was performed at 20 h post culture to further boost the plasmid yield prior to harvesting the culture and finally the fermentation was terminated at 24 h post innoculation. The culture broth was harvested, concentrated by ultrafiltration, packaged and stored at −75°C.

Plasmid DNA analysis

Pure plasmid DNA was prepared using Wizard Plus SV Minipreps according to the manufacturer's instruction (Promega, U.S.A). Clarified cell lysate containing plasmid DNA was prepared according to the protocol described in the Wizard Plus SV Minipreps manual. Briefly, 1 mL of cell culture was resuspended, alkaline lysed, neutralised and clarified by centrifugation. The pDNA concentration was determined by ethidium bromide agarose gel

electrophoresis using 1 kbp DNA ladder (Bio Labs, New England). The gel was made up in 50-fold diluted TAE buffer (242 g of Tris base, 57.1 mL acetic acid, 9.305 g of EDTA) and stained with 3 μg/mL ethidium bromide. The gel well was loaded with 1 μL of sample and electrophorased at 65 V for 70 min. Consequently, the gel was photographed using a gel analyser (BIORAD, Universal Hood II, Italy) and analysed using Quantity One software (BIORAD, USA).

List of abbreviations

a: parameter's coefficient; D: Dilution rate (h^{-1}); f : Frequency of oscillation (h^{-1}); F_i: Initial substrate feeding rate (mL/h); F_t: Substrate feeding rate at time t (mL/h); S_i: Initial substrate consumption rate (mL/h); S_t: Substrate consumption rate at time t (mL/h); t: Cultivation time (h); t_d: Biomass doubling time (h); $T(t)$: Temperature at time t (^oC); x: Coded value of nutrient concentration; X: Real value of nutrient concentration (g/L); y: Product concentration (mg/L); α: Specific exponential feeding rate (h^{-1}); μ: Specific cell growth rate (h^{-1}); ΔT : Temperature's maximum deviation (^oC); π : pi (3.142); ϕ : Phase during oscillation.

Competing interests

The authors declare that they have no competing interests.

Authors' contributions

CMO: All experiments and manuscript preparation. RP and DW: Construction of plasmid pcDNA3F. MKD: Research design and manuscript preparation.

All authors have read and approved the final manuscript.

Acknowledgements

The authors thank Monash University for funding the project and Universiti Malaysia Sabah for providing the research scholarship to CMO.

References

1. Sousa F, Duarte MF, Prazeres, Queiroz JA: **Affinity chromatography approaches to overcome the challenges of purifying plasmid DNA**. *Trends Biotechnol* 2008, **26**(9):518-525.
2. Pütz MM, Bouchee FB, Swart RLd, Muller CP: **Experimental vaccines against measles in a world of changing epidemiology**. *Int J Parasitol* 2003, **33**:525-545.

3. Prather KJ, Sagar S, Murphy J, Chartrain M: **Industrial scale production of plasmid DNA for vaccine and gene therapy: plasmid design, production, and purification**. *Enzyme Microb Technol* 2003, **33**:865-883.
4. Prazeres DMF, Ferreira GNM, Monteiro GA, Cooney CL, Cabral JMS: **Large-scale production of pharmaceutical-grade plasmid DNA for gene therapy: problems and bottlenecks**. *TIBTECH* 1999, **17**:168-174.
5. Listner K, Bentley L, Okonkowski J, Kistler C, Wnek R, Caparoni A, Junker B, Robinson D, Salmon P, Chartrain M: **Development of a highly productive and scalable plasmid DNA production platform**. *Biotechnol Prog* 2006, **22**:1335–1345.
6. Razali F, Young MM, Scharer JM, Glick BR: **Review : overexpression of protein under transcriptional regulation of lambda pL promoter system in *Escherichia coli*: consequences and bioprocess improvement approaches**. *J Chem Nat Res Eng* 2007, **1**:22-39.
7. Danquah MK, Forde GM: **Development of a pilot-scale bacterial fermentation for plasmid-based biopharmaceutical production using a stoichiometric medium**. *Biotechnol Bioprocess Eng* 2008, **13**:1-10.
8. Danquah MK, Forde GM: **Growth medium selection and its economic impact on plasmid DNA production**. *J Biosci Bioeng* 2007, **104**(6):490-497.
9. Aucoin MG, McMurray-Beaulieu V, Poulin F, Boivin EB, Chen JK, Ardelean FM, Cloutier M, Choi YJ, Miguez CB, Jolicoeur M: **Identifying conditions for inducible protein production in *E. coli*: combining a fed-batch and multiple induction approach**. *Microb Cell Fact* 2006, **5**:-.
10. Hasan CMM, Shimizu K: **Effect of temperature up-shift on fermentation and metabolic characteristics in view of gene expressions in *Escherichia coli***. *Microb Cell Fact* 2008, **7**(35).
11. Hortacsu A, Ryu DDY: **Optimal Temperature Control Policy for a Two-Stage Recombinant Fermentation Process**. *Biotechnol Progr* 1990, **6**(6):403-407.
12. Gupta JC, Jaisani M, Pandey G, Mukherjee KJ: **Enhancing recombinant protein yields in *Escherichia coli* using the T7 system under the control of heat inducible lambda P-L promoter**. *J Biotechnol* 1999, **68**(2-3):125-134.
13. Villaverde A, Benito A, Viaplana E, Cubarsi R: **Fine Regulation of Ci857-Controlled Gene-Expression in Continuous-Culture of Recombinant *Escherichia-Coli* by Temperature**. *App Environ Microbiol* 1993, **59**(10):3485-3487.

14. Demuth JP: **The effects of constant and fluctuating incubation temperatures on sex determination, growth, and performance in the tortoise Gopherus polyphemus**. *Can J Zool* 2001, **79**(9):1609-1620.
15. Les HL, Paitz RT, Bowden RM: **Experimental test of the effects of fluctuating incubation temperatures on hatchling phenotype**. *J Exp Zool Part A* 2007, **307A**(5):274-280.
16. Carnes AE: **Fermentation Process for Continuous Plasmid Dna Production**. In. Edited by CORP NT. U.S.: Hodgson, Clague P. ; 2008.
17. Park YC, Kim SG, Park. K, Lee KH, Seo JH: **Fed-batch production of D-ribose from sugar mixtures by transketolase-deficient *Bacillus subtilis* SPK1**. *Appl Microbiol Biotechnol* 2004, **66**:297-302.
18. Carnes AE, Hodgson CP, Williams JA: **Inducible *Escherichia coli* fermentation for increased plasmid DNA production**. *Biotechnol Appl Biochem* 2006, **45**:155-166.
19. Furuichi K, Katakura Y, Ninomiya K, Shioya S: **Enhancement of 1,4-dihydroxy-2-naphthoic acid production by *Propionibacterium freudenreichii* ET-3 fed-batch culture**. *Appl Environ Microbiol* 2007, **73**(10):3137-3143.
20. Meacle FJ, Zhang H, Papantoniou I, Ward JM, Titchener-Hooker NJ, Hoare M: **Degradation of supercoiled plasmid DNA within a capillary device**. *Biotechnol Bioeng* 2007, **97**(5):1148-1157.
21. Plackett RL, Burman JP: **The Design of Optimum Multifactorial Experiments**. *Biometrika* 1946, **33**(4):305-325.
22. Kalil SJ, Maugeri F, Rodrigues MI: **Response surface analysis and simulation as a tool for bioprocess design and optimization**. *Process Biochem* 2000, **35**(6):539-550.
23. Ibrahim HM, Yusoff WMW, Hamid AA, Illias RM, Hassan O, Omar O: **Optimization of medium for the production of beta-cyclodextrin glucanotransferase using Central Composite Design (CCD)**. *Process Biochem* 2005, **40**(2):753-758.
24. Booth IR, Cash P, O'Byrne C: **Sensing and adapting to acid stress**. *Antonie Van Leeuwenhoek Int J Gen Mol Microbiol* 2002, **81**(1-4):33-42.
25. Kobayashi H, Suzuki T, Unemoto T: **Streptococcal Cytoplasmic Ph Is Regulated by Changes in Amount and Activity of a Proton-Translocating Atpase**. *J Biol Chem* 1986, **261**(2):627-630.
26. Canonaco F, Schlattner U, Wallimann T, Sauer U: **Functional expression of arginine kinase improves recovery from pH stress of *Escherichia coli***. *Biotechnol Lett* 2003, **25**(13):1013-1017.

27. O'Mahony K, Freitag R, Hilbrig F, Muller P, Schumacher I: **Strategies for high titre plasmid DNA production in *Escherichia coli* DH5 alpha**. *Proc Biochem* 2007, **42**(7):1039-1049.

28. Lim HK, Jung KH: **Improvement of heterologous protein productivity by controlling postinduction specific growth rate in recombinant *Escherichia coli* under control of the P-L promoter**. *Biotechnol Progr* 1998, **14**(4):548-553.

29. Siegel R, Ryu DDY: **Kinetic-Study of Instability of Recombinant Plasmid Pplc23trpal in *Escherichia-Coli* Using 2-Stage Continuous Culture System**. *Biotechnol Bioeng* 1985, **27**(1):28-33.

30. Silva, Filomena, Passarinha L, Sousa F, Queiroz JA, Domingues FC: **Influence of growth conditions on plasmid DNA production**. *J Microbiol Biotechnol* 2009, **19**(1):1408-1414.

CHAPTER FOUR

CHROMATOGRAPHIC PURIFICATION OF PLASMID MOLECULES

Section 4.1

Process optimisation for anion exchange monolithic chromatography of 4.2 kbp plasmid vaccine (pcDNA3F)

Journal of Chromatography B. 878: 2719 – 2725 (2010)

Monash University

Declaration for Thesis Section 4.1

Declaration by candidate

In the case of Section 4.1, the nature and extent of my contribution to the work was the following:

Nature of contribution	Extent of contribution (%)
Initiation, Key ideas, Experimental, Development, Results interpretations, Writing up	90

The following co-authors contributed to the work. Co-authors who are students at Monash University must also indicate the extent of their contribution in percentage terms:

Name	Nature of contribution
Dr. Michael K. Danquah	Initiation, Key ideas, Experimental, Development, Results interpretations, Writing up

Candidate's signature		**Date**

Declaration by co-authors

The undersigned hereby certify that:

1. the above declaration correctly reflects the nature and extent of the candidate's contribution to this work, and the nature of the contribution of each of the co-authors;
2. they meet the criteria for authorship in that they have participated in the conception, execution, or interpretation, of at least that part of the publication in their field of expertise;
3. they take public responsibility for their part of the publication, except for the responsible author who accepts overall responsibility for the publication;
4. there are no other authors of the publication according to these criteria;
5. potential conflicts of interest have been disclosed to (a)granting bodies, (b) the editor or publisher of journals or other publications, and (c) the head of the responsible academic unit; and
6. the original data are stored at the following location (s) and will be held for at least five years from the date indicated below:

Location	Chemical Engineering Department, Monash University, Clayton, Australia

Signature		**Date**

Process optimisation for anion exchange monolithic chromatography of 4.2 kbp plasmid vaccine (pcDNA3F)

Clarence M. Ongkudon, Michael K. Danquah

Abstract

Anion exchange monolithic chromatography is increasingly becoming a prominent tool for plasmid DNA purification but no generic protocol is available to purify all types of plasmid DNA. In this work, we established a simple framework and used it to specifically purify a plasmid DNA model from a clarified alkaline-lysed plasmid-containing cell lysate. The framework involved optimising ligand functionalisation temperature (30-80 ^{o}C), mobile phase flow rate (0.1-1.8 mL/min), monolith pore size (done by changing the porogen content in the polymerisation reaction by 50-80 %), buffer pH (6-10), ionic strength of binding buffer (0.3-0.7 M) and buffer gradient elution slope (1-10 % buffer B/min). We concluded that preferential pcDNA3F adsorption and optimum resolution could be achieved within the tested conditions by loading the clarified cell lysate into 400 nm pore size of monolith in 0.7 M NaCl (pH 6) of binding buffer followed by increasing the NaCl concentration to 1.0 M at 3 %B/min.

Keywords: Process optimisation; Anion exchange; Monolithic chromatography; Plasmid DNA; pcDNA3F

1. Introduction

Anion-exchange chromatography (AEC) remains one of the most prominent methods in plasmid DNA (pDNA) purification due to its rapid separation, easy sanitisation, no organic solvent requirements and wide selection of available stationary phases[1]. In terms of quality and recovery, consistent results have been achieved at different scales[2]. AEC is based on the interaction between negatively charged phosphate groups of plasmid and positively charged stationary matrix[3]. A buffer containing sodium chloride salt can be used as the eluting buffer and a gradient elution can be performed at a specific slope (% eluting buffer/min) for optimum resolution [4]. Molecules with lower charge densities should elute first followed by

high negatively charged molecules, a trend, which is attributed to plasmid chain length and conformation[5].

The purification of large biomolecules, such as plasmids is obstructed by the performance of conventional chromatographic supports with a small particle pore diameter. Most of these chromatographic supports are geared towards high adsorption capacities of small molecules such as proteins and peptides. In columns packed with such particles, plasmids greater than 100 nm adsorb predominantly on the outer surface of the particles and this leads to low binding capacities [6]. A monolith is a continuous phase consisting of a piece of highly porous organic or inorganic solid material. The most essential feature of this support is that all the mobile phase is forced to flow through its large pores. As a consequence, mass transport is steered by convection; reducing the long diffusion time required by particle-based supports [7]. The pore size of the monolith plays an important role in providing spaces for both ligand attachment and plasmid mobility. Based on a previous study, it is speculated that bimodal pore sizes of 0.008 and 0.5 μm can provide the optimum condition for ligand coupling, plasmid binding and plasmid retention [8]. The pore size of the monolith can be altered by varying the composition of the reactants and porogens. One of the most studied monolithic materials is silica based monolith which has been reported in [9-11]. Silica based monolith has been used in analytical chromatography and resulted in a significantly short processing time compared to conventional packed bed column [12]. Another type of monolithic material is polymethacrylate based monolith which is the type of chromatographic column used in this work. Polymethacrylate monoliths are especially useful for large scale purification of large biomolecules owing to its enhanced mass transfer properties, pressure and flow, specific permeability, morphological and structural stability [13].

To optimise the ligand coupling on polymethacrylate, crucial parameters such as temperature, reaction time and pH can be optimised. Generally, the ligand coupling rate increases with temperature according to the Arrhenius equation [14]. At high pH values, the epoxy group of polymethacrylate is more reactive than that at low pH values. However, the maximum pH value is limited by the ligand stability which in most cases affected by deactivation, leaching and aggregation. Using high ionic strength binding buffers can also improve the ligand coupling on polymethacrylate but extra care has to be taken when using highly ionic binding buffers since they may lead into disruption of the covalent linkage of the polymethacrylate or monolith shrinkage.

pH can greatly alter the monolith charge density and thereby affect the success of the plasmid purification [8]. In this work, different pH values were tested for optimal plasmid purification. Effect of pH on the overall plasmid charge and ligand charge densities was

analysed by Zeta potential analyser. Plasmid purity, recovery and peak resolution are coherently influenced by chromatographic residence time [8]. Residence time can be altered by manipulating buffer flow rate and column length. Generally at low flow rates and high column lengths, separation will be more efficient due to an increase in retention time of the solute of interest. At low flow rates however, the peak width may be broadened resulting in low plasmid recovery and low resolution. Therefore, an optimisation of buffer flow rate is necessary and a mathematical study can be carried out to assess the trade-off between plasmid purity and recovery[15].

2. Materials and methods

Ethylene glycol dimethacrylate (EDMA) (*M*w 198.22, 98%), glycidyl methacrylate (GMA) (*M*w 142.15, 97%), cyclohexanol (*M*w 100.16, 99%), 1-dodecanol (*M*w 186.33, 98%), AIBN (*M*w 164.21, 98%), MeOH (HPLC grade, *M*w 32.04, 99.93%), DEA (*M*w 73.14, 99%) were purchased from Sigma-Aldrich. NaCl (Amresco, *M*W 58.44, 99.5%), agarose (Promega), SDS (Amresco, *M*w 288.38, 99.0%), Na_2CO_3 (SPECTRUM, *M*w 105.99, 99.5%), Tris (Amresco, Mw 121.14, 99.8%), EDTA (SERVA, *M*w 292.3, AG), EtBr (Sigma, *M*w 394.31, 10 mg/mL), 1 kbp DNA marker (BioLabs, New England), Wizard plus SV Maxipreps (Promega).

2.1. Model plasmid vaccine

E. coli DH5α carrying plasmid measles vaccine (pcDNA3F) was provided by Dr Diane Webster of School of Biological Sciences, Monash University, Australia.

2.2. Cell line propagation

10 µL of transformed cells (*E. coli* DH5*α*-pcDNA3F) was cultured in LB-agar-ampicillin plate at 37°C overnight. A single *E. coli* DH5*α*-pcDNA3F colony was picked from the LB-agar-ampicillin plate and subcultured with 250 mL of LB media containing 100 µg/mL ampicillin and 0.5% v/v glycerol at 37°C overnight under 200 rpm shaking. Subsequently, 2 mL of the culture was inoculated into 1000 mL medium containing 100 µg/mL ampicillin and 0.5% v/v glycerol. The fermentation was run at 37°C under 200 rpm shaking and was harvested at 15 hr post inoculation.

2.3. Preparation of E. coli DH5α-pcDNA3F cleared lysate

5 g of frozen *E. coli* DH5α-pcDNA3F bacterial cell paste were thawed at 37 ^{o}C and resuspended in 50 mL of 0.05 M Tris–HCl, 0.01 M EDTA, pH 8 buffer. The resuspended cells were homogenously mixed with 50 mL of lysis solution (0.2 M NaOH, 1% SDS) for 5 min by gently swirling the mixture. Neutralisation was performed by the addition of 75 mL 3 M CH_3COOK at pH 5.5 to the lysed cell suspension for 5 min. The mixture of pDNA-containing cleared lysate and the precipitated impurities, mainly gDNA were separated by centrifugation at 4600 rpm for 30 min.

2.4. Synthesis and amino functionalisation of poly(GMA-EDMA) monolithic column

The monolith was prepared via free radical co-polymerisation of EDMA and GMA monomers. EDMA/GMA mixture was combined with alcohol-based bi-porogen solvents in the proportion 20/10/60/10 (GMA/EDMA/cyclohexanol/1-dodecanol) making a solution with a total volume of 2 mL. AIBN (1% weight with respect to monomer) was added to initiate the polymerisation reaction. The polymer mixture was sonicated for 15 min and sparged with N_2 gas for 15 min to expel dissolved O_2. The mixture was gently transferred into a conical 0.8 cm × 4 cm polypropylene column (BIORAD) sealed at the bottom end. The top end was sealed with a parafilm sheet and placed in a water bath for 18 h at 60 ^{o}C. The polymer resin was washed to remove all porogens and other soluble matters by flowing through the column with methanol for 20 h at room temperature. The polymer was washed with deionised water at 0.3 mL/min for 60 min followed by a solution containing 17 mM DEA, 20 mM Na_2CO_3 and 3 mM NaCl at 0.1 mL/min for 20 h in a 60 ^{o}C water bath. The resulting functionalised polymer was washed with deionised water.

2.5. Preparation of suspended poly(GMA-EDMA) particles for Zeta potential analysis

Suspended poly(GMA-EDMA) particles for Zeta potential analysis was prepared by dispersion polymerisation. A 50 mL mixture of GMA, EDMA, cyclohexanol, 1-dodecanol (20:10:60:10 v/v respectively) and 0.15 g AIBN was prepared at room temperature in a shake flask. The polymer mixture was sonicated for 15 min and sparged with N_2 gas for 15 min. The top end was sealed with a parafilm sheet and placed in an incubator for 24 h at 60 ^{o}C under 300 RPM shaking. The polymerised poly (GMA-EDMA) was transferred into a shake flask containing 200 mL methanol for 15 h at 200 rpm. At this stage, most of the polymer existed

as finely suspended particles (< 1 μm). The suspended polymer was centrifuged and resuspended in a 50 mL solution containing 25 mM Tris–HCl, 2 mM EDTA and 0.005 M NaCl at pH 8.

2.6. Chromatographic purification of pcDNA3F

The conical column containing 2 mL of functionalised monolithic resin was connected and configured to BIORAD HPLC system. Before the chromatography was performed, column equilibration was done with buffer A (25 mM Tris–HCl, 2 mM EDTA, 0.2 M NaCl, pH 7) at 0.6 mL/min until a constant UV baseline was achieved. 1 mL of clarified cell lysate was diluted (×0.5) with buffer A and applied at 0.6 mL/min. A washing step was done with 15 column volumes (CV) buffer A at 0.6 mL/min to completely remove the unbound and weakly retained molecules especially proteins. The elution of pcDNA3F was done by mixing buffer A with buffer B (25 mM Tris–HCl, 2 mM EDTA, 1.0 M NaCl, pH 7) at 4% B/min. Column cleaning was performed by washing the column with 50 CVs of a solution containing 0.5 M NaOH and 2 M NaCl followed by 50 CVs of 70% EtOH solution. The column was then regenerated with 10 CVs of buffer B.

2.7. Plasmid DNA qualitative and quantitative analyses

Standard pcDNA3F was prepared using Wizard plus SV Maxipreps according to the manufacturer's instructions (Promega). The concentration of the plasmid was determined via UV absorbance at 260 nm. An absorbance value of 1.0 unit measured at 260 nm represents 50 mg/L double stranded DNA. Nature and size of the plasmid were determined by ethidium bromide agarose gel electrophoresis using 1 kbp DNA ladder. The gel was made up of x50 diluted TAE buffer (242 g Tris base, 57.1 mL acetic acid, 9.305 g EDTA), stained with 3 μg/mL ethidium bromide and run for 2 hr at 66 V. The gel was photographed with a gel analyser (BIORAD, Universal Hood II, Italy). The hydrodynamic size distribution and electrokinetics behaviour of plasmid and functionalised poly(GMA-EDMA) as well as their interactions at different conditions were assessed using Zetasizer and Zeta potential analyser according to the manufacturer's instructions (Malvern Instruments).

3. Results and discussion

3.1. Effect of temperature on rate of ligand functionalisation

The dependency of DEA and poly(GMA-EDMA) coupling on reaction temperature can be checked using Arrhenius equation.

$$k = Ae^{-E_a / RT} \quad (1)$$

Where k is the effective ligand coupling rate (mole/s) obtained by measuring ligand densities every minute for 1 hour, A is total number of DEA and poly(GMA-EDMA) collisions (mole/s), E_a is activation energy of poly(GMA-EDMA)-DEA (Joule/mole), R is gas constant (8.314 Joule/mole.K), and T is temperature in K. Taking ln of equation (1) yields the following equation.

$$\ln k = \left(\frac{-E_a}{R}\right)\frac{1}{T} + \ln A \quad (2)$$

By fitting equation (2) into experimental data, the correlation factor (R^2) was calculated as 0.99, A value was 8.235 x 10^{13} mole/s and activation energy for ligand coupling was 1.24 x 10^5 Joule/mole.

At high temperatures, the ligand functionalisation rate was high leading to a shorter reaction time and *vice versa* (as seen in Fig. 1). At very high temperatures however, the monolith pore structures became uneven leading to reduced binding capacities and resolution. In this study we found that the optimum temperature for ligand functionalisation was at 60 ^oC.

3.2. Optimisation of mobile phase flow rate

During chromatography, the movement of plasmids through monolith is influenced by diffusion, adsorption and convection of plasmids inside the monoliths. These factors are related to linear velocity of mobile phase as suggested by the Van Deemter equation. By running plasmid samples at different flow rates, the height equivalent to theoretical plate (HETP) can be calculated and used to determine the optimum flow rate. As depicted in Fig.

2., the optimum linear velocity is at 0.6 m/min which is equivalent to a volumetric flow rate of 0.6 ml/min. Under this condition, the resulting chromatographic peaks are sharp, symmetrical and band broadening is minimised. At flow rate < 0.6 ml/min, plasmids spend more time in the monolith and start to diffuse out from the centre to the edges thus leading to band broadening and reduced chromatographic efficiency. At flow rate > 0.6 ml/min, band broadening are more complicated. Besides the differences in residence time between plasmids in mobile phase and plasmids in stationary phase, Zochling *et al*. [16] suggested that band broadening occurring at high flow rates is also attributed to the stretching of the plasmid DNA caused by flow-induced shear stress [17]. Further to the flow-induced elongational stress, fewer amounts of plasmids are bound per unit area of the anion exchange surface thus resulting in lower plasmid yields.

We also propose herein that, as a result of a very high flow rate-induced shear stress, plasmids may become nicked thus leading to lower supercoiled plasmid DNA yields [17,18]. Shear-induced plasmid elongational and degradation are complex events and current understanding of the effects of shear rate on plasmid shapes does not provide a final answer to these proposed phenomena. In view of this, it is prudent to investigate the molecular mechanism of effect of shear stress on plasmid shape and stability to better control the monolithic chromatography of plasmids and comply with regulatory standards.

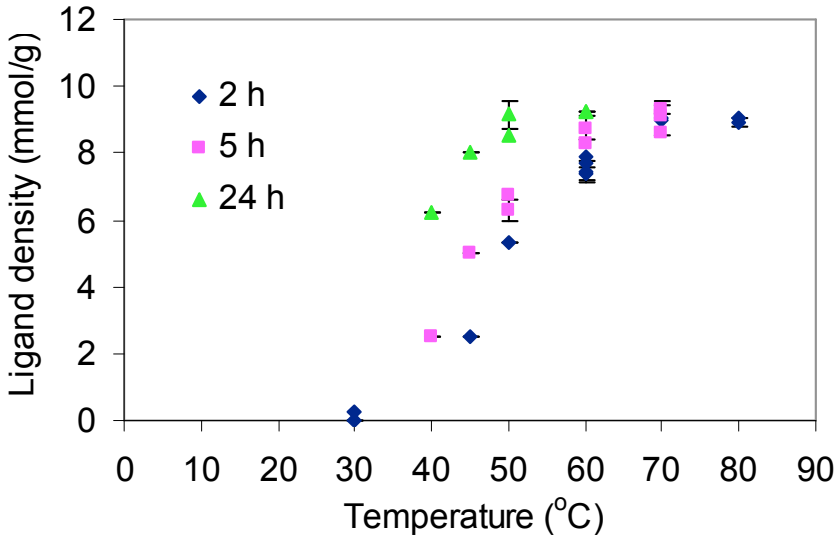

Fig. 1. Diethylamine densities measured at different functionalisation temperatures and incubation periods. Ligand densities were calculated based on the difference in dry weights of the polymer before and after functionalisation was performed. Functionalisation was done at 2 h (rhombus), 5 h (square) and 24 h (triangle) of incubation periods between 30 to 80 ^{o}C.

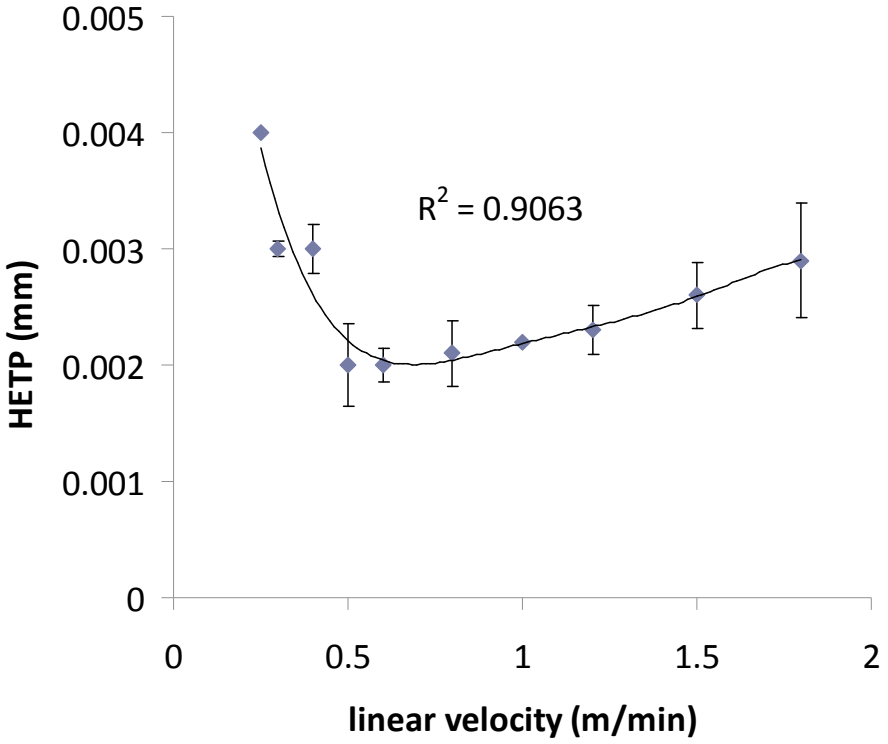

Fig. 2. Effect of flowrate on column efficiency. Buffer A (25 mM Tris–HCl, 2 mM EDTA, 0.2 M NaCl, pH 7). Buffer B (25 mM Tris–HCl, 2 mM EDTA, 1.0 M NaCl, pH 7). Sample: 0.5 mL of clarified alkaline lysed cell lysate. Washing, 30 CVs of buffer A; gradient elution, 4% B/min.

3.3. Optimisation of pore size

The chromatographic resolution of plasmid DNA significantly depends on the active surface accessibility. In this case the active surface is actually the monolith pore surfaces. The channels should be large enough to allow penetration of large plasmid DNAs (> 100 nm) and at the same time to separate other impurities of smaller sizes (< 100 nm). If the pore size is too small, not only the resolution is poor but the back pressure is high too. The first step to determine the optimum pore size of the monolith for plasmid purification is to measure the hydrodynamic size of double stranded supercoiled plasmid DNA by dynamic light scattering method. Based on the size of the plasmid, the monolith pore size can then be formed according to methods described by Danquah and Forde [19]. Further optimisation of pore size can be done for a greater plasmid resolution by fine tuning the amount of porogen in the monolith preparation.

Based on Fig. 3., the mean hydrodynamic diameter of the model plasmid pcDNA3F as measured by the Zetasize analyser (Malvern Instruments) is 137 nm. Therefore, the monolith pore size should at least be 137 nm. In a real application, the monolith pore size is much larger than the plasmid. This is to compensate with the high mobile phase flow rate and different molecules that exist in the clarified plasmid-containing cell lysate. To optimise the monolith pore size for plasmid pcDNA3F purification, different porogen contents in monolith preparation were tested. The effects of porogen on plasmid resolution and monolith pore size are shown in Fig. 4 and Fig. 5.

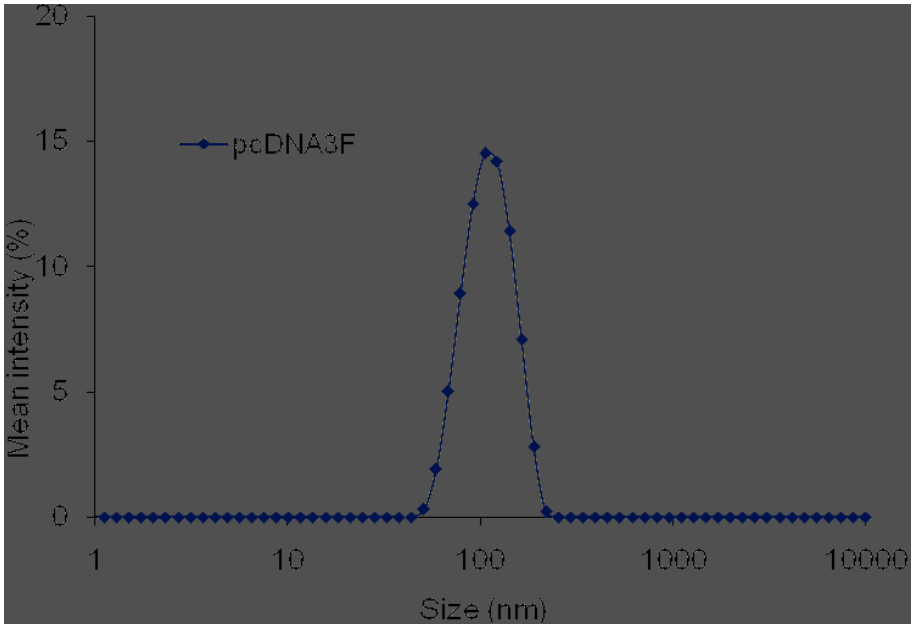

Fig. 3. Hydrodynamic size distribution of plasmid pcDNA3F. Mean size is ~137 nm in 25 mM Tris–HCl, 2 mM EDTA and 0.005 M NaCl at pH 8.

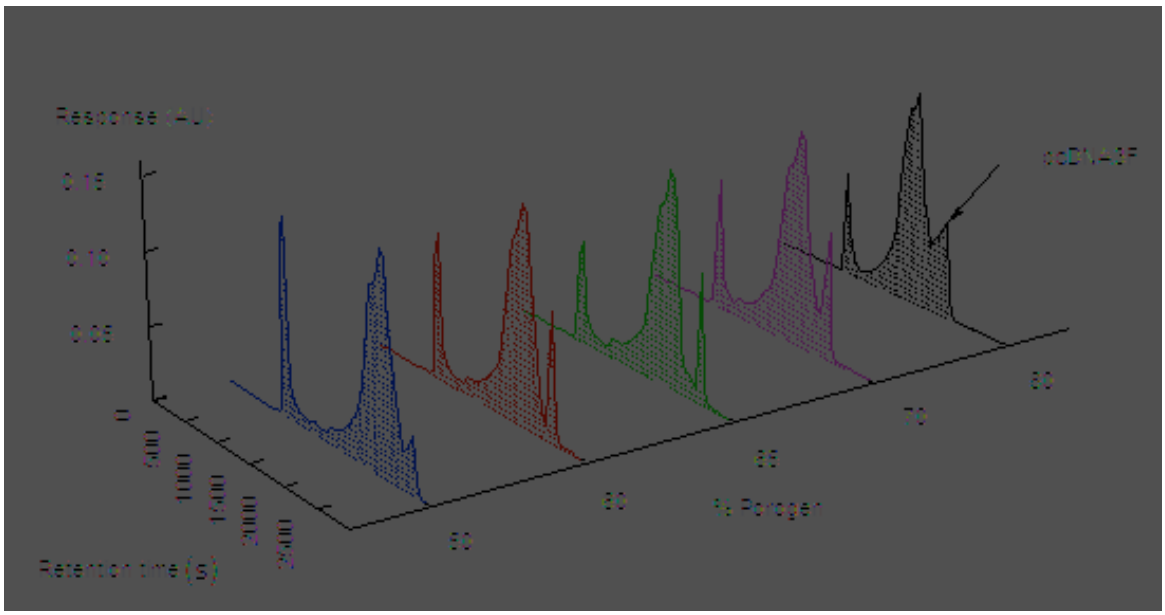

Fig. 4. Effect of porogen:monomer ratio on plasmid resolution. Flowrate 0.6 mL/min. Buffer A (25 mM Tris–HCl, 2 mM EDTA, 0.2 M NaCl, pH 7). Buffer B (25 mM Tris–HCl, 2 mM EDTA, 1.0 M NaCl, pH 7). Sample: 0.5 mL of clarified alkaline lysed cell lysate. Washing, 30 CVs of buffer A; gradient elution, 4% B/min.

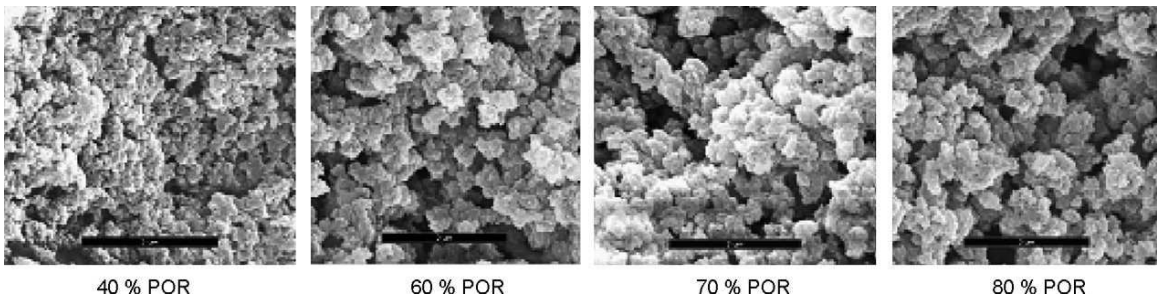

Fig. 5. SEM photographs of poly(GMA-EDMA) polymerised at different porogen:monomer ratios. Polymerisations were carried out with a constant monomer ratio (EDMA/GMA) of 40/60; porogen concentrations of 40%, 60%, 70% and 80%; polymerisation temperature of 60 ◦C; AIBN concentration of 1% (w/w) with respect to monomers. Microscopic analysis was performed at 15 kV. POR: porogen [19].

In general, smaller pore size results in the solute not entering the pores thus larger pore size is needed to cater for both ligand attachment and plasmid mobility. A decreasing trend of plasmid retention with increasing porogen content is observed in Fig. 4. This can be explained by analysing the internal structures of the monolith in Fig. 5. At 40% porogen, the modal pore diameter is 115.7 nm which is vaguely smaller than pcDNA3F. As a result of this internal resistance, the plasmids may take longer time to pass through the pores by flow-induced elongational stress and may coelute with other molecules of smaller size. Fractions of the plasmids may remain within the pores or elute at a later time thus resulting in lower plasmid yield and band broadening as depicted in Fig. 4. At 80% porogen, the modal pore size is 875.6 nm which is 8 times larger than the size of pcDNA3F. At this point, plasmid resolution may become less dependent on monolith pore size and therefore depends solely on buffer gradient elution for separation. It is also important to note that at a substantially large pore size, the surface area is greatly reduced thus resulting in a lower binding capacity. This affects the overall positive charge density of the matrix which in turn affects the electrostatic interaction and plasmid separation. In this study, the optimum monolith pore size for pcDNA3F resolution occurs at 65% porogen. This value corresponds to a pore size of approximately 400 nm according to Danquah and Forde [19].

3.4. Effect of NaCl in binding buffer on plasmid retention and binding capacity

When a clarified plasmid-containing bacterial lysate is loaded into an anion exchange monolithic column, a strong competition occurs between plasmids and negatively charged impurities for the anion exchange matrix. This leads to reduced plasmid binding capacity and low plasmid recovery during elution. One way of minimising the adsorption of lower charged impurities onto the matrix is by increasing the ionic strength of binding buffer by means of increasing NaCl concentration. Theoretically, the optimum NaCl concentration of binding buffer can be defined as the point where all impurities carry zero net surface charge leaving only plasmids with net negatively charged surface. Under this circumstance, the monolith internal surface area can be fully utilised for plasmid adsorption.

To obtain the relative surface charge of a particle, we measured the Zeta potential of the particles which is defined as the electric potential at a particular distance off the particle surface called the hydrodynamic slip plane [20]. According to Fig. 6, plasmid pcDNA3F remains negatively charged at 2 M NaCl whilst proteins and RNAs are neutralised at 0.25 M and 1.0 M NaCl respectively.

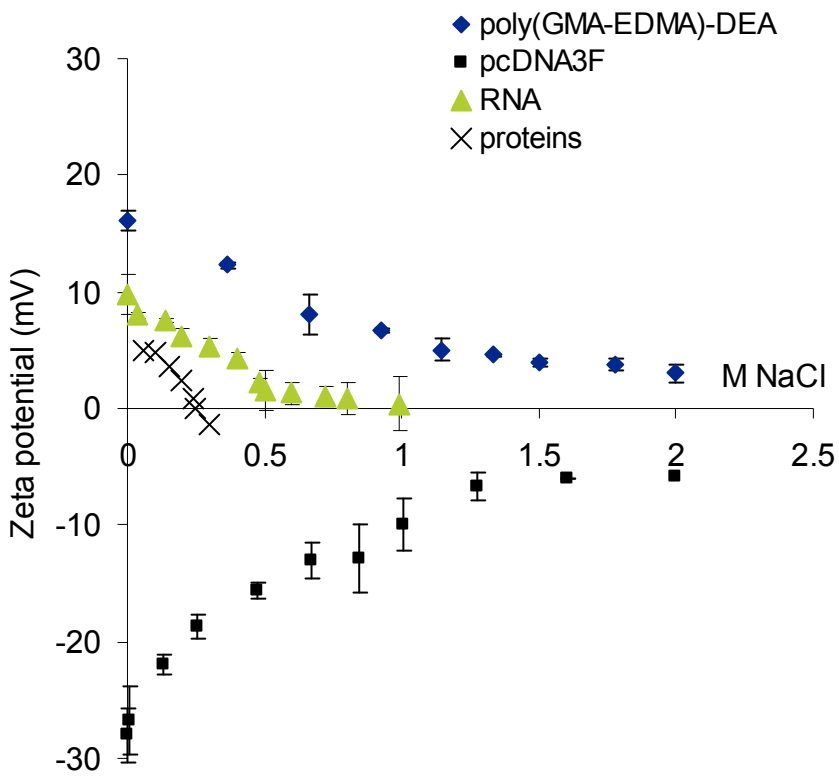

Fig. 6. Effect of buffer's ionic strength on the Zeta potential of pcDNA3F and poly(GMA-EDMA)-DEA. Base buffer (25 mM Tris–HCl, 2 mM EDTA, 0 M NaCl, pH 7). Each data point represents the average of three replicates.

We predicted that at a NaCl concentration of ~ 1.0 M in loading buffer, majority of the plasmids would stay within the monolith matrix leaving all impurities especially proteins and RNA in the flowthrough. We also hypothesised that plasmid yield would not be affected considering the same amount of sample loaded into the monolith. To verify these hypotheses, four chromatographic runs were performed at 0.3, 0.4, 0.5 and 0.7 M NaCl in loading/binding buffer. The elution step was initiated at 5 min post loading by gradient elution up to 1.0 M NaCl at 4% B/min. The chromatograms of the analyses are shown in Fig. 7. Generally the retention time was high at low ionic strength of binding buffer and *vice versa*. A decreasing trend of RNA yield with increasing ionic strength of binding buffer was observed between 0.3 and 0.7 M NaCl. RNA adsorption was virtually eliminated at 0.7 M which was slightly lower than the predicted value of 1.0 M.

The trend of plasmid yield however, did not quite agree with the hypothesis since plasmid yield seemed to decrease slightly with increasing NaCl concentration in binding buffer. This trend can be explained from the condensation theory which postulates that upon

neutralisation of negatively charged phosphate groups in the DNA backbone, the repulsive forces are weakened thus allowing the DNA to collapse into compact forms [17,21]. We also propose that at a high ionic strength of binding buffer, the amount of plasmid DNA bound per unit area of the anion exchange surface is reduced due to decreased electrostatic attraction exerted by the matrix surface. As a result of this compaction, the effective hydrodynamic diameter of the DNA is decreased and the loosely retained molecules can easily flow through the monolith pores.

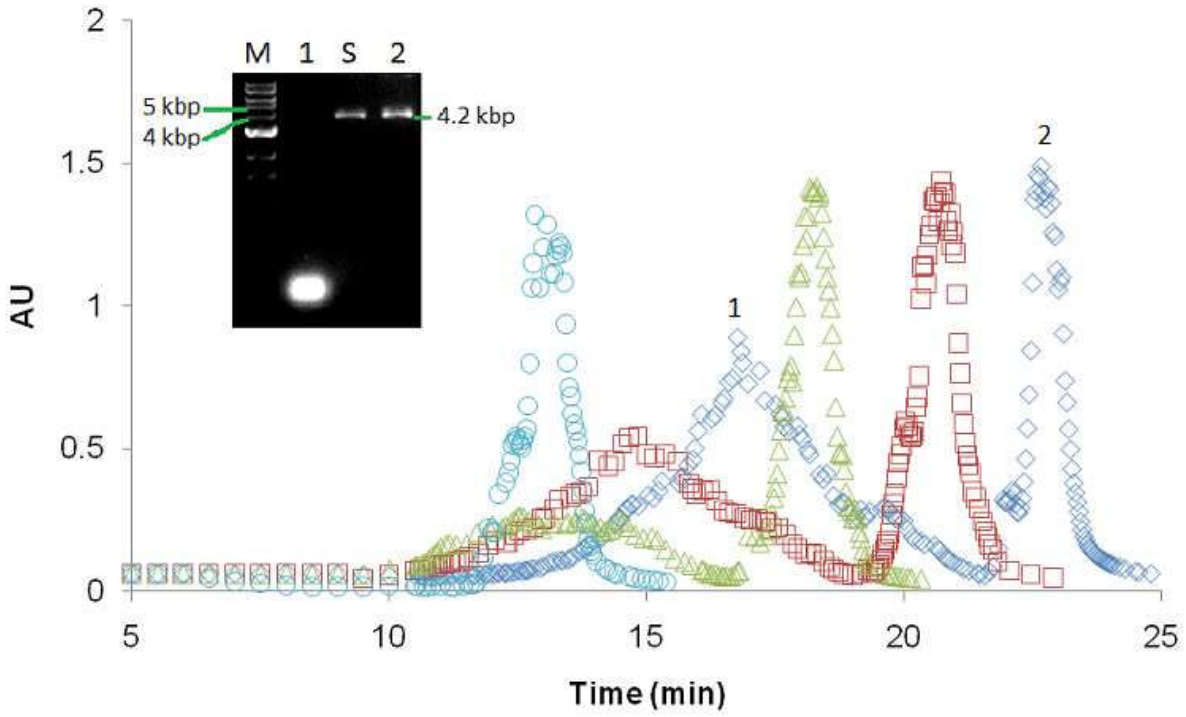

Fig. 7. Effect of ionic strength of binding buffer on plasmid retention. Buffer A (25 mM Tris–HCl, 2 mM EDTA, 0.3 M - 0.7 M NaCl, pH 7). Buffer B (25 mM Tris–HCl, 2 mM EDTA, 1.0 M NaCl, pH 7). Flowrate: 1.0 mL/min; sample: 1.0 mL of clarified alkaline lysed cell lysate; washing: 5 mL buffer A; gradient elution: 4% B/min. NaCl concentration in buffer A: 0.3 M (rhombus); 0.4 M (square); 0.5 M (triangle); 0.7 M (circle). Inset shows Ethidium bromide gel electrophoresis of different samples taken at different peak elutions. Analysis was performed using 1% agarose in 100 mL TAE×1 buffer, 0.5 µg/ml ethidium bromide at 65V for 1.7 h. Lane M is 1 kbp DNA ladder; lanes 1 and 2 represent peaks 1 (RNA) and 2 (pcDNA3F) of the chromatogram; lane S is standard Maxiprep pcDNA3F.

3.5. Optimisation of gradient elution

In ion exchange monolithic chromatography, the major mechanism that contributes to plasmid separation is attributed to size exclusion and close vicinity electrostatic interaction between the plasmid and ligand. Plasmid elution is done by increasing the ionic strength (e.g. NaCl concentration) of the mobile phase.

As discussed previously, the presence of NaCl in a mobile phase reduces the effective net charge of both plasmid and ligand. NaCl also affects the hydrodynamic size of plasmid and other impurities such as RNAs and proteins. To effectively separate plasmid DNA from contaminating species, NaCl concentration was increased gradually and each species was eluted from the column based on NaCl-induced size compaction and reduced electronegativities. Fig. 8 shows the effect of different NaCl (buffer B) gradient elutions on plasmid resolution.

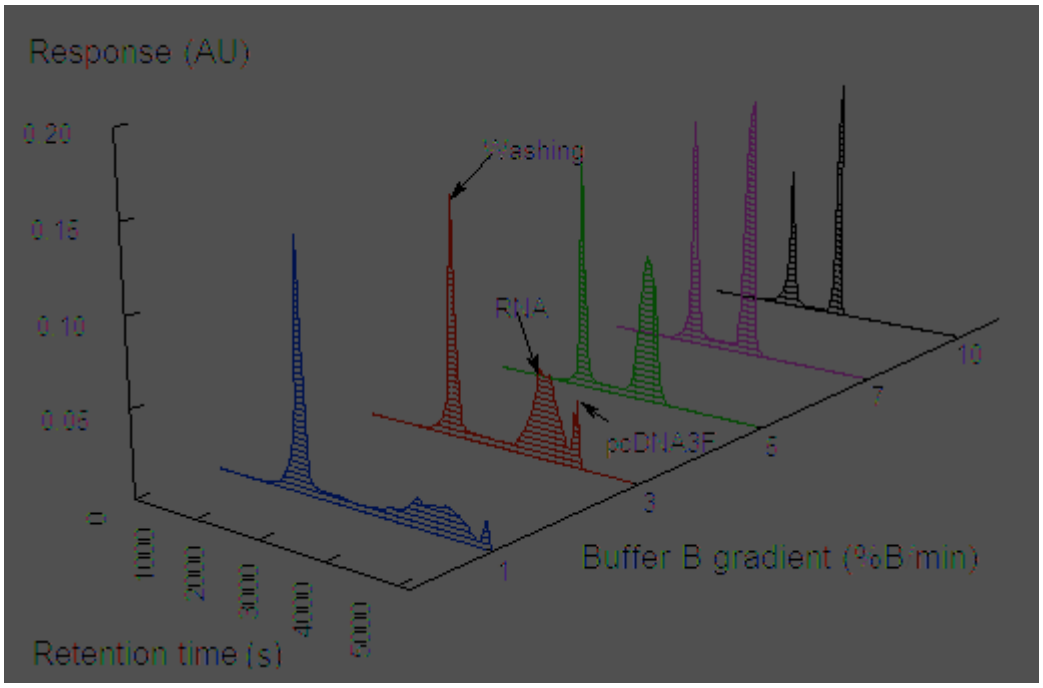

Fig. 8. Effect of buffer B gradient on plasmid resolution. Flowrate 0.6 mL/min. Buffer A (25 mM Tris–HCl, 2 mM EDTA, 0.2 M NaCl, pH 7). Buffer B (25 mM Tris–HCl, 2 mM EDTA, 1.0 M NaCl, pH 7). Sample: 0.5 mL of clarified alkaline lysed cell lysate. Washing, 30 CVs of buffer A.

There is a general trend of increasing plasmid resolution with decreasing buffer B gradient across the buffer B gradient range tested. At 7 and 10 %B/min, plasmid pcDNA3F and RNA appear as a single peak. This indicates that the increase in NaCl concentration is too abrupt and that the plasmid has too little time to separate from RNA. At 5 %B/min, pcDNA3F and RNA are scarcely separated and pcDNA3F resolution is optimum at 3 %B/min. It can also be seen that at < 3 %B/min, there is no significant improvement in resolution in addition to reduced plasmid yield. This is possibly due to a longer retention time which results in plasmid diffusion, band broadening thus lower plasmid yield.

Finding the right gradient of the eluting buffer proves to be essential in the chromatographic purification of plasmid DNA and the optimum buffer B gradient obtained in this study is plasmid-size specific. According to Smith *et al.* [4], when a specific gradient was used to elute a plasmid DNA of a different size, the resolution was considerably varied. They were unable to find a generic elution profile for plasmid DNA and discovered a size-dependent change in relative elution rates. They conducted plasmids (3.0, 5.5, 7.6 kbp) elution at different salt gradient slopes and measured the relative retention time (RRT) of supercoiled, linear and open circular plasmids.

3.6. Optimisation of pH conditions

Another important variable that plays an important role in ion exchange chromatography is pH condition of mobile phases. In this work, we investigated the effect of pH (2 to 12) on Zeta potential values of the monolith and plasmid DNA as well as on plasmid resolution. Generally, the plasmid remained negatively charged within the pH range tested (Fig. 9). Poly(GMA-EDMA)-DEA monolith displayed positive net charge at pH < 9, zero charge at pH = 9, and negative charge at pH > 10. From these observations, it can be hypothesised that the plasmid will not bind to the ligand at pH > 9 thus will move along with other impurities in the mobile phase uncaptured considering that the net charge does not take into account localized charged region. Optimum plasmid retention and resolution can be expected between pH 5 and 6 at which the difference in the magnitude of Zeta potential between the ligand and the plasmid is maximum. To verify these hypotheses, we conducted an anion exchange purification of plasmid-containing cell lysates at different pH values of the mobile phases.

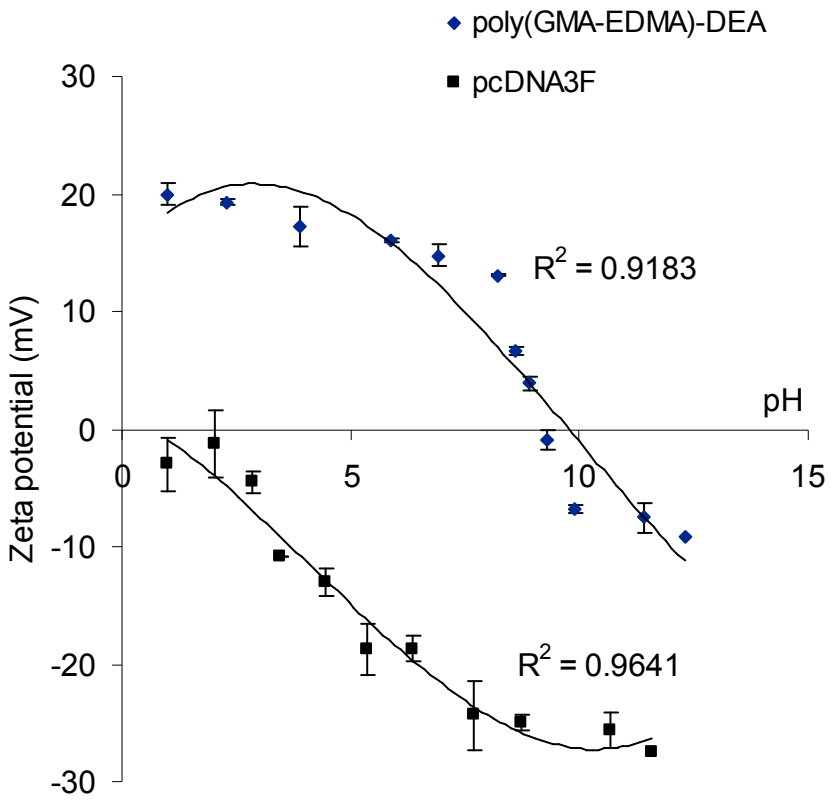

Fig. 9. Effect of buffer's pH on the Zeta potential of pcDNA3F and poly(GMA-EDMA)-DEA. Base buffer (25 mM Tris–HCl, 2 mM EDTA, 0 M NaCl, pH 7). Each data point represents the average of three replicates.

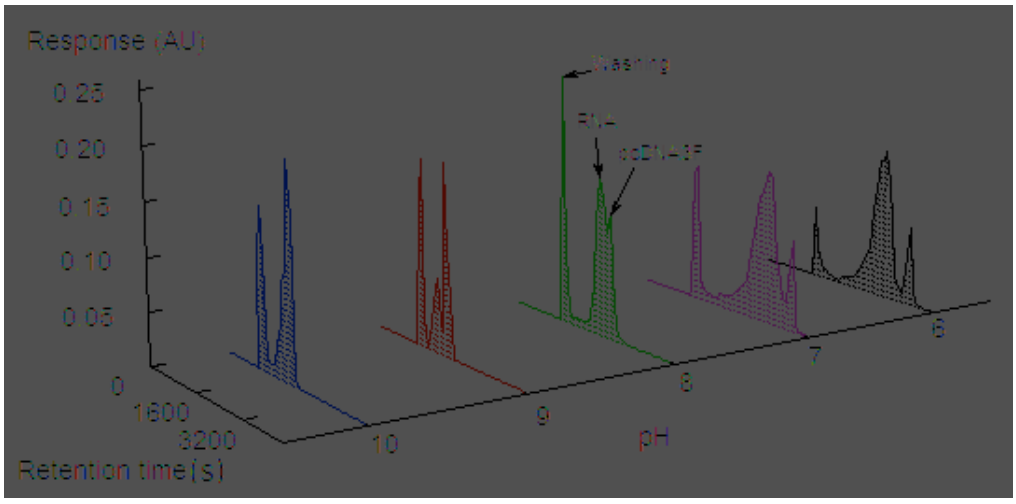

Fig. 10. Effect of pH on plasmid resolution. Flowrate 0.6 mL/min. Buffer A (25 mM Tris–HCl, 2 mM EDTA, 0.2 M NaCl). Buffer B (25 mM Tris–HCl, 2 mM EDTA, 1.0 M NaCl). Sample: 0.5 mL of clarified alkaline lysed cell lysate. Washing, 30 CVs of buffer A; gradient elution, 4% B/min.

It can be seen from Fig. 10 that at pH 9 and 10, there is no plasmid resolution since both plasmid and ligand are negatively charged. In this case, plasmid forms part of the flowthrough and co-elutes with the impurities namely RNA, nicked plasmids, proteins and lipopolysaccharides. Plasmids are best resolved from RNA at pH 6 as evident from Fig. 10 and Table 1. Under this pH value, plasmids are high negatively charged and have a strong attraction towards the positively charged anion exchange matrix thus higher retention time. In addition to that, it is speculated that under the same pH condition, other impurities mainly RNAs, proteins, gDNAs and nicked plasmids are also negatively charged but their magnitudes are substantially lower than that of supercoiled plasmids. As a consequence, plasmids and impurities can be separated during NaCl gradient elution in the order of increasing negative charge and retention time. These trends of plasmid retention as a result of pH conditions also agree with the studies done by Bencina *et al*. [22]. They studied the effect of pH of the mobile phase between 7 and 12. Retention of plasmids on a DEAHP (weak anion-exchanger) column significantly decreased at higher pH values. They concluded that the decrease in plasmid retention was attributed to DEAHP groups since the pH was not expected to significantly influence the charge on the plasmids. In this study however, we found out that the surface charge of both plasmid and anion exchange groups were significantly affected by pH as evident from Fig. 9 and were responsible for the plasmid retention.

Table 1. Plasmid-RNA resolution (Rs) at different chromatographic conditions.

pH	6	7	8	9	10
Rs	*0.81*	*0.69*	*0.51*	*0*	*0*
% buffer B/min	1	3	5	7	10
Rs	*0.73*	*0.85*	*0.43*	*0*	*0*
% porogen	50	60	65	70	80
Rs	*0.52*	*0.75*	*0.89*	*0.65*	*0.6*
buffer A ionic strength (M)	0.3	0.4	0.5	0.7	
Rs	*0.9*	*1.06*	*1.03*	*1.15*	

Rs = (T1-T2)/0.5(W1+W2), where T1: retention time of RNA (s), T2: retention time of pcDNA3F (s), W1: peak width of RNA (s), W2: peak width of pcDNA3F (s).

4. Conclusions

This work describes the optimisation of process variables for the purification of plasmid DNA (pcDNA3F) using anion exchange monolithic chromatography techniques. This work concludes that plasmid separation can successfully be achieved simply by optimising ligand functionalisation temperature, mobile phase flow rate, monolith pore size, buffer pH, ionic strength of binding buffer and buffer gradient elution slope. Temperature greatly affects the amount of ligands attached to the base monolith matrix and optimum functionalisation can be carried out at 60 ^{o}C for 24 h. Sharp, symmetrical and minimised band broadening can be achieved at a mobile phase flow rate of 0.6 m/min. Preferential plasmid adsorption and optimum resolution can be achieved by loading the clarified alkaline-lysed plasmid-containing cell lysate into 400 nm pore size of monolith in 0.7 M NaCl (pH 7) of binding buffer followed by increasing the NaCl concentration to 1.0 M at 3 %B/min.

Acknowledgements

The authors would like to thank Monash University, Australia and Universiti Malaysia Sabah, Malaysia for the financial support to carry out this project.

References

[1] A. Eon-Duval, G. Burke, J. Chromatogr. B-Analytical Technologies in the Biomedical and Life Sciences 804 (2004) 327.

[2] D.M.F. Prazeres, T. Schluep, C. Cooney, J. Chromatogr. A 806 (1998) 31.

[3] F. Sousa, M.F. Duarte, Prazeres, J.A. Queiroz, Trends Biotechnol. 26 (2008) 518.

[4] C.R. Smith, R.B. DePrince, J. Dackor, D. Weigl, J. Griffith, M. Persmark, J. Chromatogr. B 854 (2007) 121.

[5] M.M. Diogo, J.A. Queiroz, D.M.F. Prazeres, J. Chromatogr. A 1069 (2005) 3.

[6] M.W. Roberts, C.M. Ongkudon, G.M. Forde, M.K. Danquah, J. Sep. Sci. 32 (2009) 2485.

[7] J. Urthaler, R. Schlegl, A. Podgornik, A. Strancar, A. Jungbauer, R. Necina, J. Chromatogr. A 1065 (2005) 93.

[8] C.P. Bisjak, R. Bakry, C.W. Huck, G.K. Bonn, chromatographia 62 (2005) S31.

[9] H.Y. Aboul-Enein, I. Ali, H. Hoenen, Biomed. Chromatogr. 20 (2006) 760.

[10] I. Ali, V.D. Gaitonde, H.Y. Aboul-Enein, J. Chromatogr. Sci. 47 (2009) 432.

[11] H.Y. Aboul-Enein, I. Ali, Talanta 65 (2004) 276.

[12] I. Ali, H.Y. Aboul-Enein, Anal. Lett. 37 (2004) 2351.

[13] I. Ali, F.E.O. Suliman, H.Y. Aboul-Enein, LC-GC 27 (2009) 22.

[14] <http://www.biaseparations.com/products.asp?FolderId=251&TabId=322> (date last accessed: 15 May 2010).

[15] S.H. Ngiam, Y.H. Zhou, N.J. Turner, N.J. Titchener-Hooker, J. Chromatogr. A 937 (2001) 1.

[16] A. Zochling, R. Hahn, K. Ahrer, J. Urthaler, A. Jungbauer, J. Sep. Sci. 27 (2004) 819.

[17] C.S. Lengsfeld, T.J. Anchordoquy, J. Pharm. Sci. 91 (2002) 1581.

[18] S. Kong, N. Titchener-Hooker, M.S. Levy, J. Membr. Sci. 280 (2006) 824.

[19] M.K. Danquah, G.M. Forde, Chem. Eng. J. 140 (2008) 593.

[20] A.V. Delgado, F. Gonzalez-Caballero, R.J. Hunter, L.K. Koopal, J. Lyklema, Pure App. Chem. 77 (2005) 1753.

[21] G.S. Manning, Biopolymers 19 (1980) 37.

[22] M. Bencina, A. Podgornik, A. Strancar, J.Sep. Sci. 27 (2004) 801.

Section 4.2

Anion exchange chromatography of 4.2 kbp plasmid based vaccine (pcDNA3F) from alkaline lysed *E. coli* lysate using amino functionalised polymethacrylate conical monolith

Separation and Purification Technology. 78: 303 – 310 (2011)

Monash University

Declaration for Thesis Section 4.2

Declaration by candidate

In the case of Section 4.2, the nature and extent of my contribution to the work was the following:

Nature of contribution	Extent of contribution (%)
Initiation, Key ideas, Experimental, Development, Results interpretations, Writing up	90

The following co-authors contributed to the work. Co-authors who are students at Monash University must also indicate the extent of their contribution in percentage terms:

Name	Nature of contribution
Dr. Michael K. Danquah	Initiation, Key ideas, Experimental, Development, Results interpretations, Writing up

Candidate's signature		**Date**

Declaration by co-authors

The undersigned hereby certify that:

1. the above declaration correctly reflects the nature and extent of the candidate's contribution to this work, and the nature of the contribution of each of the co-authors;
2. they meet the criteria for authorship in that they have participated in the conception, execution, or interpretation, of at least that part of the publication in their field of expertise;
3. they take public responsibility for their part of the publication, except for the responsible author who accepts overall responsibility for the publication;
4. there are no other authors of the publication according to these criteria;
5. potential conflicts of interest have been disclosed to (a)granting bodies, (b) the editor or publisher of journals or other publications, and (c) the head of the responsible academic unit; and
6. the original data are stored at the following location (s) and will be held for at least five years from the date indicated below:

Location	Chemical Engineering Department, Monash University, Clayton, Australia

Signature		**Date**

Anion exchange chromatography of 4.2 kbp plasmid based vaccine (pcDNA3F) from alkaline lysed *E. coli* lysate using amino functionalised polymethacrylate conical monolith.

Clarence M. Ongkudon, Michael K. Danquah

Abstract

New strategies to economically manufacture large quantities of vaccines in less time are greatly needed to cater for the increasing global human population. This study aimed at developing a strategy to efficiently manufacture a highly purified plasmid vaccine via anion exchange monolithic chromatography. Diethylamine and triethylamine were used to provide the functional groups for polymethacrylate monoliths and used in anion exchange chromatography of plasmid pcDNA3F. Five chromatographic settings as described in the first table of this article were studied and it was concluded that the triethylamine functionalised conical monolith combined with optimum buffers' and pH conditions produced the highest quality of pcDNA3F. Plasmid yield (3003.55 mg/L), plasmid recovery (90.25%), protein (0.01 mg/L), LPS (0.12 EU/mg) with no detectable gDNA and RNA were obtained at a low NaCl concentration of 0.25 M. Apparently, this technology will have a great impact on the overall plasmid vaccine production and particularly on the development of axial flow monolithic plasmid vaccine purification.

Keywords: Plasmid; Anion exchange chromatography, Conical column; Polymethacrylate monolith

1. Introduction

The birth of recombinant DNA technology as a tool in gene therapy and more recently in DNA vaccination has fostered the development of large scale plasmid DNA (pDNA) production and purification processes. Most of currently employed cGMP plasmid purification techniques involve multi steps pre-treatment and chromatography [1, 2]. These often result in low plasmid recoveries and high operating costs. Conventional plasmid purification schemes such as chloride/ethidium bromide ultracentrifugation, miniprep and

maxiprep use alkaline lysis and disposable chromatographic columns which are not scalable and large amounts of resins, enzymes and hazardous chemicals are employed [3, 4]. Other methods such as selective precipitation, aqueous two-phase separation and tangential flow filtration have some drawbacks such as low purification effect, need for dedicated equipments, time consuming and not scalable [5-7]. Commercial scale purification of plasmid DNA (pDNA) traditionally relies on a conventional particle-based chromatography consisting of many beads with small internal pores (<100 nm) [8]. The hydrodynamic size of plasmid molecules is >100 nm hence adsorption occurs only on the outer surfaces of the beads and this leads to low binding capacities [9]. A recent advancement in large biomolecules purification has resulted in the development of a monolithic chromatographic support which provides higher binding capacity, larger pore size up to 1000 nm and higher flow rates compared to the particulate supports [10-13]. In a recent development involving plasmid purification, it has been reported that a combination of $CaCl_2$ precipitation, anion exchange chromatography and hydrophobic interaction chromatography resulted in pure pDNA satisfying all regulatory requirements [14]. The purification of larger plasmids up to 93 kb at higher flow rates and binding capacity has also been disclosed [15]. The 800ml CIM DEAE monolithic column (Boehringer Ingelheim, Austria) is currently the largest commercially available chromatographic medium that can produce up to 15g of highly concentrated and purified pDNA [7].

One of the most common problems occurs in the preparation of monolith is the introduction of air pockets or gaps between the monolith surface and column wall due to monolith shrinkage. Many researchers have attempted to provide covalent bonds between the column wall and monolith surface by introducing a coupling agent mostly silane based methacrylates [16, 17]. A much simpler method using a conical column to avoid this problem has never been published to date. Conical columns have been used to provide lower retention times, higher linear velocity, reduced mobile phase consumption, and effective converging flow [18, 19]. In addition to the dynamic efficiencies, conical column format provides greater loadability compared to the conventional analytical columns [20]. In this study, conical monoliths were simply used to eliminate side flow problems hence forcing all plasmids to flow within the pores hence interact with the anion exchange matrix.

Anion exchange chromatography (AEC) is apparently the most suitable chromatographic method for pDNA since polynucleotides are negatively charged over a wide pH range [15]. AEC is based on the interaction between negatively charged column matrix in which molecules with lower surface charge densities should elute first followed by high negatively charged molecules, a trend which is attributed to chain length and conformation

[21]. It has been reported that a lower ligand density can lead to reduced resolution [22, 23] but another group of researchers obtained the highest resolution in lower ligand densities [24]. Triethylamine (TEA) and diethylamine (DEA) are tertiary and secondary amines which are positively charged at neutrality when functionalised to the epoxy group of polymethacrylate polymer [25]. This renders their suitability in the chromatographic purification of biomolecules for human administration. It is paramount to use low charged ligands in the ion exchange chromatography of pDNA vaccine since it will result in a low salt concentration during the elution step and eliminates the need for a desalination step. Conventional chromatography often results in 0.7 to 2.0 M NaCl in the final eluate which calls for an additional salt reducing step. A low salt concentration (up to 0.3 M) in vaccine formulations is mandatory for human administration since it will affect the biological activity of the vaccine [26]. Therefore, this work aimed to develop a technique for the purification of plasmid DNA vaccine in an anion exchange chromatography using monoliths.

2. Experimental

2.1. Chemical/reagents

Ethylene glycol dimethacrylate (EDMA) (*M*w 198.22, 98%), glycidyl methacrylate (GMA) (*M*w 142.15, 97%), cyclohexanol (*M*w 100.16, 99%), 1-dodecanol (*M*w 186.33, 98%), AIBN (*M*w 164.21, 98%), MeOH (HPLC grade, *M*w 32.04, 99.93%), DEA (*M*w 73.14, 99%), TEA (*M*w 101.19, 99%), Na_2CO_3 (*M*w 105.99, 99.5%) and EDTA (*M*w 292.3, AG) were purchased from Sigma-Aldrich, Australia. NaCl (Amresco, Australia, *M*W 58.44, 99.5%), agarose (Promega, Australia), SDS (*M*w 288.38, 99.0%) and Tris (Mw 121.14, 99.8%) from Amresco, Australia, EtBr (Sigma, Australia, *M*w 394.31, 10 mg/mL), 1 kbp DNA marker (BioLabs, New England), Wizard plus SV Maxipreps (Promega, Australia).

2.2. Procedures

2.2.1. Preparation of standard pcDNA3F

The model plasmid vaccine (pcDNA3F) was constructed from measles virus fusion (MV-F) gene of plasmid pTM1-F using pcDNA3 (Invitrogen, USA) as the plasmid vector. Standard pcDNA3F purification from *E. coli* bacterial cell paste was performed with Wizard plus SV Maxipreps according to the manufacturer's instructions (Promega).

2.2.2. Preparation of E. coli DH5α-pcDNA3F cleared lysate

5 g of frozen *E. coli* DH5α-pcDNA3F bacterial cell paste was thawed at 37 ^{o}C and resuspended in 50 mL of 0.05 M Tris–HCl, 0.01 M EDTA, pH 8 buffer. The resuspended cells were homogenously mixed with 50 mL of lysis solution (0.2 M NaOH, 1% SDS) for 5 min by gently swirling the mixture. Neutralisation was performed by the addition of 75 mL 3 M CH_3COOK at pH 5.5 to the lysed cell suspension for 5 min. The mixture of pDNA-containing cleared lysate and the precipitated impurities, mainly gDNA were separated by centrifugation at 4600 rpm for 30 min.

2.2.3. Synthesis of poly(GMA-EDMA) monolithic column

The monolith was prepared via free radical co-polymerisation of EDMA and GMA monomers. EDMA/GMA mixture was combined with alcohol-based bi-porogen solvents in the proportion 20/10/60/10 (GMA/EDMA/cyclohexanol/1-dodecanol) making a solution with a total volume of 2 mL. AIBN (1% weight with respect to monomer) was added to initiate the polymerisation reaction. The polymer mixture was sonicated for 15 min and sparged with N_2 gas for 15 min to expel dissolved O_2. The mixture was gently transferred into a conical 0.8 cm × 4 cm polypropylene column (BIORAD, Australia) sealed at the bottom end. The top end was sealed with a parafilm sheet and placed in a water bath for 18 h at 60 ^{o}C. The polymer resin was washed to remove all porogens and other soluble matters by flowing through the column with methanol for 20 h at room temperature.

2.2.4. Functionalisation of poly(GMA-EDMA) with diethylamine(DEA) and triethylamine (TEA)

The column containing the monolith was connected and configured to a low pressure pump. The polymer was washed with deionised water at 0.3 mL/min for 60 min followed by a solution containing 17 mM DEA (or TEA), 20 mM Na_2CO_3 and 3 mM NaCl at 0.1 mL/min for 20 h in a 60 ^{o}C water bath. The resulting functionalised polymer was washed with deionised water for 60 min and kept at room temperature. Reaction schemes for the synthesis and TEA functionalisation of poly (GMA-EDMA) monolith are shown in Fig. 1.

2.2.5. Column's ligand density determination

Three 2 mL poly (GMA-EDMA) were prepared as described previously. The polymer was washed with deionised water for 60 min and dried in an oven at 70 ^{o}C until a constant dry weight was obtained. The polymer was derivatised with DEA (or TEA) as described before. The resulting polymer resin was washed with deionised water and dried in an oven at 70 ^{o}C

until a constant dry weight was achieved. The average ligand density was calculated based on the difference in dry weight of the polymer before and after functionalisation was carried out. Weight measurement was done using digital balance BP 110 S (Sartorius, Australia) with 0.0001 g sensitivity. The accuracy of this method was checked and agreed with results obtained using the method described by [27].

2.2.6. Anion exchange chromatographic purification of pcDNA3F

The conical column containing 2 mL of functionalised monolithic resin was connected and configured to BIORAD HPLC system. Before the chromatography was performed, column equilibration was done with buffer A (25 mM Tris–HCl, 2 mM EDTA, x M NaCl, pH y) at 1.0 mL/min until a constant UV baseline was achieved. 0.5 mL of clarified cell lysate was diluted 2-fold with buffer A and applied at 1.0 mL/min. A washing step was done with 30 column volumes (CV) buffer A at 1.0 mL/min to completely remove the unbound and weakly retained molecules especially proteins. The elution of pcDNA3F was done by mixing buffer A with buffer B (25 mM Tris–HCl, 2 mM EDTA, a M NaCl, pH b) at 4% buffer B/min. The column could easily be cleaned with 3 CVs of a solution containing 0.5 M NaOH and 2 M NaCl followed by 50 CVs of deionised water. The column was then regenerated with 10 CVs of buffer B. The chromatography was studied using DEA and TEA functionalised poly(GMA-EDMA) monoliths either as a single or combined columns. Column configurations and buffer settings are summarised in Table 1.

2.2.7. Column's binding capacity determination

The column was configured to BIORAD HPLC system and equilibrated as previously mentioned. 250 mg/L of standard pcDNA3F was diluted 2-fold with buffer A and applied at 1 mL/min until the UV absorbance reached a maximum level. The column was washed with 10 CVs buffer A and pcDNA3F was eluted with 5 CVs buffer B. The column maximum plasmid binding capacity was calculated by integrating the area under the breakthrough curves during continuous loading.

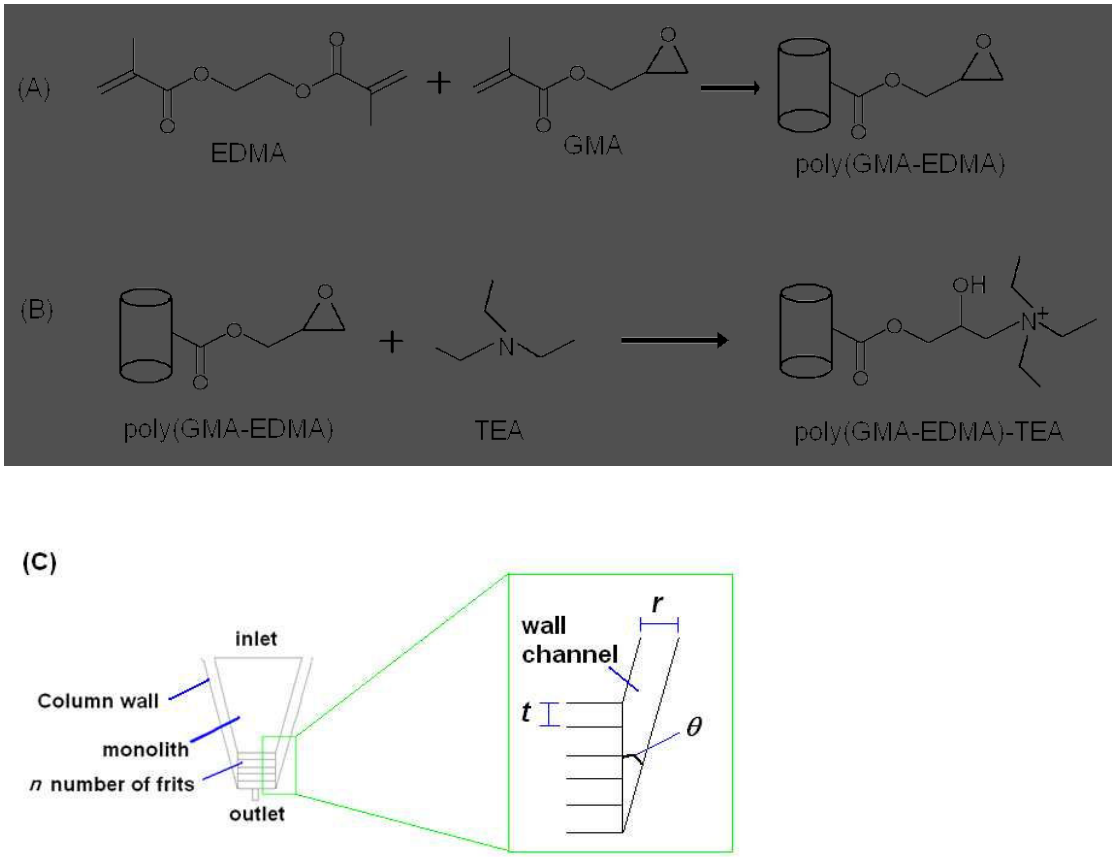

Fig. 1. (A) Copolymerisation between ethylene glycol dimethacrylate (EDMA) and glycidyl methacrylate (GMA) in the presence of cyclohexanol/dodecanol porogen and AIBN free radical initiator at 60 ^{o}C for 18 h. (B) Functionalisation of poly(GMA-EDMA) with triethylamine at 60 ^{o}C for 20 h in 20 mM Na_2CO_3 and 3 mM NaCl medium. (C) Schematic representation of the wall channeling and parameters used in equation (1).

Table 1. Column and buffer settings for anion exchange chromatography of pcDNA3F using amino functionalised polymethacrylate monoliths.

Test no.	Column configuration	Buffer A NaCl, *x* M	Buffer A pH, *y*	Buffer B NaCl, *a* M	Buffer B pH, *b*
1	1 CV poly(GMA-EDMA)-DEA	0.2	7	1.0	7
2	1 CV poly(GMA-EDMA)-TEA	0.2	7	1.0	7
3[a]	1st 0.5 CV poly(GMA-EDMA)-DEA 2nd 0.5 CV poly(GMA-EDMA)-TEA	0.2	5.7	1.0	7
4[a]	1st 0.5 CV poly(GMA-EDMA)-TEA 2nd 0.5 CV poly(GMA-EDMA)-DEA	0.2	5.7	1.0	7
5	1 CV poly(GMA-EDMA)-TEA	0.01	5.7	0.5	8

[a] Chromatographic columns for test no. 3 and no. 4 were configured by combining two conical monoliths (1st 0.5 CV poly(GMA-EDMA)-DEA, 2nd 0.5 CV poly(GMA-EDMA)-TEA) in the same column in series and *vice versa*. 1 CV = 2 mL.

2.2.8. Plasmid DNA qualitative and quantitative analyses

The concentration of the purified plasmid was determined via UV absorbance at 260 nm. An absorbance value of 1.0 unit measured at 260 nm represents 50 mg/L double stranded DNA. Nature and size of the plasmid were determined by ethidium bromide agarose gel electrophoresis using 1 kbp DNA ladder. The gel was made up of 50-fold diluted TAE buffer (242 g Tris base, 57.1 mL acetic acid, 9.305 g EDTA), stained with 3 μg/mL ethidium bromide and run for 2 hr at 66 V. The gel was photographed with a gel analyser (BIORAD, Universal Hood II, Italy). Endotoxin analysis of the plasmid solution was performed using chromogenic limulus amoebocyte lysate (LAL) technique according to the manufacturer's instruction (Genscript, USA). Protein content in the plasmid product was determined using Bicinchoninic acid assay according to the manufacturer's instructions (Sigma-Aldrich, USA). The electrokinetics behaviour of plasmid and functionalised poly(GMA-EDMA) as well as their interactions at different conditions were assessed using Zeta potential analyser according to the manufacturer's instructions (Malvern Instruments, UK). The hydrodynamic size distribution of plasmid DNA was determined using Zeta sizer according to the manufacturer's instructions (Malvern Instruments, UK).

2.2.9 Analysis of wall channeling

The conical monolith was prepared as described previously. The monolith was gently removed from the column by pushing the frit at the bottom end of the column using a needle. To construct air channels of different sizes between the monolith and the column wall, several frits with known thickness were inserted into the empty column. The monolith was inserted back into the column and configured to BIORAD HPLC system. A buffer containing 25 mM Tris–HCl, 2 mM EDTA, 0.2 M NaCl, pH 8.1 was pumped through the column at 10 mL/min and the back pressure was recorded. The size of the wall channel (side flow) was adjusted by adding or removing the frits from the column and calculated using the following equation.

$$r = nt(\tan\theta) \qquad (1)$$

Equation (1) was derived on the basis of Pythagorean theorem where r is size of wall channel (mm), n is number of frits, t is frit thickness (mm) and θ is column opening angle (^{o}). A schematic representation of the wall channeling and parameters used in equation (1) is included in Figure 1. This equation is generally applicable in any conical system with a fixed opening angle.

3. Results and discussion

3.1. Physicochemical characteristics of pcDNA3F and anion exchange conical monoliths.

The use of conical monoliths allows a great flexibility for monolith transportation since it can be stored and transported separately from the columns. Due to its unique shape, it always fills in the gaps between the column wall and monolith surface when carefully inserted. This virtually eliminates the air pocket problems usually encountered in non-modified cylindrical type monoliths. In addition, this simple method yet very effective can be used to prepare endless types of monoliths within different column materials. In this work, we developed a simple technique to investigate the correlation between the size of the wall channel and column back pressure and how this information was used to predict the degree of wall channeling in different column geometries. The conical column with an optimal opening angle was used to carry out the subsequent plasmid chromatographic purification studies. Depending on the pore size which is indicated by porogen content in Fig. 4, back pressure generally increases with decreasing size of side flow which agrees with Bernoulli's principle. At one point, the column wall is in full contact with the monolith surface and the back pressure reaches equilibrium which indicates zero side flow even when the number of frit is further reduced. At 70% porogen, the desired column back pressure at 0 cm of side flow is ~ 25 psi. A minute increase in the size of side flow is followed by a dramatic drop in the column back pressure as evident from a side flow of 1.2 mm. At < 70% porogen, the column back pressure is > 25 psi (0 cm side flow) due to decrease in pore size hence increase in flow resistance. In Fig. 5, it is apparent that there is a minimum opening angle (> 10^{o}) of a conical column that compensates for monolith shrinkage thus resulting in a steady column back pressure. Note that an opening angle of 0^{o} indicates that the column is cylindrical and the side flow is equivalent to 0.12 cm (as depicted in Fig. 4). Also note that the data depicted in Fig. 4 and Fig. 5 was generated at a constant flow rate of 10 mL/min.

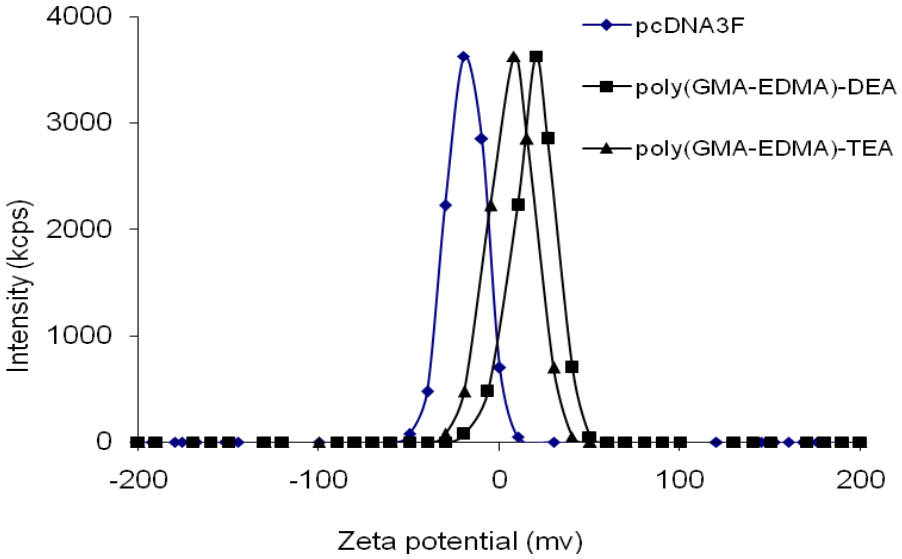

Fig. 2. Zeta potential distribution of plasmid and amino functionalised polymethacrylate sorbents. Results show mean zeta potential for plasmid pcDNA3F (~ -30 mV), poly(GMA-EDMA)-DEA (~ +16 mV) an poly(GMA-EDMA)-TEA (~ +9.5 mV). Sample buffer (25 mM Tris–HCl, 2 mM EDTA and 0.005 M NaCl at pH 8). Suspended poly(GMA-EDMA) particles were prepared by dispersion polymerisation under vigorous shaking.

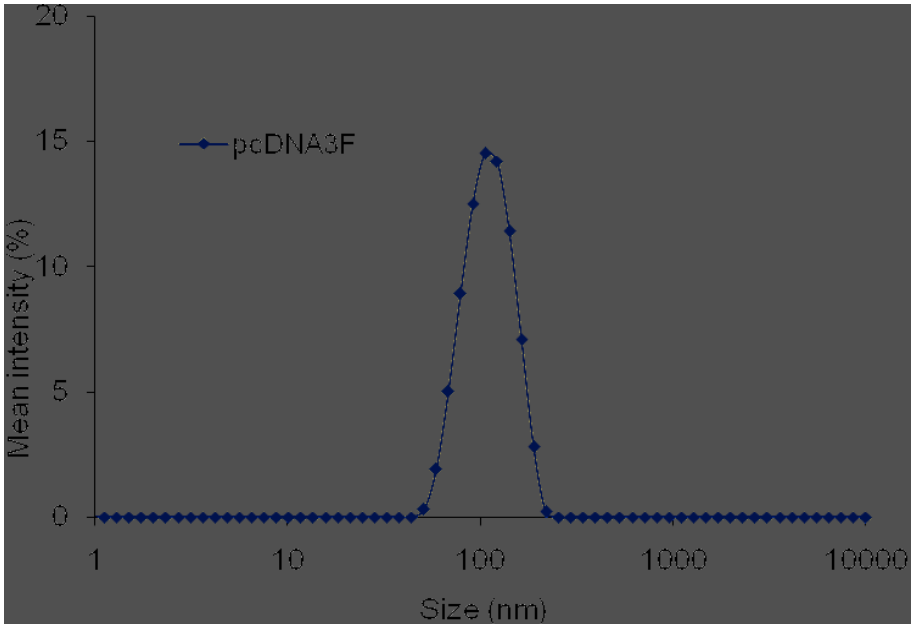

Fig. 3. Hydrodynamic size distribution of plasmid pcDNA3F. Mean size is ~137 nm in 25 mM Tris–HCl, 2 mM EDTA and 0.005 M NaCl at pH 8.

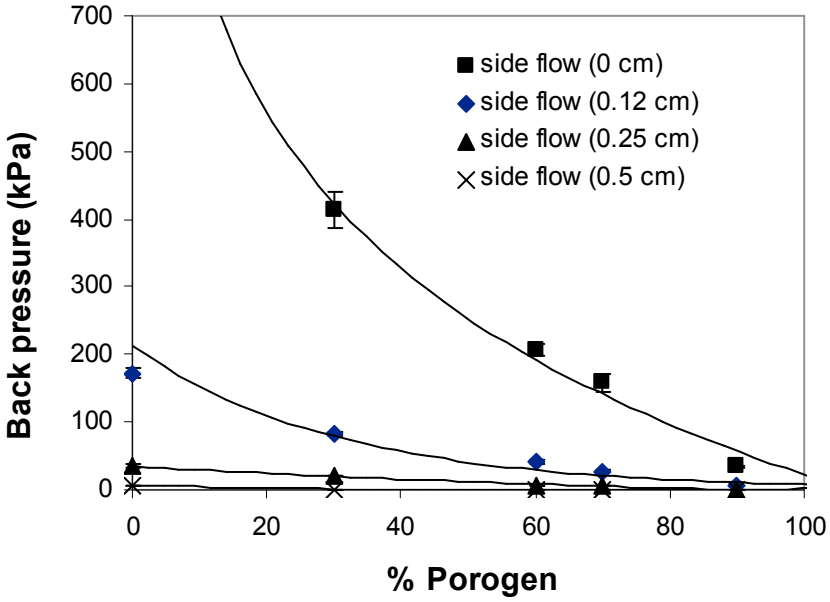

Fig. 4. Correlation between column backpressure and porogen content at different sizes of column side flow. Mobile phase flow rate (10 mL/min),

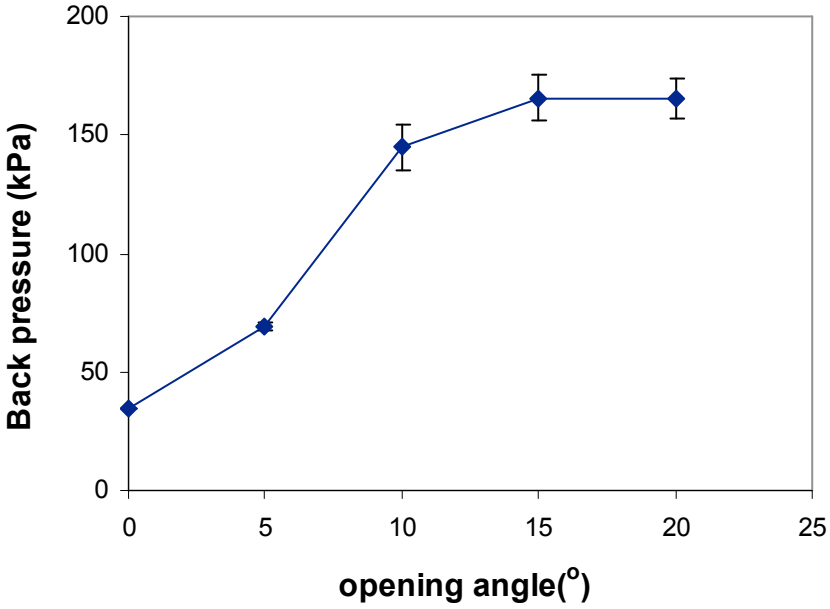

Fig. 5. Effect of conical column's opening angle on wall channeling (indicated by column back pressure). Mobile phase flow rate (10 mL/min), porogen content (70%).

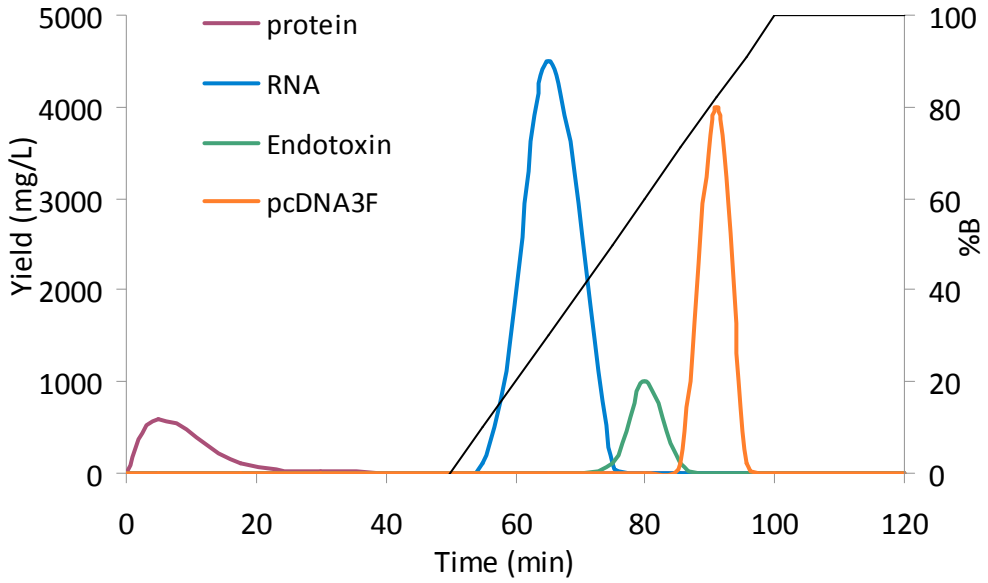

Fig. 6. Preliminary time yield analysis of different fractionated species of the clarified *E. coli* DH5α-pcDNA3F cell lysate using poly(GMA-EDMA)-DEA. Each colored bold line represents chromatogram of protein (brown), RNA (blue), endotoxin (green) and pcDNA3F (orange).

In this study, the performance of two amino based ligands in single-stage plasmid purification was compared. Diethylamine (DEA) and triethylamine (TEA) ligands were selected based on their reasonably low positive surface charge densities and the introduction of a swelling effect during functionalisation process which further reduced the wall channeling problem. The combination of a conical chromatographic column and a swelling effect gave an excellent monolith with good durability and zero side flow. During anion exchange chromatography (AEC), two factors that directly contribute to the separation mechanism are pore size of the monolith as well as surface charge of the plasmid and ligands. These factors were analysed by running Zeta potential/size analyses on suspended poly(GMA-EDMA)-DEA/TEA particles and plasmid pcDNA3F. The results for Zeta potential analysis are shown in Fig. 2. Plasmid pcDNA3F has the highest magnitude of Zeta potential of -30 mV, followed by DEA (+16 mV) and TEA ligands (+9.5 mV). The size of the intended plasmid is paramount in designing a monolith with an optimum pore size capable of resolving different types of molecules of different sizes. Based on Fig. 3, the hydrodynamic diameter of pcDNA3F is 137 nm hence the composition of all monoliths used in this study was optimised based on pcDNA3F hydrodynamic size.

3.2. Anion exchange chromatography of pcDNA3F

During the alkaline lysis procedure, most of the denatured genomic DNA and proteins were precipitated out from the cell lysate. After centrifugation at 4600 rpm for 30 min, the cleared cell lysate generally contained a small fraction of large genomic DNA, RNAs, proteins and most of the plasmid DNA. The cleared cell lysate was loaded into the anion exchange monolithic column and the cell lysate was further fractionated by means of electrostatic interaction and size exclusion of different molecules of different surface charges and hydrodynamic sizes.

Real time species separation during chromatography was studied by running specific assays at each time interval and the results are shown in Fig. 6. The plot shows how each species migrated inside the column. It is evident from this figure that most of the protein contaminants were eluted during the loading and washing stages. This proves that the proteins which were mainly membrane bound proteins of *E. coli* DH5α had negligible interactions with the positively charged ligands due to the low charge density of proteins and large pore size of monolith. The second species eluted from the column was RNA followed by endotoxin and finally pcDNA3F. RNA molecules are negatively charged, single stranded but smaller in size compared to pcDNA3F hence elute earlier than pcDNA3F. The resolution between pcDNA3F and endotoxin is lower than that of protein and RNA and endotoxin seems to coelute with pcDNA3F. This phenomenon can be expected due to the fact that endotoxin and pcDNA3F are both high negatively charged and endotoxin can form supramolecular and micellar structures and moves at a slower rate. In addition, endotoxin separation can be more difficult when a ligand with a higher positive charge is employed.

Plasmid retention time of the DEA ligand is 92.1 min whereas for TEA ligand, plasmid retention time is 75.0 min (Fig. 7A). The difference in the retention time can be explained by the surface charge and the geometrical shape of the amino ligands. DEA ligand has a higher positive charge hence higher electrostatic interaction towards plasmid compared to TEA ligand. The highly electrostatic interaction entails for higher ionic strength buffer (higher %B) for elution and longer elution time. In terms of the geometrical structure of ligands, DEA generally possesses a trigonal planar geometry which is less stable and more ‘flexible’ compared to the more stable and highly ‘rigid’ tetrahedral geometry of TEA. As a result of these conditions, the pore size of TEA-activated monolith is speculated to be slightly larger than the pore size of DEA-activated monolith. Consequently, the pore structure in DEA-activated monolith is more resistant to flow thus longer retention time compared to TEA-activated monolith. However, the geometrical shape of the ligand is assumed to have a

minimal effect on the separation mechanism compared to the electrostatic interaction. The difference in yield for RNA and plasmid DNA in both DEA and TEA cases can be explained by the ligands' binding capacities at specific chromatographic conditions. DEA ligand has a higher binding capacity (Table 2) thus higher plasmid and RNA yields compared to that of TEA ligand.

Fig. 7B shows the chromatograms of test no. 3 and no. 4 of Table 1. The retention times for both DEA-TEA and TEA-DEA column configurations are 92.9 and 97.0 min respectively. These values are much closer to the retention time for single DEA ligand column (92.1 min) and significantly higher than the retention time for single TEA column (75.0 min) in Fig. 4A. These results indicate that when two columns of different ligands of different magnitudes of positive charge are combined in AEC, plasmid retention time is more dependent on the ligand of a higher charge which in this case is DEA. In both Fig. 7A and Fig. 7B, endotoxins were eluted and partially ovelapped between RNA (peak 2) and plasmid DNA (peak 3). Another interesting result worth noting is the difference in pcDNA3F-RNA resolution in each column configuration. pcDNA3F-RNA resolution increases in the order of DEA < TEA < DEA-TEA < TEA-DEA column configurations.

Table 2. Binding capacities of poly(GMA-EDMA)-DEA and poly(GMA-EDMA)-TEA.

Column	ligand density (mmol/g)	Zeta potential (mV)	plasmid concentration (mg/L)	flow rate (mL/min)	binding capacity (mg/mL)
poly(GMA-EDMA)-DEA	6.99	+16.82 ± 1.13	125	1	21.54
poly(GMA-EDMA)-TEA	4.49	+9.73 ± 1.72	125	1	15.78

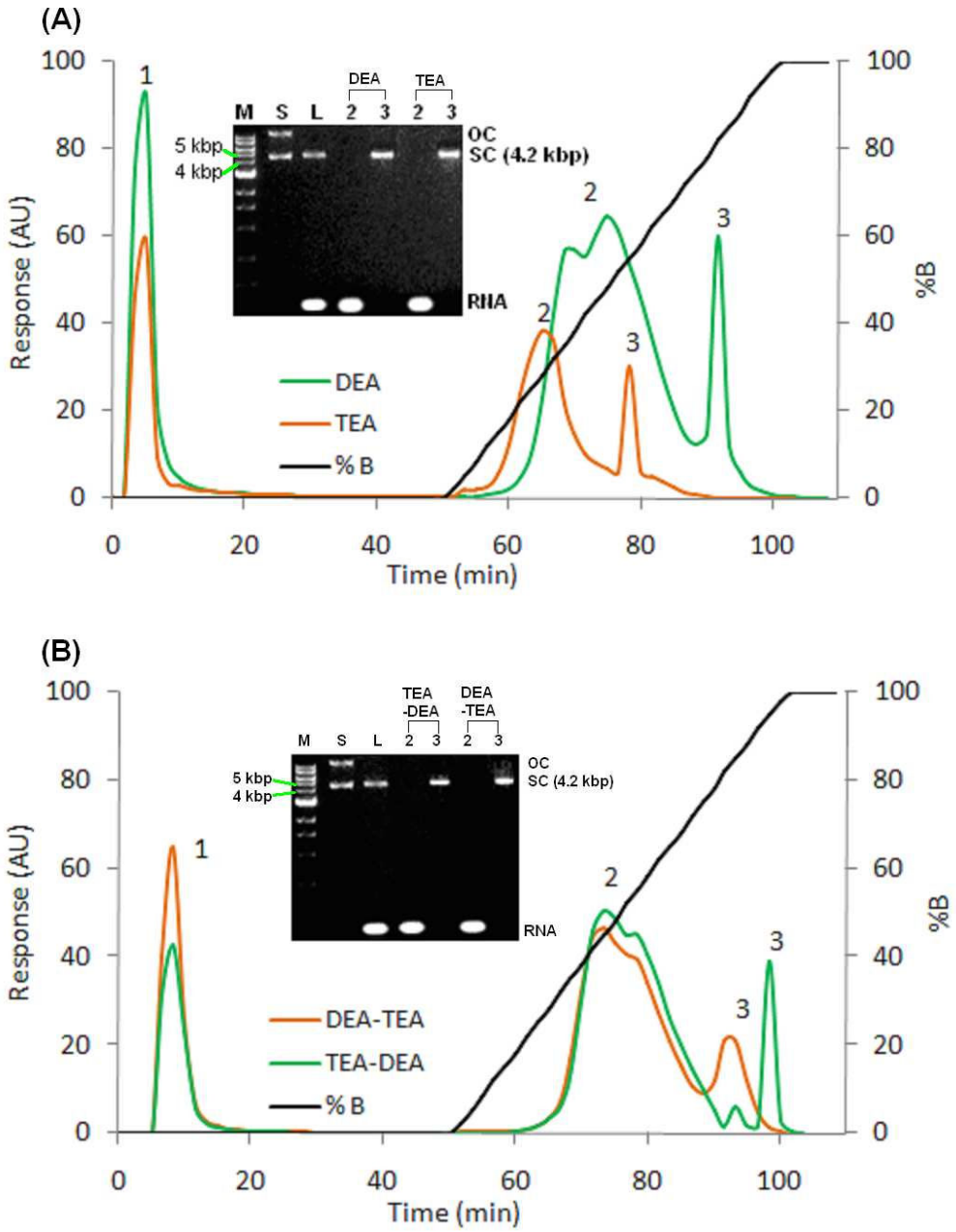

Fig. 7. Anion exchange chromatography of pcDNA3F using diethylamine (DEA) and tryethylamine (TEA) functionalised polymethacrylate monolith. Buffer conditions were given in Table 1. Flow rate 1.0 mL/min. Sample: 0.5 mL of clarified alkaline lysed cell lysate. Washing, 30 CVs; gradient elution, 30 CVs. Peaks 1, 2 and 3 represent flowthrough, RNA, and supercoiled (SC) plasmid pcDNA3F respectively. (A) Chromatograms DEA and TEA represent results from test no. 1 and no. 2 of Table 1. (B) Chromatograms DEA-TEA and TEA-DEA represent results from test no. 3 and no. 4 of Table 1. Inset shows Ethidium bromide gel electrophoresis of different samples taken at different peak elutions. Analysis was performed using 1% agarose in 100 mL TAE×1 buffer, 0.5 µg/ml ethidium bromide at 65V for 1.7 h. Lane M is 1 kbp DNA ladder; lane L is cell lysate; lanes 2 and 3 represent peaks 2 and 3 of the corresponding chromatogram; lane S is standard Maxiprep pcDNA3F.

From these observations it can be concluded that at fixed monolith pore size, flow rate and buffer composition, plasmid resolution and yield can be improved simultaneously using TEA-DEA activated chromatographic column configurations. However this method may not be commercially attractive since the amount of NaCl in the eluate is still high (~0.9 M) compared to standard vaccine formulation for human *in vivo* application [26]. A more detailed qualitative and quantitative study was carried out on test no. 1 – 4 and the results are presented in Table 3.

3.3. Column selection and optimisation of buffers' conditions

Each column setting has certain advantages as well as drawbacks. The poly(GMA-EDMA)-DEA column has about 2 fold higher plasmid yield compared to poly(GMA-EDMA)-TEA due to its higher positive charge density thus higher electrostatic attraction. However, the NaCl, protein and endotoxin levels in the final eluate of poly(GMA-EDMA)-DEA column do not meet pharmaceutical standards for *in vivo* application hence is not commercially attractive. The poly(GMA-EDMA)-TEA column in the other hand provides low levels of impurities and NaCl content but at a low plasmid yield. When the two columns are combined in series (test no. 3 and no. 4), the chromatographic performances are indeed unattractive due to low plasmid yield and increased endotoxin contamination though the plasmid DNA-RNA resolution is improved in test no. 4. Based on this assessment, the TEA activated monolithic column is selected as the most efficient column due to its ability in resolving different impurities and requires low NaCl concentration for elution. In this work, buffers' conditions for TEA functionalised column were further optimised to improve its overall efficiency.

The electrostatic interaction between plasmid and ligands can be visualised by measuring their Zeta potential values in varied buffer conditions. This information can help formulate optimal mobile phase conditions and improve the overall AEC performance. Zeta potential is a measure of the electric potential at a particular distance from the surface of a particle called the hydrodynamic shear boundary or slipping plane. The presence of sodium ions in high concentration reduces the magnitude of apparent Zeta potential values of the particles. According to Fig. 8A, the strongest electrostatic interaction between pcDNA3F and ligands (DEA and TEA) occurs at 0 M NaCl at which the difference in the magnitude of Zeta potential seems to be highest.

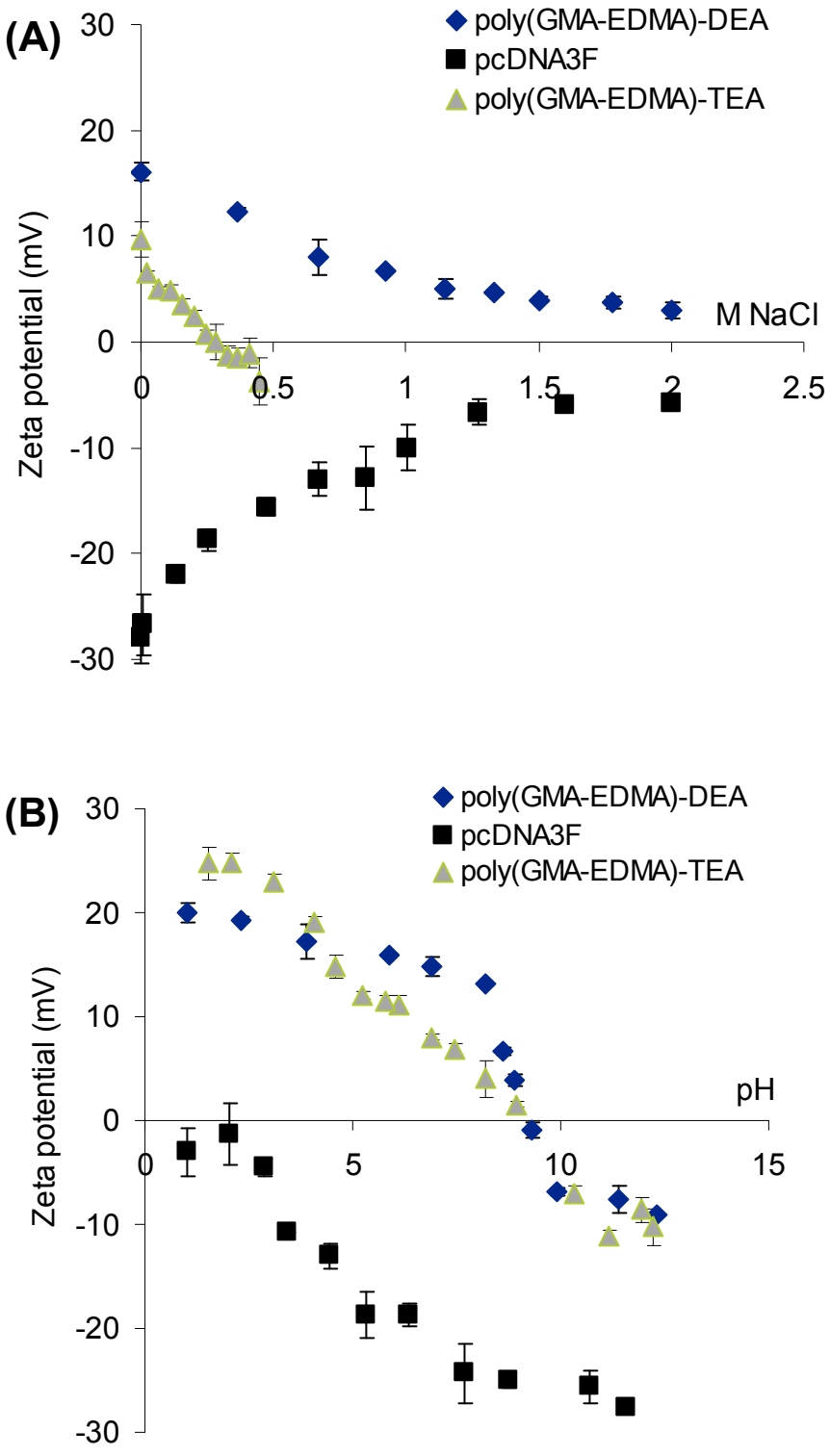

Fig. 8. (A) Effect of buffer's ionic strength on the Zeta potential of pcDNA3F, poly(GMA-EDMA)-TEA and poly(GMA-EDMA)-DEA at pH 8.1. (B) Effect of buffer's pH on the Zeta potential of pcDNA3F, poly(GMA-EDMA)-TEA and poly(GMA-EDMA)-DEA at 0 M NaCl. Buffer (25 mM Tris–HCl, 2 mM EDTA).

Zeta potential values for pcDNA3F increase whilst for DEA ligand, the zeta potential values decrease with increasing NaCl concentration in a rather similar fashion. Interestingly, for TEA ligand; Zeta potential drops substantially with a slight increase in NaCl concentration. This feature makes TEA ligand a better choice since plasmid elution can be done at less than 0.5 M NaCl.

Another factor that greatly influences the electrostatic interaction between plasmid and ligands hence their binding kinetics is pH. pH can greatly alter the monolith charge density and thereby affecting the success of plasmid purification as suggested by [28]. According to [29]; at certain pH, endotoxins can form aggregates and remain within the monolith pores. Both ligands show unique trends of Zeta potential across different pH values (Fig. 8B). The optimal electrostatic interaction between TEA and pcDNA3F is at pH ~ 5. Zeta potential values of TEA ligands gradually decrease towards neutrality and it is speculated that pcDNA3F-TEA electrostatic interaction at pH close to 7 is reasonably low. After several chromatographic runs using poly(GMA-EDMA)-TEA at different pH conditions and NaCl concentrations in mobile phases, the optimal buffers' conditions were found and shown in Table 1 (test no 5). Analyses of samples and chromatograms (Fig. 9) agree satisfactorily with the trend of plasmid elution predicted by Zeta potential analyses (Fig. 8). It is evident from Fig. 9 that the purified pcDNA3F is free from any contaminating bands of gDNA, RNA, and nicked plasmid. pcDNA3F is eluted at 78.5 min which corresponds to 50% of buffer B (or 0.25 M NaCl). Finally, pcDNA3F yield is comparable to that obtained using DEA ligand and low endotoxin level is achievable. The results presented here are optimised and specific to plasmid pcDNA3F and chromatographic column used in this study. However, the optimisation framework introduced here based on the analysis of Zeta potential at different buffer conditions is generally applicable to any AEC settings.

3.4 Economic consideration

On the basis of the results obtained in this work, the TEA functionalised monolith was found to favour better pDNA purification as opposed to that of DEA ligand. The binding capacity of current commercially available adsorbents is between 0.26 and 8.86 mg/mL [30, 31]. The total capacity of the TEA functionalised monolith estimated by dividing the total mass of bound pDNA to the volume of the monolith was found to be 15.78 mg/mL. This value of plasmid binding capacity is slightly higher than the previously reported highest binding capacity and amongst the best to date based on literature findings [30, 31].

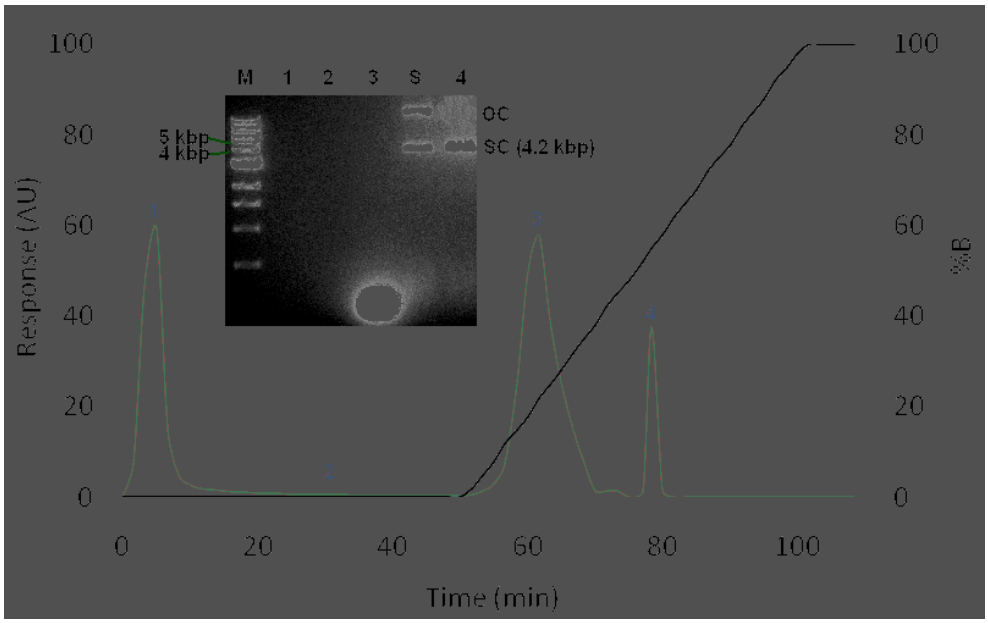

Fig. 9. Optimised anion exchange chromatography of pcDNA3F using tryethylamine (TEA) functionalised polymethacrylate monolith. Buffer conditions were optimised and displayed in Table 1. Flowrate 1.0 mL/min. Sample: 0.5 mL of clarified alkaline lysed cell lysate. Washing, 30 CVs; gradient elution, 30 CVs. Peaks 1, 2, 3 and 4 represent unbound impurities, weakly bound impurities, RNA and supercoiled (SC) plasmid pcDNA3F respectively. Inset shows Ethidium bromide gel electrophoresis of different samples taken at different peak elutions. Analysis was performed using 1% agarose in 100 mL TAE×1 buffer, 0.5 μg/ml ethidium bromide at 65V for 1.7 h. Lane M is 1 kbp DNA ladder; lanes 1, 2, 3 and 4 represent peaks 1, 2, 3 and 4 of the chromatogram; lane S is standard Maxiprep pcDNA3F.

However, it is the economic feasibility of the resin and ease of production that makes it more attractive for pDNA purification. The estimated cost of the TEA functionalised resin is US$ 86/L which is lower than the previously reported lowest cost (US$ 92.0/L) and other commercially available pDNA adsorbents [30, 31]. The cost of functionalisation with TEA ligand was evaluated by taking into account the amount of monomers, porogen, initiator, N_2, TEA ligand, washing solutions used in the monolith preparation and energy needed to maintain the temperature at 60 ^{o}C.

4. Conclusion

This article describes the production of a purified plasmid measles vaccine (pcDNA3F) in an anion exchange chromatography using triethylamine and diethylamine activated polymethacrylate conical monoliths. The pore size has been carefully designed to provide accessibility to large plasmids and high resolution for molecules of different molecular sizes.

A wall channeling effect is often encountered during the monolith synthesis as a result of polymer shrinkage. This is often followed by a decrease in the column back pressure. At fixed flow rate, column size, sample viscosity, porosity and negligible side flow effect, the column back pressure has a maximum value which is attributed to the flow resistance exerted by the interconnected pores. Equation (1) allowed us to systematically alter the size of wall channel and study its effect on column back pressure at different pore sizes and at a constant flow rate hence finds maximum value at which the side flow effect is negligible.

In this study, the TEA functionalised poly (GMA-EDMA) conical monolith combined with optimised buffer conditions provides superior performance over poly (GMA-EDMA)-DEA for the purification of plasmid based vaccine. The plasmid produced by this technique confirms to the regulatory standards and had a low NaCl content and a final pH value near neutrality. Our current (2 mL, 3.5 cm long) monolith system when used at a high flow rate (10mL/min), has not been able to satisfactorily purify our plasmid. The long processing time of ~ 40 min reported in this study was highly subjected to a velocity of 1.75 cm/min, a high volume of washing buffer and a slow rate of gradient elution required to achieve a desirable separation. Current work is underway to further reduce the amount of impurities especially LPS beyond the detection limit whilst reducing the number of chromatographic steps and processing time. Part of the current work involves modifying the buffer composition (addition of new substances) and embedding a second novel ligand into the poly (GMA-EDMA)-TEA monolith.

Table 3. Anion exchange chromatographic performance analysis of different DEA and TEA activated polymethacrylate monolithic column configurations for pcDNA3F purification.

Test no.	Column configuration	plasmid yield (mg/L)	Plasmid Recovery (%)	t_R[a] (min)	R[b] (plasmid and RNA)	protein (mg/L)	RNA (mg/L)	gDNA (mg/L)	LPS (EU/mg)
1	1 CV poly(GMA-EDMA)-DEA	3875.74	> 95	92.1	1.25	3.1	Undetected	Undetected	1.27
2	1 CV poly(GMA-EDMA)-TEA	2069.01	> 95	75.0	1.37	0.3	Undetected	Undetected	0.22
3[c]	1st 0.5 CV poly(GMA-EDMA)-DEA 2nd 0.5 CV poly(GMA-EDMA)-TEA	2129.13	> 95	92.9	1.39	0.05	Undetected	Undetected	2.21
4[c]	1st 0.5 CV poly(GMA-EDMA)-TEA 2nd 0.5 CV poly(GMA-EDMA)-DEA	2326.83	> 95	97.0	1.69	0.01	Undetected	Undetected	2.66
5	1 CV poly(GMA-EDMA)-TEA	3003.55	> 95	78.5	1.62	0.01	Undetected	Undetected	0.12

Composition of feedstock: plasmid (505 mg/L), protein (610 mg/L), RNA (2335 mg/L), gDNA (undetected), LPS (594 EU/mg)

[a] Retention time

[b] Resolution

[c] Chromatographic columns for test no. 3 and no. 4 were configured by combining in the same column two conical monoliths (1st 0.5 CV poly(GMA-EDMA)-DEA, 2nd 0.5 CV poly(GMA-EDMA)-TEA) in series and *vice versa*. 1 CV = 2 mL.

The optimization work performed in this paper is very dependent on the process environment such as the plasmid size, the porosity of the stationary phase, buffer conditions and conductivities. This means that the optimum values could change with the process conditions. However, the approach adopted in this article, even though tailored to specific process conditions, offers a generic model that can be translated to systems under different conditions. Results and equations presented in this article offer a good platform to predict optimum values of systems under different conditions.

Acknowledgements

This project is funded and supported by Monash University, Australia and Universiti Malaysia Sabah, Malaysia.

References

[1] H. Huber, W. Buchinger, J. Diewok, R. Ganja, D. Keller, J. Urthaler, R. Necina, *Industrial Manufacturing of Plasmid DNA:Boehringer's New cGMP Production System Employs Prudent Vector Design as a Backbone*. Genetic Engineering & Biotechnology News, in, USA, 2008, pp. 4-6.

[2] M. Przybylowski, S. Bartido, O. Borquez-Ojeda, M. Sadelain, I. Riviere, Production of clinical-grade plasmid DNA for human Phase I clinical trials and large animal clinical studies, Vaccine, 25 (2007) 5013-5024.

[3] K.J. Prather, S. Sagar, J. Murphy, M. Chartrain, Industrial scale production of plasmid DNA for vaccine and gene therapy: plasmid design, production, and purification, Enzyme Microb. Technol. , 33 (2003) 865-883.

[4] C.M. Ongkudon, M.K. Danquah, Mitigating the Looming Vaccine Crisis: Production and Delivery of Plasmid Vaccines, Crit. Rev. Biotechnol. , DOI: 10.3109/07388551.2010.483460 (2010).

[5] M.S. Levy, R.D. O'Kennedy, P. Ayazi-Shamlou, P. Dunnill, Biochemical engineering approaches to the challenges of producing pure plasmid DNA, Trends Biotechnol., 18 (2000) 296-305.

[6] J. Stadler, R. Lemmens, T. Nyhammar, Plasmid DNA purification, J. Gene Med., 6 (2004) S54-S66.

[7] J. Urthaler, W. Buchinger, R. Necina, Improved downstream process for the production of plasmid DNA for gene therapy, Acta Biochim. Pol., 52 (2005) 703-711.

[8] J. Urthaler, R. Schlegl, A. Podgornik, A. Strancar, A. Jungbauer, R. Necina, Application of monoliths for plasmid DNA purification development and transfer to production, J. Chromatogr. A, 1065 (2005) 93-106.

[9] M.W. Roberts, C.M. Ongkudon, G.M. Forde, M.K. Danquah, Versatility of polymethacrylate monoliths for chromatographic purification of biomolecules, J. Sep. Sci., 32 (2009) 2485-2494.

[10] A. Zochling, R. Hahn, K. Ahrer, J. Urthaler, A. Jungbauer, Mass transfer characteristics of plasmids in monoliths, J. Sep. Sci., 27 (2004) 819-827.

[11] I. Ali, F.E.O. Suliman, H.Y. Aboul-Enein, Superficially porous and monolithic columns: Tools for ultra-fast separations in HPLC, LC-GC, 27 (2009) 22-33.

[12] M.K. Danquah, G.M. Forde, Preparation of macroporous methacrylate monolithic material with convective flow properties for bioseparation: Investigating the kinetics of pore formation and hydrodynamic performance, Chem. Eng. J., 140 (2008) 593-599.

[13] I. Ali, V.D. Gaitonde, H.Y. Aboul-Enein, Monolithic Silica Stationary Phases in Liquid Chromatography, J. Chromatogr. Sci., 47 (2009) 432-442.

[14] F. Smrekar, A. Podgornik, M. Ciringer, S. Kontrec, P. Raspor, A. Strancar, M. Peterka, Preparation of pharmaceutical-grade plasmid DNA using methacrylate monolithic columns, Vaccine, 28 (2010) 2039-2045.

[15] N.L. Krajnc, F. Smrekar, J. Cerne, P. Raspor, M. Modic, D. Krgovic, A. Strancar, A. Podgornik, Purification of large plasmids with methacrylate monolithic columns, J Sep Sci, 32 (2009) 2682-2690.

[16] F. Svec, A.A. Kurganov, Less common applications of monoliths. III. Gas chromatography, J. Chromatogr. A, 1184 (2008) 281-295.

[17] J. Vidic, A. Podgornik, A. Strancar, Effect of the glass surface modification on the strength of methacrylate monolith attachment, J. Chromatogr. A, 1065 (2005) 51-58.

[18] W. Pfeiffer, Converging flow chromatography in constant-pressure mode, J. Chromatogr. A, 1006 (2003) 149-170.

[19] A. Pecavar, A. Smidovnik, M. Prosek, Determination of conical column performances using acyclovir in human plasma sample, Anal. Sci., 13 (1997) 229-234.

[20] A. Pecavar, A. Smidovnik, M. Prosek, Conically shaped chromatographic column Anal. Sci., 15 (1999) 233-240.

[21] C.M. Ongkudon, M.K. Danquah, Process optimisation for anion exchange monolithic chromatography of 4.2 kbp plasmid vaccine (pcDNA3F), J.Chromatogr. B, 878 (2010) 2719-2725.

[22] W. Kopaciewicz, M.A. Rounds, F.E. Regnier, Stationary phase contribution to retention in high-performance anion-exchange protein chromatography ligand density and mixed mode effects. , J. Chromatogr. A, 318 (1985) 16.
[23] D.L. Wu, R.R. Walters, Effects of stationary phase ligand density on highperformance ion-exchange chromatography of proteins, J. Chromatogr. A, 598 (1992) 7-13.
[24] Y. Huang, J. Bi, W. Zhou, Y. Li, Y. Wang, G. Ma, Z. Su, Improving recovery of recombinant hepatitis B virus surface antigen by ion-exchange chromatographic supports with low ligand density, Process Biochem. , 41 (2006) 2320-2326.
[25] M.K. Danquah, J. Ho, G.M. Forde, Performance of R-N(R9)-R99 functionalised poly(glycidyl methacrylate-co-ethylene glycol dimethacrylate) monolithic sorbent for plasmid DNA adsorption, J. Sep. Sci., 30 (2007) 2843 - 2850.
[26] W. Yan, L. Huang, The effects of salt on the physicochemical properties and immunogenicity of protein based vaccine formulated in cationic liposome, Int. J. Pharm., 368 (2009) 56-62.
[27] N. Lendero, J. Vidic, P. Brne, A. Podgornik, A. Strancar, Simple method for determining the amount of ion-exchange groups on chromatographic supports, J. Chromatogr. A, 1065 (2005) 29-38.
[28] C.P. Bisjak, R. Bakry, C.W. Huck, G.K. Bonn, Amino-Functionalized Monolithic Poly(glycidyl methacrylate-codivinylbenzene) Ion-Exchange Stationary Phases for the Separation of Oligonucleotides, Chromatographia, 62 (2005) S31-S36.
[29] M.B. Gorbet, M.V. Sefton, Endotoxin: The uninvited guest, Biomaterials, 26 (2005) 6811-6817.
[30] M.K. Danquah, G.M. Forde, Towards the design of a scalable and commercially viable technique for plasmid purification using a methacrylate monolithic stationary phase, J. Chem. Technol. Biotechnol., 82 (2007) 752-757.
[31] M.K. Danquah, G.M. Forde, The suitability of DEAE-Cl active groups on customized poly (GMA-co-EDMA) continuous stationary phase for fast enzyme-free isolation of plasmid DNA, J. Chromatogr. B, 853 (2007) 38-46.

CHAPTER FIVE

ENDOTOXIN REMOVAL FROM PLASMID VACCINES

Section 5.1

Endotoxin removal and plasmid DNA recovery in various metal ion solutions

Separation Science and Technology. 46: 1280 –1282 (2011)

Monash University

Declaration for Thesis Section 5.1

Declaration by candidate

In the case of Section 5.1, the nature and extent of my contribution to the work was the following:

Nature of contribution	Extent of contribution (%)
Initiation, Key ideas, Experimental, Development, Results interpretations, Writing up	90

The following co-authors contributed to the work. Co-authors who are students at Monash University must also indicate the extent of their contribution in percentage terms:

Name	Nature of contribution
Dr. Michael K. Danquah	Initiation, Key ideas, Experimental, Development, Results interpretations, Writing up

Candidate's signature		**Date**

Declaration by co-authors

The undersigned hereby certify that:

1. the above declaration correctly reflects the nature and extent of the candidate's contribution to this work, and the nature of the contribution of each of the co-authors;
2. they meet the criteria for authorship in that they have participated in the conception, execution, or interpretation, of at least that part of the publication in their field of expertise;
3. they take public responsibility for their part of the publication, except for the responsible author who accepts overall responsibility for the publication;
4. there are no other authors of the publication according to these criteria;
5. potential conflicts of interest have been disclosed to (a)granting bodies, (b) the editor or publisher of journals or other publications, and (c) the head of the responsible academic unit; and
6. the original data are stored at the following location (s) and will be held for at least five years from the date indicated below:

Location	Chemical Engineering Department, Monash University, Clayton, Australia

Signature		**Date**

Endotoxin removal and plasmid DNA recovery in various metal ion solutions.

Clarence M. Ongkudon, Michael K. Danquah

Abstract

In this brief article, we report endotoxin precipitation using different types of metal ion in plasmid DNA purification. The work involved modification and improvement of the LAL chromogenic analysis to compensate for metal ion-LAL interaction. Results (Fig. 1 and Fig. 2) show that $ZnSO_4$ gives an optimum combination of high endotoxin removal efficiency (~91%) as well as high plasmid recovery (~100%) compared to other metal ions tested.

Keywords: Lipopolysaccharide; Plasmid DNA; Selective precipitation; Free metal ion

1. Introduction

Endotoxin contamination remains as the most difficult problem in downstream processing of many therapeutic biomolecules including plasmid based vaccine. This is due to strong endotoxin characteristics such as high negatively charged, exists in different molecular sizes, amphiphilic and exerts strong interaction on biomolecules being purified [1]. In plasmid DNA production, endotoxin contamination is usually encountered during the alkaline lysis of gram negative bacteria due to the release of lipopolysaccharides (LPS) from bacterial cell wall into the lysis solution [2]. Several methods to remove endotoxins from bacterial cell lysates have been extensively studied in the past including affinity chromatography, two phase separation and ultra filtration [3, 4]. A least popular precipitation method using free metal ions has also been reported [5, 6] but the amount of studies is still lacking. Endotoxin quantitation by Limulus Amoebocyte Lysate (LAL) assay is highly sensitive to metal ions [7, 8] hence is not suitable for direct analysis of endotoxin precipitation by free metal ions. The accuracy and reliability of the LAL assay are further degraded when analysis of endotoxin precipitation by different types of metal ions is conducted simultaneously.

2. Materials and methods

2.1. Materials

$CuSO_4.5H_2O$ (99%), $ZnCl_2$ (95%) and $MgSO_4.7H_2O$ (98%) were purchased from AJAX, Australia. $CuCl_2.2H_2O$ (98%) and $ZnSO_4.7H_2O$ (99%) were purchased from BDH, Australia. $NiSO_4.6H_2O$ (99%), $MgCl_2.6H_2O$ (99%), $NiCl_2.6H_2O$ (98%) and $CaCl_2.2H_2O$ (99%) were purchased from MERCK, Germany.

2.2. Standard endotoxin (LPS) and plasmid DNA (pcDNA3F)

Standard LPS was purchased from Genscript, USA and pcDNA3F was prepared from 5 g of *E. coli* cell paste using Wizard plus SV Maxipreps according to the manufacturer's instructions (Promega, Australia).

2.3. LPS/plasmid precipitation using free metal ions

Standard LPS and pcDNA3F were mixed in 1:1 (v/v) ratio and transferred into a pyrogen free microtube and mixed with 1 M of metal ion solution. The mixture was incubated for 30 min at 22 ^oC and centrifuged at 15000 x g for 15 min. 0.5 mL of cleared supernatant was transferred into a new pyrogen free microtube and analysed for plasmid recovery and LPS removal using DNA gel electrophoresis and chromogenic LAL tests.

2.4. Chromogenic LAL analysis of LPS content in different metal ion solutions

The LAL test was performed according to the supplier's instructions (GenScript, USA) except for some modifications as explained herein. Samples, standard LPS and control contained apart from pyrogen free water, one sample volume (SV) of solution containing all cations in exact proportions. This step was highly crucial as it would eliminate any variations due to buffer composition. Minimum sample dilution (MSD) of 1000x was required to reduce the enhancement/inhibition effect of cations on LAL activity whilst maintaining high endotoxin level. 5 mM EDTA was added into each standard LPS and sample to mitigate the endotoxin-metal ion interaction. The incubation times for LAL and chromogenic substrate reactions were 20 and 3 minutes respectively at 37^oC under 50 rpm shaking.

3. Results

Fig. 1 shows that pcDNA3F is completely precipitated in Cu^{2+} solution but highly recovered in $MgSO_4$, $ZnSO_4$, $NiSO_4$ and $MgCl_2$ solutions. Interestingly, all plasmid DNA from different metal ion solutions migrate in the gel at a slower rate compared to standard pcDNA3F. This can be explained by the plasmid-metal interaction which results in a reduced overall plasmid charge density which in turn results in a reduced migration rate during gel electrophoresis. Fig. 2 shows plasmid recovery and endotoxin removal in different metal salt solutions. Plasmid recovery decreases in the order of $ZnSO_4$ > $MgSO_4$ > $MgCl_2$ > $CaCl_2$ > $NiSO_4$ > $NiCl_2$ > $ZnCl_2$ > $CuSO_4$ > $CuCl_2$ whilst endotoxin removal increases in the order of $MgCl_2$ < $MgSO_4$ < $NiSO_4$ < $CaCl_2$ < $NiCl_2$ < $ZnCl_2$ < $ZnSO_4$ < $CuSO_4$ < $CuCl_2$. The higher plasmid recoveries (> 100%) in $MgSO_4$, $ZnSO_4$ and $MgCl_2$ can be explained by the different in band intensities as measured from the DNA gel electrophoresis. It can be concluded from Fig. 2 that optimum endotoxin removal and plasmid recovery can be obtained in $ZnSO_4$ solution. Although $CaCl_2$, $CuSO_4$, $ZnCl_2$, $NiCl_2$ and $CuCl_2$ show high endotoxin removal, plasmid recovery is relatively small compared to $ZnSO_4$.

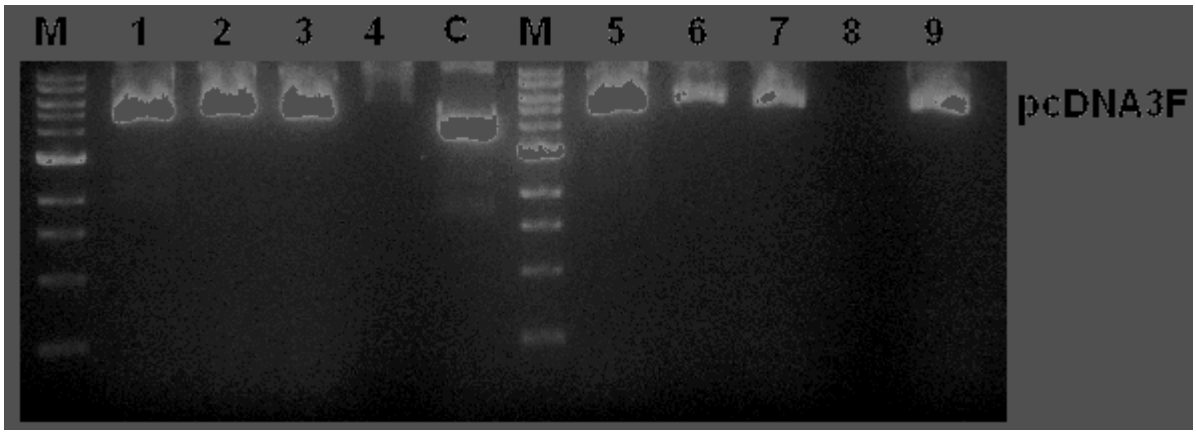

Fig. 1. DNA gel electrophoresis of pcDNA3F. Samples: 20 µL of cleared plasmid-containing metal ion solutions after centrifugation. Analysis was performed using 1% agarose in 100 mL TAE×1 buffer, 0.5 µg/ml ethidium bromide at 65 V for 90 min. Lane M is 1 kbp DNA ladder; lane C is standard pcDNA3F, lanes 1 – 9 represent supernatants of $MgSO_4$, $ZnSO_4$, $NiSO_4$, $CuSO_4$, $MgCl_2$, $ZnCl_2$, $NiCl_2$, $CuCl_2$ and $CaCl_2$.

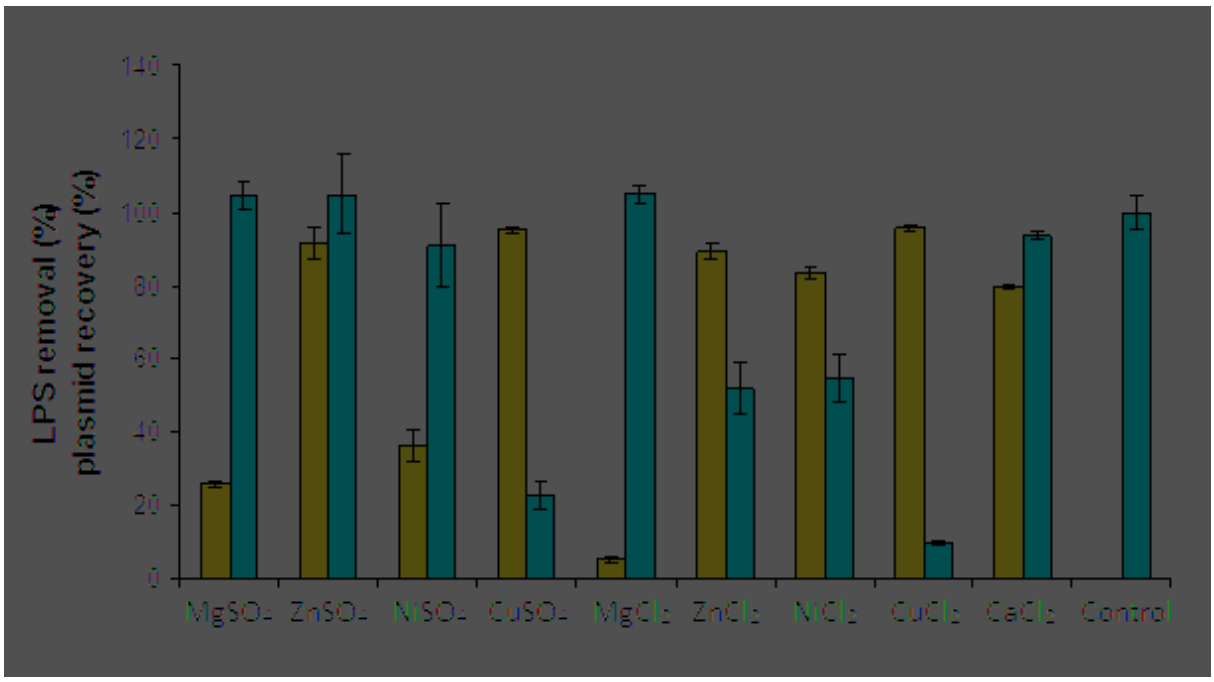

Fig. 2. Plasmid recovery and LPS removal. Plasmid recovery was calculated based on relative band intensity in DNA gel electrophoresis. LPS removal was determined based on improved LAL assay used in this study. Yellow bar represents LPS removal and blue bar represents plasmid recovery.

4. Discussion

Plasmid DNA purification using ion exchange chromatography (IEC) is generally hampered when the size of plasmid is similar to that of LPS. This is attributed to the ability of endotoxins to form different aggregate sizes and possibly carry varying charge densities. Therefore, the gradient elution in IEC may not be able to resolve the overall endotoxins as a single peak from plasmid DNA molecules. A strategy based on a high salt precipitation of endotoxins can be developed to remove large molecular size endotoxins during the alkaline cell lysis procedure. A subsequent ion exchange chromatography[9] can then conveniently separate large plasmid DNA and small endotoxins by gradient elution. Therefore, the AEC matrix can be fully utilised for plasmid DNA binding.

The chromogenic LAL analysis is often difficult to perform when the samples contain different types of metal ions. Interactions between metal ions and LAL can alter the chromogenic reactions thus affecting the accuracy of the endotoxin quantification.

A minute amount of metal ions can inhibit or enhance the LAL chromogenic reaction when added during the LAL-endotoxin incubation step but have not effect when added during the

LAL-endotoxin-chromogenic substrate incubation step[7]. Environmental factors such as pH and volume of lysate are known to further affect the LAL chromogenic reaction thus should be controlled during the analysis [8].

In order to tackle these problems, the experiments involving LAL were performed in such a way that all samples including standard LPS had similar buffer compositions (e.g. volume, pH, temperature, type of cation, and cation concentration). In addition to MSD, 5 mM EDTA was added into the samples and standards to further reduce the effect of metal ions on LAL activity. In summary, results from this work involving LAL reagents have been controlled against possible experimental errors and this work reporting selective precipitation of endotoxin directly from a plasmid DNA-LPS mixture using free alkaline earth and transitional metal ions is the first of its kind.

5. Conclusion

In this work we demonstrate that the assessment of endotoxin selective precipitation from different plasmid/endotoxin-containing metal ion solutions can be done using the technique described herein. This information is certainly vital for the design of a simplified and economic downstream purification of plasmid DNA by process integration of the existing alkaline lysis procedure.

Acknowledgement

This project is funded and supported by Monash University, Australia and Universiti Malaysia Sabah, Malaysia.

References

(1) Magalhães, P.O.; Lopes, A.M.; Mazzola, P.G.; Rangel-Yagui, C.; Penna, T.C.V.; Jr., A.P., Methods of Endotoxin Removal from Biological Preparations: a Review. *J. Pharm. Pharmaceut. Sci.* **2007,** *10*, 388-404.

(2) Diogo, M.M.; Queiroz, J.A.; Prazeres, D.M.F., Chromatography of plasmid DNA. *J. Chromatogr. A* **2005,** *1069*, 3–22.

(3) Anspach, F.B., Endotoxin removal by affinity sorbents. *J. Biochem. Biophys. Methods* **2001,** *49*, 665-681.

(4) Montbriand, P.M.; Malone, R.W., Improved method for the removal of endotoxin from DNA. *J. Biotechnol.* **1996,** *44*, 43-46.

(5) Eon-Duval, A.; Gumbs, K.; Ellett, C., Precipitation of RNA impurities with high salt in a plasmid DNA purification process: Use of experimental design to determine reaction conditions. *Biotechnol. Bioeng.* **2003,** *83*, (5), 544-553.

(6) Tan, L.; Lai, W.B.; Lee, C.T.; Kim, D.S.; Choe, W.S., Differential interactions of plasmid DNA, RNA and endotoxin with immobilised and free metal ions. *J. Chromatogr. A* **2007,** *1141*, (2), 226-234.

(7) Guyomard, S.; Darbord, J.C., Détermination quantitative des endotoxines bactériennes par la méthode «limulus chromogénique: analyse critique et étude des interactions de trois cations divalents. *Ann. Inst. Pasteur/Microbiol.* **1985,** *136B*, 49-55.

(8) Scully, M.F.; Newman, Y.M.; Clark, S.E.; Kakkar, V.V., Evaluation of a Chromogenic Method for Endotoxin Measurement. *Thromb. Res.* **1980,** *20*, 263-270.

(9) Ongkudon, C.M.; Danquah, M.K., Process optimisation for anion exchange monolithic chromatography of 4.2 kbp plasmid vaccine (pcDNA3F). *J.Chromatogr. B* **2010,** *878*, 2719-2725.

Section 5.2

Analysis of selective metal-salt-induced endotoxin precipitation in plasmid DNA purification using improved LAL assay and central composite design

Analytical Chemistry. 83: 391 – 397 (2011)

Monash University

Declaration for Thesis Section 5.2

Declaration by candidate

In the case of Section 5.2, the nature and extent of my contribution to the work was the following:

Nature of contribution	Extent of contribution (%)
Initiation, Key ideas, Experimental, Development, Results interpretations, Writing up	90

The following co-authors contributed to the work. Co-authors who are students at Monash University must also indicate the extent of their contribution in percentage terms:

Name	Nature of contribution
Dr. Michael K. Danquah	Initiation, Key ideas, Experimental, Development, Results interpretations, Writing up

Candidate's signature		**Date**

Declaration by co-authors

The undersigned hereby certify that:

1. the above declaration correctly reflects the nature and extent of the candidate's contribution to this work, and the nature of the contribution of each of the co-authors;
2. they meet the criteria for authorship in that they have participated in the conception, execution, or interpretation, of at least that part of the publication in their field of expertise;
3. they take public responsibility for their part of the publication, except for the responsible author who accepts overall responsibility for the publication;
4. there are no other authors of the publication according to these criteria;
5. potential conflicts of interest have been disclosed to (a)granting bodies, (b) the editor or publisher of journals or other publications, and (c) the head of the responsible academic unit; and
6. the original data are stored at the following location (s) and will be held for at least five years from the date indicated below:

Location	Chemical Engineering Department, Monash University, Clayton, Australia

Signature		**Date**

Analysis of selective metal-salt-induced endotoxin precipitation in plasmid DNA purification using improved LAL assay and central composite design

Clarence M. Ongkudon, Michael K. Danquah

Recent advancements in plasmid DNA (pDNA) production involve the development of innovative and cost effective methods as well as reduced number of unit operations. This study investigates the feasibilities of using a metal salt to selectively remove endotoxins from clarified cell lysates containing plasmid DNA. Screening of endotoxin precipitation in various metal salt solutions and optimisation of process conditions (pH, ion concentration, temperature and incubation time) using central composite design experiments have been carried out successfully. Results show that selective endotoxin precipitation (< 0.05 EU/µg) can economically be carried out during the alkaline cell lysis procedure (neutralisation step) at a pH condition similar to that of alkaline lysed cell lysate, a low $ZnSO_4$ concentration (0.5 M), a minimum incubation time (30 min) and a temperature of 15 ^{o}C. In summary, this method provides ease of subsequent plasmid DNA purification due to reduced bulk impurities, cost-effective and most importantly high endotoxin removal (> 80%) and plasmid recovery (> 90%).

Keywords: Endotoxin precipitation; Plasmid DNA; LAL; Central composite design; Free metal ion.

In vaccine or therapeutic drugs production, substantial endotoxin removal is paramount to avoid severe side effects such as fever, microcoagulation, degradation of organ functions and poor resistance to infections following contact with the human immune system [1]. Endotoxin or lipopolysaccharides (LPS) removal still poses major hurdles in plasmid DNA vaccine purification. Endotoxin level in plasmid DNA vaccines for i*n vivo* application has to be reduced below the threshold level of 0.1 EU/µg plasmid [2]. Endotoxins are the major component of the outer leaflet of the cell membrane of most gram negative bacteria including *E coli*. DH5α [3]. Endotoxins generally possess a negatively charged hydrophilic heteropolysaccharide (O-antigen), a core oligosaccharide region, a lipid A portion, different

aggregated sizes of 10-1000 kDa, and a pI value of 2 thus high negatively charged in basic solution [4].

The clarified alkaline lysed cell lysate generally contains genomic DNA (gDNA), endotoxins, proteins, RNA and nicked or damaged pDNA isoforms along with the intact supercoiled pDNA. The major challenge in pDNA purification is poor selectivity because most of the impurities share common features with plasmid DNA such as surface charge, size and hidrophobicity [5]. Most commercial plasmid purification schemes involve several chromatographic steps which are individually designed to remove a particular component of the cell lysate at a time [6]. Anion exchange, affinity, hydrophobic interaction chromatography, synthetic adsorbent of crystalline calcium silicate hydrate and two-phase micellar system are some of the currently used endotoxin removal techniques [6]. In anion exchange chromatography, it is difficult to separate plasmid and endotoxins mainly due to their similar binding affinities [5a]. In immobilised metal affinity chromatography, plasmid preferentially binds to Fe^{3+} compared to other metal ions. However in the presence of endotoxin and RNA, plasmid binding is least preferential. This phenomenon could be attributed to higher affinity of endotoxin and RNA towards Fe^{3+} or competition for the available binding site [7].

Apparently, the properties of the bacterial solution determine the state of the endotoxins aggregation and this information can help in designing an effective endotoxin removal scheme particularly when combined with plasmid DNA purification [8]. It has been found that addition of $CaCl_2$ into bacterial cell lysate can be used to selectively precipitate RNA from plasmid DNA but at a high concentration (1.5 M) [9]. In addition, an additional purification step such as anion exchange chromatography needs to be integrated to remove a small proportion of unprecipitated RNA [9]. Lithium chloride and magnesium chloride have also been used in RNA precipitation [10] but do not give high endotoxin removal. In this study, salts with high molal surface tension were chosen as candidates for selective endotoxin precipitant since they are antichaotropic and have salting out effect. In a study by Tan *et al.* [2], they observed that free transitional metal ions (e.g. Cu^{2+}, Ni^{2+} and Zn^{2+}) exhibited varying extent of interactions with plasmid DNA impurities hence were also included in this study. Due to the multitude interactions of metal ions on plasmid, endotoxin and RNA at different ion concentrations, it is therefore necessary to explore these interactions systematically using mathematical or statistical methods [11] and to further understand and develop strategies for plasmid DNA purification.

Limulus amoebocyte lysate (LAL) test is the most currently accepted method for endotoxin analysis due to its specificity and high sensitivity to a very low level of endotoxins. However, endotoxins cannot be accurately assayed in samples that contain different types of metal ions due to the their strong effect on the LAL-chromogenic reaction [12]. As little as 0.3 mM of metal ions strongly inhibit or enhance the LAL chromogenic reaction when added during the LAL-endotoxin incubation step but have not effect when added during the LAL-endotoxin-chromogenic substrate incubation step [12a]. As a result, there has been no comparative study of endotoxin precipitation using different metal ions to date. In this work, we have successfully determined endotoxin contents in different metal ion-containing plasmid DNA solutions and optimised the process conditions for selective endotoxin precipitation.

MATERIALS AND METHODS

Chemicals. $CuSO_4.5H_2O$ (99%), $ZnCl_2$ (95%) and $MgSO_4.7H_2O$ (98%) were purchased from AJAX, Australia. $CuCl_2.2H_2O$ (98%) and $ZnSO_4.7H_2O$ (99%) were purchased from BDH, Australia. $NiSO_4.6H_2O$ (99%), $MgCl_2.6H_2O$ (99%), $NiCl_2.6H_2O$ (98%) and $CaCl_2.2H_2O$ (99%) were purchased from MERCK, Germany. Tris base (99%), Tris-HCl (99%), acetic acid (99%), ethylenediaminetetraacetic acid (EDTA, 99%), ethidium bromide (99%), NaOH (99%), sodium dodecyl sulphate (SDS, 99%) and CH_3COOK (99%) were purchased from Sigma-Aldrich, Australia.

Controlled endotoxin (LPS) and plasmid DNA (pcDNA3F). Controlled LPS derived from *E. coli* DH5α was purchased from Genscript, USA and pcDNA3F was prepared from 5 g of *E. coli* DH5α-pcDNA3F (kindly provided by Dr. Diane Webster, Monash University, Australia) cell paste using Wizard plus SV Maxipreps according to the manufacturer's instructions (Promega, Australia).

Plasmid DNA assay. Plasmid DNA content was measured by ethidium bromide agarose gel electrophoresis using 1 kbp DNA ladder (Bio Labs, New England). The gel was made up in 50-fold diluted TAE buffer (242 g of Tris base, 57.1 mL acetic acid, 9.305 g of EDTA) and stained with 3 μg/mL ethidium bromide. The gel was electrophorased at 65 V for 70 min, imaged using a gel analyser (BIORAD, Universal Hood II, Italy) and analysed with standard plasmid DNA using software Quantity One (BIORAD, USA).

Fed-batch Fermentation. A single bacterial colony carrying the plasmid pcDNA3F (*E. coli* DH5*α*-pcDNA3F) was picked from an LB agar plate and subcultured overnight in 250 mL of LB medium containing 1 % ampicillin at 37°C and 200 rpm shaking. Subsequently, 5 mL of the culture was inoculated into a 2 L fermentor containing 1 L of LB medium and 100 µg/mL ampicillin. The temperature was set at 37°C and the dissolved oxygen (DO) value was maintained at 10% by the PID controller. The pH condition was maintained at 7.5 using 4.0 M NaOH and 1.0 M HCl. The inflowing air was set at 20 psi and foaming was controlled by using polypropylene glycol as antifoam. In the fed-batch phase, a carbon substrate feed containing 50% glycerol was added into the fermentor at a constant feeding rate of 0.1 mL/h. Temperature shift from 37 to 45°C was performed 5 h prior to harvesting the culture to boost the plasmid yield. The fermentation was terminated at 24 h post innoculation. The culture broth was harvested, concentrated by ultrafiltration, packaged and stored at −75°C.

Cell lysis and LPS precipitation using free metal ions. 50 mL of overnight grown *E. coli* cell culture was centrifuged at 5000 x g for 15 min and the cell pellet was resuspended in 3 mL of 0.05 M Tris–HCl, 0.01 M EDTA, pH 8 buffer. The resuspended cells were lysed with 3 mL of lysis solution (0.2 M NaOH, 1% SDS) for 5 min and neutralised with 4 mL of 3 M CH_3COOK at pH 5.5 for 5 min. The mixture of pDNA-containing cleared lysate and the precipitated impurities, mainly gDNA, proteins and cell debris were separated by centrifugation at 15000 x g for 10 min. 1 mL of the clarified supernatant was transferred into a fresh microtube and mixed with 1 M of metal ion solution. The mixture was gently inverted for 30-50 times, incubated for 30 min at 25 ^{o}C and centrifuged at 15000 x g for 15 min. 0.5 mL of cleared supernatant was transferred into a pyrogen free microtube and analysed for plasmid recovery and LPS removal using DNA gel electrophoresis and chromogenic LAL tests.

Chromogenic LAL analysis of LPS content in different metal ion solutions. The LAL test was performed according to the supplier's instructions (GenScript, USA) except for some modifications as explained herein. Briefly, 1 volume of sample (1 SV) was added into 1 SV of LAL solution, reacted with 1 SV of chromogenic substrate, stopped with 4 SV of color stabilisers and measured by UV spectrophotometer at 545 nm wavelength. Optimum sample dilution (OSD) of 2000x was required to reduce the enhancement/inhibition effect of cations on LAL activity at which the endotoxin activity still can be detected. Standard LPS and control cell lysate contained apart from pyrogen free water and with or without LPS, 1 SV of buffer containing alkaline lysis buffer (resuspension solution + lysis solution + neutralisation

solution) and metal salt. This was necessary to eliminate any variations due to buffer composition. Standard calibrations for endotoxins solutions containing different metal ions were performed separately for each metal ion to compensate for variable chromogenic reaction rates exerted by metal ions. 10 mM EDTA was added into each standard LPS and sample to mitigate the endotoxin-metal ion interaction. The incubation times for LAL and chromogenic substrate reactions were 20 and 3 min respectively at 37^{o}C under 50 rpm shaking. Results obtained from different metal salt solutions are shown in Table 1.

Experimental design for process optimisation. A series of 26 central composite design (CCD) experiments (Table 2) was conducted to study the effect of pH (5, 6, 7, 8, 9), metal salt concentration (0.5, 0.75, 1, 1.25, 1.5 M), incubation time (0, 10, 30, 50, 60 min) and temperature (5, 10, 15, 20, 25 ^{o}C) on plasmid recovery and endotoxin removal. LPS precipitation was carried out and analysed for plasmid DNA and endotoxin content as previously described. Ten calibration curves were constructed for endotoxin analysis at each pH value and ion concentration. Statistical analysis of the experimental data was performed using software STATISTICA (Statsoft, USA). Contour plots were constructed based on multiple-non-linear regression model and used to predict the optimum process conditions. Linear, quadratic and two-way effects of pH, ion concentration, temperature and incubation time were all incorporated in the model.

RESULTS

Effect of anion and cation on endotoxin precipitation and plasmid recovery. Prior to optimising the precipitation process, we developed a technique for measuring endotoxin contents in different metal salt solutions which facilitated in the selection of the most selective endotoxin precipitant. This method minimises errors due to variable chromogenic reaction rates in the presence of free metal ions [12] thus increasing the overall accuracy of the LAL chromogenic endotoxin analysis.

Endotoxin removal increases in the order of $MgCl_2$ < $MgSO_4$ < $NiSO_4$ < $CaCl_2$ < $NiCl_2$ < $ZnCl_2$ < $ZnSO_4$ < $CuSO_4$ < $CuCl_2$ (Table 1). From this observation, it can also be seen that endotoxin removal is more dependent on cation rather than anion. The dependency of endotoxin removal on cation increases in the order of Mg^{2+} < Ni^{2+} < Ca^{2+} < Zn^{2+} < Cu^{2+}. However, endotoxin removal does not show any preference towards $SO4^{2-}$ and Cl^{-} salt of the same cation.

Table 1. Endotoxin (LPS) and plasmid (pcDNA3F) volumetric yields after salt precipitation*.

	$MgSO_4$	$ZnSO_4$	$NiSO_4$	$CuSO_4$	$MgCl_2$	$ZnCl_2$	$NiCl_2$	$CuCl_2$	$CaCl_2$	C
Endotoxin concentration (EU/mL)	235.15	27.22	201.11	16.52	300.71	34.32	52.25	145.01	64.05	316.22
pcDNA3F concentration (μg/mL)	565.81	566.35	492.13	123.39	567.46	280.85	296.35	54.21	505.03	540.11

*Sample: 1 M of metal salt in 1 mL of clarified cell lysates. Control: 1 mL of clarified alkaline lysed cell extracts. The mixture was incubated for 30 min at 25 ^{o}C. Each value represents the average of triplicates. C: control experiment containing alkaline lysed cell lysate without metal salt. The standard deviation (SD) of each data is < 5% of the values shown.

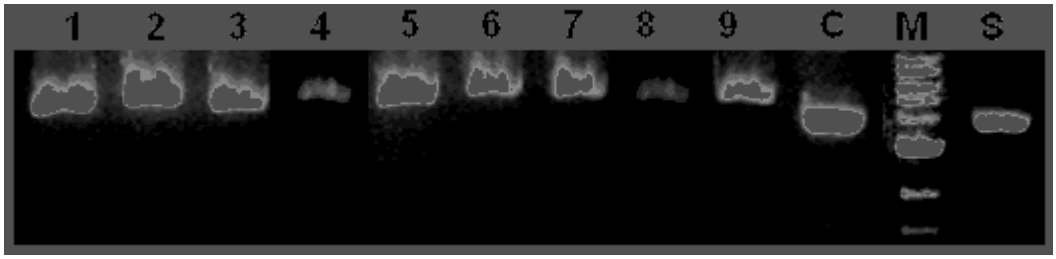

Fig. 1. DNA gel electrophoresis of pcDNA3F in various metal salt solutions. Sample: 10 μL of cell lysate-containing metal ion solutions collected after 15000 rpm centrifugation. Analysis was performed using 1% agarose in 100 mL TAE×1 buffer and 0.5 μg/ml ethidium bromide at 65 V for 70 min. Lane M is DNA ladder (from top: 10, 8, 6, 5, 4, 3, 2, 1.5 kbp); lane C is clarified cell lysate control; lane S is standard pcDNA3F; lanes 1 – 9 represent $MgSO_4$, $ZnSO_4$, $NiSO_4$, $CuSO_4$, $MgCl_2$, $ZnCl_2$, $NiCl_2$, $CuCl_2$ and $CaCl_2$ solutions respectively.

Table 2. Central composite design for the optimisation of endotoxin precipitation using $ZnSO_4$.

no.	pH	Zinc Sulphate concentration Mol/L	Temperature °C	Incubation time min	plasmid recovery %	LPS removal %
1	6	0.75	10	10	56.5	78.0
2	6	0.75	10	50	57.3	84.5
3	6	0.75	20	10	59.5	65.0
4	6	0.75	20	50	58.0	78.0
5	6	1.25	10	10	51.5	91.0
6	6	1.25	10	50	62.0	94.9
7	6	1.25	20	10	59.1	78.0
8	6	1.25	20	50	57.9	80.6
9	8	0.75	10	10	62.9	87.8
10	8	0.75	10	50	57.3	91.0
11	8	0.75	20	10	53.6	74.8
12	8	0.75	20	50	50.2	78.0
13	8	1.25	10	10	37.6	94.3
14	8	1.25	10	50	50.4	91.0
15	8	1.25	20	10	47.1	94.3
16	8	1.25	20	50	54.2	97.5
17	5	1.00	15	30	82.7	76.7
18	9	1.00	15	30	50.7	85.0
19	7	0.50	15	30	55.4	80.0
20	7	1.50	15	30	48.8	98.0
21	7	1.00	5	30	49.4	89.7
22	7	1.00	25	30	45.1	76.7
23	7	1.00	15	0	41.4	90.0
24	7	1.00	15	60	38.2	97.5
25	7	1.00	15	30	40.3	96.2

Plasmid recovery decreases in the order of $ZnSO_4$ > $MgSO_4$ > $MgCl_2$ > $CaCl_2$ > $NiSO_4$ > $NiCl_2$ > $ZnCl_2$ > $CuSO_4$ > $CuCl_2$ (Table 1 and Fig. 1). From this observation, it can be seen that in general, plasmid recovery is more dependent on cation rather than anion. The dependency of plasmid recovery on cation decreases in the order of Zn^{2+} > Mg^{2+} > Ca^{2+} > Ni^{2+} > Cu^{2+}. Also plasmid recovery is higher in $SO4^{2-}$ compared to Cl^- salt of the same cation. Apparently, plasmid pcDNA3F in lanes 1 to 9 in Fig. 1 are positioned just above pcDNA3F in lane C and S. This can be explained by the plasmid DNA – cations interaction occurred in lanes 1 to 9. The electrostatic interaction between negatively charged pcDNA3F and positively charged cations (added during precipitation step) reduced the migration rate of plasmid DNA in DNA gel electrophoresis towards the positive terminal. Due to the anecdotal effects of different metal salts on plasmid recovery and endotoxin removal, the choice of a metal salt for selective endotoxin removal in plasmid DNA purification cannot be made directly from Table 1. Therefore, we calculated the ratio of LPS:plasmid to determine the most selective precipitant. The use of $ZnSO_4$ as evident from Fig. 2 results in the lowest LPS:plasmid ratio of 0.05 which indicates optimum combination of high plasmid recovery and high endotoxin removal. LPS:plasmid ratio for $CuSO_4$, $CaCl_2$ and $ZnCl_2$ is ~1.5 which is 3-fold higher than $ZnSO_4$.

Optimisation of pH, ion concentration, incubation time and temperature for selective endotoxin precipitation using zinc sulphate. The process conditions involving $ZnSO_4$ in endotoxin precipitation were optimised using central composite design experiments and the results are portrayed in Table 2. Interestingly, LPS removal is > 80% for most of the experiments but plasmid recovery is only high (>80%) at pH 5 (Fig. 3).

To further investigate the significance of process conditions on plasmid recovery and endotoxin removal, data from central composite design experiments were subjected to analysis of variance (ANOVA). The contour plot models derived from multiple non linear regression analysis were used to study the effect of process variables on plasmid recovery and endotoxin removal hence optimum process conditions.

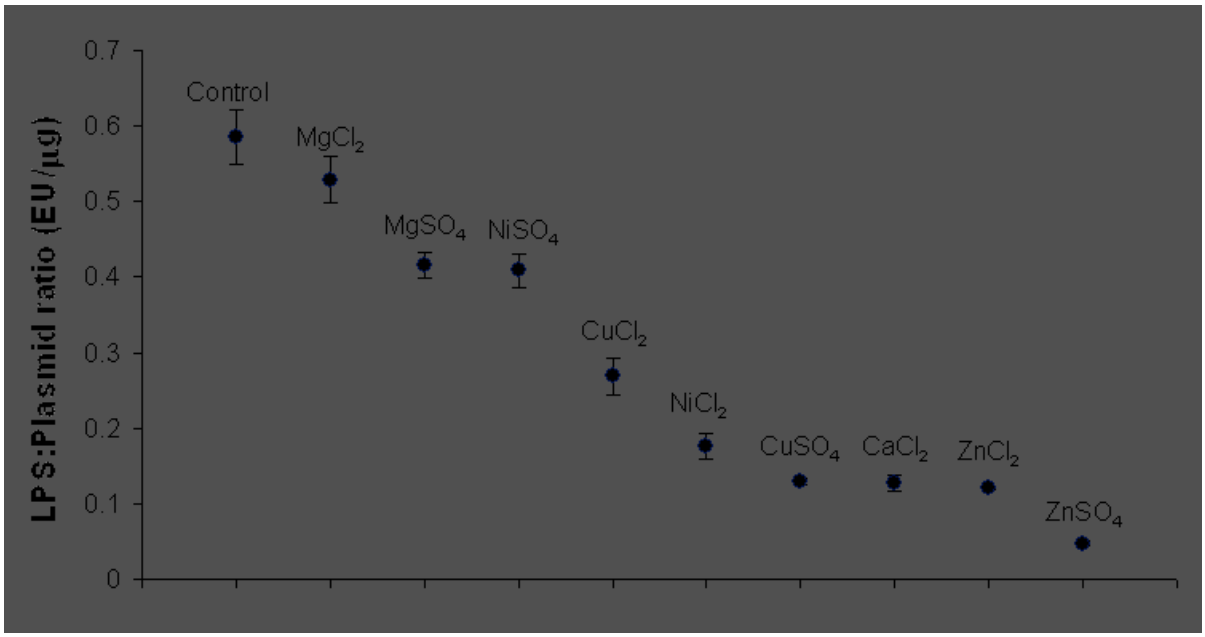

Fig. 2. Ratio between endotoxin and plasmid yields after salt precipitation. Sample: 1 M of metal salt in 1 mL of clarified cell lysates. Control: 1 mL of clarified alkaline lysed cell extracts. The mixture was incubated for 30 min at 25 ^{o}C.

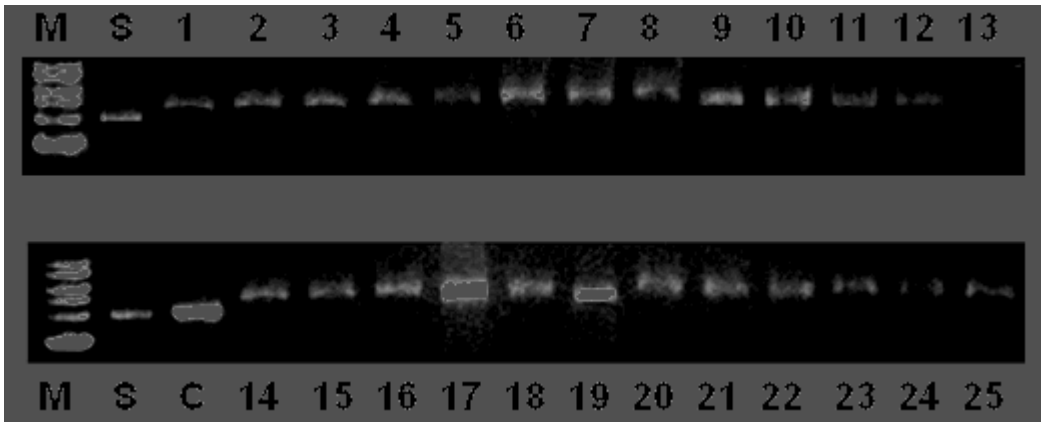

Fig. 3. DNA gel electrophoresis of clarified $ZnSO_4$ – containing cell lysate at various pH, ion concentration, temperature and incubation time. Sample: 10 µL collected after 15000 rpm centrifugation. Analysis was performed using 1% agarose in 100 mL TAE×1 buffer and 0.5 µg/ml ethidium bromide at 65 V for 70 min. Lane M is DNA ladder (from top: 10, 8, 6, 5, 4, 3 kbp); lane S is standard pcDNA3F; lane C is clarified cell lysate control; lanes 1 – 25 contain samples no. 1 – 25 of central composite design experiments in Table 1.

P value signifies the significance of variables or more specifically the probability to get larger *F* value by chance alone. As a rule of thumb, a factor with $P < 0.05$ is considered significant. pH and ion concentration have significant effect on plasmid recovery (Table 3). Temperature, incubation time and all two-way effects are not significant. *SS* value signifies the magnitude of effect of variables. pH has the largest magnitude of linear effect followed by ion concentration, incubation time and temperature. The magnitude of quadratic effects increases in the order of incubation time < temperature < ion concentration < pH. The model generated by multiple non linear regression has high *SS* value (2098.69) and low *P* value (<0.05). R^2 is a measure of the amount of reduction in the variability of response (% plasmid recovery) between model and experimental data. R^2 (0.87) indicates that 87% of the data are in good agreement with the model. For the purpose of response surface analysis, all linear, quadratic and two-way factors were included in the model to give maximum fit of the plasmid recovery data.

Plasmid DNA is highly recovered at lower pH and salt concentration regions (Fig. 4). A pH value of at least 4.5 and a salt concentration of 0.3 M are required to precipitate plasmid DNA. The lowest plasmid DNA recovery can be obtained at about pH 7 and 1 M zinc sulphate. In general, plasmid DNA recovery increases with increasing temperature and decreasing incubation time (Fig. 5). At higher temperatures, plasmid DNA obtains higher kinetic energy and the chances of plasmid precipitation is less as opposed to low temperatures.

pH, ion concentration, temperature and incubation time have significant linear and quadratic effects on endotoxin removal except for quadratic effect of incubation time (Table 4). The magnitude of linear effect on endotoxin removal increases in the order of incubation time < pH < temperature < ion concentration. All two-way effects are not significant. The model generated by multiple non linear regression has high *SS* value (1756.37) and low *P* value (<0.05). R^2 (0.92) indicates that 92% of the data are in good agreement with the model. For the purpose of response surface analysis, all linear, quadratic and two-way factors were included in the model to give maximum fit of the endotoxin removal data.

Table 3. ANOVA representing plasmid recovery in endotoxin precipitation using zinc sulphate.

Factor	*SS*	*df*	*MS*	*F*	*P*
pH (linear)	527.34	1	527.34	16.39	<0.05
pH (quadratic)	682.80	1	682.80	21.22	<0.05
Zinc Sulphate concentration (linear)	252.85	1	252.85	7.86	<0.05
Zinc Sulphate concentration (quadratic)	373.55	1	373.55	11.61	<0.05
Temperature (linear)	0.84	1	0.84	0.03	0.87
Temperature (quadratic)	64.08	1	64.08	1.99	0.19
Incubation time (linear)	10.54	1	10.54	0.33	0.58
Incubation time (quadratic)	2.96	1	2.96	0.09	0.77
pH by Zinc Sulphate concentration	71.83	1	71.83	2.23	0.17
pH by Temperature	6.63	1	6.63	0.21	0.66
pH by Incubation time	0.33	1	0.33	0.01	0.92
Zinc Sulphate concentration by Temperature	54.39	1	54.39	1.69	0.22
Zinc Sulphate concentration by Incubation time	94.58	1	94.58	2.94	0.12
Temperature by Incubation time	19.14	1	19.14	0.59	0.46
Residual	321.76	10	32.18		
Model	2098.69	14	149.91	4.66	<0.05
R^2	0.87				
R^2 adjusted	0.70				

SS : Sum of squares

df : Degrees of freedom

MS : Mean of squares

F: Fisher F-test

P : Probability test

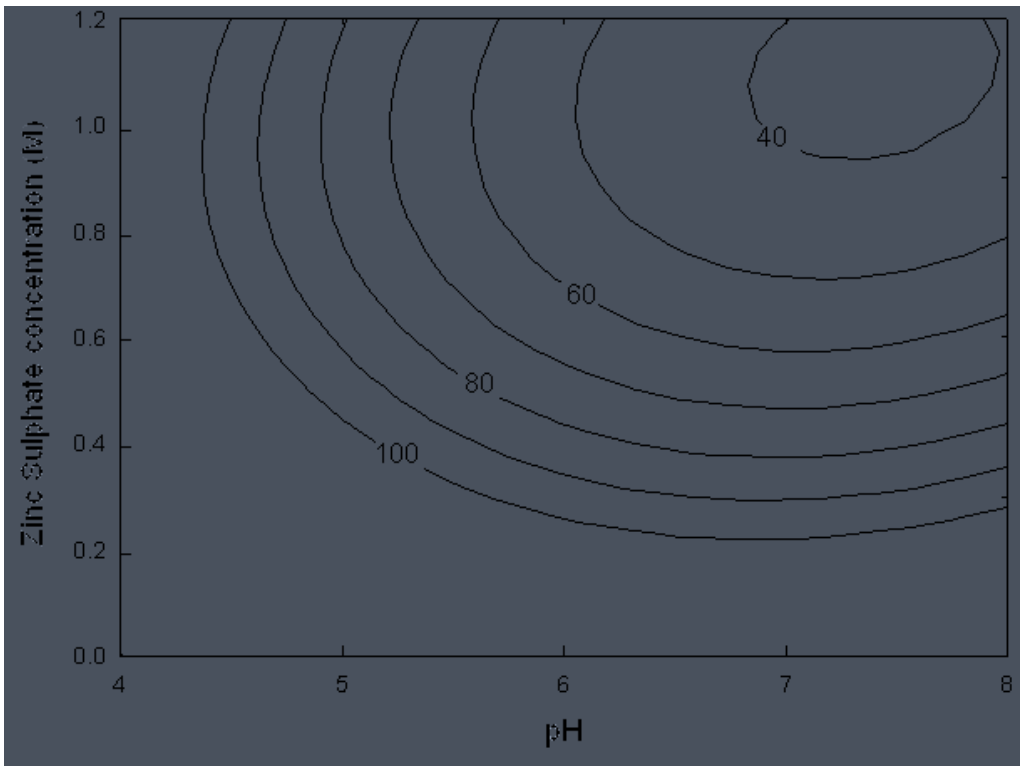

Fig. 4. Contour plots for effect of pH and zinc sulphate concentration on plasmid recovery. Values on contour plots represent plasmid recovery (%). Incubation time and temperature were fixed at 30 min and 15 ^{o}C respectively.

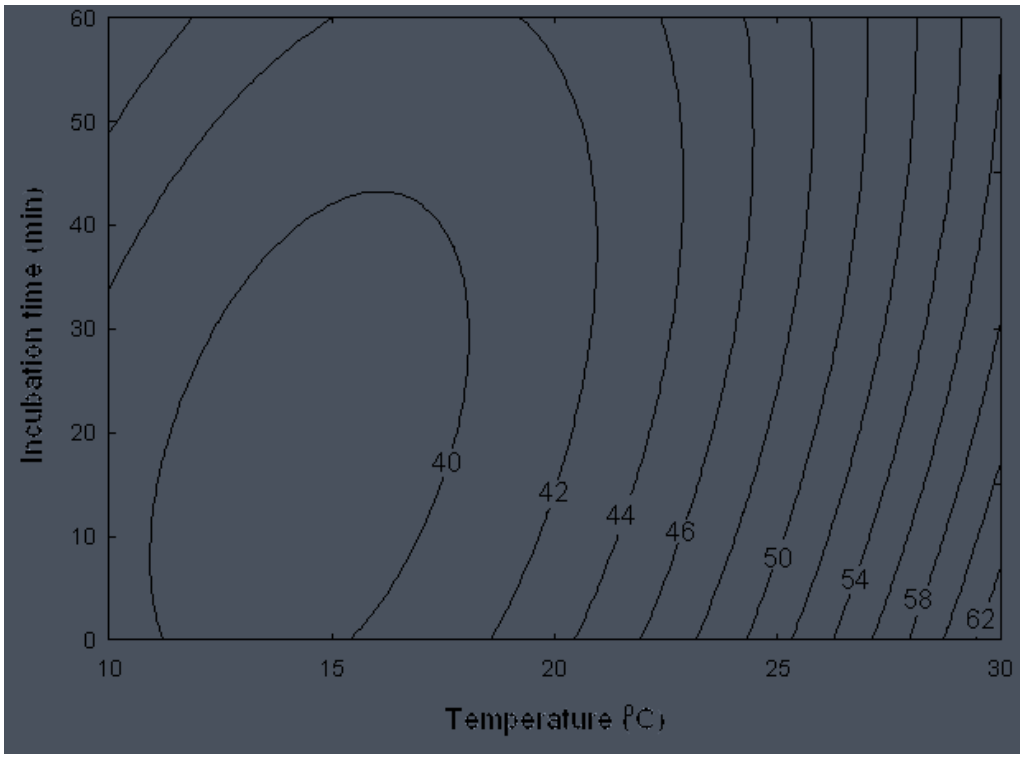

Fig. 5. Contour plots for effect of incubation time and temperature on plasmid recovery. Values on contour plots represent plasmid recovery (%). Zinc sulphate concentration and pH were set at 1 M and 7 respectively.

Table. 4. ANOVA representing endotoxin removal in endotoxin precipitation using zinc sulphate.

Factor	*SS*	*df*	*MS*	*F*	*P*
pH (linear)	236.25	1	236.25	16.31	<0.05
pH (quadratic)	244.33	1	244.33	16.87	<0.05
Zinc Sulphate concentration (linear)	605.01	1	605.01	41.77	<0.05
Zinc Sulphate concentration (quadratic)	64.58	1	64.58	4.46	0.06
Temperature (linear)	354.97	1	354.97	24.51	<0.05
Temperature (quadratic)	180.66	1	180.66	12.47	<0.05
Incubation time (linear)	92.52	1	92.52	6.39	<0.05
Incubation time (quadratic)	20.45	1	20.45	1.41	0.26
pH by Zinc Sulphate concentration	2.64	1	2.64	0.18	0.68
pH by Temperature	46.58	1	46.58	3.22	0.10
pH by Incubation time	24.26	1	24.26	1.67	0.22
Zinc Sulphate concentration by Temperature	38.13	1	38.13	2.63	0.14
Zinc Sulphate concentration by Incubation time	23.77	1	23.77	1.64	0.23
Temperature by Incubation time	8.56	1	8.56	0.59	0.46
Residual	144.83	10	14.48		
Model	1756.37	14	125.46	8.66	<0.05
R^2	0.92				
R^2 adjusted	0.82				

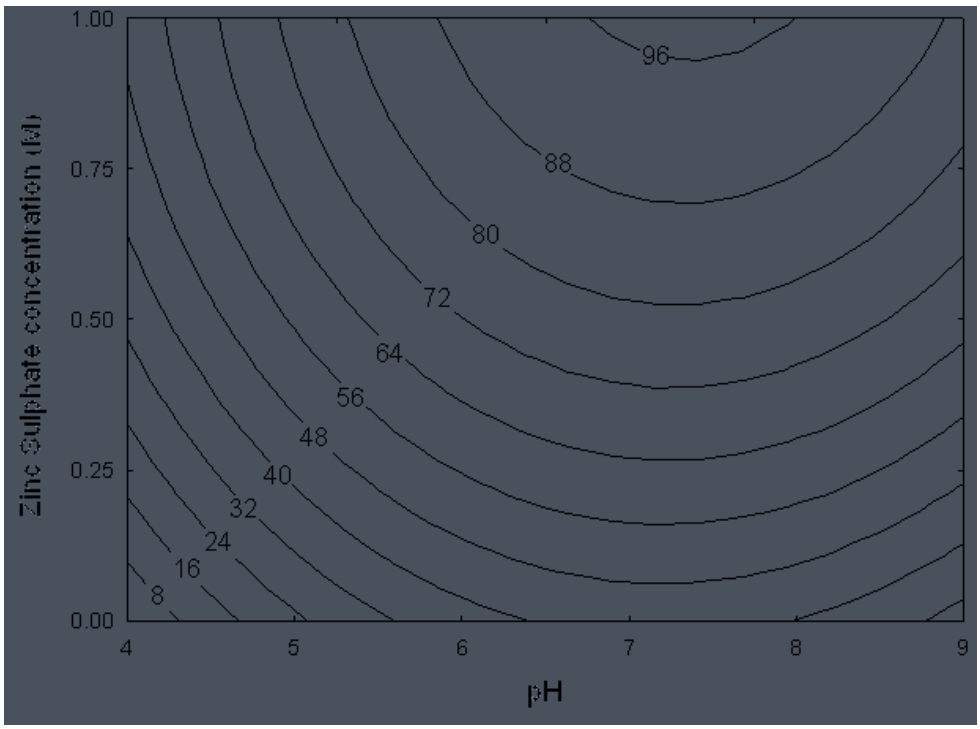

Fig. 6. Contour plots for effect of pH and zinc sulphate concentration on endotoxin removal. Values on contour plots represent endotoxin removal (%). Incubation time and temperature were fixed at 30 min and 15 ^{o}C respectively.

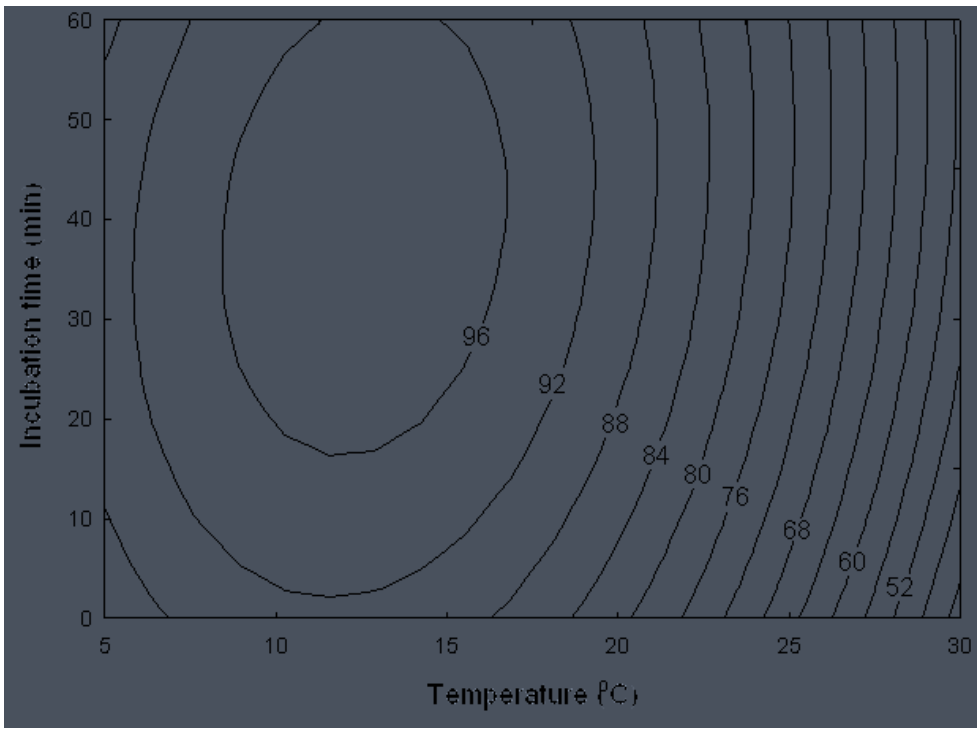

Fig. 7. Contour plots for effect of incubation time and temperature on endotoxin removal. Values on contour plots represent endotoxin removal (%). Zinc sulphate concentration and pH were set at 1 M and 7 respectively.

Endotoxins removal increases with increasing pH and zinc sulphate concentration (Fig. 6). Endotoxins are completely precipitated at pH 7.5 and 1 M zinc sulphate. At pH 6 and 0.5 M zinc sulphate, endotoxin removal is reasonably high (70%) considering plasmid recovery of 80%. In general, endotoxin removal increases with decreasing temperature and increasing incubation time (Fig. 7). At lower temperatures, endotoxins possess lower kinetic energy and the chances of endotoxin precipitation are higher as opposed to higher temperatures.

DISCUSSION

The process conditions are optimised by assuming that the precipitation step is an integral part of the alkaline lysis procedure. Plasmid recovery should be high enough prior to incorporating any subsequent purification step (e.g. anion exchange chromatography) hence should be given main priority during process optimisation. Generally, plasmid DNA recovery is high (80 – 100%) at pH < 7. In this work, pH 5 is really interesting since it is the pH of the clarified alkaline lysed cell lysate and shows the possibility to selectively precipitate endotoxin in plasmid DNA-containing solution. At pH 7 (1 M zinc sulphate), plasmid recovery is minimum (40%) but LPS removal is maximum (100%). At pH 7 (0.5 M), plasmid recovery is 70% and LPS removal is 80%. At pH 5 (1 M), plasmid recovery is 80% which is 2-fold higher than that of pH 7 (1 M) and LPS removal is 75%. Endotoxin removal of 75% is considered significant considering only large LPS are precipitated. At pH 7 – 9, LPS removal is high (>80%) at all range of zinc sulphate concentration (0.5 -1.5) tested. This gives an indication that the increase in endotoxin removal may reach a plateau at 0.5 M based on the changes of the contour plots (Fig. 8).

In view of this, we speculated that at higher salt concentrations (>1 M, pH 5), endotoxin removal could significantly be enhanced without a significant loss of plasmid DNA. A series of experiments was performed at 0 – 2 M and pH 5 to study the hypothesis. Results did not quite agree with the hypothesis. Endotoxin removal did not improve significantly at higher zinc sulphate concentrations and reached a plateau at 0.5 M (Fig. 8). On the contrary, plasmid DNA experienced a substantial loss at 1.5 and 2 M zinc sulphate (Fig. 9). Taking all the above considerations, we propose that the optimum pH and zinc sulphate concentration for selective endotoxin precipitation in plasmid-containing cell lysate are 5 and 0.5 M respectively.

In dilute solution, LPS exists as a bilayer sheet or vesicle of different molecular sizes with the hydrodynamic diameter ranging from about 50 to 500 nm [3, 8]. The different degrees of endotoxin removal efficiency at different salt concentrations may be explained by the different endotoxin aggregate structures hence different critical aggregate concentrations (CAC). The CAC is thought to be influenced by the amount of sugars linked to the lipid A portion of LPS as well as by the number and distribution of charges [13]. Above the CAC, there is equilibrium between free monomers and aggregates which may explains why only a portion of endotoxins are removed at low salt concentrations compared to at high salt concentrations. The conformation of the individual molecules in nonlamellar structure above the CAC can either be conical or wedge-shaped with the hydrophobic moiety adopting a higher cross-sectional area than the hydrophilic [13].

During the precipitation process, cations particularly divalent cations are attracted to and neutralise the negative charge of the phosphate groups of endotoxins thus increasing their potency to form aggregates and precipitate out from the solution. The size of the aggregates formed thus the degree of precipitation is presumed to further increase by cation bridging of endotoxins subunits [14]. Ion concentration, pH, temperature and incubation time contribute to different degrees of endotoxin precipitation hence can be manipulated to increase its selectivity in plasmid DNA purification.

Another interesting observation made in this study is that the selectivity of endotoxin-plasmid DNA precipitation in free metal ion solution increases in the anionic order of Mg^{2+} < Cu^{2+}/Ni^{2+} < Ca^{2+} < Zn^{2+} and cationic order of Cl^{-} < SO^{-4}. The order of selectivity is attributed to the combined effect of ionic strength and affinity of metal ion on endotoxin and plasmid DNA precipitation. The specific interaction/affinity between cations and plasmid DNA can be explained by the existence of specific binding sites for different cations within the DNA grooves as proposed by Egli, 2002 [15]. It is thought that mobile Cu^{2+} and Ni^{2+} ions have similar binding affinities on electron rich phosphate groups of endotoxin and plasmid DNA. Contradictorily, Zn^{2+} and Ca^{2+} are speculated to have specific binding affinities on endotoxin lipopolysaccharides which contribute to the selective endotoxin precipitation.

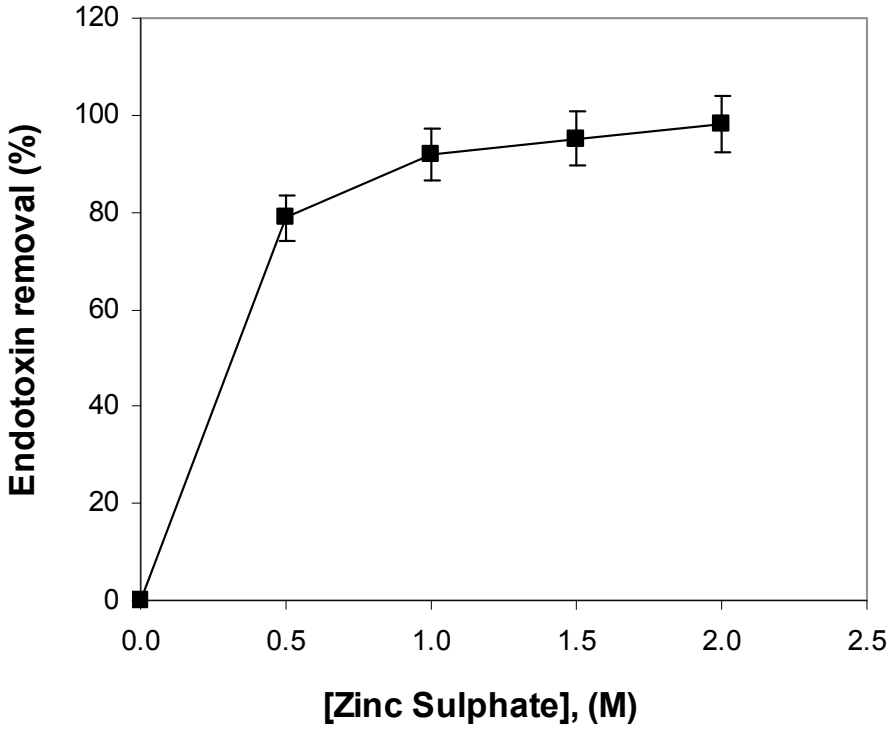

Fig. 8. Endotoxin removal at different zinc sulphate concentrations. Incubation time, pH value and temperature were fixed at 30 min, 5 and 15 ^{o}C respectively.

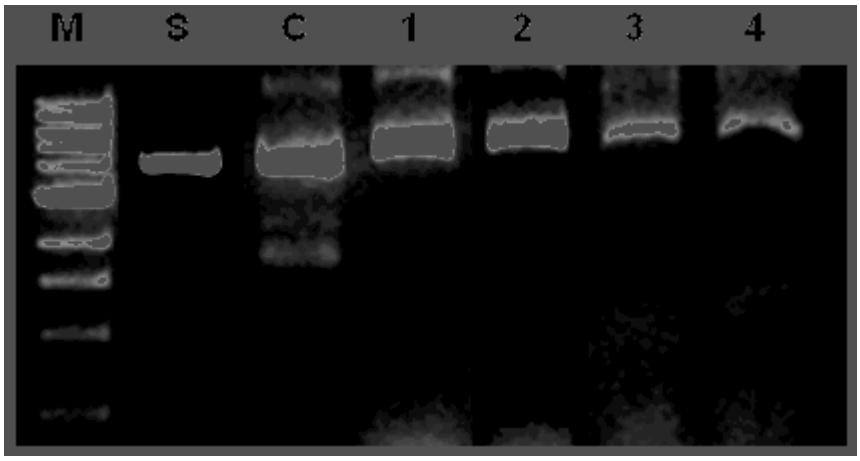

Fig. 9. DNA gel electrophoresis of clarified $ZnSO_4$ – containing cell lysate at 0, 0.5, 1, 1.5 and 2 M $ZnSO_4$. Sample: 10 µL collected after 15000 rpm centrifugation. Analysis was performed using 1% agarose in 100 mL TAE×1 buffer and 0.5 µg/ml ethidium bromide at 65 V for 70 min. Lane M is DNA ladder (from top: 10, 8, 6, 5, 4, 3, 2, 1.5, 1, 0.5 kbp); lane S is standard pcDNA3F; lane C is clarified cell lysate control (0 M $ZnSO_4$); lanes 1, 2, 3 and 4 represent 0.5, 1, 1.5 and 2 M $ZnSO_4$ respectively.

We have seen in this work, a trend of decreasing plasmid recovery with increasing salt concentration as a result of plasmid precipitation. The radius of gyration of a plasmid DNA generally decreases with increasing salt concentration from less than 10 to 100 mM [16] which can be explained by the gradual phase transition from a loosely supercoiled form to a highly compact structure [17]. Zochling *et al*. [18] observed that when salt concentration was increased from 150 mM to 2 M, the hydrodynamic size of plasmid DNA increased by 0.5-fold. The increase in molecular size thus aggregation at high salt concentration followed by salting out effect eventually results in the plasmid precipitation.

In molecular perspective, this phenomenon can be explained by the formation of cation bridges between two phosphates groups in plasmid DNA. Cation bridging in plasmid DNA occurs in two possible ways. Firstly, cations bridges are formed between phosphate groups in plasmid DNA backbone thus reducing the repulsive force and hydrodynamic size. Secondly, if plasmid concentration is sufficiently high, cation bridges are then formed between plasmids in close vicinity thus resulting in the increase of plasmid aggregate size as observed in the cation-endotoxins interaction [19].

The effect of high salt concentration on biomolecules precipitation is thought to be size-dependent [20]. Raymond *et al*. [21] reported that low molecular weight RNAs were not adequately precipitated even after 15 min incubation in 50 mM calcium chloride. Apparently, at least one additional removal step for low molecular weight molecules is required following precipitation.

Endotoxins can be completely precipitated at ~ 2 M $ZnSO_4$ (Fig. 8) but at the expense of low plasmid recovery (Fig. 9). We propose that the use of high salt concentration for complete precipitation of endotoxins can be related to the low molecular size endotoxins. This is due to the fact that only 20% endotoxin cannot be precipitated at 0.5 M $ZnSO_4$. Therefore, 2 M $ZnSO_4$ is vital to bring smaller size endotoxins to larger aggregate size and consequently precipitate out from the solution.

Plasmid DNA purification in ion exchange chromatography (IEC) is generally complicated when the size of the plasmid is similar to the size of LPS. This is due to the possibility of endotoxins to form different sizes of aggregates hence carry varying charge densities. Therefore, the degree of resolution between plasmid DNA and endotoxins in IEC is expected to be < 1 which explains why endotoxins remain in the final plasmid DNA eluate.

A strategy based on a high salt precipitation of endotoxins can be developed to remove large molecular size endotoxins during the alkaline cell lysis procedure. $ZnSO_4$ salt can be added during the neutralisation step so that endotoxins can be removed with cell debris in a single clarification step. For the clarification of a large volume of cell lysate, continuous centrifugation may not be feasible due to the shear sensitivity of plasmid DNA. Alternatively, ultrafiltration method may be employed to reduce the amount of cell debris and precipitates without a significant damage to the plasmid DNA backbone.

We also found that when using $ZnSO_4$, RNA impurities were co-precipitated with endotoxins. This further verifies the role of $ZnSO_4$ as an agent to improve the overall quality of plasmid DNA in a single precipitation step thus reducing the amount of impurities to be processed downstream. A subsequent ion exchange chromatography can then conveniently separate large plasmid DNA from small endotoxins and RNA by gradient elution [22]. Therefore, the AEC matrix can be fully utilised for plasmid DNA binding thus resulting in higher plasmid yield.

The presence of free metal ions in samples to be assayed renders the LAL quantitative analysis difficult to perform especially when the samples contain different types of metal ions. This is due to interactions between metal ions and LAL which may either enhance or inhibit the chromogenic reactions thus affecting the accuracy of the endotoxin content measurement. pH condition and volume of lysate are also known to affect the LAL assay [12b]. As little as 0.3 mM of metal ions strongly inhibit or enhance the LAL chromogenic reaction when added in the LAL-endotoxin incubation step but have no effect when added in the LAL-endotoxin-chromogenic substrate incubation step [12a].

Due to the sensitivity of LAL reagents, we have therefore carefully designed this experiment in such a way that each cation-containing sample and standard LPS had similar buffer compositions (e.g. pH, temperature, type of cation, cation concentration and volume of lysate). To further tone down the effect of metal ions, we performed OSD and addition of 10 mM EDTA into the samples and standards. Different calibration curves were constructed for each endotoxin-containing metal ion solution. In all, results from this work involving LAL reagents have been controlled against technical errors and this work reporting selective precipitation of endotoxin directly from alkaline lysed gram negative bacterial cell lysate using free alkaline earth and transitional metal ions is the first of its kind.

CONCLUSION

An extremely high endotoxin removal kit for plasmid DNA purification is fundamentally not required for *in vitro* or even *in vivo* transfection since a significantly high amount of endotoxin up to 2000 EU/μg DNA is needed to inhibit cell proliferation and transfection [23]. In this work, a simple method for selective endotoxin removal in plasmid DNA purification based on free metal ion-induced precipitation has been developed. This method can sufficiently remove a large amount of endotoxin lipopolysaccharides up to 80% from a clarified gram negative bacterial cell lysates with high plasmid DNA recovery (~100%). The optimised process is economically attractive due to its low salt consumption (0.5 M) and can be performed at a pH condition similar to that of alkaline lysed cell lysate. Furthermore, this method shows the possibility to be integrated or even replace potassium acetate usually incorporated in the neutralisation step of the alkaline cell lysis procedure. As part of the ongoing research, we are currently embarking on process intensification for plasmid DNA purification by integration of endotoxin precipitation and anion exchange chromatography in a continuous single stage process.

ACKNOWLEDGEMENT

This project was funded and supported by Monash University, Australia and Universiti Malaysia Sabah, Malaysia.

REFERENCES

1. D. Petsch, F. B. Anspach, Endotoxin removal from protein solutions. *J. Biotechnol.* 2000, *76*. 97-119.

2. L. Tan, D. S. Kim, I. K. Yoo, W. S. Choe, Harnessing metal ion affinity for the purification of plasmid DNA. *Chem. Eng. Sci.* 2007, *62*. 5809-5820.

3. N. C. Santos, A. C. Silva, M. A. R. B. Castanho, J. Martins-Silva, C. Saldanha, Evaluation of lipopolysaccharide aggregation by light scattering spectroscopy. *Chembiochem* 2003, *4*. 96-100.

4. (a) P. O. Magalhães, A. M. Lopes, P. G. Mazzola, C. Rangel-Yagui, T. C. V. Penna, A. P. Jr., Methods of Endotoxin Removal from Biological Preparations: a Review. *J. Pharm. Pharmaceut. Sci.* 2007, *10*. 388-404; (b) Y. Kang, R. G. Luo, Effects of ionic strength and pH

on endotoxin removal efficiency and protein recovery in an affinity chromatography. *Process Biochem.* 2000, *36*. 85-92.

5. (a) M. M. Diogo, J. A. Queiroz, D. M. F. Prazeres, Chromatography of plasmid DNA. *J. Chromatogr. A* 2005, *1069*. 3-22, DOI: DOI 10.1016/j.chroma.2004.09.050; (b) F. Sousa, M. F. Duarte, Prazeres, J. A. Queiroz, Affinity chromatography approaches to overcome the challenges of purifying plasmid DNA. *Trends Biotechnol.* 2008, *26*. 518-525.

6. C. M. Ongkudon, M. K. Danquah, Mitigating the Looming Vaccine Crisis: Production and Delivery of Plasmid Vaccines. *Crit. Rev. Biotechnol.* 2010, *DOI: 10.3109/07388551.2010.483460*.

7. L. Tan, W. B. Lai, C. T. Lee, D. S. Kim, W. S. Choe, Differential interactions of plasmid DNA, RNA and endotoxin with immobilised and free metal ions. *J Chromatogr. A* 2007, *1141*. 226-34, DOI: S0021-9673(06)02316-8 [pii]
10.1016/j.chroma.2006.12.023.

8. K. J. Sweadner, M. Forte, L. L. Nelsen, Filtration Removal of Endotoxin (Pyrogens) in Solution in Different States of Aggregation. *Appl. Environ. Microbiol.* 1977, *34*. 382-385.

9. A. Eon-Duval, K. Gumbs, C. Ellett, Precipitation of RNA impurities with high salt in a plasmid DNA purification process: Use of experimental design to determine reaction conditions. *Biotechnol. Bioeng.* 2003, *83*. 544-553, DOI: Doi 10.1002/Bit.10704.

10. (a) V. I. Ugarov, T. R. Samatov, H. V. Chetverina, A. B. Chetverin, Plasmid purification using hot Mg2+ treatment and no RNase. *Biotechniques* 1999, *26*. 194-+; (b) A. Chakrabarti, S. Sitaric, S. Ohi, A Procedure for Large-Scale Plasmid Isolation without Using Ultracentrifugation. *Biotechnol. Appl. Biochem.* 1992, *16*. 211-215.

11. C. M. Ongkudon, B. A. Rahman, A. A. Aziz, Optimization of critical medium components for the expression of recombinant human transferrin in insect cells baculovirus system. *J. Teknologi F.* 2006, *45*. 19-30.

12. (a) S. Guyomard, J. C. Darbord, Détermination quantitative des endotoxines bactériennes par la méthode «limulus chromogénique: analyse critique et étude des interactions de trois cations divalents. *Ann. Inst. Pasteur/Microbiol* 1985, *136B*. 49-55; (b) M. F. Scully, Y. M. Newman, S. E. Clark, V. V. Kakkar, Evaluation of a Chromogenic Method for Endotoxin Measurement. *Thrombosis Research* 1980, *20*. 263-270.

13. A. B. Schromm, K. Brandenburg, H. Loppnow, U. Zahringer, E. T. Rietschel, S. F. Carroll, M. H. J. Koch, S. Kusumoto, U. Seydel, The charge of endotoxin molecules influences their conformation and IL-6-inducing capacity. *J. Immunol.* 1998, *161*. 5464-5471.

14. M. M. Domingues, M. A. R. B. Castanho, N. C. Santos, $rBPI_{21}$ promotes lipopolysaccharide aggregation and exerts its antimicrobial effects by (hemi)fusion of PG-containing membranes. *PLoS ONE* 2009, *4*. e8385, DOI: 10.1371/journal.pone.0008385.

15. M. Egli, DNA-cation interactions: quo vadis? *Chem Biol* 2002, *9*. 277-86, DOI: S1074552102001163 [pii].

16. M. Hammermann, C. Steinmaier, H. Merlitz, U. Kapp, W. Waldeck, G. Chirico, J. angowski, Salt effects on the structure and internal dynamics of superhelical DNAs studied by light scattering and Brownian dynamics. *Biophys. J.* 1997, *73*. 2674-2687.

17. D. I. Cherny, T. M. Jovin, Electron and scanning force microscopy studies of alterations in supercoiled DNA tertiary structure. *J. Mol. Bio.* 2001, *313*. 295-307.

18. A. Zochling, R. Hahn, K. Ahrer, J. Urthaler, A. Jungbauer, Mass transfer characteristics of plasmids in monoliths. *J. Sep. Sci.* 2004, *27*. 819-27.

19. D. R. Latulippe, A. L. Zydney, Salt-induced changes in plasmid DNA transmission through ultrafiltration membranes. *Biotechnol Bioeng* 2008, *99*. 390-8, DOI: 10.1002/bit.21575.

20. J. S. Semancik, J. Szychowski, Enhanced detection of viroid-RNA after selective divalent cation fractionation. *Anal Biochem* 1983, *135*. 275-9.

21. G. J. Raymond, P. K. Bryant, 3rd, A. Nelson, J. D. Johnson, Large-scale isolation of covalently closed circular DNA using gel filtration chromatography. *Anal Biochem* 1988, *173*. 125-33, DOI: 0003-2697(88)90169-8 [pii].

22. C. M. Ongkudon, M. K. Danquah, Process optimisation for anion exchange monolithic chromatography of 4.2 kbp plasmid vaccine (pcDNA3F). *J.Chromatogr. B* 2010, *DOI:10.1016/j.jchromb.2010.08.011*. DOI: 10.1016/j.jchromb.2010.08.011.

23. K. A. Butash, P. Natarajan, A. Young, D. K. Fox, Reexamination of the effect of endotoxin on cell proliferation and transfection efficiency. *Biotechniques* 2000, *29*. 610-4, 616, 618-9.

Section 5.3

Analysis of $ZnSO_4$-induced lipopolysaccharides precipitation by measurement of hydrodynamic sizes and Zeta potentials

Process Biochemistry (Under review 2011)

Monash University

Declaration for Thesis Section 5.3

Declaration by candidate

In the case of Section 5.3, the nature and extent of my contribution to the work was the following:

Nature of contribution	Extent of contribution (%)
Initiation, Key ideas, Experimental, Development, Results interpretations, Writing up	90

The following co-authors contributed to the work. Co-authors who are students at Monash University must also indicate the extent of their contribution in percentage terms:

Name	Nature of contribution
Dr. Michael K. Danquah	Initiation, Key ideas, Experimental, Development, Results interpretations, Writing up

Candidate's signature		**Date**

Declaration by co-authors

The undersigned hereby certify that:

1. the above declaration correctly reflects the nature and extent of the candidate's contribution to this work, and the nature of the contribution of each of the co-authors;
2. they meet the criteria for authorship in that they have participated in the conception, execution, or interpretation, of at least that part of the publication in their field of expertise;
3. they take public responsibility for their part of the publication, except for the responsible author who accepts overall responsibility for the publication;
4. there are no other authors of the publication according to these criteria;
5. potential conflicts of interest have been disclosed to (a)granting bodies, (b) the editor or publisher of journals or other publications, and (c) the head of the responsible academic unit; and
6. the original data are stored at the following location (s) and will be held for at least five years from the date indicated below:

Location	Chemical Engineering Department, Monash University, Clayton, Australia

Signature		**Date**

Analysis of $ZnSO_4$-induced lipopolysaccharides precipitation by measurement of hydrodynamic sizes and Zeta potentials

Clarence M. Ongkudon, Michael K. Danquah

ABSTRACT

In our previous study on plasmid DNA isolation from *E. coli* cell lysate, we discovered that selective endotoxin precipitation was attainable using $ZnSO_4$ at a lower concentration of 0.5 M and at pH ~5. The present work studies the $ZnSO_4$–induced endotoxin precipitation process using dynamic light scattering and zeta potential analyses. Apparently, the lipopolysaccharide (LPS) aggregate size decreased for awhile at the start of $ZnSO_4$ addition and gradually increased onwards. The final low polydispersity index value of 0.04 indicated the presence of homogenously suspended supramolecular LPS particles which called for additional removal steps. It was speculated that cations close range encounter and interaction with LPS monomer contributed to LPS self aggregation whilst bridging of LPS monomers contributed to increase in LPS aggregate size. This work concludes that the LPS-plasmid DNA selective precipitation in $ZnSO_4$ solution is highly dependent on LPS solubility and critical aggregate concentration as compared to LPS-plasmid DNA-cations affinity interactions.

Keywords: Endotoxin; Lipopolysaccharide; Precipitation; Plasmid DNA; Limulus Amoebocyte lysate; Free metal ion

1. Introduction

Lipopolisaccharide (LPS) or endotoxin is composed of three major parts that include a negatively charged lipid A group attached to a polysaccharide group that anchors the LPS to the outer leaflet of the cell membrane, a core oligosaccharide covalently bound to the lipid A and a O-antigen polysaccharide group that protrudes away from the bacterial cell membrane [1]. Wild type bacterial strains express LPS with lipid A part, core oligosaccharides and O-antigen polysaccharides whilst LPS of rough mutant strains do not have the O-antigen [2]. LPS bears at least four negative charged moieties, two at 1- and 4'-phosphates of the lipid A part and two at the carboxylates adjacent to 2-keto-3-deoxyoctonate [3]. LPS in solution has

been found to be chemically and physically heterogenous in terms of the polysaccharide chain length, aggregate size and composition of the terminal glycan chains [2].

In vaccine or therapeutic drugs production, substantial endotoxin contamination could lead to severe side effects such as fever, microcoagulation, degradation of organ functions and poor resistance to infections following contact with the human immune system [4]. This so called 'biological functionality' of LPS is known to be exerted from the lipid part [5]. In the past, it was speculated that monomeric LPS was more active than aggregated LPS reflected by LAL test and induction of Egr-1 mRNA macrophages [6]. However, in a recent study, it was found that aggregated LPS induced higher tumor necrosis factor (TNF) α production [5]. LPS covers > 90% of the outer leaflet surface of the cell membrane and this highly packed LPS moieties confer bacteria resistance to most antimicrobial agents [7]. Multivalent cations were reported to be vital in stabilising the outer membrane in Gram-negative bacteria [8]. The outer membrane was found to be 3 times higher in divalent cations content compared to the inner membrane [8].

LPS is less soluble in dicationic solutions due to LPS aggregation compared to that in monocationic solutions [9]. It is assumed that a salt solution concentration of < 0.3 M does not have a significant effect on LPS solubility and hydrophobicity thus can be used for LPS sample preparation [1]. The amphiphilic nature of LPS gives an opportunity for self aggregation above the critical aggregate concentration (CAC) which can be in the nanomolar range [2]. CAC which determines the state of LPS aggregation is a function of polysaccharide chain length. Techniques for analysing LPS aggregation include fluorescence spectroscopy, light scattering and equilibrium analysis [2]. Electric double layer studies indicate that divalent cations are 100 times more effective than monovalent cations in lowering the membrane surface potential of LPS [9]. Addition of divalent cations changes the in-plane arrangement of LPS by converting the hydrocarbon chain packing from a hexagonal to a nonhexagonal lattice [9].

At pH 7, LPS carries at least four negative charges considering pK values of 1.0 for the phosphate groups and 2.5 for the carboxylate groups [10]. At lower pH values, a species A in solution is in equilibrium with the solid phase and as the pH is increased a new species B is generated from species A by the dissociation of a proton [10]. Thus, the total solubility is the sum of the concentration of A and B. The decrease in solubility observed with decreased pH can be explained by the charge transition of LPS from a highly anionic to a less anionic form [10].

Precipitation has been widely used in the bioprocess industry as a tool for product concentration or isolation. In plasmid DNA purification, numerous precipitation agents have

been explored including polyethylene glycol, ammonium sulphate, ammonium acetate, lithium chloride, spermidine, spermine, and cationic detergent (CTAB) [11]. A number of studies suggest the use of precipitants particularly multivalent cations as agents for precolumn treatment or early capture step in plasmid purification [11-13]. In our recent study on plasmid DNA isolation from clarified *E. coli* cell lysate, we found that Ca^{2+} and Zn^{2+} could selectively precipitate bacterial endotoxins out of solution [14]. In that study, we also observed that the highest LPS-plasmid DNA resolution was attainable using $ZnSO_4$ at a lower concentration of 0.5 M and at a pH condition similar to that of clarified cell lysate. These interesting observations motivated us to study the hydrodynamic behaviour of endotoxins at the aforementioned conditions using state of the art dynamic light scattering and zeta potential analyses. We speculated that at pH 5 and 0.5 M $ZnSO_4$, lipopolysaccharides possessed a zero net charge and a larger aggregate size compared to that corresponding to its critical aggregate concentration (CAC). We also presumed that the precipitation process occurred spontaneously as a result of gravitational pull, increased aggregate size and reduced solubility but at a substantially slow rate.

2. Materials and Methods

2.1. Materials

$ZnSO_4.7H_2O$ (99%) was purchased from BDH, Australia. Tris base (99%), Tris-HCl (99%), acetic acid (99%), ethylenediaminetetraacetic acid (EDTA, 99%), NaOH (99%), sodium dodecyl sulphate (SDS, 99%) and CH_3COOK (99%) were purchased from Sigma-Aldrich, Australia. Controlled LPS prepared from *E. coli* DH5α was purchased from Genscript, USA.

2.2. LPS precipitation using $ZnSO_4$ in neutralised lysis solution

1 mL of neutralised lysis solution or buffer was prepared from Solution A (0.05 M Tris–HCl, 0.01 M EDTA, pH 8), Solution B (0.2 M NaOH, 1% SDS) and Solution C (3 M CH_3COOK at pH 5.5) in the proportion of 3:3:4/A:B:C. The mixture was centrifuged at 15000 x g for 10 min to remove the precipitates and the supernatant was collected by filtering through a 0.45 μm membrane filter (Millipore). 1 mL of the cleared supernatant was transferred into a fresh microtube and mixed with 0.5 M $ZnSO_4$ (pH 5). A predetermined amount of freeze-dried LPS was resuspended in the $ZnSO_4$ solution, gently inverted for 30-50

times, incubated for 30 min at 25 ^{o}C and centrifuged at 15000 x g for 15 min. 0.5 mL of cleared supernatant was transferred into a pyrogen free microtube and analysed for LPS content.

2.3. Chromogenic Limulus Amoebocyte Lysate (LAL) analysis of LPS content in $ZnSO_4$-containing solutions

The LAL chromogenic test of divalent-metal-ion-containing alkaline cell lysate solutions was performed based on the methods described by Ongkudon and Danquah[14]. Briefly, 1 volume of sample (1 SV) was added into 1 SV of LAL solution, reacted with 1 SV of chromogenic substrate, stopped with 4 SV of color stabilisers and measured by UV spectrophotometer at 545 nm wavelength. Optimum sample dilution (OSD) of 2000x was required to reduce the enhancement/inhibition effect of cations on LAL activity at which the endotoxin activity still can be detected. 10 mM EDTA was added into the controlled LPS and sample solutions to mitigate the endotoxin-metal ion interaction. The incubation times for LAL and chromogenic substrate reactions were 20 and 3 minutes respectively at 37^{o}C under 50 rpm shaking.

2.4. Dynamic light scattering of lipopolysaccharide aggregates in the presence of $ZnSO_4$

A predetermined amount of LPS was dissolved in 1 mL pyrogen free water and filtered through a 0.45 μm filter (Millipore) into a low volume disposable cuvvette. 0.5 M $ZnSO_4$ were added into the LPS solution and equilibrated at room temperature for 10 min. The hydrodynamic size of the LPS aggregates were measured by Malvern Zetasizer Nano ZS (Malvern, UK) with a backscattering detection at 173^{o}, equipped with a He-Ne laser (λ =632.8 nm), at 25 ^{o}C, 3.25 mm measurement position, 15 runs/measurement, 5 measurements and 10 sec/ run. The hydrodynamic diameter of LPS was obtained from the peak with the highest intensity in the light scattering intensity distributions. Control samples that contained 0 M $ZnSO_4$ at pH 7 were included in all experiments.

2.5. Zeta potential analysis of lipopolysaccharide aggregates in the presence of $ZnSO_4$

Samples for zeta potential analysis were prepared as described in the dynamic light scattering analysis. The zeta potential of the LPS aggregates were measured in liquid suspensions using Laser Doppler Velocimetry (LDV) of Malvern Zetasizer Nano ZS

(Malvern, UK). The zeta potentials reported here were obtained from the average of three separate samples prepared under the same conditions.

3. Results

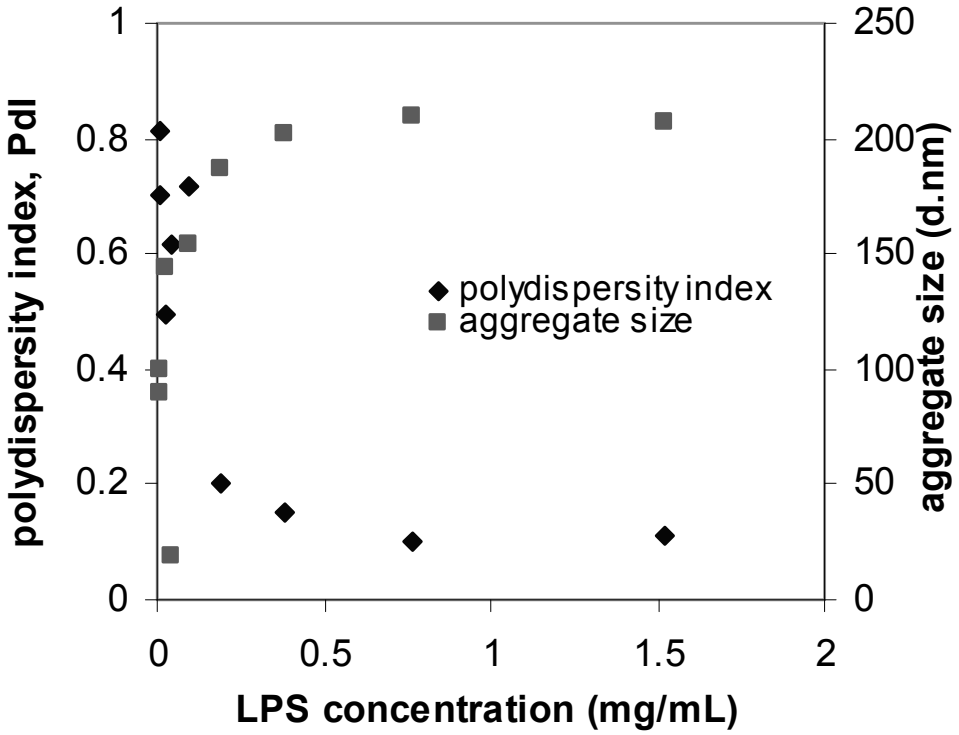

Fig. 1. Effect of LPS concentration on PdI and aggregate size. Buffer was prepared from Solution A (0.05 M Tris–HCl, 0.01 M EDTA, pH 8), Solution B (0.2 M NaOH, 1% SDS) and Solution C (3 M CH_3COOK at pH 5.5) in the proportion of 3:3:4/A:B:C, centrifuged at 15000 g for 10 min and filtered through a 0.45 μm membrane filter.

The structural arrangement of LPS molecules (e.g. unilamelar, multilamellar) varies over LPS concentrations thus affecting its hydrodynamic size distribution. The precipitation process commenced with the addition of $ZnSO_4$ into a homogenous supramolecular LPS solution. Prior to obtaining the homogenous LPS solution, different concentrations of LPS solutions were prepared and analysed for hydrodynamic diameter and polydispersity index (Fig. 1) using the Malvern Zetasizer Nano ZS instrument. Generally, the region where the polydispersity index (PdI) value was minimal signified formation of organised supramolecular LPS and the region where an increase in PdI values became appreciable was

typically labelled as critical aggregate concentration (CAC) or critical micelle concentration (CMC) [15]. Thus, homogenous supramolecular LPS solutions were prepared at a concentration at which the LPS hydrodynamic diameter was constant and the PdI value was minimal. In this work, the LPS precipitation was carried out in a buffer solution similar to that of clarified *E. coli* cell lysate with the exclusion of *E. coli* cells. This was to give the ideal representation of the clarified cell lysate where the LPS precipitation was actually performed in a real application.

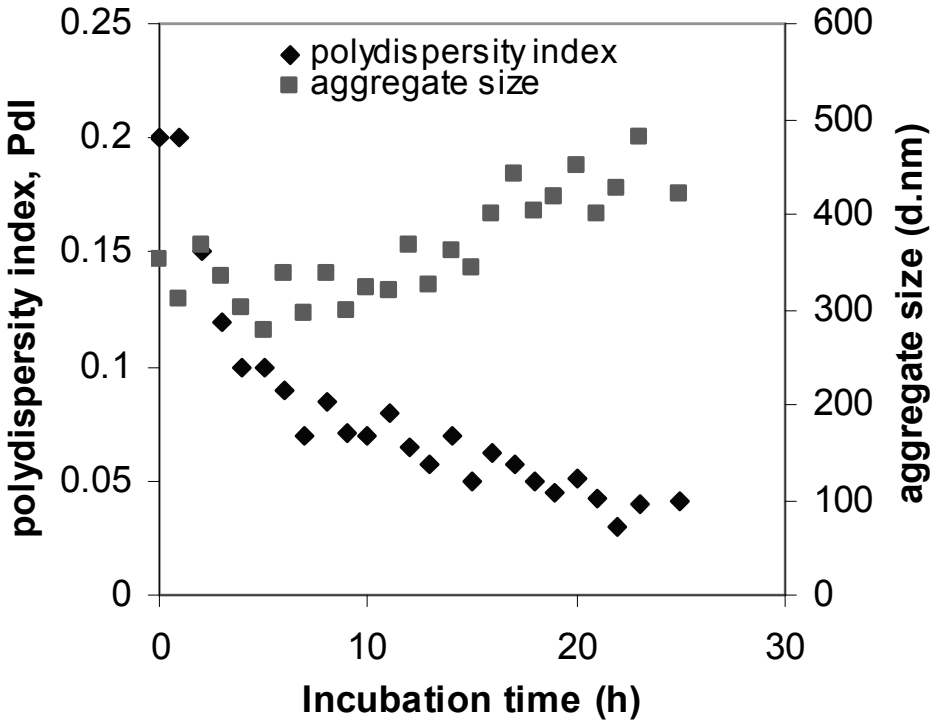

Fig. 2. Time course analysis of LPS precipitation in 0.5 M $ZnSO_4$ (pH 5) at 25 ºC. Buffer was prepared from Solution A, Solution B and Solution C in the proportion of 3:3:4/A:B:C, centrifuged at 15000 g for 10 min and filtered through a 0.45 µm membrane filter.

LPS precipitation was carried out with the incorporation of $ZnSO_4$ into the LPS solution (Fig. 2). At the commence of $ZnSO_4$ addition, the average size (hydrodynamic diameter) of LPS aggregates was around 350 nm. This value was greater than that without $ZnSO_4$ hence indicated that LPS aggregation took place instantaneously. The hydrodynamic diameter of LPS reported in this work was obtained from the maxima of size distribution of the dynamic light scattering analysis. Based on the PdI value at 0 h, it was further concluded

that the LPS solution was highly polydispersed at the beginning of the precipitation process due to the presence of varied LPS aggregate sizes resulting from initial LPS aggregation. The initial precipitation process also exhibited a concomitant small decrease in LPS aggregate size for about 5 h before gradually increased onwards. Interestingly, the PdI decreased steadily to a final value of about 0.04 which corresponded to an LPS aggregate size of approximately 450 nm. In other words, natural $ZnSO_4$–induced LPS precipitation process resulted in an overall increase in LPS aggregate size of 100 nm within a time span of 24 h. All time-based samples were further analysed using the chromogenic LAL method. It was found that the LPS contents observed over the precipitation process were still considerably high reaching 200 EU/mL at 24 h (Fig. 3). This phenomenon indicated that the size of LPS aggregates at 24 h was insufficiently large to precipitate all LPS aggregates out of the solution. Based on Fig. 2, the complete LPS precipitation might have taken at least 3 days assuming that a minimum aggregate size (hydrodynamic diameter = 1000 nm) was needed to precipitate LPS out of solution. Therefore in a real application, centrifugation or membrane filtration is normally incorporated to accelerate the precipitation process.

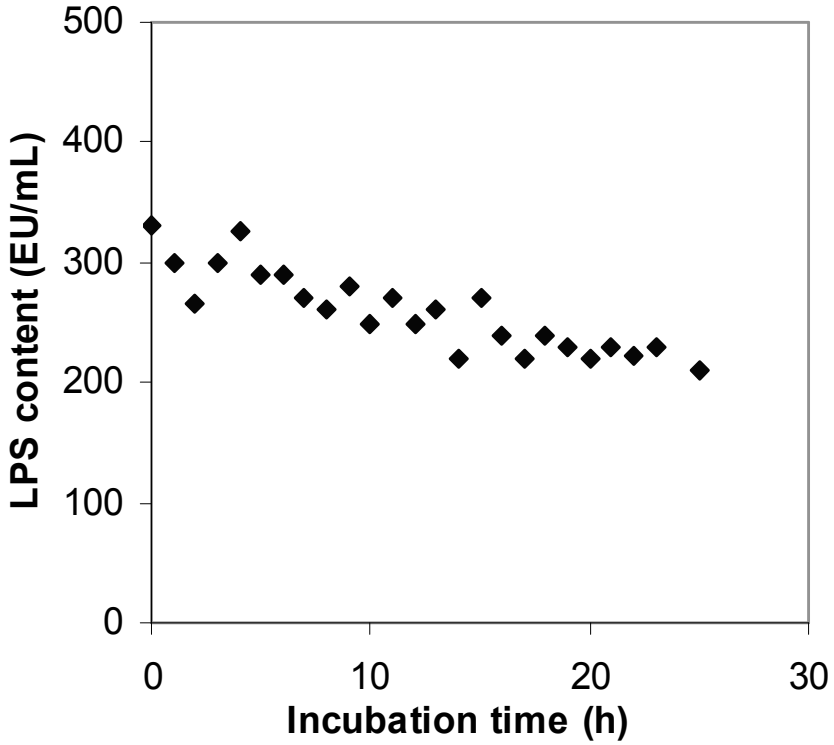

Fig. 3. Chromogenic LAL analysis of $ZnSO_4$-induced LPS precipitation. Concentration of $ZnSO_4$ was 0.5 M at pH 5 and 25 ºC.

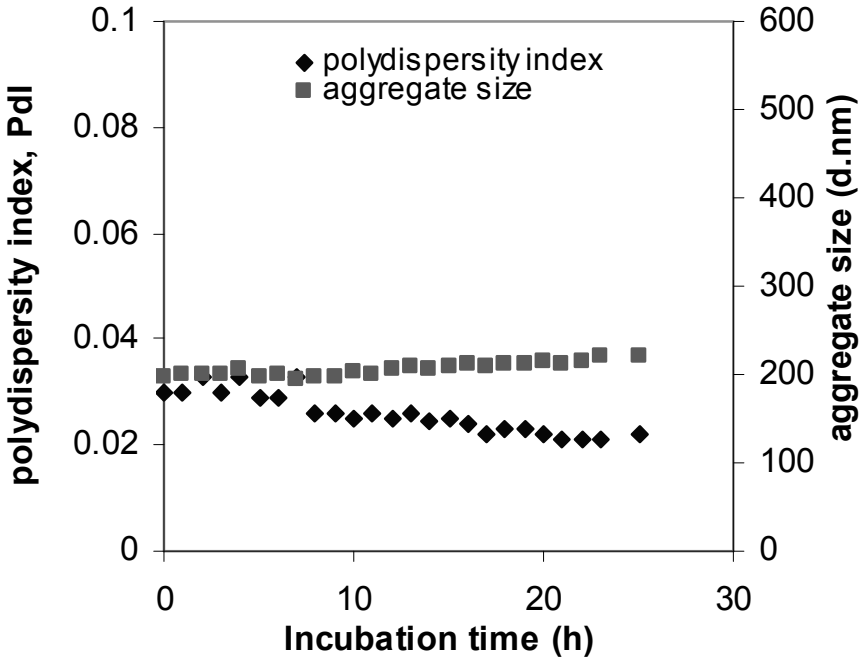

Fig. 4. Time course analysis of LPS precipitation in 0 M $ZnSO_4$ (pH 7) at 25 ºC. Buffer was prepared from Solution A, Solution B and Solution C in the proportion of 3:3:4/A:B:C, centrifuged at 15000 g for 10 min and filtered through a 0.45 μm membrane filter.

Fig. 4 represented the change in LPS aggregate size and PdI value of $ZnSO_4$-lacking solution over the period of 24 h. It was interesting to note that, in $ZnSO_4$-lacking solution, LPS were somehow subjected to aggregation process which took place at a considerably slow rate as depicted in Fig. 4. However, the total increase in aggregate size was relatively small (< 15 nm) with a final PdI value of about 0.02. Apparently, the aggregation process was possible due to the presence of high level of other positively charged molecules in the buffer solution. These counter ions could lead to the formation of larger LPS aggregates probably in the same manner observed in $ZnSO_4$-induced LPS precipitation.

Earlier in this work, we speculated that LPS was highly negatively charged in $ZnSO_4$–lacking cell lysate solution whilst in 0.5 M $ZnSO_4$ solution, the LPS were mostly positively charged as a result of Zn^{2+} distribution. The repulsive force among negatively charged LPS headgroups in $ZnSO_4$–containing solution was reduced and led into the formation of larger supramolecular aggregates compared to that without $ZnSO_4$. In this work, a predetermined amount of pure LPS was prepared in a buffer containing resuspension, lysis and neutralisation solutions. It could be seen in Fig. 5. that the average zeta potential of LPS in buffer solution was ~ –15 mV despite the high level of positive ions (pH = 5) and ~ +15 mV in 0.5 M $ZnSO_4$-containing buffer solution.

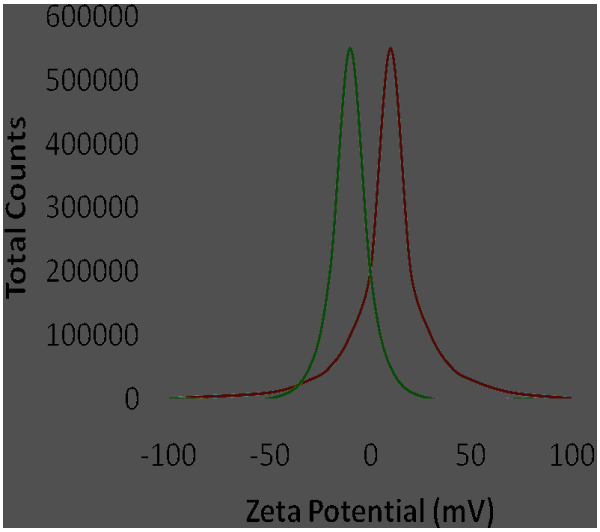

Fig. 5. Zeta potential analysis of LPS solutions. Buffer was prepared from Solution A (0.05 M Tris–HCl, 0.01 M EDTA, pH 8), Solution B (0.2 M NaOH, 1% SDS) and Solution C (3 M CH_3COOK at pH 5.5) in the proportion of 3:3:4/A:B:C, centrifuged at 15000 g for 10 min and filtered. Green line: 0 M $ZnSO_4$; red line: 0.5 M $ZnSO_4$.

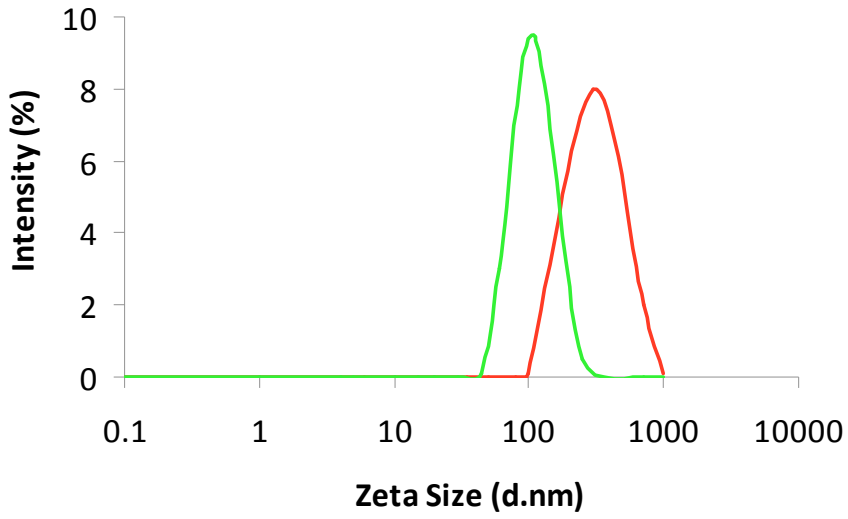

Fig. 6. Effect of centrifugation on the hydrodynamic diameter distribution of LPS in 0.5 M $ZnSO_4$ (pH 5). Buffer was prepared from Solution A (0.05 M Tris–HCl, 0.01 M EDTA, pH 8), Solution B (0.2 M NaOH, 1% SDS) and Solution C (3 M CH_3COOK at pH 5.5) in the proportion of 3:3:4/A:B:C and filter-centrifuged to remove debris. Green line: after centrifugation; red line: before centrifugation.

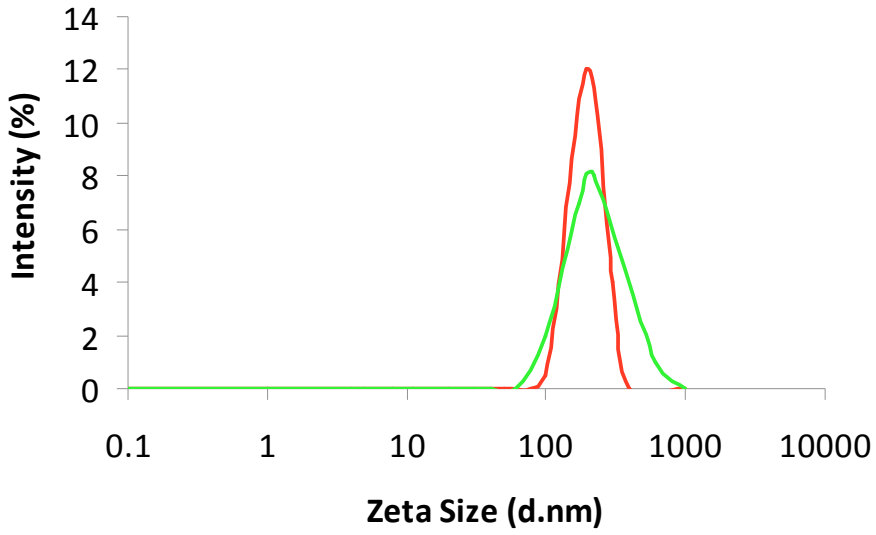

Fig. 7. Effect of centrifugation on the hydrodynamic diameter distribution of LPS in 0 M $ZnSO_4$ (pH 7). Buffer was prepared from Solution A (0.05 M Tris–HCl, 0.01 M EDTA, pH 8), Solution B (0.2 M NaOH, 1% SDS) and Solution C (3 M CH_3COOK at pH 5.5) in the proportion of 3:3:4/A:B:C and filter-centrifuged to remove debris. Green line: after centrifugation; red line: before centrifugation.

Table 1. Analysis of LPS content in $ZnSO_4$-containing buffer before and after centrifugation.

Sample no.	pH	Before or after centrifugation	* $ZnSO_4$ (mol/L)	PdI	LPS (EU/mL)	% LPS removal
1	7	Before	0	0.1	430	0
2	7	After	0	0.1	320	25
3	5	Before	0.5	0.1	399	0
4	5	After	0.5	0.4	35	91

*Buffer was prepared from Solution A (0.05 M Tris–HCl, 0.01 M EDTA, pH 8), Solution B (0.2 M NaOH, 1% SDS) and Solution C (3 M CH_3COOK at pH 5.5) in the proportion of 3:3:4/A:B:C and filter-centrifuged to remove debris.

Fig. 6 showed that there was a removal of larger LPS aggregates after the centrifugation step. Although there were some LPS aggregates (mainly 100 nm) left after the centrifugation step, the corresponding PdI value was high (Sample no. 4 of Table 1) which indicated that the centrifuged solution might contain a relatively low concentration of smaller LPS aggregates. LAL analysis further suggested that there was a high removal (91%) of LPS as a result of $ZnSO_4$ addition and centrifugation (Table 1). Therefore, the sample solution obtained after centrifugation contained only about 9% of LPS which were mainly the 100 nm aggregates. It was interesting to note that a small proportion (25%) of LPS aggregates were precipitated in a non $ZnSO_4$ – containing solution by centrifugation. This phenomenon was understandable since the centrifugal force exerted during the centrifugation step was high enough to precipitate any suspended particles including LPS out of solution. Based on the dynamic light scattering data in Fig. 7, the maxima of size distribution generally remained at 200 nm although a slight drop in intensity was observed after centrifugation. The drop in intensity could represent LPS precipitation as depicted by 25% LPS removal in Table 1. An apparent increase in size distribution was also seen alongside the drop in intensity. This interesting observation indicated that even in aqueous solutions, LPS precipitation was possible by centrifugation due to increased rate of particles collision hence rate of aggregation.

4. Discussion

4.1. Mechanism of $ZnSO_4$-induced LPS precipitation

In dilute solutions, LPS molecules usually exist as mixtures of monomers of different sizes resulting from self entanglement or rigidification. However, at fairly high concentrations, several physical properties such as osmotic pressure, turbidity, electrical conductance, and surface tension may be altered and lead to the formation of organised supramolecular structures (micelles) [15]. The micellar structure of LPS is highly advantageous when characterisation of LPS aggregation is concerned. It will eliminate any misinterpretations of data resulting from the nonuniform LPS structures. In this study, a method based on the analysis of hydrodynamic diameter and polydispersity of particles in solution was employed to determine the experimental conditions necessary for the preparation of homogenous LPS micelles. Dynamic light scattering techniques are by far the most powerful method to determine the hydrodynamic structures of microparticles compared to other techniques such as surface tension, electrical conductivity and dye solubilisation due to

the fact that information concerning the sizes and shapes of micelles as well as CAC can be determined more accurately [15].

Earlier in this work, it was hypothesised that $ZnSO_4$-induced LPS aggregation occurred spontaneously at a considerably reduced rate as a result of gravitational pull and reduced solubility. At the start of the $ZnSO_4$ addition, the LPS aggregate size apparently decreased for awhile before gradually increased until the precipitation was halted. The low PdI values observed at the end of the incubation period signified that most of the aggregated LPS were homogenously suspended in the solution and might have taken several days to settle to the bottom of the solution. In a real application, these aggregates could be removed by centrifugation or membrane filtration thus significantly reducing the processing time. The time taken for the reverse process of LPS aggregation or monomerisation of aggregated LPS is generally 24 h @ 22 ^{o}C [6] which agrees with results obtained in this study (24 h @ 25 ^{o}C). Although results from this work somewhat agree with the hypothesis, further explanation is needed for the rather unique trend of LPS aggregation observed.

Cations are preferentially located between the carboxylate and phosphate groups of LPS headgroup [16]. It was speculated that, at the commence of the $ZnSO_4$ addition into the LPS solution, cations close range encounter and interaction with LPS monomer took place and resulted in self rigidification, entanglement and compaction of LPS monomer as well as reduced number of water molecules around the LPS hydration shell. This was due to reduced repulsive force between negatively charged LPS headgroups. Water molecules, which were partially negatively charged, were also attracted and accumulated at the hydrophilic headgroup of LPS where cations were preferentially located. However, it has been observed that cations are not completely neutralised by water molecules and negatively charged LPS headgroups [16]. This created a possibility of molecular bridging between two phosphate groups of two LPS monomers and further increase in the aggregate size as seen during the later stage of the aggregation/precipitation process.

Investigation into the influence of externally added divalent cations on the mobility and aggregate structure of LPS by [3] concludes that cations reduce the activity of LPS and mobility of lipid A whilst the structure shifts from unilamellar to multilamellar arrangements. Lipopolysaccharides are more rigid at pH 5 than at pH 10.5. At pH 7, head group mobility of LPS-divalent cations is substantially lower that of LPS-monovalent cations but at pH 12 both are equally fluid [17]. Again, the above statements validate the use of low pH in $ZnSO_4$-induced precipitation. The increased LPS aggregation state transition from pH 7 (0 M $ZnSO_4$) to pH 5 (0.5 M $ZnSO_4$) as depicted by –ve zeta potential in Fig. 5 can also be explained by the

reduced ionisation state of LPS and increased cations electrostatic binding assuming an LPS isoelectric point of between 5 and 7.

The anionic LPS on the outer membrane and the underlying peptidoglycan provide multiple sites for cation binding. LPS binding to Zn^{2+} has been reported and shown to reduce the toxicity of endotoxin-challenged mice by inhibition of LPS adsorption and not by LPS inactivation [18, 19]. Ca^{2+} and Mg^{2+} were found in higher concentrations whilst Zn^{2+} was found in lower concentrations [8]. The levels of cations bound to the cell membrane can also be affected by the composition of the growth medium [8]. Although Ca^{2+} and Mg^{2+} contents are reported to be higher in LPS, it is interesting to note that Zn^{2+}, which exists only in a fraction amount, has the capacity to precipitate LPS selectively from plasmid DNA-containing solution when externally added [14]. It is also important to note that Ca^{2+} and Zn^{2+} have higher affinities towards the anionic group of LPS molecule compared to the phosphate group of plasmid DNA. On the basis of these considerations, it is concluded that the LPS-plasmid DNA resolution induced by Zn^{2+}, Ca^{2+} and Mg^{2+} is less dependent on their affinities but rather on other factors such as solubility and CAC. In addition, this selectivity can be maintained if the concentration is kept below 0.5 M for Zn^{2+}. Above this concentration, the resolution between LPS and plasmid DNA is greatly reduced as observed in our previous study [14].

In a study by [20], they investigated the aggregation state of LPS at different concentrations of cations and found that the concentration giving 50% aggregation, (K_m) values of Ca^{2+} and Mg^{2+} were higher than that of other cations. This finding is rather true since higher levels of Ca^{2+} and Mg^{2+} have been reported in the stable form of native monomeric LPS molecule [8]. Thus, the lower level of Zn^{2+} in LPS may indicate a lower K_m value. The concentration giving 50% aggregation, (K_m) is proportionately related to the concentration causing loss of LPS infectivity, (K_m*infection*). In another study, it was found that $ZnSO_4$ substantially reduced the fluidity of LPS with a concomitant increase in LPS polarisation compared to that of cobalt, nickel and magnesium salts [21]. In that study, fluorescence was measured using a Spex fluorescence spectrometer F1 T11 (Spex Instruments, Edison, NJ) and the polarization, P was calculated using equation (1) where I_1 and I_2 were the emission intensities (λ = 420 nm) measured simultaneously behind two polarisation analysers, vertical (I_1) and parallel (I_2) respectively.

$$P = (I_2 - I_1)/(I_2 + I_1) \quad (1)$$

4.2. Research implication: Plasmid DNA downstream processing platform

The demand for plasmid DNA in the biopharmaceutical industries is currently skyrocketing hence there is a great need to reinvent the way plasmid DNA is manufactured. The major bottleneck in the development of scalable and continuous plasmid DNA downstream processing is poor selectivity due to common features found in plasmid DNA and its impurities which are mainly RNA and endotoxins. Conventional plasmid purification using chloride/ethidium bromide ultracentrifugation is not scalable because of hazardous materials whilst commercial purification kits such as miniprep and midiprep use disposable chromatographic columns and a large amount of resins and enzymes. However, chromatographic method is currently the most reliable method due to its ability to exploit different plasmid DNA characteristics such as size, charge, hydrophobicity, and affinity.

It is important to note that, in plasmid DNA chromatographic purification, endotoxin removal is highly complicated by endotoxins tendency to form varied aggregate sizes and charge densities. As a result, a considerable amount of endotoxins may still present in the final plasmid DNA eluate which calls for additional endotoxin removal steps. Increasing the number of unit operation is inevitably followed by an increase in product loss and production cost. When developing a large scale plasmid DNA purification process, the design should aim at volume reduction, high flow rate, better resolution and higher capacity as these will have significant impacts on the overall economics hence production cost.

A strategy based on metal salt-induced precipitation of endotoxins can be developed to remove larger endotoxin aggregates (> 200 nm) prior to column purification. $ZnSO_4$ salt can be added after the neutralisation step or even replace potassium acetate, which is usually found in a traditional neutralisation solution. Consequently, endotoxins and cell debris can be removed in a single clarification step by centrifugation or membrane filtration. Anion exchange chromatography can then be incorporated to separate large plasmid DNA from traces of endotoxins [22]. The optimised process is economically attractive due to its low salt consumption (0.5 M) and can be performed at a pH condition similar to that of clarified cell lysate. Most importantly, there is no increase in the number of unit operation since the selective endotoxin precipitation step is done as an integral part of the clarified cell lysate preparation.

5. Conclusion

Currently, there is a lack of understanding and experimental evidences to support the role of $ZnSO_4$ in LPS precipitation. The data presented herein and their interpretation cannot completely or satisfactorily describe the complexity of LPS aggregation or its precipitation characteristics in cation-containing LPS solution**.** This is partly due to the fact that these particles, as natural isolates, exhibit numerous inherent properties. For example, each strain exhibits high variability of the polysaccharide part of *0*-specific chain and number of fatty acid residues. Nevertheless, our results suggest that, at least over certain concentrations, LPS precipitation occurs spontaneously as a result of self entanglement and cross-bridging between LPS monomers whereby $ZnSO_4$ and centrifugation are incorporated to induce the rate of aggregation hence precipitation process. It is suggested that an X-ray diffraction analysis and surface plasmon resonance be performed on LPS solutions in order to gain a better understanding of the structural changes involved in $ZnSO_4$-induced LPS precipitation as compared to that induced by other metal ions.

Acknowledgement

The authors wish to thank Monash University, Australia for funding this project and University Malaysia Sabah, Malaysia for providing the scholarship to CMO.

References

[1] Aurell CA, Wistrom AO. Critical Aggregation Concentrations of Gram-Negative Bacterial Lipopolyscaccharides (LPS). Biochem Biophys Res Com 1998;253:119-123.

[2] Sasaki H, White SH. Aggregation behavior of an ultra-pure lipopolysaccharide that stimulates TLR-4 receptors. Biophys J 2008;95:986-993.

[3] Garidel P, Rappolt M, Schromm AB, Howe J, Lohner K, Andra J, Koch MHJ, Brandenburg K. Divalent cations affect chain mobility and aggregate structure of lipopolysaccharide from Salmonella minnesota reflected in a decrease of its biological activity. Biochim Biophys Acta-Biomembranes 2005;1715:122-131.

[4] Petsch D, Anspach FB. Endotoxin removal from protein solutions. J Biotechnol 2000;76:97-119.

[5] Mueller M, Lindner B, Kusumoto S, Fukase K, Schromm AB, Seydel U. Aggregates are the biologically active units of endotoxin. J Biol Chem 2004;279:26307-26313.

[6] Takayama K, Mitchell DH, Din ZZ, Mukerjee P, Li C, Coleman DL. Monomeric Re Lipopolysaccharide from *Escherichia-Coli* Is More Active Than the Aggregated Form in the Limulus Amebocyte Lysate Assay and in Inducing Egr-1 Messenger-Rna in Murine Peritoneal-Macrophages. J Biol Chem 1994;269:2241-2244.

[7] Domingues MM, Lopes SCDN, Santos NC, Quintas A, Castanho MARB. Fold-Unfold Transitions in the Selectivity and Mechanism of Action of the N-Terminal Fragment of the Bactericidal/Permeability-Increasing Protein (rBPI(21)). Biophys J 2009;96:987-996.

[8] Coughlin RT, Tonsager S, Mcgroarty EJ. Quantitation of Metal-Cations Bound to Membranes and Extracted Lipopolysaccharide of *Escherichia-Coli.* Biochem 1983;22:2002-2007.

[9] Snyder S, Kim D, McIntosh TJ. Lipopolysaccharide bilayer structure: Effect of chemotype, core mutations, divalent cations, and temperature. Biochem 1999;38:10758-10767.

[10] Din ZZ, Mukerjee P, Kastowsky M, Takayama K. Effect of Ph on Solubility and Ionic State of Lipopolysaccharide Obtained from the Deep Rough Mutant of *Escherichia-Coli.* Biochem 1993;32:4579-4586.

[11] Wahlund PO, Gustavsson PE, Izumrudov VA, Larsson PO, Galaev IY. Precipitation by polycation as capture step in purification of plasmid DNA from a clarified lysate. Biotechnol Bioeng 2004;87:675-684.

[12] Eon-Duval A, Gumbs K, Ellett C. Precipitation of RNA impurities with high salt in a plasmid DNA purification process: Use of experimental design to determine reaction conditions. Biotechnol Bioeng 2003;83:544-553.

[13] Tan L, Lai WB, Lee CT, Kim DS, Choe WS. Differential interactions of plasmid DNA, RNA and endotoxin with immobilised and free metal ions. J Chromatogr A 2007;1141:226-234.

[14] Ongkudon CM, Danquah MK. Analysis of selective metal-salt-induced endotoxin precipitation in plasmid DNA purification using improved LAL assay and central composite design Anal Chem 2011;83:391-397.

[15] Santos NC, Silva AC, Castanho MARB, Martins-Silva J, Saldanha C. Evaluation of lipopolysaccharide aggregation by light scattering spectroscopy. Chembiochem 2003;4:96-100.

[16] Obst S, Kastowsky M, Bradaczek H. Molecular dynamics simulations of six different fully hydrated monomeric conformers of *Escherichia coli* re-lipopolysaccharide in the presence and absence of Ca2+. Biophys J 1997;72:1031-1046.

[17] Coughlin RT, Peterson AA, Haug A, Pownall HJ, McGroarty EJ. A pH titration study on the ionic bridging within lipopolysaccharide aggregates. Biochim Biophys Acta-Biomembranes 1985;821:404-412.

[18] Snyder SL, Walker RI. Inhibition of Lethality in Endotoxin-Challenged Mice Treated with Zinc Chloride. Infect Immun 1976;13:998-1000.

[19] Sobocinski PZ, Powanda MC, Canterbury WJ, Machotka SV, Walker RI, Snyder SL. Role of Zinc in Abatement of Hepatocellular Damage and Mortality Incidence in Endotoxemic Rats. Infect Immun 1977;15:950-957.

[20] Field AM, Rowatt E, Williams RJP. The interaction of cations with lipopolysaccharide from *Escherichia coli* C as shown by measurement of binding constants and aggregation reactions. Biochem J 1989;263:695-702.

[21] Wellinghausen N, Schromm AB, Seydel U, Brandenburg K, Luhm J, Kirchner H, Rink L. Zinc enhances lipopolysaccharide-induced monokine secretion by alteration of fluidity state of lipopolysaccharide. J Immunol 1996;157:3139-3145.

[22] Ongkudon CM, Danquah MK. Process optimisation for anion exchange monolithic chromatography of 4.2 kbp plasmid vaccine (pcDNA3F). JChromatogr B 2010;878:2719-2725.

Section 5.4

The study of aggregative interaction of cations with endotoxins and plasmid DNA

Chemical Engineering Journal (Under review 2011)

Monash University

Declaration for Thesis Section 5.4

Declaration by candidate

In the case of Section 5.4, the nature and extent of my contribution to the work was the following:

Nature of contribution	Extent of contribution (%)
Initiation, Key ideas, Experimental, Development, Results interpretations, Writing up	85

The following co-authors contributed to the work. Co-authors who are students at Monash University must also indicate the extent of their contribution in percentage terms:

Name	Nature of contribution
Emma Hodges (5%) Kathleen Murphy (5%) Dr. Michael K. Danquah	Initiation, Key ideas, Experimental, Development, Results interpretations, Writing up

Candidate's signature		**Date**

Declaration by co-authors

The undersigned hereby certify that:

1. the above declaration correctly reflects the nature and extent of the candidate's contribution to this work, and the nature of the contribution of each of the co-authors;
2. they meet the criteria for authorship in that they have participated in the conception, execution, or interpretation, of at least that part of the publication in their field of expertise;
3. they take public responsibility for their part of the publication, except for the responsible author who accepts overall responsibility for the publication;
4. there are no other authors of the publication according to these criteria;
5. potential conflicts of interest have been disclosed to (a)granting bodies, (b) the editor or publisher of journals or other publications, and (c) the head of the responsible academic unit; and
6. the original data are stored at the following location (s) and will be held for at least five years from the date indicated below:

Location	Chemical Engineering Department, Monash University, Clayton, Australia

Signature		**Date**

The study of aggregative interaction of cations with endotoxins and plasmid DNA

Clarence M. Ongkudon*, Emma Hodges, Kathleen Murphy and Michael K. Danquah

Bio Engineering Laboratory, Department of Chemical Engineering, Monash University, Clayton campus, Wellington road, Victoria 3800, Australia.

* Corresponding author. Tel.: [redacted]. Fax: [redacted]
E-mail address: [redacted] (C.M. Ongkudon).

ABSTRACT

DNA is the third generation of vaccine technology surpassing previous viral methods, due to decreased storage and transport issues and faster production rates. The aim of the experiments detailed in this paper was to examine the potential use and advantages of using divalent cation-induced aggregation as a purification method for endotoxin removal. Zeta analysis, including Zeta potential, particle size analysis, percentage of aggregation; UV_Vis spectroscopy and electron microscopy were used to validate the hypothesis that Zn^{2+} (as $ZnSO_4$) is the cation of choice for preferential aggregation of LPS over pDNA. The results from the Zeta size analysis showed that the addition of Zn^{2+} results in the largest number of LPS particles per aggregate. pDNA aggregates had the largest number of particles per molecule when it was left untreated with cation. The value of aggregation constant (K_m) for LPS-Zn^{2+} was substantially low (0.28) and considerably large (> 2M) for pDNA-Zn^{2+}. Scatchard plots show positive slopes when calculated for pDNA-cation indicating unusual binding kinetics. It can be concluded that of the three cations examined in this research, Zn^{2+} was found to have the optimal performance characteristics for aggregation with LPS making secondary purification techniques viable.

Key words: Endotoxin Removal; Lipopolysaccharides; Plasmid DNA Purification; Binding Constants; Aggregation

INTRODUCTION

Plasmid DNA (pDNA) is a promising new blockbuster that could potentially lead to the discovery of novel vaccines for the prevention of diseases such as that caused by HIV or HCV. Research on innovative and cost effective pDNA production strategies is currently hindered by the majority of researches being focused on lab scale applications which routinely depend on commercially available, high cost disposable pDNA purification kits. Of interest is fast and reliable endotoxin removal technique which currently poses a major bottleneck in large scale production.

Endotoxins or lipopolysaccharides (LPS) are a natural component of gram-negative bacterial expression systems including the widely used *E. coli* [1]. Endotoxin regulates trans-membrane transport, intercellular communication and makes up part of the outer surface of the cell membrane of Gram-negative bacteria. Endotoxin has three distinct regions, an O-specific chain, a core oligosaccharide part and a lipid moiety one of which is very hydrophobic and the molecule also has a negative charge at neutral pH [2]. High levels of endotoxin are inevitably introduced into crude cell lysate when the cell membrane is lysed or through non-sterile process conditions [2]. The presence of endotoxins even at a small concentration is highly toxic to humans and could lead to severe health conditions including death. Endotoxins are stable molecules and thus difficult to destroy once introduced into the human body. Extreme treatments with heat (up to 250°C) or pH (over 1 M of strong acid or base) are needed to destroy endotoxins on glasswares and other laboratory equipments [3], however, cannot be employed on shear sensitive plasmid DNA.

Recent developments in the field of pDNA vaccine research include an improved method for pDNA purification through the use of a pre-column removal of impurities by selective metal cation induced precipitation [4]. Free transitional metal ions (e.g., Cu^{2+}, Mg^{2+}, and Zn^{2+}) are known to exhibit different degrees of interactions with plasmid DNA and impurities. It has been found that addition of $CaCl_2$ into the bacterial cell lysate can be used to selectively precipitate RNA from plasmid DNA but at a reasonably high concentration making it economically unattractive [5]. In addition, an additional purification step such as chromatographic removal step needs to be integrated to remove a small proportion of unprecipitated RNA [5]. Apparently, the properties of the bacterial solution determine the state of the endotoxins aggregation and this information can help in designing an effective endotoxin removal scheme particularly when combined with plasmid DNA purification [6].

Endotoxins also demonstrate better interaction with free metal ions than pDNA suggesting that there is a huge potential for selective removal of endotoxins using metal ions to be integrated into a commercial pDNA production line [4].

The study by [7] looked at optimising the process conditions (pH, ion concentration, temperature and incubation time) using central composite design experiments and concluded that selective endotoxin removal can conveniently be carried out at a pH condition similar to that of alkaline-lysed cell lysate and at a low ZnSO4 concentration. It was also reported that this method provided ease of subsequent plasmid DNA purification due to reduced bulk impurities, cost-effective and most importantly high level of endotoxin removal (>80%) and plasmid recovery (>90%) [7]. However, the underlying reasons for this strong selectivity were not well understood. Another drawback of the study by [7] is that the main purification steps are performed in an isolated manner and thus the results may not reflect the actual performance when the whole process is integrated into a continuous process line.

Ionic strength has been shown to be a key factor for both immobilised and free metal ions in determining the degree of interaction. It is currently unknown about the fundamental role of Zn^{2+} in selective pDNA-LPS precipitation process observed by the previous researchers. This body of work was developed to investigate the precipitation mechanism and in particular aggregation kinetics of pDNA-cation and LPS-cation by measurement of variables such as the amount of cations bound, particle size, mean Zeta potential, aggregate structure, and concentration of cation giving an appreciable degree of aggregation.

MATERIALS AND METHODS

Chemicals

Zinc Sulphate ($ZnSO_4.7H_20$), Magnesium Chloride ($MgCl_2.6H_20$ from APS, NSW, Australia) and Calcium Chloride ($CaCl_2.2H_2O$, Merck, Germany) were made up with deionised water to a concentration of 1000 μM. The weight of $CaCl_2$ to make up the 1000 μM solution was 0.0147 g; $ZnSO_4$ was 0.0276 g and $MgCl_2$ 0.0205 g. These were further diluted to a concentration of 100 μM. Arsenazo III, bovine serum albumin (BSA) and phosphotungstic acid were purchased from Sigma-Aldrich Australia.

Zeta potential analysis

1 mL of 0.5 M solution of divalent cations was made up using deionised water and then added to 1 mL of 25 kbp pDNA solution. The control solution contained only pDNA with deionised water. Each solution was run through the Malvern Zetasizer Nano ZS (Malvern, UK) three times consecutively for both Zeta potential and Zeta size. Manual setting was used and the temperature was set at 25 ºC. A similar experiment using endotoxin lipopolysaccharide (LPS) solution instead of pDNA was carried out. To form this LPS solution, endotoxin (6 EU) from *E*. coli standard Lot no. R30101006 (GenScript, USA) was diluted with 10 mL of LAL (endotoxin free) reagent water Lot no. R30041006 (GenScript, USA). The LAL reagent water was also used to prepare the 0.5 M cation solutions.

Zeta size analysis

An analogous method of preparation to that of determination of Zeta potential was used. The hydrodynamic size of the LPS aggregates were measured by Malvern Zetasizer Nano ZS (Malvern, UK) with a backscattering detection at 173^{o}, equipped with a He-Ne laser (λ =632.8 nm), at 25 ^{o}C, 3.25 mm measurement position, 15 runs/measurement, 5 measurements and 10 sec/ run.

Determination of the relative number of molecules in an average aggregate particle

A method to assess the effectiveness of the aggregation that occurred when cation was present in solution was by determining the number of molecules, pDNA or LPS, which were bound in an average aggregate particle. The average diameter was determined as the highest peak of the particle size intensity distribution. The average volume, V (nm^3) was calculated using the formula shown in equation (1), where D is the average diameter in nm.

$$V = \frac{\pi \times D^3}{6} \qquad (1)$$

It was assumed that the particles formed perfect spheres and that the contribution of cation in size and weight of aggregate was negligible when compared to the large macromolecules (pDNA and LPS). The average number of LPS molecules was then found by dividing the average volume, V (nm^3) by 8.3 nm^3. This value was calculated as follows: molecular weight

(Mw) of LPS was approximately 5000g/mol [8]; this was divided by the number of molecules in a mole (6 x 10^{23} molecules/mole), to find the weight of a single LPS molecule; 5000/6 x 10^{23} gave 0.83 x 10^{-20} g/molecule. The density of LPS was assumed to be 1 g/cm^3 thus one molecule of LPS occupies a volume of 8.3 nm^3.

An analogous method was used to calculate the number of pDNA molecules in an average pDNA aggregate, however, the average volume (nm^3) was divided by 27500 due to molecular weight of pDNA molecules. The number of base pair of the pDNA molecule was 25 kbp. A single base pair is approximately equivalent to 6,600 daltons [9]. One dalton is equivalent to 1g/mole, thus the molecular weight was approximated to be 1.65 x 10^8 g/mole. Divided by 6 x 10^{23} molecules/mole gave 27500 g/molecule. Again density was assumed to be 1gm/cm^3.

Determination of cation concentration at 50% aggregation (K_m value)

The K_m value represented the concentration of cations that resulted in 50% aggregation. These values were generated from a graph of cation concentration vs. percentage aggregation with either LPS or pDNA using the method outlined by [7], which was based on absorbance measurements. The model was expected to be linear and pass through the initial point (0, 0) of the graph. Microsoft Excel software was used to generate an equation for the straight line passing all the experimental values and the point (0, 0). These equations were used to find the required concentration to achieve 50% aggregation.

Determination of number of cations bound per molecule of LPS or pDNA

The purpose of this experiment was to look at how much of the cation was being extracted from the solution to form aggregates with endotoxin and plasmid. A unique pH-dependent dye called Arsenazo was used to measure the concentration of cations in solution by measuring the change in the light absorbance of the Arsenazo reactions. Wavelengths between 590-610 nm were examined as per [10], however it was decided that for the purpose of this experiment a wavelength of 610 nm was most suitable. A 250 μM stock solution of Arsenazo reagent was made by mixing 0.0197 g of Arsenazo III (Lot no. A927755G) to 100 mL of deionised water. This was further diluted to 50 μM by adding 20 mL of this solution to 80 mL of deionised water and the final pH was adjusted to a value of 9 using 40 g/L NaOH. 0.02 mL of 0.061 μM pDNA was added into separate microcentrifuge tubes containing 0, 5, 10, 15, 20, 25, 30, 35 μM cation solutions respectively and incubated for 10 mins at 25 °C. 1 mL of 50

μM Arsenazo (pH 9) was added into each tube, inverted gently several times, incubated for 10 mins and the absorbance of each sample was measured via a UV-Vis spectrophotometer at a wave length of 610 nm. For LPS analysis, 50 μM of LPS solution were added into each cation solution, incubated, mixed with Arsenazo and the absorbance was measured as described above. All solutions used in this work were prepared at pH 7 except for the working Arsenazo solution (50 μM) which was prepared at pH 9. The amount of remaining cations in solutions was measured by correlating the absorbance data to a standard curve generated for each cation.

Electron microscopy

Visualisation of LPS and pDNA molecules under an electron microscope was undertaken to determine if exposure to particular cations resulted in a change in the quantity and magnitude of particle size. 100 μM of lipopolysaccharide (pH 7) were mixed with 50 mM cation and incubated at 25°C for 10 min. 0.01% bovine serum albumin and 0.2% phosphotungstic acid (pH 7) were added and applied on a carbon-coated grid. The surplus liquid was removed using a filter paper and the grid was air dried. Micrographs were taken using the Hitachi electron microscope at magnifications of 6kx, 40kx and 200kx. For pDNA analysis, the above protocols were repeated using 1 μM pDNA.

RESULTS AND DISCUSSIONS

Zeta potential analysis

The average mean Zeta potential of the control pDNA (No cation addition) for the three runs was calculated to be -52.1 mV (Table 1). The data suggests that pDNA aggregates are strongly anionic, a consequence of the presence of negatively charged DNA phosphate groups on the pDNA helical backbone. The strongly anionic nature of the pDNA indicates higher colloidal stability and thus a decreased amount of aggregation [11]. As hypothesised, the addition of positively charged cationic particles to the negatively charged pDNA molecules causes a cancellation effect on the charge observed. The mean Zeta potential decreased from -52.1mV for the control solution to a mean value of -12.3 when Zn^{2+} was present. It is also suggested that an effectively neutral Zeta potential may correspond to an increased quantity of aggregation occurring due to a decreased existence of charge-charge repulsion allowing the particles to improve on their natural tendency to aggregate [12]. In Mg^{2+} solution, the mean

Zeta potential was found to be -2.5mV, the closest to neutrality that was found for the pDNA mixtures. This should theoretically correspond to a greater ability of the particles to aggregate due to reduction in charge dependent repulsion [11]. Ca^{2+} formed aggregates with a mean Zeta potential between that of Zn^{2+} and Mg^{2+} with a value of -4.24. Comparison of the three types of cations showed that, qualitatively, a similar trend of decreasing Zeta potential did occur. However, Zn^{2+} showed a Zeta potential value that was closest to neutrality thus possessed the highest degree of aggregation.

Table 1. Analysis of Zeta potential of pDNA in free cation solutions.

Cation	Cation concentration (M)	pDNA concentration (μM)	Mean Zeta potential (mV)	Standard deviation
-	-	5	-52.1	± 5.2
Zn^{2+}	0.5	5	-12.3	± 2.1
Ca^{2+}	0.5	5	-4.2	± 1.9
Mg^{2+}	0.5	5	-2.5	± 1.5

Samples were made up in deionised water and measurements were done in triplicates at room temperature.

Table 2. Analysis of Zeta potential of LPS in free cation solutions.

Cation	Cation concentration (M)	LPS concentration (μM)	Mean Zeta potential (mV)	Standard deviation
-	-	10	-9.7	± 0.8
Zn^{2+}	0.5	10	1.4	± 0.3
Ca^{2+}	0.5	10	1.5	± 0.3
Mg^{2+}	0.5	10	8.8	± 0.5

Samples were made up in deionised water and measurements were done in triplicates at room temperature.

An analogous experiment was conducted using LPS instead of pDNA and the results are presented in Table 2. Similar to pDNA, it was again hypothesized that the addition of cation to the anionic LPS particles caused a charge cancellation. The control sample (contained only LPS) gave a -9.7 mV mean Zeta potential. In Zn^{2+} solution, the mean Zeta potential was slightly positive with a value of 1.4 mV. This suggests that the average LPS aggregates were more cationic when Zn^{2+} was present than when the LPS was untreated. The mean Zeta potential of the LPS with Mg^{2+} present was also positive, surpassing neutrality, with a value of 8.8 mV. This value is still lower than ±30 mV and consequently sufficient aggregation

could still occur. Calcium cations were added to the LPS and the resultant Zeta potential was also found to be in the positive region with a value of 1.5 mV.

The differences observed between the three replicates, indicated by the standard deviations in Table 1 and Table 2 can be explained by the time dependent changes in the aggregation of the particles. A slight pH deviation could also be a factor due to the substantial dependence Zeta potential had on the pH, though all the pDNA-cation solutions were prepared at pH 7. A comparison between Table 1 and Table 2 suggests that unlike pDNA, which has a larger deviation of Zeta potentials when untreated, the untreated LPS produced a small deviation. Assuming a negligible experimental error, this phenomenon could be explained by looking into the hydrodynamic shape of the molecules. The 25 kbp pDNA is substantially larger in size hence degree of self-entanglement or rigidification compared to LPS. This self-entanglement could possibly result in the charge being hidden within the inner part of the aggregate thus varying the mean Zeta potential. Unlike pDNA, LPS shows a smaller Zeta potential deviation due to the well exposed negatively charged groups.

Zeta size analysis

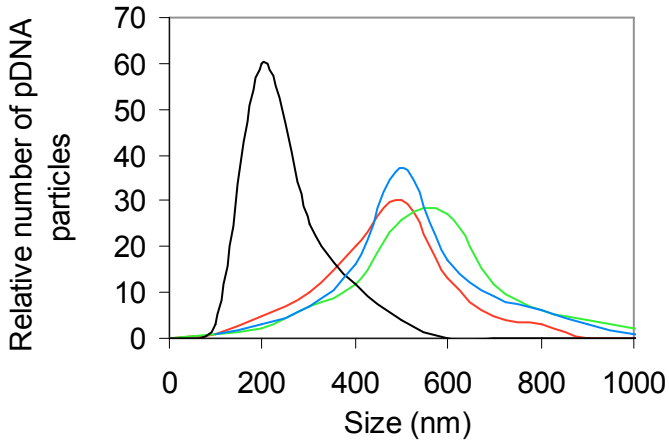

Fig. 1. Relative number of pDNA particles in each size range for different type of cations. 1 mL of 25 kbp pDNA solution was mixed with 0.5 M cation and measured for hydrodynamic diameter. Relative number of particles was obtained from the size intensity distribution of Malvern Zetasizer Nano ZS (Malvern, UK). Lines represent Mg^{2+} (Black), Zn^{2+} (Blue), Ca^{2+} (Green) and No cation (Red).

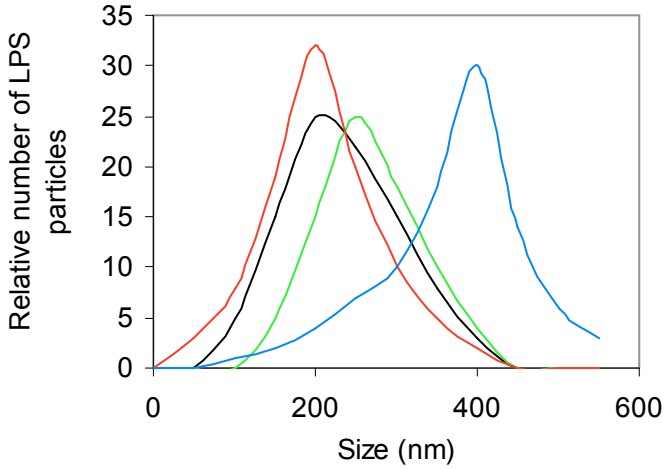

Fig. 2. Relative number of LPS particles in each size range for different type of cations. 1 mL of LPS solution was mixed with 0.5 M cation and measured for hydrodynamic diameter. Relative number of particles was obtained from the size intensity distribution of Malvern Zetasizer Nano ZS (Malvern, UK). Lines represent Mg^{2+} (Black), Zn^{2+} (Blue), Ca^{2+} (Green) and No cation (Red).

The Zeta size analyser used a process called Dynamic Light Scattering (DLS) to perform the particle size measurements. The DLS method measures Brownian motion of the particles being analysed to enable the size of the particles to be calculated. The Stokes-Einstein equation relates the speed of a particle (due to Brownian motion) to its size. By utilising a combination of this equation and analysis of the intensity fluctuations, produced by light bouncing off illuminated particles, the size of the aggregates can be measured [13].

Based on Fig. 1, it is observed that the size of the pDNA aggregates (in this case without cation addition) covers a broad range, from around 100 nm up to 1000 nm. The peak number of particles was found in 400-600 nm range. Although the addition of Zn^{2+} resulted in an increased number of particles in the higher size range (> 900 nm), the peak size was relatively similar to that of the control, with the majority of particles still in the 400-600 nm range. Equivalent to that of the control and Zn^{2+} solutions, the peak size for Ca^{2+} was found to be in the 400-600 nm range. Interestingly, the peak size for Mg^{2+} was found at a significantly lower aggregation size range of 100-300 nm, indicating that the addition of magnesium ions might affect the 3-D structure of the plasmid causing it to become more compact and that the concentration of Mg^{2+} was not sufficient to form bridges between pDNA molecules hence larger aggregates.

Fig. 2. above shows that the mean size of untreated LPS particles is larger than that estimated using equation (1) for one LPS molecule. This implies that the untreated LPS prepared in this work were consisted of partially aggregated LPS particles. LPS is known to self aggregate [14] and thus it can be hypothesised that the lower size range evident at around 0-50 nm is due to the presence of less or non-aggregated LPS molecules and the self-aggregation results in the formation of the higher LPS particle size in the 50-600 nm range.

The addition of zinc ions enhances the aggregate formation. The size range on the X-axis of Fig. 2 shows that the average aggregation size of the LPS particles, when Zn^{2+} is present, is larger than the control with a peak of approximately 400 nm. Furthermore, the number of particles in the lower size range is lower than in the control solution (No cation addition). The larger number of particles in the higher size range when Zn^{2+} is present compared to that of Mg^{2+} or Ca^{2+} further suggests $ZnSO_4$ as a potential LPS precipitant. Ca^{2+} shows a normal distribution relatively similar to that of the control and Mg^{2+} with a mean aggregate size of around 250 nm. Although the mean aggregate size is higher than that in the control and Mg^{2+} solutions, it is considerably lower than that in the Zn^{2+} solution.

Relative number of molecules in average aggregate particle

Table 3. Relative number of pDNA molecules per particle.

	Plasmid DNA particles		
Cation	**Average diameter (nm)**	**Volume (nm^3)**	**No. of molecules/particle**
No cation	501	6.6E+08	240
Zn^{2+}	507	6.8E+07	250
Mg^{2+}	166	2.4E+06	8.7
Ca^{2+}	542	8.3E+07	300

Table 4. Relative number of LPS molecules per particle.

	LPS particles		
Cation	**Average diameter (nm)**	**Volume (nm^3)**	**No. of molecules/particle**
No cation	157	2.0E+06	2.4E+05
Zn^{2+}	399	3.3E+07	4.0E+06
Mg^{2+}	166	2.4E+06	2.9E+05
Ca^{2+}	175	2.8E+06	3.4E+05

As shown in Table 3, the control pDNA (No cation) was found to have 240 molecules per particle. The addition of cations caused the number of pDNA molecules in an aggregate to decrease or increase. Ca^{2+} solution had the highest amount of pDNA molecules per particle with a value of 300 followed by Zn^{2+} with 250 and Mg^{2+} only 8.7. The data suggests that under the experimental conditions, addition of Zn^{2+} and Ca^{2+} enhances aggregate formation of pDNA whilst Mg^{2+} decreases the size of aggregates.

It is interesting to note that the number of pDNA molecules per particle in solutions without cation addition is substantially large. It is estimated that the volume of a single pDNA molecule is 275000 nm^3 which is far smaller than the value reported in Table 3 for 'No cation'. From our overall observation, we speculated that the large volume of pDNA particle was a result of the pDNA's porous-like spherical arrangement. Since the Zetasize instrument could not distinguish between compact and porous particles, the final value of the number of molecules/particles was calculated by assuming that the particle was compact and contained only pDNA molecules instead of pores.

Table 4 indicates that the addition of Zn^{2+} resulted in the largest number of LPS molecules per aggregate particle with a value of 4x10^6 followed by 2.4x10^5 in control solution, 2.9x10^5 in Mg^{2+} and 3.4x10^5 in Ca^{2+}. These results are in agreement with the results of Zeta size analysis that suggest Zn^{2+} has the most profound aggregate forming capabilities for LPS.

K_m values

The K_m value represents the concentration of cations that results in 50% aggregation and can generally be used to classify the aggregating efficiencies of precipitants. The smaller the K_m value, the more efficient the precipitant is. A major outcome of the analysis of Table 5 was the existence of selective aggregating efficiencies for LPS and pDNA. Such information is definitely useful to the development of pDNA purification strategy particularly with respect to selective pDNA-LPS precipitation.

Cu^{2+} demonstrates a strong interaction with both pDNA and LPS. This aggregative interaction between Cu^{2+} and pDNA/LPS renders its unsuitability as a candidate for cation-based endotoxin removal as this would result in both endotoxin and plasmid forming large aggregates making consequential separation based on size inefficient. It is assumed that those cations with $K_m > 2$ M do not have any interaction with

pDNA or LPS. Of particular interest are cations (in the form of salt) that display high K_m value for pDNA and low K_m value for LPS which are $ZnSO_4$, $CaCl_2$ and $MgCl_2$. These particular metal salts, which were represented by Zn^{2+}, $Ca^{2+}$and Mg^{+2} respectively throughout the paper, were found to have the ability to selectively precipitate by means of increasing the aggregate size of LPS whilst maintaining the size of pDNA particle to a minimum. It can be seen from Table 5 that, in combination with endotoxin, Zn^{2+} has a K_m value of 0.28, less than Ca^{2+} at 0.31 and Mg^{2+} at 0.49. This suggests that Zn^{2+} is more selective than Ca^{2+} and Mg^{2+} as it requires a lesser concentration to achieve the same degree of aggregation.

Table 5. K_m values for pDNA and LPS in different cation solutions.

Cation	Concentration (M) of cation giving 50% aggregation, K_m	
	pDNA	LPS
$CuCl_2$	0.28	0.26
$ZnSO_4$*	> 2	0.28
$ZnCl_2$	0.52	0.28
$NiCl_2$	0.55	0.3
$CaCl_2$*	> 2	0.31
$NiSO_4$*	> 2	0.69
$MgSO_4$*	> 2	0.98
$MgCl_2$*	> 2	0.49
$CuSO_4$	0.32	0.26

*In regard to interaction with pDNA, the data indicate that the interaction between these cations and pDNA is minimal or negligible.

All solutions contained only metal salts, deionised water and either pDNA or LPS.

Determination of cation quantity in aggregate

In this experiment, Arsenazo III was used to bind divalent cations and form complexes that displayed different spectrophotometric absorbance characteristics. It was observed that the differences in absorbance of Zn^{2+}, Ca^{2+}, and Mg^{2+} containing solutions were highly dependent on pH. At pH < 7, the differences in absorbance were quite insignificant over all cation concentrations tested. This indicated that Arsenazo-cation binding was weak and undistinguishable in acidic conditions. However at pH 9 as depicted in Fig. 3, the absorbance profile of each cation was distinct as evident from the slopes of each plot.

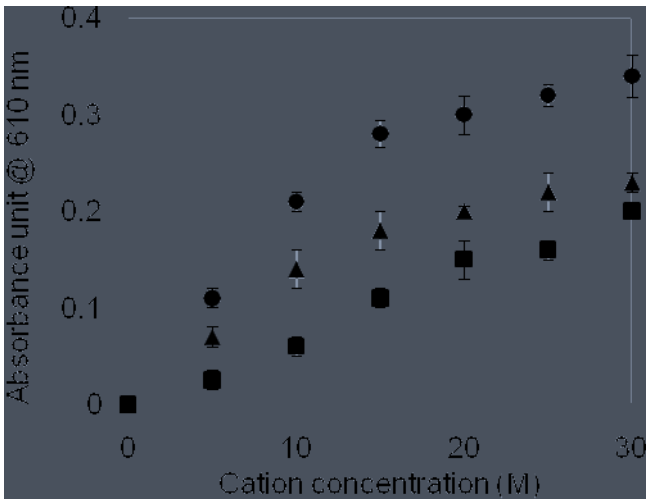

Fig. 3. Spectrophotometry of cation-Arsenazo III reactions. A series of solutions of varying concentration of cation in combination with 50 μM Arsenazo III was prepared with deionised water as solvent. Absorbance at 610 nm wave length was measured at room temperature. A straight line equation was found at the linear region of this plot and used to determine the cation concentration remaining in solutions after the addition of endotoxin or plasmid. ●: $CaCl_2$; ▲: $MgCl_2$; ■: $ZnSO_4$.

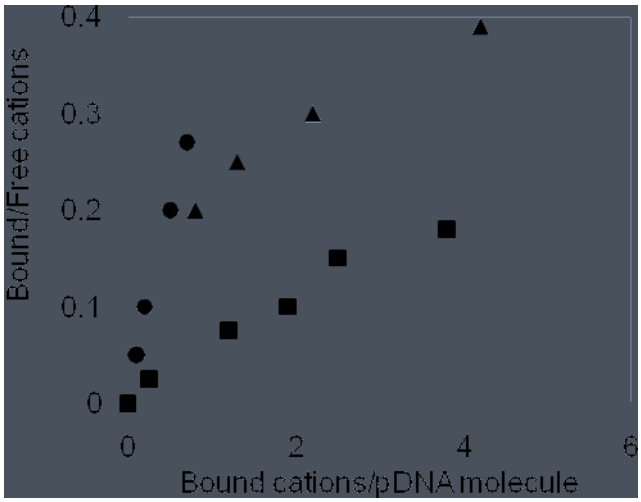

Fig. 4. Scatchard plot for pDNA-cation binding analysis. 0.061μM pDNA (25 kbp) was mixed with 0, 5, 10, 15, 20, 25, 30 and 35 μM cations in separate microcentrifuge tubes. Ten minutes of incubation time at 25°C was allowed for pDNA-cation binding before 25 μM Arsenazo III was added. Absorbance at 610 nm wave length of each sample was measured. The concentration of unbound cations was determined by using a standard curve for each experiment. Both X- and Y- axes were subjected to deviation due to the measured bound cations, however error analysis showed that the overall magnitude of deviation was < 10 % of each data point. ●: $CaCl_2$; ▲: $MgCl_2$; ■: $ZnSO_4$.

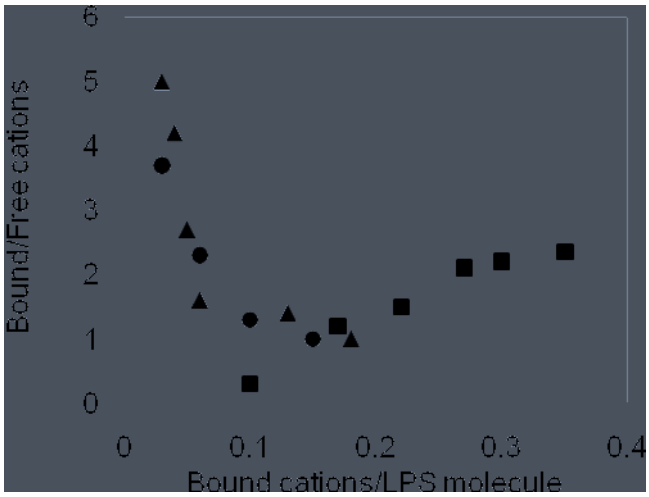

z

Fig. 5. Scatchard plot for LPS-cation binding analysis. 50 μM LPS was mixed with 0, 5, 10, 15, 20, 25, 30 and 35 μM cations in separate microcentrifuge tubes. 10 minutes of incubation time at 25°C was allowed for LPS-cation binding before 25 μM Arsenazo III was added. Absorbance at 610 nm wave length of each sample was measured. The concentration of unbound cations was determined by using a standard curve for each experiment. Both X- and Y- axes were subjected to deviation due to the measured bound cations, however error analysis showed that the overall magnitude of deviation was < 10 % of each data point. ●: $CaCl_2$; ▲: $MgCl_2$; ■: $ZnSO_4$.

The Scatchard plots generated for the result of pDNA interaction with Zn^{2+}, Ca^{2+} and Mg^{2+} display an unusual phenomenon that is cited in a small number of journal articles including those by [15, 16] on ligand binding. The unusual behaviour is that the gradient of the graph (Fig. 4) is positive, suggesting an inverse dependence of binding constants (nK). Similar to these articles when pDNA was used as the ligand, only positive gradients were observed. From the literature there is some suggestion that the dependence of the value of nK is dependent on the concentration of the protein (plasmid in this case) [16]. What can be deduced is that a single plasmid concentration is insufficient to characterise cation-plasmid interaction adequately thus further experimentation is required. The data in Fig. 4 indicate that Zn^{2+} demonstrated a small amount of binding with the plasmid. This binding increased with increasing Zn^{2+} concentration; however, the standardisation of the data allows us to conclude that this increase is still fairly insignificant.

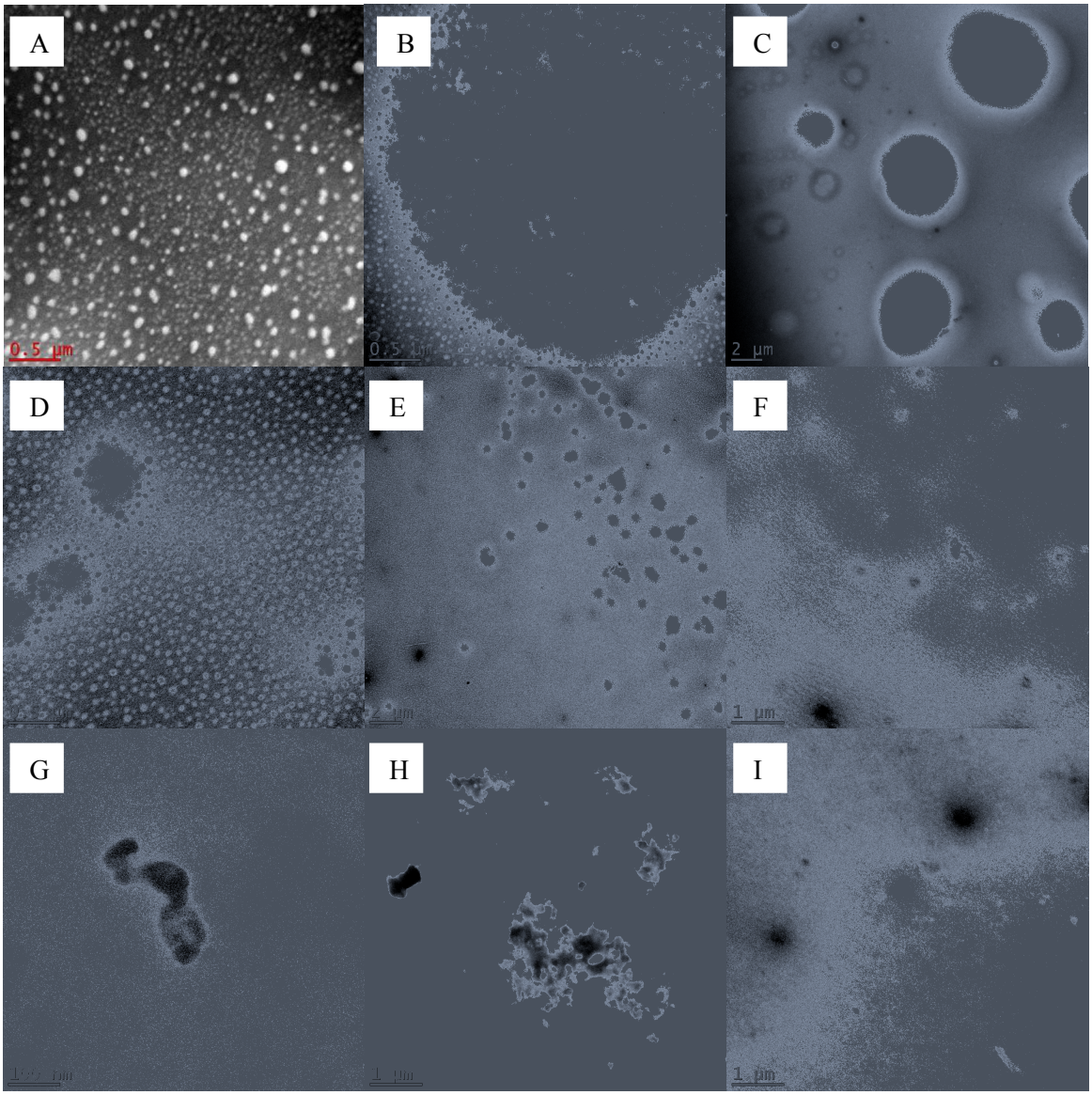

Fig. 6. Electron microscopy of pDNA and LPS under different aggregation conditions. 100 µM lipopolysaccharide were mixed with 50 mM cation and incubated at 25°C for 10 min. Bovine serum albumin (0.01%) and phosphotungstic acid (0.2%) were added into the mixture, applied on a carbon-coated grid and air dried. All solutions were prepared at pH 7. Micrographs were taken using Hitachi electron microscope at magnifications of 6kx, 40kx and 200kx. The experiments were repeated for pDNA (1 µM) instead of lipopolysaccharide. The white bar represents the actual scale of the image. **A**: LPS (6kx); **B**: LPS-Zn^{2+} (40kx); **C**: LPS-Zn^{2+} (6kx); **D**: LPS-Mg^{2+} (40kx); **E**: LPS-Mg^{2+} (6kx); **F**: pDNA (6kx); **G**: pDNA (200kx); **H**: pDNA-Ca^{2+} (6kx); **I**: pDNA-Zn^{2+} (6kx).

A small amount of binding was seen to be occurring between pDNA and Ca^{2+} and an increase in binding was observed as the concentration of Ca^{2+} was increased. Mg^{2+} too was shown to have an affinity with pDNA as the concentration of cation in the solution reduced to a greater extent than Zn^{2+} and Ca^{2+} upon the addition of plasmid as demonstrated by the reduction of absorbance in the solution of Arsenazo III (data not shown). [17] also brings to light the fact that Scatchard methods of examining binding data are suitable when only one class of sites is displayed by the ligand but are at best approximate when more than a single class exists thus results hint that concentration and multiple binding sites could play a role in the binding kinetics of pDNA and cations. The general implication of this positive gradient could be that there is a minimum concentration of plasmid that is required before a significant binding between itself and cations and consequential aggregation occur or that pDNA/ cation binding is not appreciable at small cation concentrations.

In an analogous method, a similar series of experiments were carried out for LPS. Fig. 5 shows that the concentration of the LPS solutions and consequently the ratio of cation concentration to LPS concentration had a marked effect on the binding kinetics as observed by the different curves produced on the Scatchard plots. Due to negative and near zero points produced when LPS concentrations were very low (0.5 and 5 μM) it was decided that the subsequent cation-LPS absorbance data be carried out using 50 μM of LPS. At higher concentrations of LPS, Mg^{2+} indicated that the bound/free cation ratio was high when the bound cation/LPS ratio was low and gradually dropped onwards (with increasing bound cation/LPS ratio). A similar trend was observed for Ca^{2+} with an initial bound/free cation value of 3.7. The general trend for the Scatchard plots of Ca^{2+} and Mg^{2+} at higher concentration is a negative gradient. Similarly, [15] found that at higher concentration of ligand, the gradient of the standard curve was negative, but the unusual phenomenon of a positive gradient was found at lower ligand levels. As mentioned earlier, the theory of concentration dependence of ligand-cation binding emerges to agree with results from this work and literatures. This phenomenon may also be correlated to ligand-ligand interactions, agglomeration or that it is even a function of pH.

Visualisation of aggregate particles

LPS particles were examined electron microscopically and the results were shown in Fig. 6. Partially dense spherical particles were observed for the LPS control as shown in Fig. 6A. Fig. 6B and Fig. 6C display lipopolysaccharide particles when Zn^{2+} is present. The pronounced

increase in density of particles present indicates an enhancement of LPS aggregation, when exposed to Zn^{2+}. Magnesium cations are also seen to induce aggregate formation (Fig. 6D and Fig. 6E) as evident by the presence of dense spherical particles, which indicates a higher quantity of aggregation than what is observed in the control case. However, as a consequence of the higher LPS aggregate density in the Zn^{2+} solution (Fig. 6B and Fig. 6C), the superiority of Zn^{2+} over Mg^{2+} as a LPS aggregation inducer is further supported. Fig. 6 F – I representing pDNA shows that no apparent change in particle size occurred in Zn^{2+} solutions. However, significantly aggregated pDNA particles were present in Ca^{2+} solutions. These highly aggregated structures could be due to the extended aggregation experienced during the air drying of the grid where the samples were placed.

CONCLUSIONS

The aim of this study was to undertake an in depth analysis of endotoxin and pDNA aggregation in order to gain a greater understanding of the potential use of cation-induced aggregation as a viable secondary purification technique in plasmid DNA manufacture. The four stages of investigation looked at the different physicochemical aspects of aggregation. Stage one found that the greatest number of LPS molecules in an average LPS aggregate particle occurred in the presence of Zn^{2+} whereas in pDNA solutions, Mg^{2+} had a significant effect on the number of pDNA molecules/particle. This information supported the hypothesis that zinc cation showed the greatest potential as a distinguishing aggregation inducer compared to other cations investigated. Stage two reiterated the superiority of Zn^{2+} and in particular zinc sulphate as it had the lowest K_m value, indicating a lesser amount of zinc ions was required, than any of the other cations, to produce 50% aggregation in the LPS. Stage three investigated the number of cations bound to a single LPS or pDNA molecule using a Scatchard plot analysis. Results from this analysis showed that under the experimental conditions, Zn^{2+}-LPS had a positive Scatchard plot gradient suggesting high affinity interaction thus high saturation point. Stage four allowed for a visual confirmation of the aggregating potential of cations in particular Zn^{2+}. It was evident from the electron microscopy results that Zn^{2+} induced a greater density of aggregates compared to other cations studied. This body of work and all the new information gathered herein are significant to the current research on plasmid DNA production as it considerably highlights zinc cations strong selectivity for LPS over pDNA and its ability to enhance the formation of LPS aggregates making a secondary size- based purification technique viable. As part of the ongoing research project, we are also conducting a further study on the binding kinetics of

zinc cation with LPS using different methods such as LAL assay and plasmid emission spectroscopy [18], which do not require the use of toxic Arsenazo III dye. We are also looking at the integration of this novel secondary purification technique into the downstream processing of plasmid DNA, possibly in combination with other novel technique such as the use of a monolith-based purification technology.

ACKNOWLEDGEMENTS

The authors would like to thank Monash University, Australia for funding this project.

DECLARATION OF INTEREST

The authors declare that they have no competing interests.

SAFETY REQUIREMENTS

The following general safety conditions were applied to all experiments.

- Enclosed shoes, long pants, lab coats, and safety goggles were worn at all times.
- No objects that entered the laboratory left without first being autoclaved.
- All persons using the BEL laboratory underwent a safety induction.
- Arsenazo (III) is a toxic reagent and care was taken when handling including the wearing of gloves.
- LPS and pDNA pose a biohazard as they are genetically engineered. Gloves were worn when handling and all care was taken to contain these substances within the laboratory. Similarly all equipments which came into contact were autoclaved after use. Also wastes were treated as biohazards and disposed of through the appropriate route.

REFERENCES

[1] R.H. Chen, C.J. Huang, B.S. Newton, G. Ritter, L.J. Old, C.A. Batt, Factors affecting endotoxin removal from recombinant therapeutic proteins by anion exchange chromatography, Protein Expression and Purif., 64 (2009) 76-81.

[2] D. Petsch, F.B. Anspach, Endotoxin removal from protein solutions, J. Biotechnol., 76 (2000) 97-119.

[3] P.O. Magalhães, A.M. Lopes, P.G. Mazzola, C. Rangel-Yagui, T.C.V. Penna, A.P. Jr., Methods of Endotoxin Removal from Biological Preparations: a Review, J. Pharm. Pharmaceut. Sci., 10 (2007) 388-404.

[4] C.M. Ongkudon, M.K. Danquah, Endotoxin Removal and Plasmid DNA Recovery in Various Metal Ion Solutions, Sep. Sci. Technol., 46 (2011) 1-3.
[5] A. Eon-Duval, K. Gumbs, C. Ellett, Precipitation of RNA impurities with high salt in a plasmid DNA purification process: Use of experimental design to determine reaction conditions, Biotechnol. Bioeng., 83 (2003) 544-553.
[6] K.J. Sweadner, M. Forte, L.L. Nelsen, Filtration Removal of Endotoxin (Pyrogens) in Solution in Different States of Aggregation, Appl. Environ. Microbiol., 34 (1977) 382-385.
[7] C.M. Ongkudon, M.K. Danquah, Analysis of Selective Metal-Salt-Induced Endotoxin Precipitation in Plasmid DNA Purification Using Improved Limulus Amoebocyte Lysate Assay and Central Composite Design, Anal. Chem., 83 (2011) 391-397.
[8] A.M. Field, E. Rowatt, R.J.P. Williams, The interaction of cations with lipopolysaccharide from *Escherichia coli* C as shown by measurement of binding constants and aggregation reactions, Biochem. J., 263 (1989) 695-702.
[9] Conversion and Calculations, in, Nordic Biosite, 2011.
[10] V. Michaylova, L. Yuroukva, Arsenazo III as a soectriohotometric reagent for zinc and cadmium, Anal. Chim. Acta (1974) 73-82.
[11] Characterization of Aggregative Stability, in, Dispersion Technology Inc., 2002.
[12] Zeta Potential Overview, in, Brookhaven Instruments Corporation, 2010.
[13] Zetasizer Nano Series User Manual, in, Malvern Instruments Ltd., 2004.
[14] J.W. Shands, The Dispersion of Gram-negative Lipopolysaccharide by Deoxycholate, J. Biol. Chem., 255 (1980) 1221.
[15] L. Clegg, W. Lindup, Scatchard plots with a positive slope: dependence upon ligand concentration, J. Pharm. Pharmacol., (1984) 776-779.
[16] A. Miller, J. Adir, R.E. Vestal, Scatchard Plots with a Positive Slope and Role of Albumin Concentration, J. Pharmaceut. Sci., (1978) 1193-1194.
[17] J.J. Vallner, Binding of Drugs by Albumin and Plasma Protein, J. Pharm. Sci., 66 (1977) 447-465
[18] R.T. Coughlin, S. Tonsager, E.J. Mcgroarty, Quantitation of Metal-Cations Bound to Membranes and Extracted Lipopolysaccharide of Escherichia-Coli, Biochem., 22 (1983) 2002-2007.

CHAPTER SIX

ECONOMIC EVALUATION OF PLASMID VACCINE PRODUCTION

Section 6.1

Inactivated influenza virus vaccine versus plasmid DNA influenza vaccine: Cost per dose estimation and economic comparison

BMC Health Service Research (Under review 2011)

Monash University

Declaration for Thesis Section 6.1

Declaration by candidate

In the case of Section 6.1, the nature and extent of my contribution to the work was the following:

Nature of contribution	Extent of contribution (%)
Initiation, Key ideas, Experimental, Development, Results interpretations, Writing up	35

The following co-authors contributed to the work. Co-authors who are students at Monash University must also indicate the extent of their contribution in percentage terms:

Name	Nature of contribution
Lorraine Angstetra Dr. Michael K. Danquah Dr. Gareth M. Forde	Initiation, Key ideas, Experimental, Development, Results interpretations, Writing up

Candidate's signature		**Date**

Declaration by co-authors

The undersigned hereby certify that:

1. the above declaration correctly reflects the nature and extent of the candidate's contribution to this work, and the nature of the contribution of each of the co-authors;
2. they meet the criteria for authorship in that they have participated in the conception, execution, or interpretation, of at least that part of the publication in their field of expertise;
3. they take public responsibility for their part of the publication, except for the responsible author who accepts overall responsibility for the publication;
4. there are no other authors of the publication according to these criteria;
5. potential conflicts of interest have been disclosed to (a)granting bodies, (b) the editor or publisher of journals or other publications, and (c) the head of the responsible academic unit; and
6. the original data are stored at the following location (s) and will be held for at least five years from the date indicated below:

Location	Chemical Engineering Department, Monash University, Clayton, Australia

Signature		**Date**

Inactivated influenza virus vaccine versus plasmid DNA influenza vaccine: Cost per dose estimation and economic comparison

Clarence M. Ongkudon, Lorraine Angstetra, Michael K. Danquah, Gareth M. Forde

Abstract

This study focused on the cost per dose estimation and economic analysis of two different types of influenza vaccine manufacturing facilities which were the inactivated influenza virus vaccine and plasmid DNA influenza vaccine. Analysis showed that the project's success was highly dependent on the selling price and production volume of influenza vaccine. Both facilities incurred a similar cost per dose of about $2 although most of the manufacturing costs for plasmid DNA vaccine were lower than inactivated virus vaccine. However, plasmid DNA vaccine had the advantage of producing the vaccine one year ahead of the inactivated virus vaccine.

*Keywords***:** Influenza vaccine; Plasmid DNA vaccine; Inactivated virus vaccine; Economic evaluation

INTRODUCTION

Current method for the preparation of an inactivated influenza virus vaccine through embryonated eggs may not be viable in the case of a pandemic. The viruses derived from embryonated hens' eggs are variants with substitutions in their haemagglutinin (HA) in the vicinity of the receptor binding site that are often antigenically significant (1). Therefore, an alternative technology is greatly needed to prevent its widespread in a timely manner. The inaugural use of plasmid DNA has been successfully reported in 2003 for the immunization of the California condors against West Nile virus (2). The veterinarian at the Los Angeles zoo has reported that the condors had no effects and the birds responded very well (Weiss R (http://www.washington-post.com)).

Although there have been several documented methods for plasmid DNA vaccine manufacture, these methods are presumably similar to the manufacture of recombinant protein products using bacterial hosts (3). These methods can be divided into two main categories

which are the plasmid production and plasmid DNA purification. Plasmid DNA cultivation is similar to the fermentation methods used for the production of recombinant protein. However, the growth conditions required for optimal production vary in each technique (4).

Studies on the economic aspects of vaccine production generally focus on the application and administration of vaccines amongst children. There have been no studies that combine the technical advancement findings with the economic evaluation of influenza vaccines which could be useful to pharmaceutical or biotechnology companies to consider into their investment strategy. The manufacturing facilities modeled in this study were to be built and based in the United States; hence, all economic analysis was for the United States market and was expressed in US dollars.

The cost per dose analysis focused on the research and development phase from discovery through to the end of phase 3 clinical trials. It also focused on the nature and dose of immunogen and the route of administration of vaccine. Plant costs, manufacturing costs and sterile filling costs were calculated based on case studies of intracellular protein production by a recombinant microorganism (5) and plasma- derived hepatitis B vaccine production (6). The economic analysis did not include costs for storage; transportation and vaccine administration (e.g. labour to administer injections).

EXPERIMENTAL

Basis and assumptions

The study compared the cost per dose incurred by two different technologies which were the inactivated virus and the plasmid DNA vaccine. Table 1 and 2 showed the data for calculation for both facilities. 73 million doses were the annual influenza vaccine capacity calculated using the basis and cost per dose model for plasmid DNA flu vaccine. Due to the known lengthy processing time to manufacture inactivated influenza virus vaccine (i.e. 9 month), there would only be 1 campaign in a year (i.e. 1 batch I year). Hence, the fermentor had been sized with this assumption. The correlation between kg of influenza virus in litres of liquid buffer was linear. This was an arbitrary assumption in the absence of published literature data on this aspect. Having sized the fermentor required for each process, the manufacturing cost for each process was then calculated. The following organogram (Fig. 1) was the model used to calculate the manufacturing cost for each process. The cost of bulk production process was proportionately related to the size of the fermentor. The sterile filling process for both inactivated virus and plasmid DNA vaccines were similar. Any differences in the processing parameters between the two technologies might not be significant to the manufacturing cost.

Table 1. Data for inactivated influenza virus vaccine facility

Description	Value
Required virus (in weight) annually for ca. 73 million dose	ca. 1 kg of virus
Fermentor size calculated	ca. 12,000 L
Fermentor size required	15,000 L

Table 2. Data for plasmid DNA vaccine facility

Description	Value
Plasmid DNA	104 g / batch
No of doses per batch	ca. 10 million doses / batch
No of batches per year (potential)	7.8 batches / year
No of production cycles per year (actual)	7 production cycles / year (taking shut down for maintenance, plant modification, etc into consideration)
No of doses per year	ca. 73 million doses / year

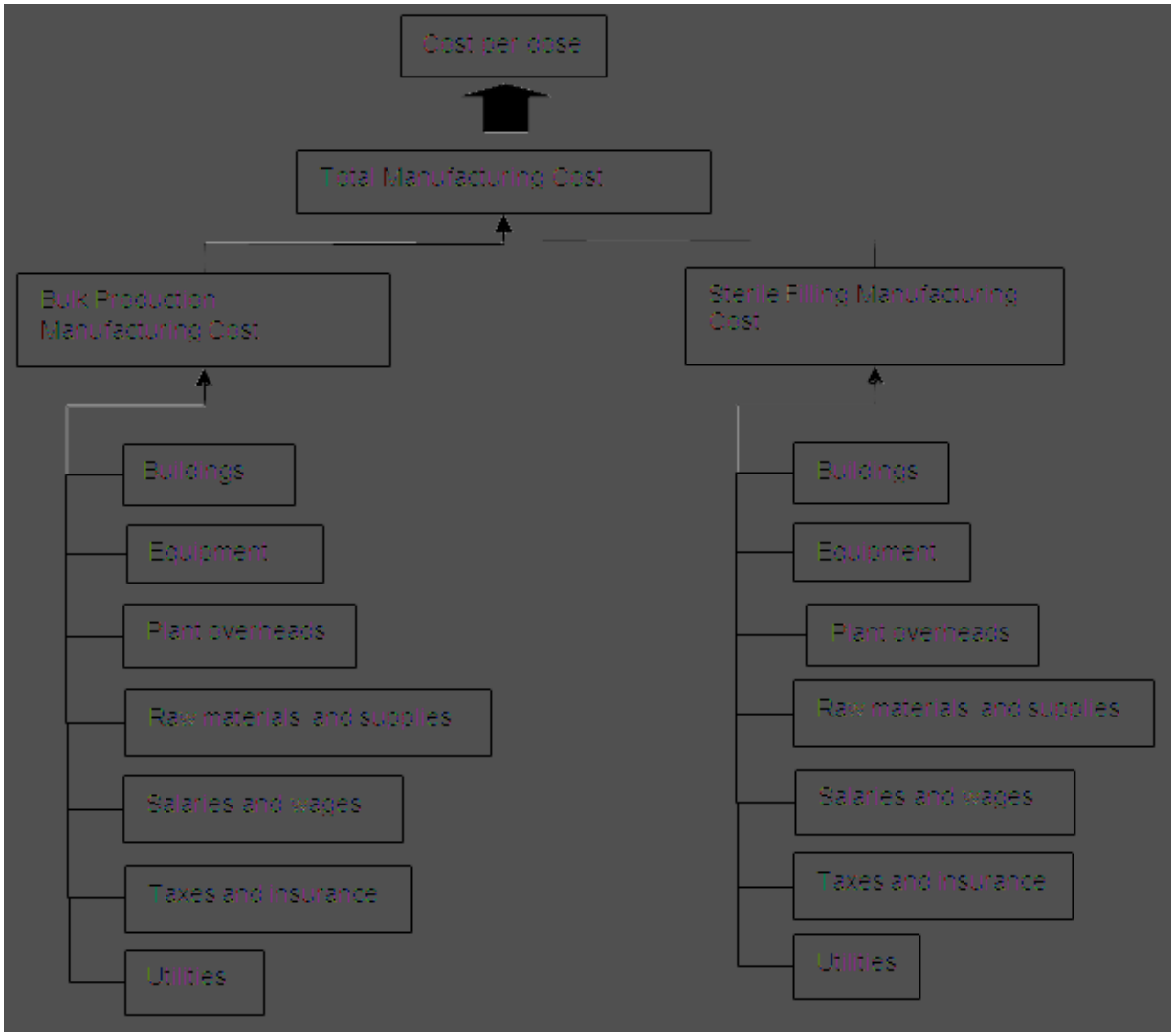

Fig. 1. Manufacturing cost model

Fixed capital cost

The first calculation made was the fixed capital cost as described elsewhere (7). Fixed capital cost consisted of equipments, buildings (15% of fixed capital), land and site development (7% of fixed capital) and start-up cost (10% of fixed capital). Hence, having calculated the equipment cost, the cost of the fixed capital cost, building, land and site development, and start-up cost were then derived. Equipment cost was calculated using capacity change and cost indices formulae (U.S. Department of Labor (http://data.bls.gov)). For sterile filling production facility, the equipment cost was calculated based on the number of doses to be produced per cycle (i.e. ca. 21 million doses) instead of the annual capacity.

Research and development cost

The R&D cost associated to the development of inactivated virus vaccine was assumed to be ca. $460 million. This is 40% of the general cost required to launch a new vaccine product, which has been quoted to be ca. $1 billion in 2004. This 40% was an arbitrary number assuming that the main R&D cost for inactivated virus vaccine was for clinical trial. There was no substantial R&D resource required to develop the technology as it was not a novel technology. This cost was amortized over 10 years. Plasmid DNA was a novel technology for influenza vaccine, thus the R&D cost was estimated to be ca. $1 billion which was the typical R&D cost in the industry.

Other costs

Marketing cost for both inactivated virus and plasmid DNA vaccine facilities were estimated to be ca. US$ 25 million. This was based on the marketing cost that MedImmune incurred to launch EluMist (Rosenwald SM (http://www.washingtonpost.com)). The relationship between salaries and fermentor size was linear. Hence, the salary for the bulk production was calculated using the salaries cost from the intracellular protein production case study as a basis. The ratio of staff between bulk production and sterile filling was 14 to 28. This number was taken from the plasma-derived hepatitis B vaccine case study (6). Hence, this ratio was used to estimate the salary required for sterile filling section. The salaries cost for chicken egg factory was not calculated as the cost of eggs had been included as part of the raw material cost. This cost would take all aspects of operating costs associated to the chicken egg factory. Salaries cost model for plasmid DNA vaccine was the same as for inactivated virus vaccine. Other costs such plant overhead (25% of fixed capital cost) and tax/insurance (4%) were selected based on the calculation for intracellular protein production (5). The calculation carried out for utilities and raw materials was similar to the one done for salary cost with the

exception of the raw material cost for chicken egg factory, which was calculated based on the assumption that one chicken egg provided enough vaccine for 1 dose. This was an arbitrary assumption in the absence of literature data. Cost of 1 dozen of eggs was $2 (U.S. Department of Labor (http://data.bls.gov)).

Economic evaluation

The economic evaluation was carried out through cash flow diagrams, internal rate of return, rate of return, payback period and sensitivity analysis between cost per dose and some of the input variables (i.e. Raw material cost, R&D cost, and Marketing Cost) (8). All costs mentioned in this study were in US dollars. Cash flow diagram was calculated using 9% (9) as the interest rate. The 9% rate used in this study was based on the suggested weighted average cost of capital (WACC) mentioned in (9). This was derived based on the suggested 12% WACC for the pharmaceutical industry. This 12% consisted of risk-free rate of return of 6% on a 30-year US Treasury bond, 3% of development risk and 3% of sales (market) risk. The 3% of sales (market) risk was excluded from this study as it was perceived that due to the nature of this product (i.e. Pandemic Preparation), there was no associated risk on this aspect. The selling price determined in this study was based on the lowest listed pricing stipulated in the (CDC (http://www.cdc.gov)). US$ 11.10 price was selected for this study, which was of the lower range of the influenza vaccine price in the market to provide a conservative approach to this study.

RESULTS AND DISCUSSION

Cost per dose calculation

The cost per dose final calculation for both plasmid DNA and inactivated virus vaccine was detailed in Table 3. Both plasmid DNA and inactivated virus vaccine process had similar cost per dose at $2.20 and $2.13 respectively. Reviewing the cost components in detail, plasmid DNA seemed to provide lower capital and operating costs than the inactivated virus technology. This was due to the smaller fermentor scale that plasmid DNA technology required. With plasmid yield of 80 g/m^3 and dosage requirement of 10 µg/dose, 1,500 L fermentor size which with 7 batches per year was adequate to provide ca. 73 million doses target. To attain the same capacity in this case study, a 15,000 L fermentor was required for the inactivated virus technology as it had 90 g/m^3 yield with dosage requirement of 15 µg/dose.

Table 3. Final cost per dose for both plasmid DNA and inactivated influenza virus vaccine facilities

	Plasmid DNA Influenza Vaccine	**Inactivated Influenza Virus Vaccine**
Manufacturing Cost	**(USD)**	**(USD)**
Fixed Cost	$1,511,274	$12,715,738
Variable Cost	$19,592,592	$71,739,058
R&D cost (amortisation)	$114,188,790	$45,675,516
Marketing Cost/year	$25,000,000	$25,000,000
Total	$160,292,656	$155,130,312
Cost per dose	$2.20	$2.13

Table 4. Projected production volume for plasmid DNA and inactivated influenza virus vaccine facility

Year	**Projected Production (Plasmid DNA)**	**Projected Production (Inactivated Influenza Virus) Vaccine)**
1	10,000,000	-
2	20,000,000	20,000,000
3	30,000,000	30,000,000
4	40,000,000	40,000,000
5	50,000,000	50,000,000
6	60,000,000	60,000,000
7	72,800,000	72,800,000
8	72,800,000	72,800,000
9	72,800,000	72,800,000
10	72,800,000	72,800,000

The basis calculation indicated that the major difference between the two technologies seemed to be the fermentor size where plasmid DNA vaccine plant had a smaller fermentor at 1,500 L as compared to the required fermentor size of 15,000 L for inactivated virus vaccine plant. The major contributing factor to this significant difference could be the processing time. Due to the short processing time of 3 weeks required for plasmid DNA as compared to nine months for the inactivated virus vaccine plant, the fermentor could be designed in a small size to meet the annual capacity requirement. The selling price per dose was estimated to be $7.77 per dose. This was based on 70% of the current flu vaccine price for FluLaval (a GlaxoSmithKline influenza vaccine for age 18 years or older) as indicated on the CDC website which was US$11.10 per dose (CDC (http://www.cdc.gov)). The 30% reduction was done to allow for distribution cost, which was to provide profit margin to the distributors.

Cost components comparison

Fig. 2 showed the cost component distribution for both plasmid DNA and inactivated virus influenza vaccine facilities. The values indicated that, due to the difference in the fermentor size, the bulk production's cost for plasmid DNA vaccine plant was lower than for inactivated virus vaccine plant. The sterile filling plant for the plasmid DNA technology seemed to require lower cost as well as shorter processing time (i.e. 3 weeks as compared to 9 months for inactivated virus vaccine process). This allowed the sterile filling equipment to be designed at smaller capacity as this plant could manufacture multiple cycles (i.e. 7 per year) to meet the required annual capacity of ca.73 million. Hence, the overall equipment cost for inactivated virus vaccine plant appeared to be higher by a factor of ca. 4 to that of plasmid DNA vaccine plant. This was mainly due to the difference in the fermentor size (i.e. 1,500 L for plasmid DNA versus 15,000 L for inactivated virus vaccine plant) and the large difference in the sterile filling capacity (i.e. ca. 10 million doses for plasmid DNA versus ca. 73 million doses for inactivated virus vaccine).

Economic evaluation

The economic analyses for both vaccine plants were carried out through cash flow diagrams, analysis of payback period, internal rate of return, rate of return and sensitivity analysis between cost per dose and some of the input variables (i.e.Raw material cost, R&D cost, and Marketing Cost).

The projected production volumes in ten years of operation for both facilities were given in Table 4. With the production volume of plasmid DNA vaccine increasing steadily for the first 7 year from ca. 10 million to ca. 73 million doses, the cash flow increased from ca.

$80 million on its 1st year of sales to ca. $600 million on the 7th year of sales onwards. The cumulative cash flow for this facility (Fig. 3) was at ca. negative US$ 1 billion for the first year of production and it was only positive from the 5th year at ca. $100 million. Hence, the payback period suggested for this project was ca. 5 year.

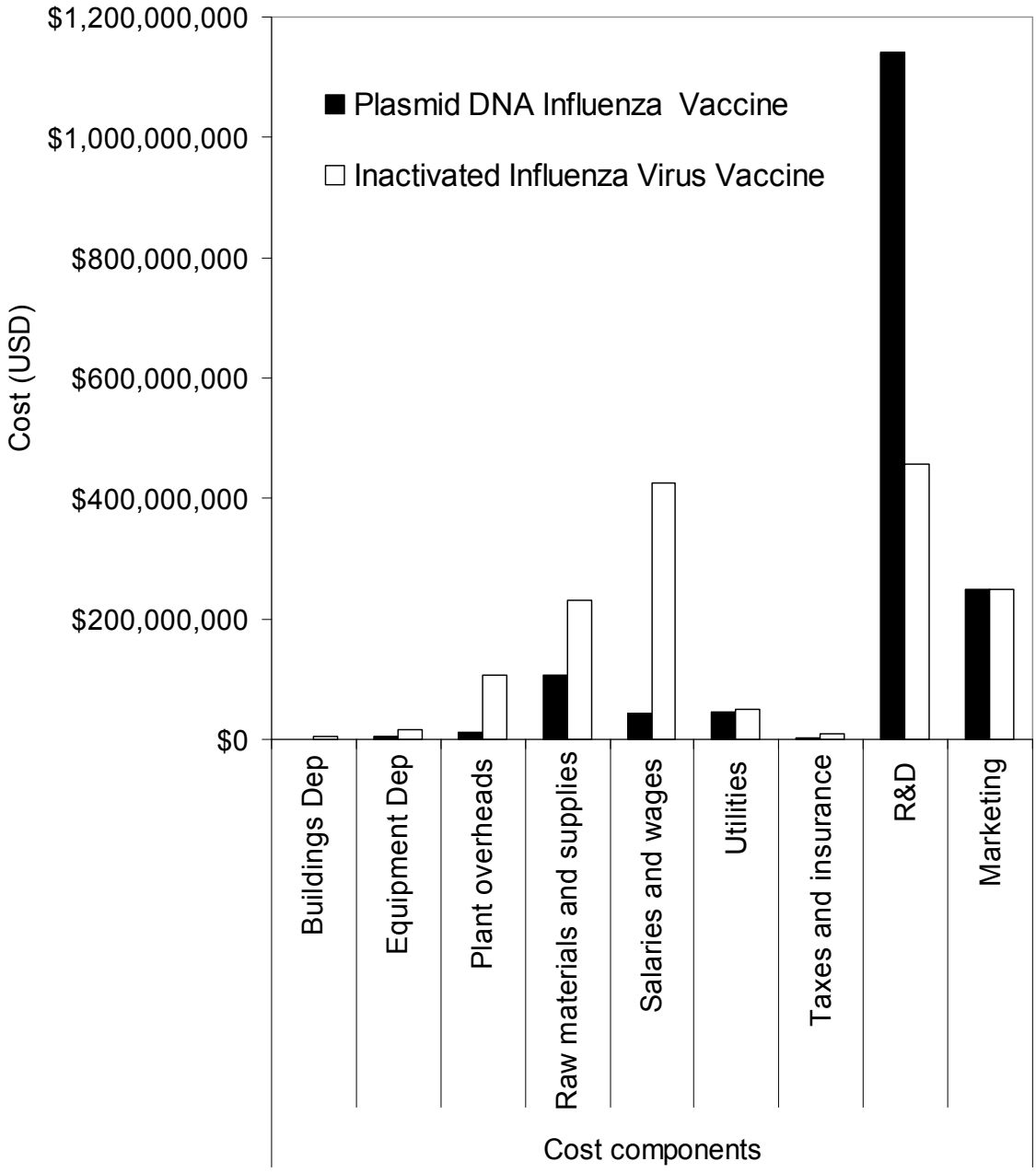

Fig. 2. Cost component distribution of the production of plasmid DNA and inactivated influenza virus vaccine. Costs calculated for 10 years production.

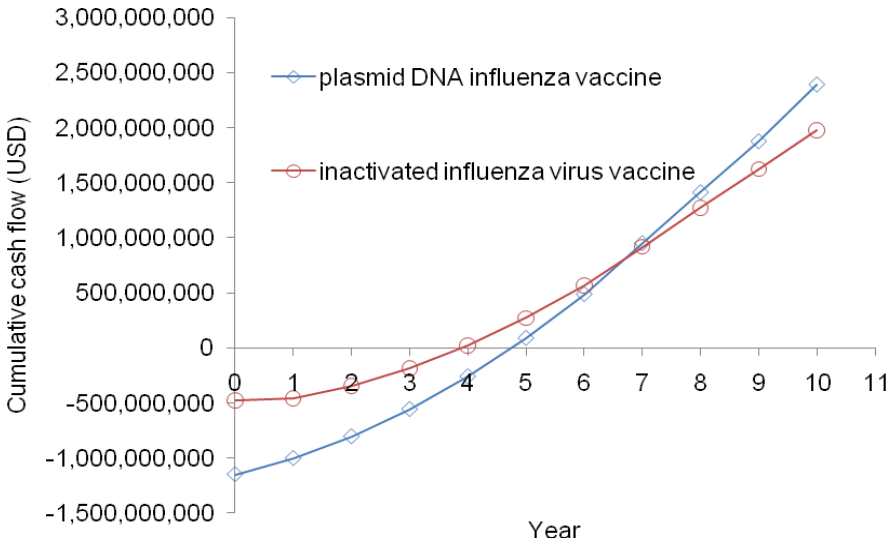

Fig. 3. Cumulative cash flow for plasmid DNA influenza vaccine and inactivated influenza virus vaccine.

For inactivated virus vaccine, the product would only reach the market one year following the completion of the project. This meant that the sales would only start on the second year. However, as this was a conventional technology, the initial production volume would not have to start from ca. 10 million per year and it should be able to produce ca. 20 million per year during its first year of production (i.e. Year 2). With the production volume increasing steadily for the first 7 year from ca. 20 million to ca. 73 million doses, the cash flow increased from ca. $160 million on year 2 of sales to ca. $600 million on the 7th year of sales onwards. This meant that the cumulative cash flow (Fig. 3) was at ca. negative US$ 500 million during its first year of production and it was only positive from the 4th year at ca. $30 million. Hence, the payback period suggested for this project was ca. 4 year. The payback period indicated that plasmid DNA has longer payback period than the inactivated virus vaccine facility.

Rate of return was the ratio of annual profit to investment. This was a simple index of the performance of the money invested. Though basically a simple concept, the calculation of the ROR was complicated by the fact that the annual profit (net cash flow) would not be constant over the life of the project. The simplest method was to base the ROR on the average income over the life of the project and the original investment. The calculated rate of return for both plasmid DNA and inactivated virus influenza vaccine facilities were 20% and 40% respectively. It is in this light that the inactivated virus vaccine was seen as a better investment compared to the pDNA vaccine.

Sensitivity analysis

The sensitivity analysis was carried out by varying the following components (Selling price; Plant and R&D cost; Marketing cost; Raw material and supplies; Cost of capital; Production volume; Cost per dose; and Plasmid DNA dose) with variations of -50%, -25%, 25%, and 50%: These components were selected as these were assessed to be the major contributors to the manufacturing cost and there were uncertainties around these factors due to the assumptions made in this study.

From the sensitivity analysis graph (Fig. 4), it was suggested that Net Present Worth of plasmid DNA influenza vaccine facility was most sensitive to the selling price and production volume of the facility. The selling price to the distributor indicated in this study was $7.77 and this was based on current selling price. As the selling price was reduced by 50%, the NPW of this project was reduced from ca. US$ 1 billion to ca. US$ 200 million. This suggested that this would not be the preferred investment anymore. When the selling price was increased by 50%, the NPW of this project increased by ca. 50%, from ca. US$ 1 to ca. US$ 2 billion.

From the sensitivity analysis graph (Fig. 5), it indicated that Net Present Worth of the inactivated influenza virus vaccine facility was most sensitive to the production volume of the facility. When the production volume was reduced by 50%, the NPW for this project decreased from ca. US$1 billion to ca. US$20 million. This suggested that this would not be the preferred investment anymore. When the production volume was increased by 50%, the NPW of this project increased to ca. US$ 2 billion.

The sensitivity analysis suggested that the success of any project depended largely on the production volume and the selling price of the vaccine. With the potential influenza pandemic, hence, the need for preventive measures, production volume should not become a concern. The facility in this study has been designed for ca. 73 million which was only a fraction of the world population. According to an article in GSK website (http://www.gsk.com), a pandemic can affect up to 25% of the world's population , which translates to around 1.6 billion population calculated based on world's population of 6,535,640,775 (U.S. Census Bureau (http://www.census.gov)). In addition, an article in the Centre for Disease Control and Prevention (CDC) (http://www.cdc.gov) has also highlighted that in 2005-06, 85 million doses of influenza vaccine has been distributed in U.S alone. The selling price for this study was US$ 7.77, which was of the lower range of the influenza vaccine price in the market. Hence, the NPW calculated in this study was conservative.

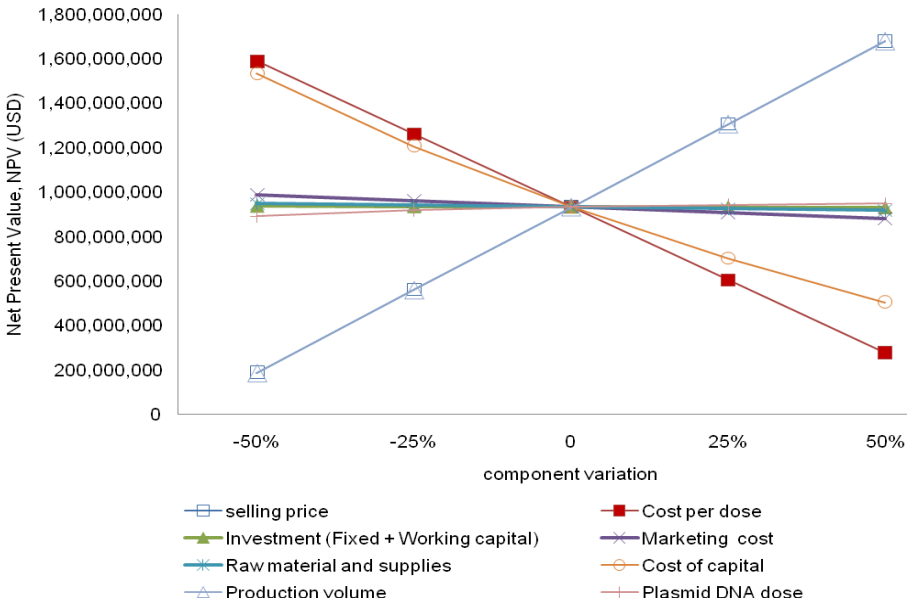

Fig. 4. Sensitivity analysis for plasmid DNA influenza vaccine facility. Net Present Value (NPV) for selling price was the same as the production volume. Base values for selling price ($8), cost per dose ($2), investment ($8,829,279), marketing cost ($25,000,000), raw material and supplies ($10,563,732), cost of capital (9%), production volume (72,800,000) and plasmid DNA dose (10).

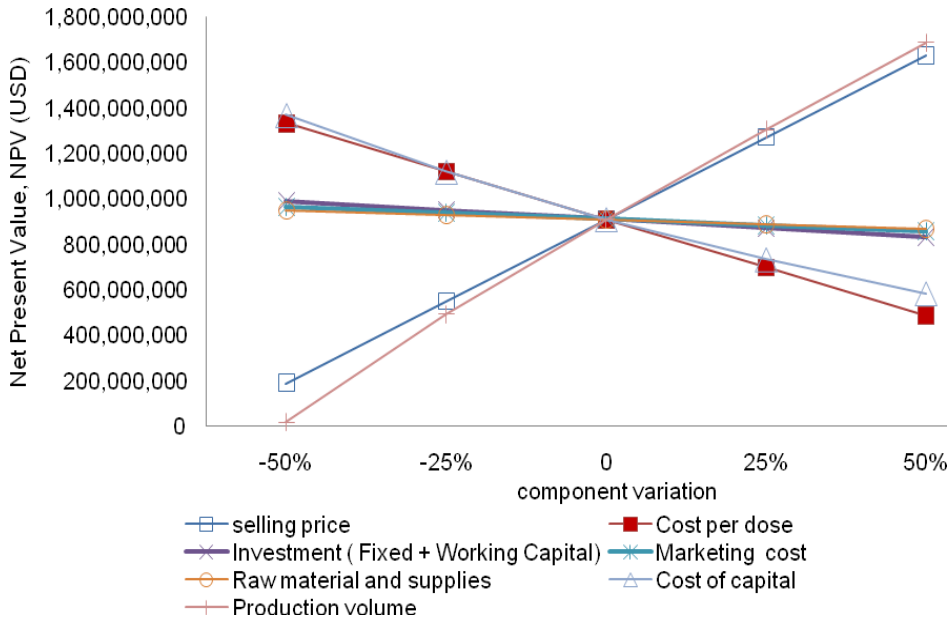

Fig. 5. Sensitivity analysis for inactivated influenza virus vaccine facility. Base values for selling price ($8), cost per dose ($2), investment ($160,450,520), marketing cost ($25,000,000), raw material and supplies ($23,155,087), cost of capital (9%), production volume (72,800,000).

The next influencing factor for any project's success indicated in this analysis was the cost of capital. The 9% rate used in this study was based on the suggested weighted average cost of capital (WACC) by (9). This was derived based on the suggested 12% WACC for the pharmaceutical industry. This 12% consisted of Risk-free rate of return of 6% on a 30-year US Treasury bond, 3% of development risk and 3% of sales (market) risk. The 3% of sales (market) risk was excluded from this study as it was perceived that due to the nature of this product (i.e. Pandemic Preparation); there was no associated risk on this aspect. As stipulated in Fig. 4 and Fig. 5, the increase in cost of capital by 50% suggested a decrease in the NPW for both plasmid DNA and inactivated influenza virus vaccine facility from ca. US$ 1 billion to ca. US$ 500 - 600 million. The cost of capital for the biotechnology industry was highly variable due to the uncertainty and development risk associated to this industry. The derived WACC calculated for this study was 9%. WACC for biotechnology could be higher than this calculated value and this could range from 20% to 50% while the WACC for the big pharma typically ranged 8% to 12% (10).

With an investment of US$1 billion for plasmid DNA vaccine facility, WACC rates of 20% and 50% would provide NPW of ca. US$ 80 million and ca. negative US$ 700 million. Hence, this was certainly one element which needed to be considered and calculated immaculately. However, it was to be noted that these NPW values were calculated assuming that the production volume and selling price was constant (note: Production Volume and Selling Price seemed to be the most influencing factor, followed by Cost of Capital). For the inactivated influenza virus vaccine facility, the increase of WACC rate to 20% and 50% had a similar effect where the NPW decreased to ca. US$ 300 million and ca. negative US$ 300 million respectively.

CONCLUSIONS

This report detailed the economic analysis to determine the cost per dose for two different types of influenza vaccine: an inactivated influenza virus vaccine derived from chicken eggs and a plasmid DNA influenza vaccine. Sensitivity analysis for both facilities indicated that the two most important determining factors for the project's success were selling price and production volume followed by cost of capital and cost per dose. A comparison of the manufacturing cost for both facilities seemed to suggest that both manufacturing methods provided a similar cost per dose at approximately $2 per dose. However, when the manufacturing components were examined in detail, the data indicated that many of the manufacturing factors for a plasmid DNA facility had a lower cost than the inactivated virus vaccine facility. R&D costs were the only components which were higher for plasmid DNA

facility compared to the inactivated virus vaccine facility. When the economic analysis was carried out for both facilities, however, the plasmid DNA vaccine facility did not seem to emerge as a better investment as compared to the inactivated influenza virus vaccine facility. The payback periods for the DNA and inactivated vaccine facilities were 5 and 4 years respectively, despite the advantage that the plasmid DNA facility had in producing the vaccine 1 year ahead of the inactivated influenza virus vaccine facility. However, it was worth noting that the cash inflow for the plasmid DNA vaccine facility was higher at negative US$1 billion compared to the negative US$500 million cash inflow required for the inactivated influenza virus vaccine facility.

REFERENCES

1. Robertson, J. S., Cook, P., Attwell, A. M. and Williams, S. P. (1995) Replicative Advantage in Tissue-Culture of Egg Adapted Influenza-Virus over Tissue-Culture Derived Virus - Implications for Vaccine Manufacture. Vaccine, **13,** 1583-1588.
2. Bouchie, A. (2003) In Brief. Nat. Biotechnol., **21,** 9-11.
3. Durland, R. H. and Eastman, E. M. (1998) Manufacturing and quality control of plasmid-based gene expression systems. Adv Drug Delivery Rev, **30,** 33-48.
4. Prather, K. J., Sagar, S., Murphy, J. and Chartrain, M. (2003) Industrial scale production of plasmid DNA for vaccine and gene therapy: plasmid design, production, and purification. Enzyme Microb Technol, **33,** 865-883.
5. Kalk, J. P. and Langlykke, A. E. (1986), in Manual of Industrial Microbiology and Biotechnology, (Demain, A. L. and Solomon, N. A., eds.), American Society of Microbiology, Washington, pp. 363-385.
6. Mahoney, R. T. (1990) Cost of Plasma-Derived Hepatitis-B Vaccine Production. Vaccine, **8,** 397-401.
7. Atkinson, B. and Mavituna, E. (1991) Biochemical Engineering and Biotechnology Handbook. 2nd ed. Stockton Press, New York.
8. Coulson, J. M., Richardson, J. F. and Sinnott, R. K. (1999) Chemical Engineering -Volume 6: An Introduction to Chemical Engineering Design. 3rd ed. Butterworth- Heinemann.
9. Moscho, A., Hodits, R. A., Janus, F. and Leiter, J. M. E. (2000) Deals that make sense. Nat Biotechnol, **18,** 719-722.
10. Villiger, R. and Bogdan, B. (2005) Getting real about valuations in biotech. Nat Biotechnol, **23,** 423-428.

CHAPTER SEVEN

CONCLUSION

Plasmid DNA (pDNA) vaccines have the potential to prevent future pandemics primarily due to their ease of manufacturing and high safety profile. To date, limitations in the ability to produce large quantities of pDNA vaccines cost-effectively, amongst other major reasons, have impinged on rigorous pre-clinical and clinical research and have ultimately restricted the full-scale implementation of pDNA vaccines in the main stream drug market. One of the major factors preventing the production of clinical-grade plasmid has been the inability to effectively remove endotoxins. Improved chromatographic purification including the use of uniquely designed conical-shaped monolithic adsorbents and efficient endotoxin removal through selective lipopolysaccharide precipitation has been very promising towards rapid production of high plasmid volumetric titres. An integrated process for the production of clinical-grade pDNA molecules, as shown in Figure 1, has been developed in this research.

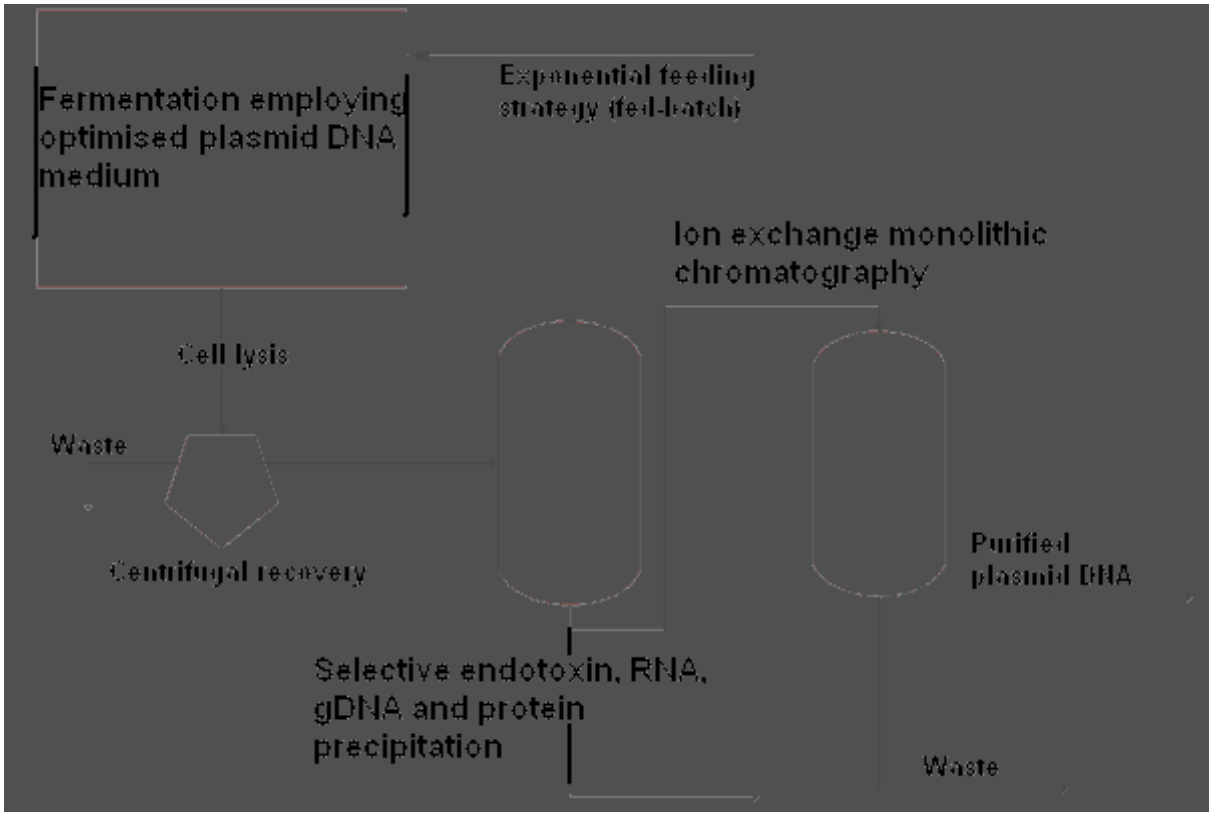

Figure 1. Bioprocess development for clinical-grade pDNA production.

In the upstream section, the most commonly used fermentation method is batch fermentation. A more preferred type of batch fermentation is fed-batch which elongates the batch exponential phase. The elongated exponential phase could lead to an increased nucleotide replication through the optimisation of substrate levels such as glucose and phosphate concentrations to ensure that bacteria have a continuous extra-chromosomal replication. Glycerol can be used as an alternative carbon source to the commonly used glucose substrate to increase plasmid production. Glycerol supports slower cell growth than glucose which creates an opportunity to direct cellular metabolism towards optimum plasmid replication. This is so as glycerol has slower uptake kinetics and molecular transporting mechanism than glycolysis and this leads to higher levels of plasmid replication and pDNA yields. A low-cost semi-defined medium for optimal plasmid replication was developed through experimental design and optimisation. The medium allows for increased plasmid replication rate at the expense of cell wall synthesis thus resulting in high plasmid specific and volumetric yields.

Clarified bacteria lysate typically contains fragmented gDNA, endotoxins, proteins, RNA, nicked and supercoiled DNA therefore rigorous purification protocols to obtain pure and homogenous supercoiled pDNA are required. Careful design of purification steps in the downstream process is essential to ensure maximum attainment of intact supercoiled pDNA in the final product fraction. Plasmid purification from clarified bacteria lysate requires a series of stages to ensure that all contaminants are removed or reduced to below the threshold limits for *in vivo* administration. This is usually achieved in successive chromatography steps. Some major limitations in current plasmid purification techniques include high operating costs, difficulty in scaling up, use of hazardous materials and low plasmid recoveries, being the result of multiple chromatographic steps. One of the main impediments to current pDNA purification system is poor selectivity since pDNA molecules share common physicochemical features with the contaminating biomolecules. A novel technique based on anion-exchange monolithic chromatography has been developed in this project. By using monoliths as adsorbent, a major issue that occurs with conventional chromatography that is the obstruction of large biomolecules due to small particle pore diameter, is resolved leading to higher binding capacity and reduced diffusion time. However, a drawback of monolithic technology, being the introduction of air pockets between the monolith surface and column wall due to monolith shrinkage is addressed in this project by applying conical monoliths. It has been established that conical monolithic formats can be used to seal out these gaps whilst maintaining column efficiency and allowing better process hydrodynamics.

A challenging and critical stage in pDNA purification is the removal of endotoxins. As *E. coli* is still the production host of choice, finding efficient ways to remove endotoxins is of great interest. The difficulty when employing anion-exchange columns for endotoxin removal in pDNA purification is the likely presence of competitive ionic interactions of pDNA and endotoxins with the resin, thus resulting in co-elution of endotoxins. The unique aggregation characteristics of endotoxins were exploited in this research to improve endotoxin removal. Endotoxins demonstrated better interaction with free metal ions than nucleic acids suggesting a huge potential for selective removal of endotoxins relative to nucleic acids. Free metal ions (Cu^{2+}, Ni^{2+}, Ca^{2+}, Mg^{2+} and Zn^{2+}) exhibited varying extents of interactions with plasmid DNA and endotoxins. The study further analysed optimal process conditions (pH, ion concentration, temperature and incubation time) using central composite design experiments. It was found that maximum selective endotoxin removal can be achieved using $ZnSO_4$ as a precipitant. This method provides ease of pDNA purification due to reduced bulk impurities, with high endotoxin removal (>80%) and plasmid recovery (>90%).

The objectives of this PhD research as outlined in Chapter 1 have been realised and the core findings/achievements are reiterated below.

- A simple bioprocess framework has been developed and employed to improve the production of plasmid molecules by utilising controlled fed-batch fermentation, employing strategic glycerol feeding, growth pH modification and temperature fluctuation. This resulted in a significant plasmid volumetric yield of 110 mg/L and a specific yield of 14 mg/g using off-the-shelf pDNA purification kit.
- An optimised cultivation medium for plasmid-bearing *E. coli* cells containing 10.6 g/L tryptone, 6.5 g/L glucose and 15.7 g/L disodium hydrogen orthophosphate has been developed through statistical design experiments and response surface methodology.
- Improved chromatographic purification of plasmid DNA has been realised through optimisation of adsorbent ligand density, mobile phase flow rate, monolith pore size, buffer pH, ionic strength of binding buffer and buffer elution gradient. Optimum resolution was achieved by loading the clarified plasmid-containing lysate into 400 nm pore size monolithic adsorbent in 0.7 M NaCl (pH 7) of binding buffer followed by increasing NaCl concentration to 1.0 M at 3 %B/min.

- At fixed flow rate, column size, sample viscosity, porosity and negligible side flow effect, the column back pressure has a maximum value which is attributed to the flow resistance exerted by the interconnected pores of the monolithic adsorbent.
- A uniquely designed conical column capable of producing a chromatographic stationary system with no wall-channel effect has been developed. Briefly, the monolith is prepared by *in situ* polymerisation followed by gradual reduction of the size of the wall channel.
- Triethylamine activated polymethacrylate conical monolith when integrated with optimal process conditions can produce high plasmid yield (up to 3003 mg/L), plasmid recovery (90%), protein (0.01 mg/L), LPS (0.1 EU/mg) with no detectable gDNA and RNA molecules. The final eluate contains less than 0.3 M NaCl.
- The use of an improved LAL assay developed in this research work has enabled screening of potential divalent cations for selective endotoxin precipitation.
- Selective endotoxin precipitation can effectively be performed as an integral part of the cell lysis procedure at a pH condition similar to that of the clarified alkaline-lysed cell lysate using 0.5 M $ZnSO_4$.
- The use of $ZnSO_4$ as a selective endotoxin precipitant in pDNA purification has been validated using Zeta potential analysis, dynamic light scattering, electron microscopy, Scatchard plot analysis and UV spectroscopy. Results from these analyses indicate high affinity interaction between endotoxins and Zn^{2+}.

It is suggested that future work resulting from this thesis focus on the development of an integrated process for pDNA purification based on the findings from this thesis. This proposed work would definitely expand the perspective of the potential application of the developed technology, identify further improvements relating to large-scale production and consequently give a more reliable indication of the process economics.

References

Carnes, A. E., Hodgson, C. P., and Williams, J. A. 2006. Inducible *Escherichia coli* fermentation for increased plasmid DNA production. *Biotechnol. Appl. Biochem.* 45: 155-166.

Carnes, A. E. 2007. *Process for Plasmid Dna Fermentation*. U.S. patent 20070254342.

Danquah, M. K., and Forde, G. M. 2008c. Development of a pilot-scale bacterial fermentation for plasmid-based biopharmaceutical production using a stoichiometric medium. *Biotechnol. Bioprocess Eng.* 13: 1-10.

Diogo, M. M., Queiroz, J. A., and Prazeres, D. M. F. 2005. Chromatography of plasmid DNA. *J. Chromatogr. A*. 1069: 3-22.

Filomena, S., Passarinha, L., Sousa, F., Queiroz, J. A., and Domingues, F. C. 2009. Influence of growth conditions on plasmid DNA production. *J. Microbiol. Biotechnol.* 19: 51-54.

Han, Y., and Forde, G. M. 2008. Single step purification of plasmid DNA using peptide ligand affinity chromatography. *J. Chromatogr. B*. 874: 21-26.

Nan, X. Z., He, S. W., Hao, C., and Lin, C. P. 2005. Effects of medium composition on the production of plasmid DNA vector potentially for human gene therapy. *J. Zhejiang Univ. SCI.* 6B: 396-400.

Prather, K. J., Sagar, S., Murphy, J., and Chartrain, M. 2003. Industrial scale production of plasmid DNA for vaccine and gene therapy: plasmid design, production, and purification. *Enzyme Microb. Technol.* 33: 865-883.

Prazeres, D. M. F., Ferreira, G. N. M., Monteiro, G. A., Cooney, C. L., and Cabral, J. M. S. 1999. Large-scale production of pharmaceutical-grade plasmid DNA for gene therapy: problems and bottlenecks. *Trends Biotechnol.* 17: 168-174.

Sousa, F., Prazeres, D. M. F., and Queiroz, J. A. 2008. Affinity chromatography approaches to overcome the challenges of purifying plasmid DNA. *Trends Biotechnol.* 26: 518-525.

APPENDICES

Appendix A1

AUSTRALIA

Patents Act 1990

Monash University

PROVISIONAL SPECIFICATION 2011900918

Invention Title:

A liquid chromatography column

Name of Inventors:

1) CLARENCE M. ONGKDUDON

2) MICHAEL K. DANQUAH

The invention is described in the following statement:

A liquid chromatography column

Field of the Invention

The present invention relates to chromatographic columns, and to methods of their use.

Background to the Invention

High performance liquid chromatography (HPLC) is a widely-used laboratory technique in which a liquid sample (the 'mobile phase') is passed through a solid material (the 'stationary phase') in a column under greater than atmospheric pressure. Different components of the sample interact to different degrees with the material of the stationary phase, and thus will travel at different rates through the stationary phase, allowing the components to be separated.

In one form of HPLC, the stationary phase is formed by packing the column with particles such as silica. In order to decrease run times and increase selectivity in particulate columns, the particle size can be decreased to enhance interactions. However, this increases the backpressure in the column in inverse proportion to the square of the particle size. Furthermore, pores in a packed particle column are susceptible to drying, and hence reduced reaction surface area, unless the column is maintained in a wet environment.

An alternative form of HPLC employs monolithic structures within the column. These are porous rod structures having high permeability, large reaction surface area, and a high degree of connectivity between pores. This allows high flow rates, and thus decreased run times, to be achieved without excessive backpressure.

Traditionally, monolithic HPLC columns have included a cylindrical solid structure within a cylindrical column, although more recently conical columns have been found to provide lower retention times, higher linear velocity, reduced mobile phase consumption and effective converging flow (W. Pfeiffer, 'Converging flow chromatography in constant-pressure mode', J. Chromatogr. A, 1006 (2003) 149-170; A. Pecavar, A. Smidovnik, M. Prosek, 'Determination of conical column performances using acyclovir in human plasma sample', Anal. Sci., 13 (1997) 229-234). In addition to the dynamic efficiencies, conical columns are thought to provide greater loadability compared to conventional analytical

columns (A. Pecavar, A. Smidovnik, M. Prosek, Conically shaped chromatographic column Anal. Sci., 15 (1999) 233-240).

For both cylindrical and conical columns, the monolith is generally made of silica or a polymeric material. These monolithic materials are susceptible to shrinkage, leading to the development of a gap or 'wall channel' between the monolithic resin and the column wall. This in turn results in a portion of the mobile phase containing sample molecules effectively bypassing the stationary phase and remaining unseparated, thereby reducing the resolution of chromatographic peaks and/or contaminating the product fraction.

Attempts have been made to address the above described 'wall channelling problem' by providing covalent bonds between the column wall and the monolith by introducing a coupling agent, for example a silane-based methacrylate (F. Svec, A.A. Kurganov, 'Less common applications of monoliths. III. Gas chromatography, J. Chromatogr. A, 1184 (2008) 281-295'; J. Vidic, A. Podgornik, A. Strancar, 'Effect of the glass surface modification on the strength of methacrylate monolith attachment', J. Chromatogr. A, 1065 (2005) 51-58). However, these methods are rather tedious to implement and may not provide a long-term solution to wall channelling. There is also a risk of leaching out the coupling agent during a column run and this can interfere with the product fraction. The interference may be toxic, and even if biocompatible, would necessitate further downstream purification, especially if the product fraction is to be used in biopharmaceutical applications.

There is therefore a need for a method and a monolithic column which addresses the wall channelling problem.

Summary of the invention

Accordingly, the present invention provides, in a first aspect, a monolithic column for liquid chromatography, including:

a conical column having a column wall and an outlet end;

a conical monolith disposed within the conical column; and

height adjustment means for the conical monolith;

wherein the height adjustment means is operable to move the conical monolith within the column such that a wall channel between the conical monolith and the column wall is reduced in size.

The height adjustment means allows the relative position of the monolith and column wall to be adjusted and, due to the inclined surfaces of the monolith and the column wall, any gap between the monolith and the column wall can be reduced or even eliminated.

Preferably, the height adjustment means comprises a plurality of displacer elements disposed between the outlet end and a lower end of the conical monolith. The displacer elements may be individually removable to incrementally reduce the size of the wall channel.

Preferably, the height adjustment means is effective to set a predetermined backpressure in the conical column. The predetermined backpressure may be an equilibrium pressure, which can be determined, for example, for a monolith of a particular porosity by generating at least one standard curve for the dependence of backpressure on wall channel size. If the backpressure is lower than expected for a wall channel size of zero, the height adjustment means can be used to progressively adjust the monolith position until the desired backpressure is reached.

In a further aspect, the invention provides a method of reducing wall channelling in a monolithic liquid chromatography column, including:

providing a conical column having a column wall and an outlet end;

disposing a conical monolith within the conical column; and

moving the conical monolith within the column such that a wall channel between the conical monolith and the column wall is reduced in size.

The conical monolith is preferably moved by a height adjustment means which may be located adjacent to the outlet end. The height adjustment means may comprise a plurality of displacer elements disposed between the outlet end and a lower end of the conical monolith.

In one embodiment, the displacer elements are individually removed to incrementally reduce the size of the wall channel.

In preferred embodiments of the monolithic column and method, the displacer elements are non-porous frits having holes at or near their centres. These may be of substantially equal thickness. The frits may also vary in cross-sectional shape and in one embodiment, take the form of truncated cones.

In particularly preferred embodiments, the column wall has an opening angle of at least 10 degrees. It has been found that increasing the opening angle beyond 10 degrees further reduces wall channelling.

In one embodiment of the method, the size of the wall channel is adjusted until a predetermined backpressure, for example an equilibrium backpressure, within the column is reached.

The method may further include generating at least one standard curve for the dependence of backpressure on the size of the wall channel. The standard curve or curves may be generated by:

(i) setting the size of the wall channel by adjusting the position of the conical monolith;

(ii) running a test buffer through the column;

(iii) measuring the backpressure in the column; and

(iv) repeating steps (i) to (iii).

In one embodiment, the method further includes a step of preparing the monolith *in situ* in the absence of the displacer element.

Brief description of the drawings

Preferred embodiments of the invention will now be described, by way of non-limiting example only, by reference to the accompanying drawings in which:

Figure 1 shows one embodiment of a monolithic column;

Figure 2 shows an alternative monolithic column;

Figure 3 shows a series of standard curves for estimating wall channelling in a monolithic column;

Figure 4 depicts the dependence of column backpressure on opening angle; and

Figure 5 shows the reaction schemes for synthesising and functionalising an exemplary monolith for use with embodiments of the invention.

Description of preferred embodiment

Referring to Figure 1, there is shown a monolithic column 10 including a conical column 11 having a column wall 12 and an outlet end 14. Disposed within the conical column 11 is a conical monolith 20. The monolith 20 may include a porous frit at its lower end (not shown).

As seen in the magnified view at the right of Figure 1, the wall 12 of the conical column 11 makes an angle θ with the vertical, usually referred to as the 'opening angle' of the column.

In Figure 1, the monolith 20 has experienced shrinkage and therefore has a smaller cross-section than the internal cross-section of the conical column 11. Accordingly, a wall channel 25 exists between the monolith 20 and the column wall 12. The wall channel 25 has a width r, this being the horizontal distance from the surface of the monolith 20 to the column wall 12.

Disposed between the monolith 20 and the outlet end 14 of the column 11 is a plurality 30 of displacer elements 32. The displacer elements are preferably identically constructed non-porous frits each having thickness *t.* The width *r* of the wall channel is thus given by:

$$r = nt(\tan\theta) \ , \qquad (1)$$

where r is size of wall channel (mm), n is the number of frits, t is frit thickness (mm) and θ is column opening angle (^{o}).

If the frits 32 are of differing thicknesses t_i, $i = 1, \ldots, n$, then it will be appreciated that Equation (1) can be generalised by replacing the product nt by the sum over i of the n frit thicknesses t_i.

The displacer elements 32 can be individually added or removed as desired, and thus serve as height adjustment means 30 for the monolith 20. By removing frits 32, the monolith 20 is lowered relative to the column 11 and the width *r* of the wall channel 25 thereby reduced.

It will of course be appreciated that Equation (1) is applicable for any conical column with a fixed opening angle θ.

Figure 2 shows an alternative monolithic column 110 including a conical column 111 having a column wall 112 and an outlet end 114. A conical monolith 120 having a porous frit 122 at its lower end is disposed within the conical column 111.

As shown in Figure 2(a), the monolithic column 110 also includes height adjustment means 130 comprising non-porous frits 132(a), 132(b), 132(c), and 132(d), each of which has a hole 133 at its centre. In order to reduce or eliminate the wall channel 125 between the monolith 120 and the column wall 112, frits 132(a) and 132(b) can be removed so that the monolith 120 is lowered relative to the column 111 (Figure 2(b)).

There will now be described a method of generating a standard curve for estimating the degree of wall channelling in a conical column.

The inventors of the present invention have realised that the dependence of column backpressure on monolith porosity and wall channel size can be exploited in order to predict the degree of wall channelling. That is, if the porosity and backpressure are known, the wall channel size can be predicted.

After being prepared *in situ* in the column 11, the surface of the monolith 20 will be in contact with the column wall 12, so that no wall channel exists. The monolith 20 has a porosity which depends on synthesis conditions and materials used. For example, in polymer

monoliths suitable for use with embodiments of the present invention, such as poly (GMA-EDMA) (see Figure 4), increasing the synthesis temperature decreases the porosity of the monolith matrix.

To adjust the height of the monolith 20 above the outlet end 14, the monolith 20 is gently removed from the column 11 by pushing a frit at the outlet end 14. One or more frits 32 of known thickness *t* can then be inserted into the empty column 11 to produce a wall channel 25 of known size *r* as set out in Equation (1).

The monolith 20 can then be inserted back into the column 11 and configured for operation with an HPLC system, for example a BIORAD (trade mark) HPLC system. A buffer solution is pumped through the column 11 at a predetermined flow rate, and the resulting backpressure in the column 11 is recorded.

The size of the wall channel 25 is adjusted by adding or removing the frits 32 from the column 11, and the backpressure as a function of wall channel size *r* is measured.

The above procedure is then repeated with monoliths having different porosity. The result is a series of standard curves as shown in Figure 3, in which column backpressure in kPa is shown plotted against monolith porosity, as measured by % porogen. These curves can be used to predict the degree of side flow (wall channelling). For example, under the same flow and synthesis conditions as in Figure 2, for a monolith with 70% porogen content, the column backpressure should be about 25 psi (170 kPa) for zero side flow as can be seen from the upper curve 210.

A small increase in the degree of wall channelling results in a dramatic drop in the column backpressure, as can be seen from curve 220 which corresponds to a wall channel of width 1.2 mm. A monolith with 70% porogen would produce a backpressure of about 20 kPa with a wall channel of this size.

Advantageously, the wall channelling problem can be further addressed by increasing the opening angle of the conical column. In Figure 4, the curve 310 depicts the dependence of column backpressure on opening angle for a mobile phase flow rate of 10 mL/min, a porosity at 70% porogen, no wall channel, and the same buffer as was used to generate the standard curves of Figure 3. In Figure 3, it can be seen that for opening angles of around 10^{o} or more, the geometry of the conical column further compensates for monolith shrinkage, thus resulting in a steady column backpressure.

Modifications and variations as could be deemed obvious to the person skilled in the art are included within the ambit of the present invention as claimed in the appended claims.

CLAIMS:

1. A monolithic column for liquid chromatography, including:
a conical column having a column wall and an outlet end;
a conical monolith disposed within the conical column; and
height adjustment means for the conical monolith;
wherein the height adjustment means is operable to move the conical monolith within the column such that a wall channel between the conical monolith and the column wall is reduced in size.

2. A monolithic column according to claim 1, wherein the height adjustment means comprises a plurality of displacer elements disposed between the outlet end and a lower end of the conical monolith.

3. A monolithic column according to claim 2, wherein the displacer elements are individually removable to incrementally reduce the size of the wall channel.

4. A monolithic column according to any one of claims 1 to 3, wherein the height adjustment means is effective to set a predetermined backpressure in the conical column.

5. A monolithic column according to any one of claims 2 to 4, wherein the displacer elements are non-porous frits having holes at or near their centres.

6. A monolithic column according to claim 5, wherein the frits take the form of truncated cones.

7. A monolithic column according to claim 5 or claim 6, wherein the frits are of substantially equal thickness.

8. A monolithic column according to claim 5 or claim 6, wherein the frits vary in thickness.

9. A monolithic column according to any one of claims 1 to 8, wherein the column wall has an opening angle of at least 10 degrees.

10. A method of reducing wall channelling in a monolithic liquid chromatography column, including:

providing a conical column having a column wall and an outlet end;

disposing a conical monolith within the conical column; and

moving the conical monolith within the column such that a wall channel between the conical monolith and the column wall is reduced in size.

11. A method according to claim 10, wherein the conical monolith is moved by height adjustment means.

12. A method according to claim 11, wherein the height adjustment means is located adjacent to the outlet end.

13. A method according to claim 11 or claim 12, wherein the height adjustment means comprises a plurality of displacer elements disposed between the outlet end and a lower end of the conical monolith.

14. A method according to claim 13, further including the step of producing the conical column with the displacer elements.

15. A method according to claim 13 or claim 14, wherein the displacer elements are individually removed to incrementally reduce the size of the wall channel.

16 A method according to any one of claims 13 to 15, wherein the displacer elements are non-porous frits having holes at or near their centres.

17. A method according to claim 16 wherein the frits take the form of truncated cones.

18. A method according to claim 16 or claim 17, wherein the frits are of substantially equal thickness.

19. A method according to claim 16 or claim 17, wherein the frits vary in thickness.

20. A method according to any one of claims 10 to 19, wherein the column wall has an opening angle of at least 10 degrees.

21. A method according to any one of claims 10 to 20, wherein the size of the wall channel is adjusted until a predetermined backpressure within the column is reached.

22. A method according to claim 21, wherein the predetermined backpressure is an equilibrium backpressure.

23. A method according to claim 21 or claim 22, further including generating at least one standard curve for the dependence of backpressure on the size of the wall channel.

24. A method according to claim 23, wherein the at least one standard curve is generated by:

(i) setting the size of the wall channel by adjusting the position of the conical monolith;

(ii) running a test buffer through the column;

(iii) measuring the backpressure in the column; and

(iv) repeating steps (i) to (iii).

25. A method according to claim 24, further including the step of preparing the monolith *in situ* in the absence of the displacer elements.

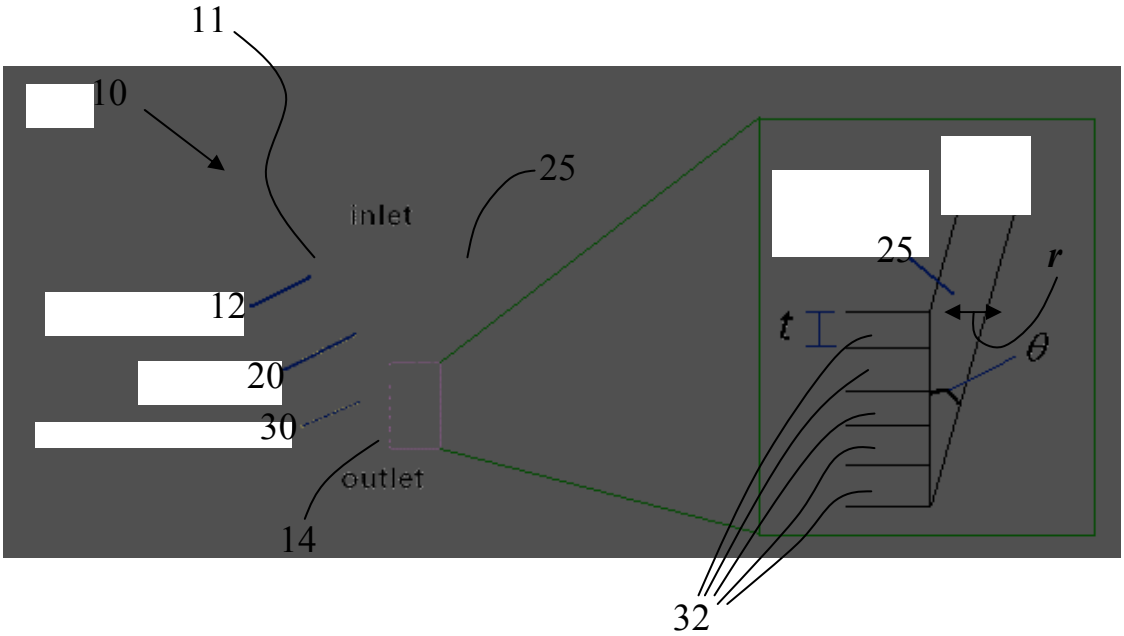

FIG 1

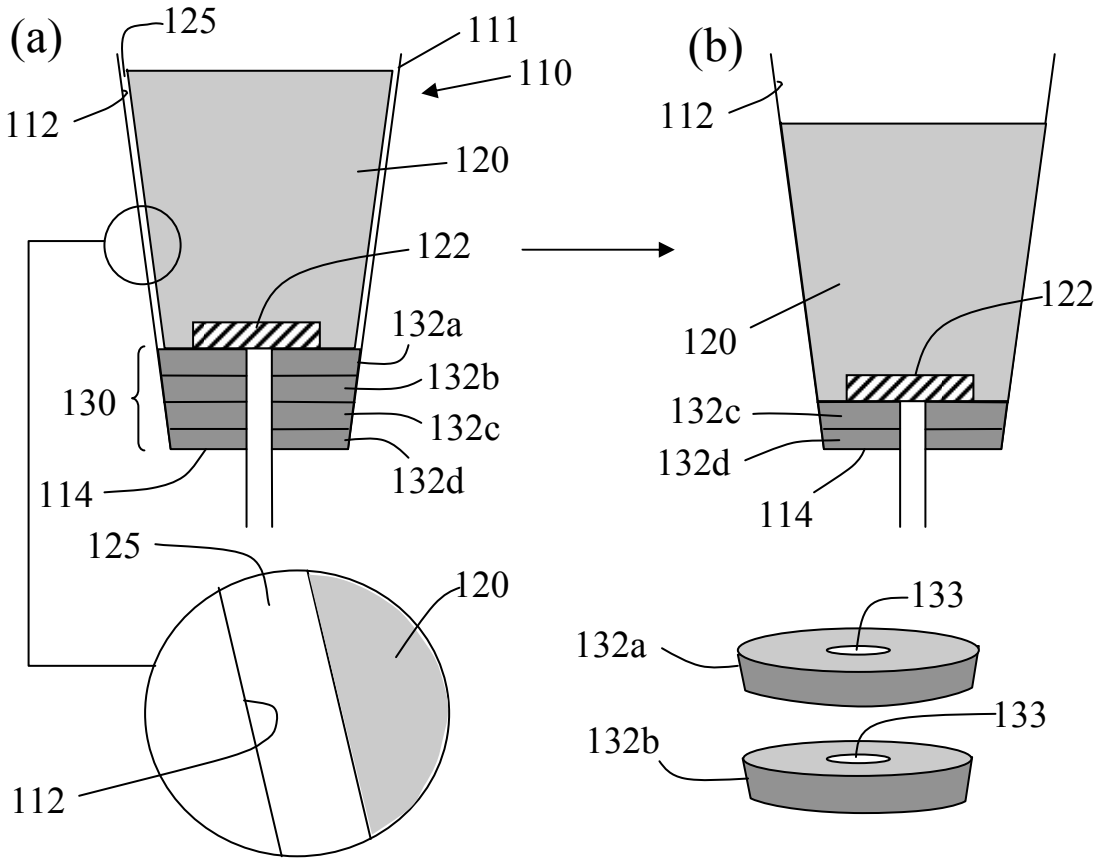
(a)
125
111
110
112
120
122
132a
132b
130
132c
132d
114
125
120
112
(b)
112
122
120
132c
132d
114
133
132a
133
132b

FIG 2

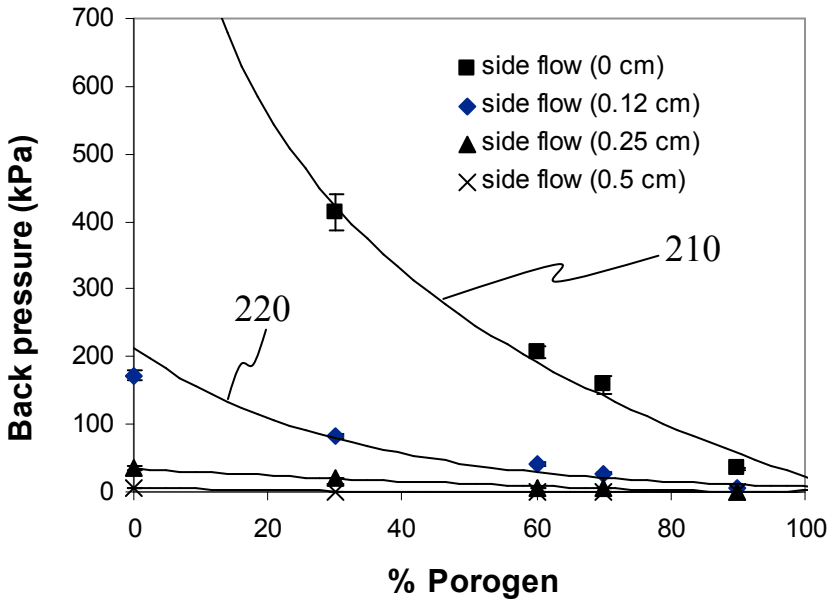
700
600
500
400
300
200
100
0
Back pressure (kPa)
0
20
40
60
80
100
% Porogen
side flow (0 cm)
side flow (0.12 cm)
side flow (0.25 cm)
side flow (0.5 cm)
210
220

FIG 3

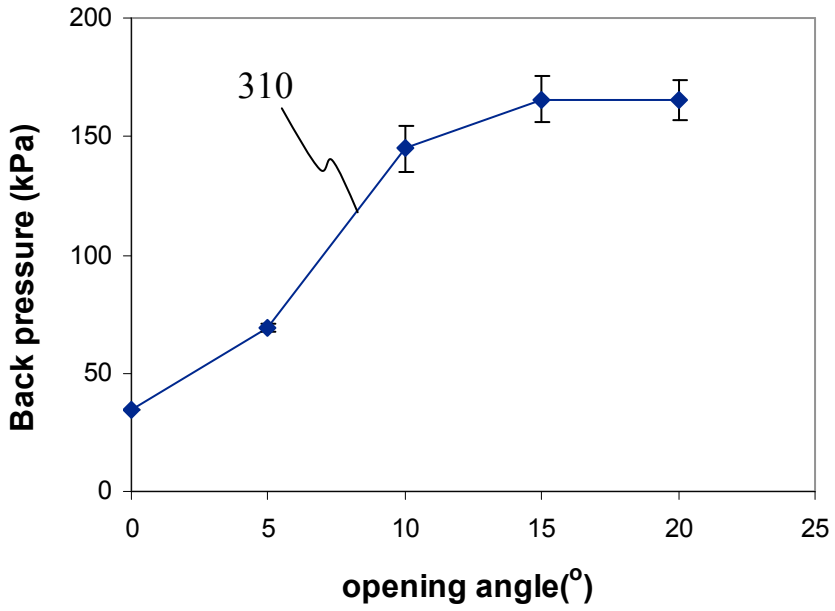
200
150
100
50
0
Back pressure (kPa)
310
0
5
10
15
20
25
opening angle(°)

FIG 4

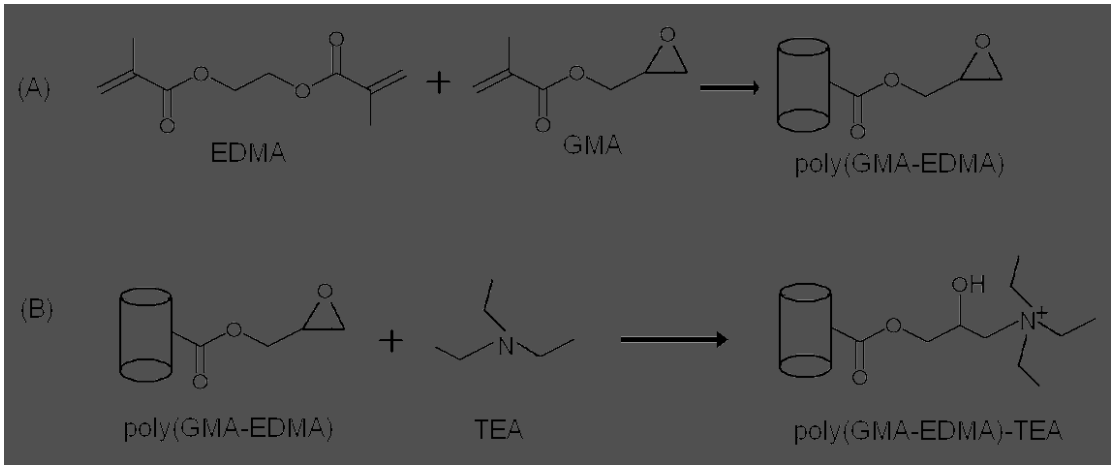
(A)
EDMA
GMA
poly(GMA-EDMA)
(B)
poly(GMA-EDMA)
TEA
poly(GMA-EDMA)-TEA
OH
N
N+

FIG 5

Appendix B1

Clarence M. Ongkudon and Michael K. Danquah. The performance of a triethylamine activated polymethacrylate conical monolith for plasmid vaccine purification. **Victorian Infection and Immunity Network symposium**, Melbourne, Australia, 3rd June 2010.

Abstract: Commercial scale purification of plasmid DNA (pDNA) relies on a conventional particle-based chromatography consisting of many beads with small internal pores (<100 nm). The hydrodynamic size of plasmid molecules is >100 nm hence adsorption occurs only on the outer surfaces of the beads and this leads to low binding capacities. pDNA purification by particle-based chromatography is also hindered by low flow rates and high pressure drops. A recent advancement in plasmid purification has resulted in the development of polymethacrylate monolithic chromatographic support which provides higher capacity and flow rates at lower pressure drops compared to the particulate supports. This study aims at developing a technology to efficiently manufacture a clinical grade, endotoxin free plasmid DNA vaccine via monolithic chromatography. Consequently, this technology will have a great impact on the overall vaccine production and its economic viability.

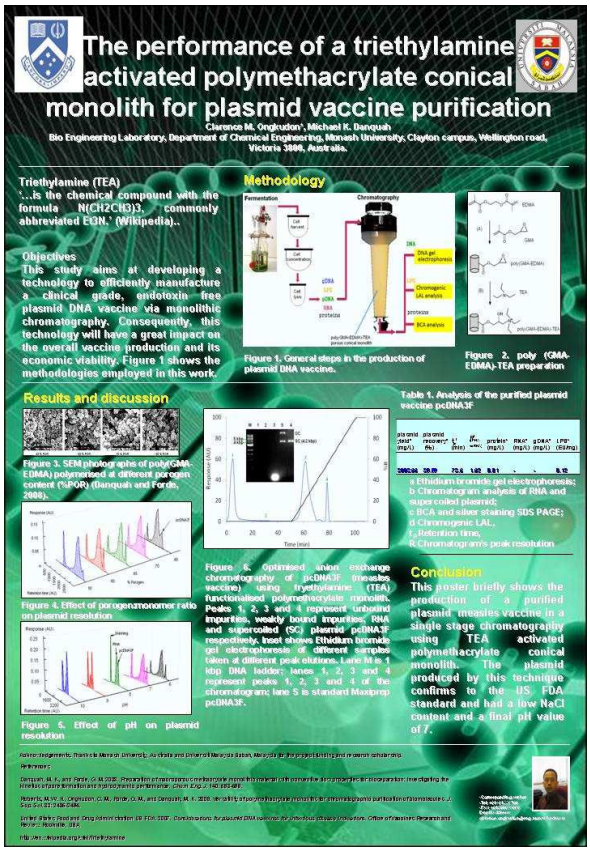

Appendix B2

Clarence M. Ongkudon and Michael K. Danquah. A Novel Technology for Continuous Enzyme Free Isolation of Plasmid DNA. **Bioprocessing Network conference**, Melbourne, Australia, 12th – 14th October 2010.

Abstract: Plasmid DNA purification in ion exchange chromatography (IEC) is generally complicated when the size of the plasmid is similar to the size of endotoxins (LPS). This is due to the ability of endotoxins to form different sizes of aggregates and possibly carry varying charge densities. Therefore, the gradient elution in IEC may not be able to resolve the overall endotoxins as a single peak from plasmid DNA molecules. A strategy based on a high salt precipitation of endotoxins is underway to remove large molecular size endotoxins during the alkaline cell lysis procedure. A subsequent ion exchange chromatography can then conveniently separate large plasmid DNA and small endotoxins by gradient elution. Therefore, the AEC matrix can be fully utilised for plasmid DNA binding.

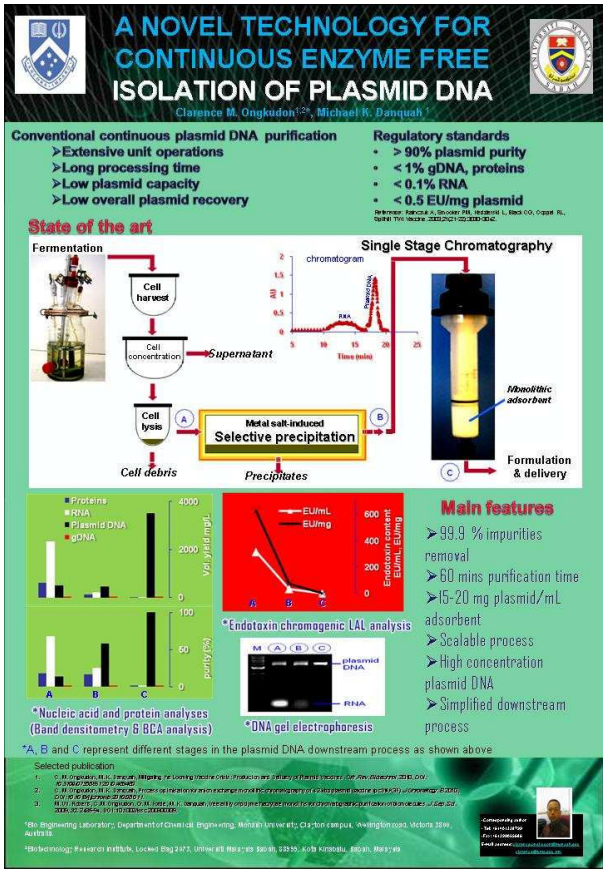

Appendix B3

Clarence M. Ongkudon and Michael K. Danquah. A novel technology for continuous isolation of large biomolecules: A study on plasmid DNA production. **UMS Biotechnology Symposium IV**, Kota Kinabalu, Malaysia, 1st – 3rd December 2010

Abstract: Continuous large scale purification of large biomolecules such as genomic DNA, plasmid DNA or virus is often hampered by the low yield, slow recovery and high cost of conventional techniques such as particle or membrane based chromatography and phase separation techniques. This work describes a novel technology for the production of such molecules particularly plasmid DNA by controlled host cell growth and anion exchange monolithic purification (BEL monolith). Cell growth was optimised for plasmid propagation by controlled glycerol feeding employing optimised medium and pH-temperature induction techniques. The BEL monolithic system was optimised for high yield and high quality plasmid DNA using diethylamine as the anion exchange group. A selective endotoxin precipitation by $ZnSO_4$ was introduced as an integral part of the alkaline lysis procedure and showed nearly 100% preliminary endotoxin removal and plasmid recovery. Problems that were encountered during the process development are also put forward. Consequently, this study indicates that the technology can be performed for routine production of large amount of endotoxin and enzyme free plasmid DNA or any large biomolecules from laboratory to commercial scale thus eliminating the dependency on high cost disposable commercial kits and extensive unit operations.

Appendix C1

Critical Reviews in Biotechnology, 2011; 31(1): 32–52

ISSN 0738-8551 print/ISSN 1549-7801 online
DOI: 10.3109/07388551.2010.483460

informa
healthcare

REVIEW ARTICLE

Mitigating the looming vaccine crisis: production and delivery of plasmid-based vaccines

Clarence M. Ongkudon, Jenny Ho, and Michael K. Danquah

Department of Chemical Engineering, Bio Engineering Laboratory, Monash University, Victoria, Australia

Abstract
The exponentially growing human population and the emergence of new diseases are clear indications that the world can no longer depend solely on conventional vaccine technologies and production schemes. The race to find a new vaccine technology is crucial to help speed up and complement the World Health Organization (WHO) disease elimination program. The ultimate goal is to uncover fast and efficient production schemes in the event of a pandemic, and also to effectively fight deadly diseases such as malaria, bird flu, hepatitis, and human immunodeficiency virus (HIV). Plasmid DNA vaccines, if properly formulated, offer specific priming of the immune system and similar or even better prophylactic effects than conventional vaccines. This article discusses many of the critical issues that need to be considered when developing fast, effective, and reliable plasmid DNA vaccine manufacturing processes. Different modes of plasmid production via bacterial fermentation are compared. Plasmid purification by chromatography is specifically discussed as it is the most commercially viable bioprocess engineering technique for continuous purification of supercoiled plasmid DNA. Current techniques and progress covering the area of plasmid DNA vaccine design, formulation, and delivery are also put forward.

Keywords: Plasmid DNA, DNA vaccine, vaccine production, vaccine delivery, bioprocess

Introduction

Vaccine evolution

The so-called first generation or conventional vaccines involve the introduction of whole-organism vaccines into the immune system to induce immunological responses. These vaccines could be in the form of live, attenuated, or killed pathogens such as smallpox and polio vaccines (WHO, 2007). The efficiency of these vaccines lies in their ability to trigger both B- and T-cell responses. T-cell-mediated response is the generation of cytolytic T-lymphocytes (CTL) against viral infection and tumor while B-cell response is the antibody production against antigens (Shroff *et al.*, 1999). A list of some current vaccines in the market and under evaluation is given in Table 1. Measles vaccine (MV) was first formulated in the 1960s using formalin- or Tween-inactivated virus adjuvanted with alum. This formulation, however, is incapable of inducing relatively sufficient amounts of CTL and was discontinued in 1967. Live-attenuated vaccine (LAV) was introduced later and resulted in a major decline of measles casualties even though it led to rash and fever in almost 50% of the children immunized. The presence of maternally derived MV-specific antibodies and immunological maturity of the recipient has the most profound effect on the success of measles vaccination (Vries *et al.*, 2008). In 2005, after nearly a decade of intensive research, the Food and Drug Administration (FDA) issued a license to a new vaccine combining measles, mumps, rubella, and varicella (MMRV) vaccines. The MMRV that is commercially known as ProQuad® contains LAV and albumin. The level of antibody response reflects in a similar way in patients who are given separate vaccines but contraindicated in patients with known hypersensitivity to any component of the vaccine including neomycin and gelatine (Buck, 2005). The second generation vaccines consist of subcomponent vaccines such as defined protein antigens and recombinant viral proteins. Examples of these vaccines are tetanus, diphtheria toxoid, and hepatitis B surface antigen. Merozoite surface proteins, such as MSP1, MSP2, and MSP3 or the apical membrane antigen (AMA)-1, are among the target

Address for Correspondence: Dr. Michael K. Danquah, Department of Chemical Engineering, Bio Engineering Laboratory, Monash University, Clayton campus, Wellington Road, Victoria 3800, Australia. E-mail: michael.danquah@eng.monash.edu.au

(Received 17 April 2009; revised 28 January 2010; accepted 05 March 2010)

Appendix C2

J. Sep. Sci. 2009, *32*, 2485–2494

Michael W. H. Roberts[1]
Clarence M. Ongkudon[2]
Gareth M. Forde[2]
Michael K. Danquah[2]

[1]Department of Chemical Engineering, Loughborough University, Loughborough, Leicestershire, United Kingdom
[2]Bio Engineering Laboratory (BEL), Department of Chemical Engineering, Monash University, Victoria, Australia

Review

Versatility of polymethacrylate monoliths for chromatographic purification of biomolecules

Polymethacrylate monoliths, specifically poly(glycidyl methacrylate-*co*-ethylene dimethacrylate) or poly(GMA-*co*-EDMA) monoliths, are a new generation of chromatographic supports and are significantly different from conventional particle-based adsorbents, membranes, and other monolithic supports for biomolecule purification. Similar to other monoliths, polymethacrylate monoliths possess large pores which allow convective flow of mobile phase and result in high flow rates at reduced pressure drop, unlike particulate supports. The simplicity of the adsorbent synthesis, pH resistance, and the ease and flexibility of tailoring their pore size to that of the target biomolecule are the key properties which differentiate polymethacrylate monoliths from other monoliths. Polymethacrylate monoliths are endowed with reactive epoxy groups for easy functionalization (with anion-exchange, hydrophobic, and affinity ligands) and high ligand retention. In this review, the structure and performance of polymethacrylate monoliths for chromatographic purification of biomolecules are evaluated and compared to those of other supports. The development and use of polymethacrylate monoliths for research applications have grown rapidly in recent times and have enabled the achievement of high throughput biomolecule purification on semi-preparative and preparative scales.

Keywords: Biomolecules / Chromatography / Polymethacrylate monolith / Purification

Received: May 1, 2009; revised: May 23, 2009; accepted: May 23, 2009

DOI 10.1002/jssc.200900309

1 Introduction

There are many different ways in which biomolecule separation and purification are performed. Of all the techniques available, liquid chromatography is the most versatile technique for the purification of different biomolecules. Stationary phases for chromatographic purification of biomolecules have conventionally been particulate-based supports consisting of many beads with small internal pores. These supports are designed for efficient separation of smaller biomolecules. Issues arise when larger biomolecules are to be separated. These large biomolecules are too large to enter the pores of a bead so interactions occur only on the outer surface, thus leading to poor binding. Poor binding results in under-exploitation of the available capacity of the resin and may also result in high levels of non-specific binding in the intraparticle volume [1].

Monolithic supports are new developing technology and have many benefits over particulate supports. In the past decade there has been increasing research and development in the area of monolithic supports for use as the stationary phase in chromatographic separation. Monolithic supports comprise a single structure with a highly interconnected or honey-combic network of channels, a significant variation from conventional particulate supports. Monolithic supports have many inherent advantages when compared to conventional particulate based supports due to their physical and chemical structure. A major reason for many of the advantages of monolithic supports is the large pores (>200 nm in diameter) found in the matrix [2, 3]. These pores are much larger than those found in particulate supports and allow convective mass transport, far superior to mass transfer by diffusion found in particulate supports. In chromatographic separations, with the exception of affinity purification, mass transfer has been considered the rate-limiting factor [4]. With the convective transport mechanism of monolithic structures, this bottleneck has largely been relieved especially for larger molecules which are too

Correspondence: Dr. Michael K. Danquah, Bio Engineering Laboratory (BEL), Department of Chemical Engineering, Monash University, Victoria 3800, Australia
E-mail: michael.danquah@eng.monash.edu.au
Fax: +61-3-99055686

Abbreviations: **AC**, affinity chromatography; **CIM**, convective interaction media; **DEAE**, diethylaminoethyl; **HIC**, hydrophobic interaction chromatography; **IEC**, ion-exchange chromatography; **poly(GMA-co-EDMA)**, poly(glycidyl methacrylate-*co*-ethylene dimethacrylate)

Appendix C3

Ongkudon *et al. Microbial Cell Factories* 2011, **10**:16
http://www.microbialcellfactories.com/content/10/1/16

MICROBIAL CELL FACTORIES

RESEARCH Open Access

Cultivation of *E. coli* carrying a plasmid-based Measles vaccine construct (4.2 kbp pcDNA3F) employing medium optimisation and pH-temperature induction techniques

Clarence M Ongkudon[1*], Raelene Pickering[2], Diane Webster[2], Michael K Danquah[1]

Abstract

Background: Plasmid-based measles vaccines offer great promises over the conventional fertilised egg method such as ease of manufacture and mimic wild-type intracellular antigen expression. The increasing number of clinical trials on plasmid-based measles vaccines has triggered the need to make more in less time.

Results: In this work, we investigated the process variables necessary to improve the volumetric and specific yields of a model plasmid-based measles vaccine (pcDNA3F) harboured in *E. coli* DH5α. Results from growth medium optimisation in 500 mL shake flasks by response surface methodology (RSM) generated a maximum volumetric yield of 13.65 mg/L which was 1.75 folds higher than that of the base medium. A controlled fed-batch fermentation employing strategic glycerol feeding and optimised growth conditions resulted in a remarkable pcDNA3F volumetric yield of 110 mg/L and a specific yield of 14 mg/g. In addition, growth pH modification and temperature fluctuation between 35 and 45°C were successfully employed to improve plasmid production.

Conclusion: Production of a high copy number plasmid DNA containing a foreign gene of interest is often hampered by the low plasmid volumetric yield which results from the over expression of foreign proteins and metabolic repressors. In this work, a simple bioprocess framework was employed and successfully improved the production of pcDNA3F.

Background

Plasmid DNA (pDNA) vaccine is a third generation of vaccine technology which offers an attractive new alternative to conventional immunisation techniques. In human trials, pDNA has been shown to induce protective immunity similar to that of natural infection for not only measles, but across a broad range of virus families [1]. From a production stand point, the lyophilised form of the current vaccine lacks thermal stability, requiring an uninterrupted cold chain for maximum efficacy [2]. The enhanced thermal stability of plasmid DNA at room temperature and above offers a great promise for the treatment of measles and other diseases in tropical and economically disadvantaged areas [3]. General steps involve in the production of plasmid vaccines are similar to that of protein production that include fermentation, primary isolation and purification [4]. It is presumed that the mechanisms that contribute to yield improvement are reduced metabolic burden during plasmid synthesis; reduced plasmid mediated protein production and altered DNA compaction during plasmid induction [5]. Various bioprocess engineering approaches that can be employed to alter the growth of *E. coli* hence gene expression have extensively been discussed by Razali *et al.* [6] that include temperature shift techniques, feeding strategies, timing of induction and plasmid stabilisation.

It is important to note that like chromosomal DNA, plasmid DNA is made up of sugar-phosphate backbone and nitrogen base nucleotides (ATGC). Carbon, phosphorus and nitrogen are the main ingredients in DNA biopolymers unlike proteins. Also, in the central dogma of molecular biology, only replication is required for

* Correspondence: clarence.ongkudon@monash.edu
[1]Bio Engineering Laboratory, Department of Chemical Engineering, Monash University, Clayton campus, Wellington road, Victoria 3800, Australia
Full list of author information is available at the end of the article

Appendix C4

Journal of Chromatography B, 878 (2010) 2719–2725

Contents lists available at ScienceDirect

Journal of Chromatography B

journal homepage: www.elsevier.com/locate/chromb

Process optimisation for anion exchange monolithic chromatography of 4.2 kbp plasmid vaccine (pcDNA3F)

Clarence M. Ongkudon*, Michael K. Danquah

Bio Engineering Laboratory, Department of Chemical Engineering, Faculty of Engineering, Monash University, Clayton Campus, Wellington Road, Clayton, Victoria 3800, Australia

ARTICLE INFO

Article history:
Received 1 July 2010
Accepted 12 August 2010
Available online 19 August 2010

Keywords:
Process optimisation
Anion exchange
Monolithic chromatography
Plasmid DNA
pcDNA3F

ABSTRACT

Anion exchange monolithic chromatography is increasingly becoming a prominent tool for plasmid DNA purification but no generic protocol is available to purify all types of plasmid DNA. In this work, we established a simple framework and used it to specifically purify a plasmid DNA model from a clarified alkaline-lysed plasmid-containing cell lysate. The framework involved optimising ligand functionalisation temperature (30–80 °C), mobile phase flow rate (0.1–1.8 mL/min), monolith pore size (done by changing the porogen content in the polymerisation reaction by 50–80%), buffer pH (6–10), ionic strength of binding buffer (0.3–0.7 M) and buffer gradient elution slope (1–10% buffer B/min). We concluded that preferential pcDNA3F adsorption and optimum resolution could be achieved within the tested conditions by loading the clarified cell lysate into 400 nm pore size of monolith in 0.7 M NaCl (pH 6) of binding buffer followed by increasing the NaCl concentration to 1.0 M at 3%B/min.

1. Introduction

Anion-exchange chromatography (AEC) remains one of the most prominent methods in plasmid DNA (pDNA) purification due to its rapid separation, easy sanitisation, no organic solvent requirements and wide selection of available stationary phases [1]. In terms of quality and recovery, consistent results have been achieved at different scales [2]. AEC is based on the interaction between negatively charged phosphate groups of plasmid and positively charged stationary matrix [3]. A buffer containing sodium chloride salt can be used as the eluting buffer and a gradient elution can be performed at a specific slope (% eluting buffer/min) for optimum resolution [4]. Molecules with lower charge densities should elute first followed by high negatively charged molecules, a trend, which is attributed to plasmid chain length and conformation [5].

The purification of large biomolecules, such as plasmids is obstructed by the performance of conventional chromatographic supports with a small particle pore diameter. Most of these chromatographic supports are geared towards high adsorption capacities of small molecules such as proteins and peptides. In columns packed with such particles, plasmids greater than 100 nm adsorb predominantly on the outer surface of the particles and this leads to low binding capacities [6]. A monolith is a continuous phase consisting of a piece of highly porous organic or inorganic solid material. The most essential feature of this support is that all the mobile phase is forced to flowthrough its large pores. As a consequence, mass transport is steered by convection; reducing the long diffusion time required by particle-based supports [7]. The pore size of the monolith plays an important role in providing spaces for both ligand attachment and plasmid mobility. Based on a previous study, it is speculated that bimodal pore sizes of 0.008 and 0.5 μm can provide the optimum condition for ligand coupling, plasmid binding and plasmid retention [8]. The pore size of the monolith can be altered by varying the composition of the reactants and porogens. One of the most studied monolithic materials is silica based monolith which has been reported in [9–11]. Silica based monolith has been used in analytical chromatography and resulted in a significantly short processing time compared to conventional packed bed column [12]. Another type of monolithic material is polymethacrylate based monolith which is the type of chromatographic column used in this work. Polymethacrylate monoliths are especially useful for large-scale purification of large biomolecules owing to its enhanced mass transfer properties, pressure and flow, specific permeability, morphological and structural stability [13].

To optimise the ligand coupling on polymethacrylate, crucial parameters such as temperature, reaction time and pH can be optimised. Generally, the ligand coupling rate increases with temperature according to the Arrhenius equation [14]. At high pH values, the epoxy group of polymethacrylate is more reactive than

* Corresponding author. Tel.: +61 401338799; fax: +61 399055686.
E-mail addresses: clarence.ongkudon@monash.edu, clarence.ongkudon@eng.monash.edu.au (C.M. Ongkudon).

1570-0232/$ – see front matter © 2010 Elsevier B.V. All rights reserved.
doi:10.1016/j.jchromb.2010.08.011

Appendix C5

Separation and Purification Technology 78 (2011) 303–310

Contents lists available at ScienceDirect

Separation and Purification Technology

journal homepage: www.elsevier.com/locate/seppur

Anion exchange chromatography of 4.2 kbp plasmid based vaccine (pcDNA3F) from alkaline lysed *E. coli* lysate using amino functionalised polymethacrylate conical monolith

Clarence M. Ongkudon*, Michael K. Danquah

Bio Engineering Laboratory, Department of Chemical Engineering, Monash University, Clayton Campus, Wellington Road, Victoria 3800, Australia

ARTICLE INFO

Article history:
Received 20 August 2010
Received in revised form
10 November 2010
Accepted 26 January 2011

Keywords:
Plasmid
Anion exchange chromatography
Conical column
Polymethacrylate monolith

ABSTRACT

New strategies to economically manufacture large quantities of vaccines in less time are greatly needed to cater for the increasing global human population. This study aimed at developing a strategy to efficiently manufacture a highly purified plasmid vaccine via anion exchange monolithic chromatography. Diethylamine and triethylamine were used to provide the functional groups for polymethacrylate monoliths and used in anion exchange chromatography of plasmid pcDNA3F. Five chromatographic settings as described in the first table of this article were studied and it was concluded that the triethylamine functionalised conical monolith combined with optimum buffers' and pH conditions produced the highest quality of pcDNA3F. Plasmid yield (3003.55 mg/L), plasmid recovery (90.25%), protein (0.01 mg/L), LPS (0.12 EU/mg) with no detectable gDNA and RNA were obtained at a low NaCl concentration of 0.25 M. Apparently, this technology will have a great impact on the overall plasmid vaccine production and particularly on the development of axial flow monolithic plasmid vaccine purification.

1. Introduction

The birth of recombinant DNA technology as a tool in gene therapy and more recently in DNA vaccination has fostered the development of large scale plasmid DNA (pDNA) production and purification processes. Most of currently employed cGMP plasmid purification techniques involve multi steps pre-treatment and chromatography [1,2]. These often result in low plasmid recoveries and high operating costs. Conventional plasmid purification schemes such as chloride/ethidium bromide ultracentrifugation, miniprep and maxiprep use alkaline lysis and disposable chromatographic columns which are not scalable and large amounts of resins, enzymes and hazardous chemicals are employed [3,4]. Other methods such as selective precipitation, aqueous two-phase separation and tangential flow filtration have some drawbacks such as low purification effect, need for dedicated equipments, time consuming and not scalable [5–7]. Commercial scale purification of plasmid DNA (pDNA) traditionally relies on a conventional particle-based chromatography consisting of many beads with small internal pores (<100 nm) [8]. The hydrodynamic size of plasmid molecules is >100 nm hence adsorption occurs only on the outer surfaces of the beads and this leads to low binding capacities [9]. A recent advancement in large biomolecules purification has resulted in the development of a monolithic chromatographic support which provides higher binding capacity, larger pore size up to 1000 nm and higher flow rates compared to the particulate supports [10–13]. In a recent development involving plasmid purification, it has been reported that a combination of $CaCl_2$ precipitation, anion exchange chromatography and hydrophobic interaction chromatography resulted in pure pDNA satisfying all regulatory requirements [14]. The purification of larger plasmids up to 93 kb at higher flow rates and binding capacity has also been disclosed [15]. The 800 mL CIM DEAE monolithic column (Boehringer Ingelheim, Austria) is currently the largest commercially available chromatographic medium that can produce up to 15 g of highly concentrated and purified pDNA [7].

One of the most common problems occurs in the preparation of monolith is the introduction of air pockets or gaps between the monolith surface and column wall due to monolith shrinkage. Many researchers have attempted to provide covalent bonds between the column wall and monolith surface by introducing a coupling agent mostly silane based methacrylates [16,17]. A much simpler method using a conical column to avoid this problem has never been published to date. Conical columns have been used to provide lower retention times, higher linear velocity, reduced mobile phase consumption, and effective converging flow [18,19]. In addition to the dynamic efficiencies, conical column format provides greater loadability compared to the conventional analytical columns [20]. In this study, conical monoliths were simply used to eliminate side flow problems hence forcing all plasmids

* Corresponding author. Tel.: +61 401338799; fax: +61 399055686.
E-mail address: clarence.ongkudon@eng.monash.edu.au (C.M. Ongkudon).

1383-5866/$ – see front matter © 2011 Published by Elsevier B.V.
doi:10.1016/j.seppur.2011.01.039

Appendix C6

Separation Science and Technology, 46: 1280–1282, 2011

ISSN: 0149-6395 print/1520-5754 online
DOI: 10.1080/01496395.2011.557027

Taylor & Francis
Taylor & Francis Group

Endotoxin Removal and Plasmid DNA Recovery in Various Metal Ion Solutions

Clarence M. Ongkudon and Michael K. Danquah
Bio Engineering Laboratory, Department of Chemical Engineering, Faculty of Engineering, Monash University, Victoria, Australia

In this brief article, we report endotoxin precipitation using different types of metal ion in plasmid DNA purification. The work involved modification and improvement of the LAL chromogenic analysis to compensate for metal ion-LAL interaction. Results (Figs. 1 and 2) show that $ZnSO_4$ gives an optimum combination of high endotoxin removal efficiency (~91%) as well as high plasmid recovery (~100%) compared to other metal ions tested.

Keywords free metal ion; lipopolysacharide; plasmid DNA; selective precipitation

INTRODUCTION

Endotoxin contamination remains as the most difficult problem in downstream processing of many therapeutic biomolecules including plasmid based vaccine. This is due to strong endotoxin characteristics such as high negatively charged, exists in different molecular sizes, amphiphilic, and exerts strong interaction on biomolecules being purified (1). In plasmid DNA production, endotoxin contamination is usually encountered during the alkaline lysis of gram negative bacteria due to the release of lipopolysacharides (LPS) from bacterial cell wall into the lysis solution (2). Several methods to remove endotoxins from bacterial cell lysates have been extensively studied in the past including affinity chromatography, two-phase separation, and ultra filtration (3,4). A least popular precipitation method using free metal ions has also been reported (5,6) but the amount of studies is still lacking. Endotoxin quantitation by Limulus Amoebocyte Lysate (LAL) assay is highly sensitive to metal ions (7,8) hence is not suitable for direct analysis of endotoxin precipitation by free metal ions. The accuracy and reliability of the LAL assay are further degraded when analysis of endotoxin precipitation by different types of metal ions is conducted simultaneously.

Received 26 August 2010; accepted 19 January 2011.
Address correspondence to Clarence M. Ongkudon, Bio Engineering Laboratory, Department of Chemical Engineering, Faculty of Engineering, Monash University, Clayton Campus, Wellington Road, Victoria 3800, Australia. Tel.: +61401338799; Fax: +61399055686. E-mail: clarence.ongkudon@monash.edu

MATERIALS AND METHODS

Materials

$CuSO_4 \cdot 5H_2O$ (99%), $ZnCl_2$ (95%) and $MgSO_4 \cdot 7H_2O$ (98%) were purchased from AJAX, Australia. $CuCl_2 \cdot 2H_2O$ (98%) and $ZnSO_4 \cdot 7H_2O$ (99%) were purchased from BDH, Australia. $NiSO_4 \cdot 6H_2O$ (99%), $MgCl_2 \cdot 6H_2O$ (99%), $NiCl_2 \cdot 6H_2O$ (98%), and $CaCl_2 \cdot 2H_2O$ (99%) were purchased from MERCK, Germany.

Standard Endotoxin (LPS) and Plasmid DNA (PcDNA3F)

Standard LPS was purchased from Genscript, USA and pcDNA3F was prepared from 5 g of *E. coli* cell paste using Wizard plus SV Maxipreps according to the manufacturer's instructions (Promega, Australia).

LPS/Plasmid Precipitation Using Free Metal Ions

Standard LPS and pcDNA3F were mixed in 1:1 (v/v) ratio and transferred into a pyrogen free microtube and mixed with 1 M of metal ion solution. The mixture was incubated for 30 min at 22°C and centrifuged at 15000× g for 15 min. 0.5 mL of cleared supernatant was transferred into a new pyrogen free microtube and analyzed for plasmid recovery and LPS removal using DNA gel electrophoresis and chromogenic LAL tests.

Chromogenic LAL Analysis of LPS Content in Different Metal Ion Solutions

The LAL test was performed according to the supplier's instructions (GenScript, USA) except for some modifications as explained herein. Samples, standard LPS and control contained apart from pyrogen free water, one sample volume (SV) of solution containing all cations in exact proportions. This step was highly crucial as it would eliminate any variations due to buffer composition. Minimum sample dilution (MSD) of 1000× was required to reduce the enhancement/inhibition effect of cations on LAL activity while maintaining a high endotoxin level. 5 mM EDTA was added into each standard LPS and the sample to mitigate the endotoxin-metal ion interaction. The incubation

Appendix C7

Anal. Chem. **2011**, *83*, 391–397

Analysis of Selective Metal-Salt-Induced Endotoxin Precipitation in Plasmid DNA Purification Using Improved Limulus Amoebocyte Lysate Assay and Central Composite Design

Clarence M. Ongkudon* and Michael K. Danquah

Bio Engineering Laboratory, Department of Chemical Engineering, Faculty of Engineering, Monash University, Clayton Campus, Wellington Road, Victoria 3800, Australia

Recent advancements in plasmid DNA (pDNA) production involve the development of innovative and cost-effective methods as well as reduced number of unit operations. This study investigates the feasibilities of using a metal salt to selectively remove endotoxins from clarified cell lysates containing plasmid DNA. Screening of endotoxin precipitation in various metal salt solutions and optimization of process conditions (pH, ion concentration, temperature, and incubation time) using central composite design experiments have been carried out successfully. Results show that selective endotoxin precipitation (<0.05 EU/μg) can economically be carried out during the alkaline cell lysis procedure (neutralization step) at a pH condition similar to that of alkaline-lysed cell lysate, a low $ZnSO_4$ concentration (0.5 M), a minimum incubation time (30 min), and a temperature of 15 °C. In summary, this method provides ease of subsequent plasmid DNA purification due to reduced bulk impurities and cost-effective and most importantly high endotoxin removal (>80%) and plasmid recovery (>90%).

In vaccine or therapeutic drugs production, substantial endotoxin removal is paramount to avoid severe side effects such as fever, microcoagulation, degradation of organ functions, and poor resistance to infections following contact with the human immune system.[1] Endotoxin or lipopolysaccharides (LPS) removal still poses major hurdles in plasmid DNA vaccine purification. Endotoxin level in plasmid DNA vaccines for in vivo application has to be reduced below the threshold level of 0.1 EU/μg plasmid.[2] Endotoxins are the major component of the outer leaflet of the cell membrane of most Gram-negative bacteria including *E. coli.* DH5α.[3] Endotoxins generally possess a negatively charged hydrophilic heteropolysaccharide (O-antigen), a core oligosaccharide region, a lipid A portion, different aggregated sizes of 10−1000 kDa, and a pI value of 2, thus highly negatively charged in basic solution.[4,5]

The clarified alkaline-lysed cell lysate generally contains genomic DNA (gDNA), endotoxins, proteins, RNA, and nicked or damaged pDNA isoforms along with the intact supercoiled pDNA. The major challenge in pDNA purification is poor selectivity because most of the impurities share common features with plasmid DNA such as surface charge, size, and hydrophobicity.[6,7] Most commercial plasmid purification schemes involve several chromatographic steps which are individually designed to remove a particular component of the cell lysate at a time.[8] Anion-exchange, affinity, hydrophobic interaction chromatography, synthetic adsorbent of crystalline calcium silicate hydrate, and the two-phase micellar system are some of the currently used endotoxin removal techniques.[8] In anion-exchange chromatography, it is difficult to separate plasmid and endotoxins mainly due to their similar binding affinities.[6] In immobilized metal affinity chromatography, plasmid preferentially binds to Fe^{3+} compared to other metal ions. However, in the presence of endotoxin and RNA, plasmid binding is least preferential. This phenomenon could be attributed to higher affinity of endotoxin and RNA toward Fe^{3+} or competition for the available binding site.[9]

Apparently, the properties of the bacterial solution determine the state of the endotoxins aggregation, and this information can help in designing an effective endotoxin removal scheme particularly when combined with plasmid DNA purification.[10] It has been found that addition of $CaCl_2$ into bacterial cell lysate can be used to selectively precipitate RNA from plasmid DNA but at a high concentration (1.5 M).[11] In addition, an additional purification step such as anion-exchange chromatography needs to be

* To whom correspondence should be addressed. Phone: +61401338799. Fax: +61399055686. E-mail: clarence.ongkudon@monash.edu.

(1) Petsch, D.; Anspach, F. B. *J. Biotechnol.* **2000**, *76*, 97–119.
(2) Tan, L.; Kim, D. S.; Yoo, I. K.; Choe, W. S. *Chem. Eng. Sci.* **2007**, *62*, 5809–5820.
(3) Santos, N. C.; Silva, A. C.; Castanho, M. A. R. B.; Martins-Silva, J.; Saldanha, C. *ChemBioChem* **2003**, *4*, 96–100.
(4) Magalhães, P. O.; Lopes, A. M.; Mazzola, P. G.; Rangel-Yagui, C.; Penna, T. C. V.; Pessoa, A. P., Jr. *J. Pharm. Pharm. Sci.* **2007**, *10*, 388–404.
(5) Kang, Y.; Luo, R. G. *Process Biochem.* **2000**, *36*, 85–92.
(6) Diogo, M. M.; Queiroz, J. A.; Prazeres, D. M. F. *J. Chromatogr., A* **2005**, *1069*, 3–22.
(7) Sousa, F.; Prazeres, D. M. F.; Queiroz, J. A. *Trends Biotechnol.* **2008**, *26*, 518–525.
(8) Ongkudon, C. M.; Danquah, M. K. *Crit. Rev. Biotechnol.* [Online early access]. DOI: 10.3109/07388551.2010.483460. Published Online: Sept 29, **2010**. http://informahealthcare.com/doi/abs/10.3109/07388551.2010.483460.
(9) Tan, L.; Lai, W. B.; Lee, C. T.; Kim, D. S.; Choe, W. S. *J Chromatogr., A* **2007**, *1141*, 226–234.
(10) Sweadner, K. J.; Forte, M.; Nelsen, L. L. *Appl. Environ. Microbiol.* **1977**, *34*, 382–385.

10.1021/ac1026379
Published on Web 11/30/2010